

DEVELOPING AND USING A HEAD-MOUNTED  
MINIATURE MICROSCOPE TO INVESTIGATE  
MEMORY FORMATION IN MOUSE MODEL OF  
ALZHEIMER'S DISEASE

by

Chen Yan

A thesis submitted in conformity with the requirements  
for the degree of Doctor of Philosophy  
Institute of Medical Science  
University of Toronto



# ABSTRACT

---

## **Developing and using a head-mounted miniature microscope to investigate memory formation in mouse model of Alzheimer's Disease**

Chen Yan

Doctor of Philosophy

Institute of Medical Science

University of Toronto

2018

Alzheimer's Disease (AD) is characterized by progressive memory loss. Results from many experiments suggest AD begins as a disease of synaptic dysfunction. However, how synaptic dysfunction translates into circuit dysfunction and, ultimately, memory impairment is entirely unknown. To address the circuit-level dysfunction in AD, I developed a miniature fluorescent microscope that can be mounted on the head of a behaving mouse. We showed this mini-microscope is capable of imaging hundreds of neurons in the cornu ammonis area 1 (CA1) region of the hippocampus, and with minor modifications, also in deeper brain structures and in two colour channels.

To investigate the circuit dysfunction in AD, we used transgenic mice designed to model AD in humans. These TgCRND8 mice (referred to as AD mice) express human familial AD genes and similarly develop memory impairments. As expected, we showed that AD mice have robust memory deficits in a contextual fear conditioning paradigm, in which mice were trained to associate an aversive stimulus with a context. Imaging data from

our mini-microscope showed that compared to control mice, CA1 cells in AD mice were hyperexcitable and contained less information related to memory recall. Moreover, cells from AD mice showed a deficit in coordinated activity, suggesting that these mice are impaired in pattern completion, a process important in recalling hippocampal-dependent memories.

Previous studies suggest that AD mice have excessive endocytosis of GluA2-containing AMPAR, which accounts for their synaptic dysfunction. We found disrupting GluA2 endocytosis using an interfering peptide (TAT-GluA2<sub>3Y</sub>) before training was sufficient to rescue the memory and circuitry deficits in AD mice. Moreover, we showed disrupting GluA2 endocytosis during a reminder three days after training also restored memory. These results argue that AD mice still retain some aspect of the memory days after training, and that strengthening this weakened memory allowed mice to recall it.

In conclusion, I developed and used a novel calcium imaging method to investigate the circuit dysfunction in a mouse model of AD. Using this tool, I revealed an important link between the synaptic and circuit deficits in AD mice. These findings may have important implications for designing the next generation of tools and therapies for AD.

# ACKNOWLEDGEMENTS

---

I am among the lucky few to enter graduate school under the exceptional mentorship of Dr. Sheena Josselyn, and it's hard to overstate my gratitude for Sheena's motivation, guidance and advice over my PhD program. Sheena's unwavering encouragement and support gave me the courage to transition from molecular biology to engineering and computational neuroscience with no prior experience, and made the journey extremely fulfilling. Sheena has shown me what an iconic scientist is: knowledgeable yet humble, rigorous yet open-minded, passionate yet meticulous. These attributes are what I will strive to achieve. I would also like to thank my program advisory committee members: Dr. Junchul Kim, Dr. Christopher Yip and Dr. Fang Liu. Your insightful suggestions and feedbacks during committee meetings have greatly pushed the project forward.

I would like to thank Dr. Paul Frankland for discussions about experiments and analyses, and always being helpful and supportive. I have been tremendously privileged to work with the brilliant members of the Josselyn / Frankland lab during the PhD program. I would like to express my gratitude to Dr. Valentina Mercaldo, who volunteered to be the unfortunate pilot user of the bug-ridden mini-microscope prototype and actually endured it — this work would not exist if not for her unreasonable perseverance and enthusiasm. Furthermore, I would like to thank Alexander Jacob for help with building and refining the mini-microscope design, and Dr. Ying Meng for discussions about Alzheimer's disease and input for this thesis. I would also like to particularly thank Dr. Asim Rashid, with whom I have collaborated since I first came to the lab. His infectious composedness, both towards science and life in general, has made me feel much less stressed in graduate school than I am supposed to be. Besides the Josselyn / Frankland lab members, I have also received

tremendous help from Dr. Nathan Insel and Dr. David Redish. I am grateful for their sharp ideas, deep insights and constructive critiques for the mini-microscope data and analysis.

This long journey of graduate school is not without exceptional support from my friends and family. I would like to thank Miao, Xiangyuan, and Mengchen for the many sleepless nights where failures in graduate school were laughed at. I would also like to thank my parents for their unconditional support and encouragement for me to pursue my passion. Last but not the least, I could not have come this far without the tremendous love and support from my wife Wei. Thank you for your understanding and patience, and for making me feel like a giant by keeping my head in the clouds and my feet on the ground.

# CONTRIBUTIONS

---

The author (Chen Yan) planned and conducted the experiments, as well as analyzed the data and prepared this thesis either in whole or in part. The following contributions by other individuals are acknowledged:

**Dr. Sheena Josselyn (Supervisor)** Mentorship, laboratory resources, assistance of experiment planning, interpretation of data, and thesis preparation.

**Dr. Junchul Kim (Committee member)** Guidance in experiment planning, interpretation of data, and thesis preparation.

**Dr. Christopher Yip (Committee member)** Guidance in experiment planning, interpretation of data, and thesis preparation.

**Dr. Fang Liu (Committee member)** Guidance in experiment planning and interpretation of data.

**Dr. Paul Frankland** Guidance in interpretation of results.

**Dr. Valentina Mercaldo** Assistance in the behavioural experiments for Chapter 3.

**Dr. Nathan Insel** Guidance in data analysis.

**Dr. David Redish** Guidance in data analysis.

**Alexander Jacob** Assistance in designing and building the mini-microscope in Chapter 2 and in thesis preparation.

**Dr. Ying Meng** Assistance in thesis preparation.

**Wei Zhao** 3D rendering of mini-microscope schematic in Chapter 2.

# Contents

<b>1 Literature Review</b>	<b>1</b>
1.1 Clinical presentation of AD . . . . .	1
1.1.1 Prevalence . . . . .	1
1.1.2 Progression . . . . .	2
<i>Introduction</i> . . . . .	2
<i>Preclinical stage</i> . . . . .	2
<i>Clinical stage</i> . . . . .	3
1.1.3 Pharmacological intervention . . . . .	5
1.2 Neuropathology in AD . . . . .	7
1.2.1 Introduction . . . . .	7
1.2.2 Cholinergic hypothesis . . . . .	8
1.2.3 Amyloid cascade hypothesis . . . . .	9
1.2.4 Tau hypothesis . . . . .	11
1.3 Hippocampus and memory . . . . .	13
1.3.1 History . . . . .	13
1.3.2 Anatomy of hippocampus . . . . .	14
1.3.3 Theories of hippocampus function . . . . .	15
<i>Introduction</i> . . . . .	15
<i>Marr model</i> . . . . .	16
<i>Standard model of memory consolidation</i> . . . . .	18
<i>Multiple trace theory (memory transformation theory)</i> . . . . .	20

<i>Cognitive mapping theory</i>	21
<i>Relational theory</i>	23
1.4 Synaptic mechanisms for memory . . . . .	25
1.4.1 Introduction . . . . .	25
1.4.2 The $\alpha$ -amino-3-hydroxy-5-methyl-4-isoxazolepropionic acid (AMPA) receptor . . . . .	25
1.4.3 long-term potentiation (LTP) . . . . .	27
1.4.4 long-term depression (LTD) . . . . .	28
1.4.5 Homeostatic plasticity . . . . .	30
1.4.6 Synaptic plasticity and memory hypothesis . . . . .	31
1.5 Hippocampal deficits in AD . . . . .	33
1.5.1 Initiation of AD pathology in hippocampus . . . . .	33
1.5.2 Synaptic deficits . . . . .	34
1.5.3 Hyperexcitability . . . . .	36
1.5.4 Circuit function deficits . . . . .	37
<i>Place encoding</i> . . . . .	37
<i>Pattern separation and completion</i> . . . . .	39
1.6 Methods and tools for investigating neural population activity . . . . .	40
1.6.1 <i>In vivo</i> electrophysiological recording . . . . .	40
1.6.2 Immunohistochemistry and <i>in situ</i> hybridization against immediately-early genes (IEGs) . . . . .	42
1.6.3 <i>In vivo</i> two-photon calcium imaging . . . . .	44
1.6.4 Fluorescent endoscopy . . . . .	46
<i>Fiber bundle based fluorescence endoscopes</i> . . . . .	47
<i>Miniature integrated fluorescence endoscopes</i> . . . . .	47
1.6.5 Conclusion . . . . .	48
1.7 Hypothesis and research aims . . . . .	49

<b>2 Construction of a Miniature Epi-fluorescence Microscope</b>	<b>53</b>
2.1 Introduction . . . . .	53
2.2 Material and methods . . . . .	54
2.2.1 General design of the mini-microscope . . . . .	54
<i>Lens configuration</i> . . . . .	55
<i>Filter selection</i> . . . . .	56
<i>Electronics</i> . . . . .	56
<i>Casing and assembly</i> . . . . .	57
<i>Objective lens assembly for deep brain imaging</i> . . . . .	57
2.2.2 Viral infusion . . . . .	60
2.2.3 Implantation of the mini-microscope . . . . .	60
2.2.4 <i>In vivo</i> mini-microscope testing . . . . .	61
2.2.5 Image analysis . . . . .	61
<i>Extracting cells from calcium imaging videos</i> . . . . .	61
<i>Mapping cells across session</i> . . . . .	62
2.3 Results . . . . .	62
2.3.1 Capability and <i>in vitro</i> testing of the mini-microscope . . . . .	62
2.3.2 Measuring blood flow with mini-microscope . . . . .	64
2.3.3 Recording calcium transients in CA1 . . . . .	65
2.3.4 Video preprocessing . . . . .	70
<i>Illumination correction</i> . . . . .	70
<i>Motion correction</i> . . . . .	71
2.3.5 Between session stability . . . . .	72
2.3.6 Deep brain imaging . . . . .	72
2.3.7 Two colour . . . . .	73
2.4 Discussion . . . . .	75
<b>3 Memory Formation in Alzheimer's Disease</b>	<b>77</b>

3.1	Introduction . . . . .	77
3.2	Material and methods . . . . .	79
3.2.1	Animals and vectors . . . . .	79
	<i>TgCRND8 mice</i> . . . . .	79
	<i>GP5.17 mice</i> . . . . .	79
	<i>Viral vectors</i> . . . . .	79
	<i>TAT-GluA2<sub>3Y</sub> peptide</i> . . . . .	80
3.2.2	Viral infusion . . . . .	80
3.2.3	Histology . . . . .	80
3.2.4	Contextual fear conditioning . . . . .	81
3.2.5	Motion tracking . . . . .	81
	<i>Features</i> . . . . .	82
	<i>Tracking</i> . . . . .	83
3.2.6	Analysis . . . . .	84
	<i>Freezing behaviour</i> . . . . .	84
	<i>Preprocessing for calcium transients</i> . . . . .	84
	<i>Mutual information</i> . . . . .	85
	<i>Machine learning</i> . . . . .	87
	<i>Statistics</i> . . . . .	91
	<i>Bayesian modelling</i> . . . . .	91
3.3	Results . . . . .	92
3.3.1	TAT-GluA2 <sub>3Y</sub> rescues memory deficits in transgenic (Tg) mice . . . . .	92
3.3.2	Tg mice can initiate freezing . . . . .	95
3.3.3	TAT-GluA2 <sub>3Y</sub> rescues hyperactivity in Tg cells . . . . .	97
3.3.4	TAT-GluA2 <sub>3Y</sub> rescues contextual fear memory recall by decreasing activity . . . . .	101
3.3.5	TAT-GluA2 <sub>3Y</sub> rescues freezing encoding deficit in Tg cells . . . . .	103
3.3.6	Network encoding of freezing behaviour . . . . .	105

3.3.7	Freezing encoding precedes freezing behaviour . . . . .	107
3.3.8	Memory recall in Tg mice is unstable . . . . .	111
3.3.9	Memory deficits in Tg mice are not a result of forgetting . . . . .	113
3.4	Discussion . . . . .	115
<b>4</b>	<b>General Discussion</b>	<b>123</b>
4.1	Construction of the mini-microscope . . . . .	123
4.1.1	Advantages of the current mini-microscope . . . . .	123
4.1.2	Advantages of using the mini-microscope to study AD . . . . .	125
4.2	Examining circuitry deficits in a mouse model of AD . . . . .	126
4.2.1	CA1 hyperexcitability . . . . .	126
4.2.2	Contextual fear memory . . . . .	128
4.2.3	Encoding . . . . .	129
4.2.4	Pattern completion . . . . .	130
4.2.5	TAT-GluA <sub>2</sub> <sub>3Y</sub> treatment is able to rescue circuitry deficits in AD . .	136
<b>5</b>	<b>Conclusions and Future Directions</b>	<b>139</b>
5.1	Conclusion . . . . .	139
5.2	Future directions for mini-microscope development . . . . .	142
5.2.1	Technical improvement for the mini-microscope . . . . .	142
5.2.2	Combining mini-microscope with other techniques for investigating circuitry function . . . . .	143
5.3	Effect of TAT-GluA <sub>2</sub> <sub>3Y</sub> in strengthening memory trace . . . . .	145
5.4	Pattern completion and pattern separation . . . . .	146
5.5	Effect of TAT-GluA <sub>2</sub> <sub>3Y</sub> in correcting AD pathology . . . . .	147
<b>Bibliography</b>		<b>149</b>



## **List of Tables**

1.1 Comparison of techniques for studying neural activity at cellular level. . . .	49
--	----



# List of Figures

2.1	Assembly of deep brain imaging doublet.	59
2.2	Schematic of the miniature microscope.	63
2.3	Resolution of the mini-microscope.	64
2.4	<i>In vivo</i> image of blood vessels.	65
2.5	Image of CA1 neurons in a freely behaving mouse.	66
2.6	Sample analysis data from a calcium imaging video.	67
2.7	Cells identified in a single imaging session.	68
2.8	Detection of potential place cells in CA1 calcium imaging.	69
2.9	Illumination correction.	70
2.10	Motion correction.	71
2.11	Cell alignment between sessions.	72
2.12	Calcium imaging in lateral amygdala (LA) during fear conditioning.	73
2.13	Images under both green and red channel.	74
3.1	hidden Markov chain (HMM) model for tracking mice.	83
3.2	Experimental paradigm for contextual fear conditioning.	93
3.3	Sample cell image and calcium transients.	94
3.4	Percent of freezing during memory test.	94
3.5	Freezing lengths and number of freezing bouts.	96
3.6	Cell activity during training and memory test.	99
3.7	Cell activity difference between training and memory test.	100
3.8	Cell activity during freezing.	102

3.9	Freezing information during memory test. . . . .	104
3.10	Position-controlled freezing information. . . . .	105
3.11	Accuracy of machine learning classifiers in predicting freezing. . . . .	107
3.12	Bayes model for change point detection. . . . .	108
3.13	Average classifier prediction accuracy at initiation of freezing behaviour. . .	110
3.14	Normalized distance to the Gaussian support vector machine (gSVM) classification boundary. . . . .	112
3.15	TAT-GluA2 <sub>3Y</sub> treatment during a brief reminder rescues memory deficit. . .	114
3.16	TAT-GluA2 <sub>3Y</sub> treatment does not rescue memory recall without reminder. .	115

# GLOSSARY

---

**A $\beta$**  amyloid  $\beta$ -peptide

**A/P** anteroposterior

**AAV** adeno-associated virus

**ACh** acetylcholine

**AChE** acetylcholinesterase

**AD** Alzheimer's Disease

**AFC** auditory fear conditioning

**AICD** APP intracellular domain

**AMPA**  $\alpha$ -amino-3-hydroxy-5-methyl-4-isoxazolepropionic acid

**AMPAR** AMPA receptor

**ANOVA** analysis of variance

**AP2** assembly polypeptide 2

**APP** amyloid  $\beta$  precursor protein

**arc** activity-regulated cytoskeleton-associated protein

**a.u.** arbitrary units

**BBB** blood brain barrier

**BLA** basolateral amygdala

**BOLD** blood-oxygen-level dependent

**CA1** cornu ammonis area 1

**CA2** cornu ammonis area 2

**CA3** cornu ammonis area 3

**CaMKII**  $\text{Ca}^{2+}$ /calmodulin-dependent protein kinase II

**CaMKIV**  $\text{Ca}^{2+}$ /calmodulin-dependent protein kinase IV

**catFISH** cellular compartment analysis of temporal activity by fluorescent *in situ* hybridization

**CDK5** cyclin-dependent protein kinase 5

**CLARITY** clear lipid-exchanged anatomically rigid imaging/immunostaining-compatible tissue hydrogel

**CMOS** complimentary metal-oxide-semiconductor

**CNMF** constrained non-negative matrix factorization

**CNS** central nervous system

**CSF** cerebrospinal fluid

**D/V** dorsoventral

**DAG** diacylglycerol

**DC** direct current

**DG** dentate gyrus

**dHPC** dorsal hippocampus

**DNA** deoxyribonucleic acid

**EC** entorhinal cortex

**eEF2** eukaryotic elongation factor 2

**EEG** electroencephalogram

**EPSC** excitatory postsynaptic current

**EPSP** excitatory postsynaptic potential

**ER** endoplasmic reticulum

**FAD** familial AD

**FAST** Functional Assessment Staging

**FDM** fused deposition modelling

**FISH** fluorescent *in situ* hybridization

**FITC** fluorescein isothiocyanate

**fMRI** functional magnetic resonance imaging

**FOV** field of view

**GABA**  $\gamma$ -aminobutyric acid

**GDS** Global Deterioration Scale

**GECI** genetically encoded calcium indicator

**GFP** green fluorescence protein

**GLM** general linear model

**GRIN** gradient-index

**GRIP-1** glutamate receptor-interacting protein

**GSK3** glycogen synthase kinase 3

**gSVM** Gaussian support vector machine

**HIV** Human Immunodeficiency Virus

**H.M.** Henry Molaison

**HMM** hidden Markov chain

**HSV** herpes simplex virus

**hSyn** human synapsin

**ICA** independent component analysis

**IEG** immediately-early gene

**IHC** immunohistochemistry

**i.p.** intraperitoneal

**IP3** inositol triphosphate

**KLE** Kozachenko–Leonenko entropy estimator

**KS test** Kolmogorov-Smirnov test

**LA** lateral amygdala

**LED** light-emitting diode

**LFP** local field potential

**LTD** long-term depression

**LTP** long-term potentiation

**M/L** mediolateral

**MAPK** mitogen-activated protein kinase

**MAPT** microtubule associated protein tau

**MCI** mild cognitive impairment

**MCMC** Monte-Carlo Markov chain

**mGluR** metabotropic glutamate receptor

**MMSE** Mini Mental State Examination

**MRI** magnetic resonance imaging

**mRNA** messenger RNA

**MTL** medial temporal lobe

**mTor** mechanistic target of rapamycin

**NAc** nucleus accumbens

**NBC** naive Bayes classifier

**NCS-1** neuronal calcium sensor 1

**NFT** neurofibrillary tangle

**NIAAA** National Institute on Aging-Alzheimer's Association

**NMDAR** N-methyl-D-aspartate receptor

**NSF** N-ethylmaleimide-sensitive factor

**PBS** phosphate-buffered saline

**PCA** principle component analysis

**PET** positron emission tomography

**PFA** paraformaldehyde

**PICK1** protein interacting with C Kinase - 1

**PKA** protein kinase A

**PKC** protein kinase C

**PLA** polylactic acid

**PP1** protein phosphatase 1

**PrP<sup>C</sup>** cellular prion protein

**PSD** post-synaptic density

**PTP** protein tyrosine phosphatases

**RNA** ribonucleic acid

**SNR** signal-to-noise ratio

**SVM** support vector machine

**TARP** transmembrane AMPAR regulatory protein

**Tg** transgenic

**TRAP** targeted recombination in active populations

**TrICP** the trimmed iterative closest point algorithm

**TRITC** tetramethylrhodamine

**tTA** tetracycline-off transcriptional activator

**USAF** United States Air Force

**USB** universal serial bus

**UV** ultraviolet

**vHPC** ventral hippocampus

**WHO** the World Health Organization

**WT** wild-type



# 1

## LITERATURE REVIEW

---

### 1.1 Clinical presentation of Alzheimer's Disease (AD)

#### 1.1.1 Prevalence

It is estimated that 35.6 million people have dementia worldwide (World Health Organization, 2013). This illness costs more than \$604 billion USD each year and creates substantial burden to family members and caregivers of the patients (World Health Organization, 2013). AD is the most common form of dementia, contributing to 60–80 % of all clinical cases (Alzheimer's Association, 2016). More than 11 % of population older than 65 are affected by AD in North America, and the risk triples to 33 % for individuals beyond 85 (Hebert et al., 2013). The real number of patients affected by AD is likely larger than reported, as instances of AD are often under-diagnosed and under-reported (Barrett et al., 2006; Zaleta et al., 2012). While the prevalence of AD in individuals beyond 65 is stable over the years, as the population ages, the burden of AD is expect to continue to rise. The instances of AD is expected to double every 20 years (World Health Organization, 2013; Hebert et al., 2013). This will translate into more than 8 million AD patients in the United States in 2030, and as many as 16 million in 2050. The World Health Organization (WHO) estimated in 2040, cases of dementia worldwide will reach 81.1 million, most of which are caused by AD (World Health Organization, 2013).

### 1.1.2 Progression

#### Introduction

AD is named after Dr. Alois Alzheimer, who first described the disease in 1906 (Goedert and Spillantini, 2006). A patient in her early fifties named Auguste D. was admitted with progressive memory loss, hallucinations and focal neurologic symptoms. After her death, Dr. Alzheimer examined her post-mortem brain tissue with silver staining, and made the crucial observation of senile plaques and neurofibrillary tangles (NFTs), both of which became the pathologic hallmarks of AD (Goedert and Spillantini, 2006; Dubois et al., 2016). The importance of senile plaques in the early pathogenesis of AD was further cemented by the discovery of autosomal dominant AD. Patients with familial AD have disordered amyloid  $\beta$ -peptide (A $\beta$ ) metabolism, namely mutations in genes presenilin 1, presenilin 2, and amyloid precursor protein (APP). For these patients, the onset of clinical symptoms is predictable and early, before the age of 65 (Goedert and Spillantini, 2006; Dubois et al., 2016).

#### Preclinical stage

The pathogenesis of AD starts well before clinical symptoms appear (Dubois et al., 2016). Atrophy of brain structures particularly the medial temporal lobe can be detected by magnetic resonance imaging (MRI) before the onset of AD (Jack et al., 1992; Scheltens et al., 1992; Chetelat and Baron, 2003), and is considered a diagnostic biomarker for AD at the mild cognitive impairment stage (Jack et al., 1999). Moreover, positron emission tomography (PET) imaging allows detection of amyloid plaques (the senile plaques originally described by Dr. Alois Alzheimer), and more recently hyperphosphorylated *tau* protein (which forms the neurofibrillary tangles) *in vivo* (Mathis et al., 2003; Maruyama et al., 2013; Okamura et al., 2013). These results from PET studies have shown to reliably predict AD risk in mild cognitive impairment (MCI) or asymptomatic participants (Klunk et al., 2004; Chien et al., 2014; Sepulcre et al., 2016).

Cerebrospinal fluid (CSF) protein levels are another biomarker for AD in the preclinical stage. As CSF circulates through extra-cellular space in the brain, its molecular composition reflects that of the central nervous system (CNS). Core biomarkers such as  $\text{A}\beta_{42}$ , *tau* and hyper-phosphorylated *tau* have consistently been shown to differentiate AD from other aging-related cognitive disorders (Blennow et al., 2010). Moreover, longitudinal studies of CSF biomarker levels in families with autosomal-dominant (familial) AD, where the participants have a predictable earlier age of AD onset, have shown detectable changes of  $\text{A}\beta_{42}$  and *tau* concentrations in CSF 5–20 years before symptom onset (Bateman et al., 2012; Fagan et al., 2014). Studies in asymptomatic and MCI patients display a similar timeline, where the biomarker changes are detectable 5–10 years before AD symptoms onset (Buchhave et al., 2012; Vos et al., 2013).

In conclusion, there is robust evidence to support that the pathology of AD exists as a continuum, and is present long before clinical diagnosis. As a result, neuroimaging and CSF biomarkers have been proposed to be included in the clinician's toolbox to increase the accuracy of diagnosis and earlier recognition of preclinical AD (Alzheimer's Association, 2016). Recognizing AD before the onset of clinical symptoms also provides an optimal window for intervention and optimization of treatment.

### Clinical stage

As a result of the broad clinical AD pathology spectrum, the algorithm for diagnosis of AD is complex and nuanced. Because an autopsy with neuropathological examination showing amyloid plaques and NFTs is the gold-standard of diagnosing AD, “probable AD” is the terminology for clinical diagnosis of AD (Hyman et al., 2012). The most recent guidelines from the National Institute on Aging-Alzheimer's Association (NIAAA) describes the following criteria for probable AD: the patient's presentation **a)** satisfies the criteria for dementia (as opposed to delirium), **b)** is insidious in onset over months to years, **c)** is progressive, **d)** consists of cognitive deficits that are evident in domains of learning, language, visuospatial or executive functions, and **e)** is not explained by other causes such as stroke, drug abuse,

vitamin deficiency, or other dementia types (McKhann et al., 2011). The diagnosis of possible AD is given to patients who would otherwise meet the criteria for probable AD but present with an atypical course or concurrent diseases (*e.g.*, cerebrovascular) that may impact the person's cognition or be difficult to disentangle. The diagnostic category of probable AD with evidence of AD pathophysiological process incorporates biomarker evidence, which can increase the confidence that the symptoms from probable AD is a result of the AD pathophysiological process (McKhann et al., 2011). The Mini Mental State Examination (MMSE) is the most commonly used test for detecting and tracking cognitive decline. The functional decline of AD patients can be further measured by Global Deterioration Scale (GDS) scales (Reisberg et al., 1982) and Functional Assessment Staging (FAST) (Sclan and Reisberg, 1992). AD patients' disease progression generally begins with a decline in memory, language, and spatial navigation performance. The symptoms then progress to difficulties in routine tasks, changes in emotion and personality, and disturbances in diurnal rhythms. In the end, the patient shows completely loss of verbal ability, problems in eating, incontinence, as well as psychomotor problems. At this stage the patient will require full time assistance for basic activities of daily living (Reisberg et al., 1982; Sclan and Reisberg, 1992).

While the stages of AD are well described, the rate of progression is highly variable from patient to patient (Komarova and Thalhauser, 2011; Tschanz et al., 2011). This suggests that AD patients are a heterogeneous population, and the progression of AD may be under the influence of various latent factors. The Cache County Study on Memory in Aging systematically followed 5000 elderly residents of Cache County, Utah, USA to map the natural course for up to 12 years. The study found several factors that are predictive of rate of cognitive decline in AD. Cardiovascular disease history predicts a faster rate of decline (Mielke et al., 2007), and better general health was protective to AD (Leoutsakos et al., 2012). Moreover, various aspects of the care-giving environment are also influence the rate of cognitive decline in AD patients. For example, AD patients benefit from more engagement in cognitive stimulating activities (Treiber et al., 2011) as well as

closer relationships to the caregivers (Norton et al., 2009).

As AD is a progressive disorder with no effective disease-modifying treatment, the prognosis for an AD patient is poor. The average survival after diagnosis is 4–8 years (Larson et al., 2004; Helzner et al., 2008). Moreover, patients will spend more than 40 % of the time after diagnosis at the most severe stage of dementia (Arrighi et al., 2010). Given the prevalence of AD and the burden it creates, delaying the progression of the disease by only a few months can reduce the cost of care by more than \$ 2000 per patient per year even if no effective treatment is available (Zhu and Sano, 2006). This will translate to more than \$ 15 billion total reduction of cost over a decade in Canada (Alzheimer's Society of Canada, 2010).

### 1.1.3 Pharmacological intervention

Currently only four drugs are approved for AD: three acetylcholinesterase (AChE) inhibitors - donepezil, rivastigmine and galantamine, and one N-methyl-D-aspartate receptor (NMDAR) antagonist - memantine (Nelson and Tabet, 2015). Rivastigmine and galantamine are approved for treatment of mild-moderate AD, and donepezil is available for AD patients at all stages (Bassil and Grossberg, 2009; Smith, 2009). Memantine is only available to moderate-severe AD patients, used either by itself or combined with donepezil (Nelson and Tabet, 2015).

AChE inhibitors aim to increase the amount of acetylcholine (ACh), which has been found to be depleted in circuits implicated in memory (*e.g.*, hippocampus) in the AD brain (discussed in Section 1.2.2). The AChE inhibitors act by blocking AChE, and therefore inhibiting the reuptake of ACh in the synapse, allowing its concentration to increase. AChE inhibitors are effective in improving the cognitive function of AD patients. For mild–moderate AD patients, large-scale double-blind studies have found significant cognitive protection effects with donepezil (Rogers et al., 1998), rivastigmine (Farlow et al., 2000), and galantamine treatment (Wilkinson and Murray, 2001). A more recent meta-analysis of double-blind studies has confirmed the effectiveness of AChE inhibitors on the cognitive outcome in

mild–moderate AD patients, and found no difference in the effectiveness between AChE inhibitors at their prescription dose (Tan et al., 2014).

While the effects of AChE inhibitors have been demonstrated in multiple late phase clinical trials, the effect size is small. Therefore, the cognitive benefit to individual patients may not be clinically meaningful, particularly in terms of overall function and independent living (Lin et al., 2013). Moreover, not all patients respond to AChE inhibitor treatment, and the factors influencing drug responsiveness are still unclear (Van Der Putt et al., 2006). AChE inhibitors unfortunately also lose their effectiveness as the patient progresses beyond moderate stage (Gillette-Guyonnet et al., 2011), except donepezil, which has been found to be mildly effective at high dose in moderate – severe AD patients (Sabbagh et al., 2013).

Memantine aims to protect neurons from NMDAR-mediated excitotoxicity in AD. NMDAR are calcium-permeable glutamate receptors which are central for learning and memory. The NMDAR is blocked by a  $Mg^{2+}$  ion in a voltage-dependent manner. In AD, the  $Mg^{2+}$  block is compromised by  $A\beta$  accumulation, leading to a pathological influx of  $Ca^{2+}$  into the post-synaptic neuron, and eventually cell death (Danysz and Parsons, 2012). Memantine replaces the  $Mg^{2+}$  and blocks the NMDAR in a  $A\beta$ -independent manner, therefore preventing the pathological influx of  $Ca^{2+}$ . Moreover, as the memantine block of NMDAR is also voltage dependent, it does not affect physiological  $Ca^{2+}$  influx during learning and memory (Danysz and Parsons, 2012).

Memantine only shows significant effects in moderate – severe AD patients (Reisberg et al., 2003; Tariot et al., 2004; Schneider et al., 2011), and is often prescribed with AChE inhibitor for a positive additive effect (Rountree et al., 2009). Double blind studies have shown that memantine is able to improve cognitive function in moderate – severe AD patients (Reisberg et al., 2003; Tariot et al., 2004), although the improvement is not consistent (Porsteinsson et al., 2008).

In conclusion, the currently approved pharmacological treatments of AD are only able to provide relief from the cognitive symptoms of AD, and their effectiveness varies from patient to patient. None of these therapies have effects on AD-related behavioural symptoms, or

show any benefits for the general functioning of AD patients (Tan et al., 2014). The drugs are, at best, able to delay the progression of AD, but unable to alter the course or improve the outcome of the disease. Together with a high drop-off rate and reports of adverse effect in many randomized clinical trials, more effective or disease-modifying therapies are urgently needed (Bond et al., 2012).

## 1.2 Neuropathology in AD

### 1.2.1 Introduction

Understanding the aetiology of AD will facilitate the discovery of more effective interventions. The most widely accepted cause of AD is synapse and neuronal loss, which are the best pathological correlates of disease progression and have been the focus of clinical investigation for over a decade (Selkoe, 2002; Coleman et al., 2004). Unfortunately given the progressive nature of AD, slowing or reversing neurodegeneration is difficult to achieve without a thorough understanding of its upstream players. In this section, I will first discuss the cholinergic hypothesis, upon which the currently available pharmaceutical AD treatments are based. This is followed by a discussion of the amyloid hypothesis and the tau hypothesis. These hypotheses are based on the hallmarks of AD pathology: amyloid plaques and NFTs.

It should be noted that although not discussed, other theories for the pathophysiology of late-onset AD are also supported by empirical evidence, and have gained various levels of attention over the years. The glutamate hypothesis, the basis for the memantine (Section 1.1.3), suggests that neuronal death is a result of excess glutamate activity. Excess glutamate activity results in a toxic overload of  $\text{Ca}^{2+}$  in neurons and initiates neuronal death (Greenamyre et al., 1988; Parsons et al., 2007). The oxidative stress hypothesis proposes that heavy metal ions and other molecules accumulate in the AD brain and induce the generation of free radicals, which cause neuronal damage either directly or indirectly (Markesberry, 1997; Smith et al., 2010).

Another group of hypotheses propose that central to AD pathophysiology is abnormal neuronal metabolism and insufficient energy supply. The mitochondrial hypothesis suggests AD is caused by decreased mitochondrial function, leading to insufficient energy in the cell (Zhu et al., 2006; Swerdlow et al., 2014). The vascular hypothesis states that AD is caused by the abnormal constriction and hardening of blood vessels in the brain, making the brain deficient of energy (Luchsinger et al., 2005; Mamelak, 2017). The inflammatory hypothesis proposes that chronic inflammation leads to AD. A chronic elevated inflammatory response impairs the metabolic balance of neurons, resulting in pathological changes to axons, plaque deposition and tangle formation (Krstic and Knuesel, 2013).

It is important to bear in mind that although each of the hypotheses for AD aetiology is presented as separate, linear sequences of causes and effects, there is significant overlap between them. Moreover, given the heterogeneity of late-onset AD patients (Komarova and Thalhauser, 2011; Tschanz et al., 2011), it is likely that the aetiology of AD is multifactorial and mixed (Schneider et al., 2007). Grouping AD aetiologies into multiple hypotheses is an artificial construct. In reality, a patients can show multiple aetiologies simultaneously where the symptoms are the result of their interactions.

### **1.2.2 Cholinergic hypothesis**

First proposed in 1982 by Bartus et al., the cholinergic hypothesis is the oldest theory of AD pathogenesis. Bartus et al. (1982) proposed that cognitive deficits seen in AD are the result of impairments in cholinergic system function. The cholinergic system is important in learning and memory (Deutsch, 1971). Young human experimental participants administered scopolamine, a nicotinic ACh receptor antagonist, showed impaired memory performance at the same level as elderly participants. This impairment could be rescued by ACh agonists such as physostigmine (Drachman and Leavitt, 1974). Together with the evidence that cholinergic synapses in AD undergo profound degeneration (Whitehouse et al., 1982), these results led to the development of AChE inhibitors donepezil, rivastigmine and galantamine. Currently, these are the only three drugs available to mild-moderate AD

patients (Bartus, 2000, also see Section 1.1.3).

The reception of the cholinergic hypothesis was mixed. Studies of the cholinergic neural projections in AD found cholinergic neurons have impaired synthesis pathway for ACh (Milner et al., 1987). AD is also found to correlate with a decrease of nicotinic ACh receptor density, however the muscarinic ACh receptors are not affected (Nordberg et al., 1992; Burghaus et al., 2000). Moreover, the degeneration of cholinergic synapses is most prominent in areas involved in learning and memory (Geula and Mesulam, 1996).

On the other hand, the cholinergic hypothesis was challenged primarily by paucity of evidence for early development of AD. For example, degeneration of cholinergic neurons is only found in late-stage AD, but not present in preclinical and early-stage patients (Davis et al., 1999). In fact, cholinergic neurons in hippocampus and frontal cortex are increased in early AD patients (DeKosky et al., 2002). Moreover, the limited clinical effect of AChE inhibitors suggests that cholinergic degeneration may be a secondary effect. This has generated significant doubt on the role of cholinergic system in AD aetiology, and the popularity of cholinergic hypothesis has declined. The cholinergic hypothesis is now often viewed as either a result of the amyloid cascade (Discussed in Section 1.2.3), or a cofactor for other risk factors for neuronal degeneration (Roberson and Harrell, 1997; Contestabile, 2011).

### 1.2.3 Amyloid cascade hypothesis

The amyloid cascade hypothesis, first proposed by Hardy and Higgins in 1992, states that the abnormal accumulation of the protein A $\beta$  is a primary trigger for AD. Accumulation of A $\beta$  initiates a series of pathological events in the brain, including tangle formation, neuritic injury, and finally dysfunction and death of neurons. This hypothesis is based on the discovery that the “senile plaques”, which characterized AD, are composed of A $\beta$  (Masters et al., 1985). A $\beta$  is the result of sequential cleavage of the amyloid  $\beta$  precursor protein (APP) on chromosome 21. APP is over-expressed in Down syndrome patients, whose genome contains an extra chromosome 21. As a result, all Down syndrome patients

have early onset of AD-like neural pathology, including amyloid plaque deposition and NFT formation (Wisniewski et al., 1985; Hardy and Selkoe, 2002). Moreover, mutation of APP (Dutch type) causes cerebral hemorrhage and deposition of A $\beta$  (Hardy and Selkoe, 2002).

Subsequent genetic and molecular studies described how A $\beta$  is processed from APP in detail. APP can be processed in two pathways: an amyloidgenic pathway and a non-amyloidgenic pathway. In the non-amyloidgenic pathway, APP is cleaved by  $\alpha$ -secretase into a soluble N-terminal fragments, APP $\alpha$ , and a 83-amino-acid C-terminal peptide, C83. C83 is then cleaved by  $\gamma$ -secretase into a small p3 peptide and the APP intracellular domain (AICD). However in the amyloidgenic pathway, the APP is first processed by  $\beta$ -secretase into N-terminal fragments, APP $\beta$ , and a 99-amino-acid C-terminal peptide, C99. The C99 is then cleaved by  $\gamma$ -secretase to form an extracellular peptide containing 38-43 amino acids, A $\beta$  and the AICD (Barage and Sonawane, 2015). The most toxic forms of A $\beta$  are A $\beta_{40}$  and A $\beta_{42}$ . While A $\beta_{40}$  is more abundant, A $\beta_{42}$  is more hydrophobic and aggregates faster (Walsh and Selkoe, 2007).

Evidence from animal models and familial AD (FAD) patients supports a causal role of A $\beta$  in AD symptoms. Autosomal dominant mutations in genes encoding the  $\gamma$ -secretase (*PSEN1* and *PSEN2*) renders the non-amyloidgenic pathway for APP processing defective, allowing more A $\beta$  production through the amyloidgenic pathway (Suzuki et al., 1994; Levy-Lahad et al., 1995; Rogaev et al., 1995). The effect of mutation in FAD has also been confirmed in mouse models in which the human mutant gene is expressed. These mouse models develop amyloid plaques in the brain, together with learning and memory deficits (Hsiao et al., 1996; Dodart et al., 1999; Chishti et al., 2001; Westerman et al., 2002). Moreover, acute treatment of A $\beta$  is toxic to hippocampal and neocortical neurons, both in cultured cells and *in vivo* (Lacor et al., 2004; Shankar et al., 2008). Additionally, genome-wide association studies have found a link between AD and regions associated with increased A $\beta$  levels (Kehoe et al., 1999; Myers et al., 2000).

However, more recent evidence suggests the aetiology of AD, especially the late-onset type, is more complicated than stated by amyloid cascade hypothesis. Longitudinal PET

studies have shown that while amyloid plaque load in humans poses a significant risk of cognitive decline in both cognitively normal and MCI subjects, it is only weakly associated with cognitive decline and not predictive of disease progression in AD patients (Chen et al., 2014). Moreover, amyloid plaque prevalence in elderly subjects is more than twice of AD prevalence (Rowe et al., 2010; Alzheimer's Association, 2016), suggesting a large population carrying significant plaque load without cognitive impairment. Recent clinical trials of immunotherapies aimed at amyloid plaque removal in AD patients have been successful in reducing the plaque load, however were unable to demonstrate clinical effect (Farlow et al., 2015; Siemers et al., 2016; Sevigny et al., 2016). These results suggest that the role of A $\beta$  in the development of AD is more nuanced than initially stated in the amyloid cascade hypothesis.

Amendments to the amyloid cascade hypothesis have attempted to reconcile the relationship between plaque load and cognitive performance. It has been proposed that the soluble fraction of A $\beta$  oligomers, which is most toxic to neurons, is cardinal to AD and insoluble plaques are irrelevant (Ferreira et al., 2015). A $\beta$  toxicity on synapses and neurons is evident (Ferreira et al., 2015), and synaptic degeneration correlates with the cognitive decline in AD (Selkoe, 2002; Coleman et al., 2004). Moreover, Canter et al. (2016) proposed A $\beta$  destabilizes synapses and impairs normal function of neural networks, resulting in cognitive deficits AD. In conclusion, the amyloid cascade hypothesis is supported by the most compelling evidence to date, however evidence suggest the reality of AD aetiology is more complex than what the initial hypothesis suggested.

#### 1.2.4 Tau hypothesis

NFTs are another key pathological signature of AD. NFTs are composed of hyper-phosphorylated *tau* proteins (Grundke-Iqbali et al., 1986). The *tau* hypothesis states that abnormal function of these *tau* proteins leads to a series of pathological events that are responsible for neurodegeneration and clinical symptoms (Goedert and Spillantini, 2011).

Under physiological conditions, *tau* proteins, expressed by the microtubule associated

protein tau (MAPT) gene, are widely expressed in the brain. The *tau* proteins assemble and stabilize microtubules in the cell, which is important for cell structure maintenance and intracellular transport. However, in AD, *tau* is found hyper-phosphorylated by multiple kinases, including glycogen synthase kinase 3 (GSK3), cyclin-dependent protein kinase 5 (CDK5) and mitogen-activated protein kinase (MAPK) (Singh et al., 1994). This hyper-phosphorylated *tau* is unable to bind to the microtubule building block tubulin, and is thought to result in destabilization of microtubules (Bramblett et al., 1993; Yoshida and Ihara, 1993; Alonso et al., 1994). Unbound *tau* proteins, under high concentrations, are likely to aggregate and form twisted paired helical filaments, which are the main component of NFTs (Kidd, 1963; Kuret et al., 2005). Destabilized microtubules and the toxicity of NFTs leads to failure in axonal transportation of vesicles and mitochondria, and finally the death of the neuron.

Importantly, the presence of NFTs is significantly correlated with the cognitive deficits of patients with AD (Hyman et al., 2012). Moreover, the spread of *tau* pathology is stereotypical and corresponds to the progression of AD symptoms. *tau* affects brain regions important for learning and memory, such as hippocampus and amygdala before spreading out to the neocortex (Braak and Braak, 1991). These early results from post-mortem studies have recently been confirmed by PET studies using *tau* tracers. PET scans allow detection of the amount and distribution of the *tau* protein in patients (Ossenkoppele et al., 2016; Schöll et al., 2016). *tau* is likely to be of key importance in the development of AD.

*tau* is implicated in many other neurodegenerative disorders where amyloid plaques are not present (e.g. Williams and Lees, 2009; McKee et al., 2016). For instance, primary *tau* pathology, such as mutation in the MAPT gene which encodes the *tau* protein, causes a familial form of frontotemporal dementia, but not AD (Hutton et al., 1998; Poorkaj et al., 1998). These findings suggest that *tau* pathology is sufficient for causing neurodegeneration. However, as there are no amyloid plaques in these disorders or mouse models of *tau* pathology (Götz et al., 2004), *tau* pathology is unlikely to be the primary cause for AD.

*tau* is now viewed as a downstream element in the pathophysiology of AD, causing di-

rect neurotoxicity. Further evidence suggests that *tau* may be downstream of the amyloid cascade. Plaque formation in AD proceeds tangle formation (Price and Morris, 1999). Furthermore, A $\beta$  binds to the *tau* protein *in vitro*, and accelerates *tau* hyper-phosphorylation (Guo et al., 2006; Zempel et al., 2010). In mouse models of *tau* pathology, A $\beta$  accelerates NFT formation and neural degeneration (Lewis et al., 2001; Terwel et al., 2008).

In conclusion, evidence suggests *tau* pathology is secondary to the cause of AD. However, given its strong correlation with the cognitive deficits in AD and important role in neurodegeneration, further studies aimed at understanding the underlying mechanism are necessary.

## 1.3 Hippocampus and memory

### 1.3.1 History

The hippocampus first came into the spotlight of learning and memory research following reports of the patient, Henry Molaison (H.M.) (Scoville and Milner, 1957; Squire, 2009). H.M. suffered from severe epilepsy which was not responsive to pharmaceutical treatments. As a last resort, H.M. received bilateral resection of the medial temporal lobe including hippocampus and brain areas surrounding it. While this surgery cured his epilepsy, it created profound anterograde amnesia, to the point that H.M. forgot daily events minutes after they occurred (Scoville and Milner, 1957; Squire, 2009). The amnesic effects of H.M.'s surgery were unanticipated, primarily due to the earlier work of Karl Lashley showing that memory was not stored in a localized fashion (Bruce, 2001). Further studies of H.M.'s memory deficit and animal models of hippocampus lesion have suggested that hippocampus is important for governing the formation of long-term memories, which form the basis for Squire and Zola-Morgan (1991)'s theory of hippocampal function (discussed in Section 1.3.3).

Another breakthrough in understanding hippocampal function stemmed from the discovery of place cells (O'Keefe and Dostrovsky, 1971). O'Keefe and Dostrovsky (1971) recorded

single unit signals from cornu ammonis area 1 (CA1) and cornu ammonis area 3 (CA3) subregions of hippocampus in rats, and found cells that fired only when the rat was in a specific location within the environment. These cells were consequently named “place cells”. This discovery forms the basis for the cognitive mapping theory (O’Keefe, 1976), and has inspired further research that confirms the important role of hippocampus and surrounding areas in processing location-related information (discussed in Section 1.3.3).

### 1.3.2 Anatomy of hippocampus

The anatomy and cellular structure of hippocampus was first described by Cajal (1893), and more recently reviewed in detail by Strien et al. (2009). While the anatomy described here is mostly based on rodent studies, the organization, connectivity and function of the hippocampus are very similar across mice, rats, monkeys and humans (Clark and Squire, 2013).

The hippocampus is a large brain area in the medial temporal cortex consisting of multiple subregions, including dentate gyrus (DG), CA1, cornu ammonis area 2 (CA2), CA3 and subiculum. While original studies regarded hippocampus as a single brain region, it is now recognized that the hippocampus is heterogeneous along the dorsal-ventral axis (Moser et al., 1998; Fanselow and Dong, 2010). The dorsal hippocampus (dHPC) (septal pole) has strong connections to cingulate and retrosplenial cortex as well as thalamus, and is important for cognition and spatial navigation. The ventral hippocampus (temporal pole), as well as the subregion CA2, preferentially connect to regions such as hypothalamus and amygdala, and have been implicated in emotion and stress regulation (Fanselow and Dong, 2010; Chevaleyre and Piskorowski, 2016). In this thesis, the discussion will be limited to dHPC, as it is the focus of all of the experiments.

The standard view regards the dHPC as a tri-synaptic loop (Strien et al., 2009). The entorhinal cortex (EC) collects multimodal sensory information and sends projections from layer II to DG and CA3, through axons in the perforant path. Axons from granular cells in DG, the mossy fibers, then synapse onto CA3. Pyramidal cells in CA3 project to the

ipsilateral CA1 through Schaffer colaterals, and to contralateral CA1 through commissural pathway. CA1 pyramidal cells in turn synapses on the deep layer of EC either directly or through subiculum (Strien et al., 2009).

While the standard view of hippocampus connectivity is unidirectional, there are also significant recurrent projections and back projections in the hippocampus. The CA3 subregion is well known to form recurrent connections, and these recurrent connections are proposed to be critical for encoding and retrieving episodic memories (Nakazawa et al., 2002; Rolls, 2007). Weaker recurrent connections in CA1 and DG are also reported (Swanson et al., 1981; Ishizuka et al., 1990; Buckmaster et al., 1993). Moreover, outside the standard view there also exist back projections from CA3 back to DG, as well as back projections from CA1 to CA3 (Swanson et al., 1981; Li et al., 1994). Back projections from subiculum to CA1 are also reported (Finch et al., 1983).

### **1.3.3 Theories of hippocampus function**

#### **Introduction**

While it has been established that hippocampus plays a cardinal role in learning and memory, the exact role of hippocampus, and the mechanism by which hippocampus enables these cognitive processes are still unclear. Many theories have been proposed to answer these questions, and some of the most prominent theories are discussed here. I will start with the earlier Marr model (Marr, 1971) which has been hugely influential on the development of later theories of hippocampal function. The standard model of memory consolidation (Squire, 1992) and the competing multiple trace theory (Nadel and Moscovitch, 1997), are mostly influenced by the studies of the famous patient H.M., who received bilateral medial temporal lobe lesions and displayed anterograde amnesia along with other cognitive symptoms. The cognitive mapping theory and its extension, relational theory, stem from the discovery of place cells in hippocampus (O'Keefe and Dostrovsky, 1971).

Readers are also reminded that these theories should be regarded as multiple facets, in-

stead of competing hypotheses, of hippocampal functions. There are significant overlaps between the theories, and each theory aims to provide a different perspective of hippocampal function. In light of this, there has been a recent push for unification of many of these theories, and each theory is also continually supported or challenged by emerging experimental evidence.

### Marr model

In his seminal paper, Marr (1971) first used mathematical terms to describe the computational aspect of brain function. He proposed that the neocortex, being a complex structure, must perform complex computational tasks, while the archicortex, with a simpler structure, must perform simpler computational functions. In terms of memory function, and based on the symptoms of patient H.M., he proposes that the role of hippocampus is to provide short-term storage for “simple memories”, where sensory inputs are stored with minimal modification. The representations of “simple memories” are then transferred to neocortex, in a process where statistical regularities of the “simple memories” are extracted, and stored in the neocortex to form long-term memory.

In his model, Marr (1971) also described how the hippocampus stores “simple memories”. He argued this task could be completed with a three-layer neural network: an input layer, a codon layer and an output layer. The input layer represents sensory patterns. These patterns are then encoded with the codon layer, which has a larger number of nodes with sparse activity in order to store patterns reliably. He also proposed that the output layer should have a recurrent connection, which will allow the system to reconstruct a pattern with only a partial input pattern.

The Marr model is remarkable even viewed from today’s perspective. While in the original paper Marr (Marr, 1971) regarded the neocortex, entorhinal cortex and the whole hippocampus as the input, codon and output layer respectively, under modern interpretation the entorhinal cortex is better fit as the input layer, DG as the codon layer and both CA3 and CA1 as the output layer (Willshaw et al., 2015). Not only do the large number of

sparserly active granular cells in DG and the recurrent connections in CA3 fit the anatomy described in Marr (1971)'s model, the functions of DG and CA3 are also congruent with the model. For example, the DG has been shown to perform pattern separation, and the CA3 is shown to perform pattern completion through its recurrent connections (Knierim and Neunuebel, 2016). Moreover, the idea of dissociating the memory system into a fast, simple system and a slow, complex system also forms the basis of the modern theory of systems memory consolidation (Squire, 1992; McClelland, 2013).

One of the most important predictions of the Marr model (Marr, 1971) is the concepts of pattern separation and pattern completion. The Marr model predicts that the DG, with its large number of neurons, performs the function of pattern separation, where similar inputs are mapped onto more different representations in DG. On the other hand in CA3, the strong recurrent connections are able to perform the function of pattern completion, which maps partial or noisy input patterns back into their complete representation (Rolls, 2013b; Knierim and Neunuebel, 2016).

While the processes of pattern separation and pattern completion have been inferred from DG and CA1 ensemble activity or even behavioural performance (Santoro, 2013; Rolls, 2013b), direct evidence for pattern separation and pattern completion has not been available until recently, mostly due to the difficulty of simultaneously recording large number of neurons in behaving animals (Knierim and Neunuebel, 2016). Using multi-tetrode arrays, Neunuebel and Knierim (2014) simultaneously recorded neural activity from both DG and CA3 in behaving rats. The rats were placed in an environment where local spatial cues and global spatial cues were presented in conflict. The authors found while DG responses are highly different from the degree of environmental conflict, CA3 responses are more coherent (Neunuebel and Knierim, 2014). This result, therefore, directly confirms the long-standing prediction from Marr's model (Rolls, 2013b; Knierim and Neunuebel, 2016).

However, the Marr (1971) model is unfortunately limited by the data available at its time. The discovery of place cells (O'Keefe and Dostrovsky, 1971) and other specialized position-related cells in entorhinal cortex and hippocampus, such as grid cells and head-direction

cells (Taube et al., 1990; Fyhn et al., 2004; Hafting et al., 2005), suggest hippocampus also processes contextual information about the environment (discussed in 1.3.3), and is not a mere pattern store. Modern theoretical development has also shown that Marr (1971)'s proposal of an overnight transfer from the fast system to the slow system is also overly simplified (Squire, 2009).

In conclusion, while Marr (1971)'s model is sometimes regarded as a "noble failure" (Willshaw et al., 2015), the model and its ideas have inspired modern theoretical development and still exerts a strong influence on the learning and memory literature today.

### **Standard model of memory consolidation**

The standard model of memory extends the Marr model to take into account studies of medial temporal lobe lesion in humans and animals, as well as neural imaging studies of hippocampal and cortical activity after memory encoding (Squire, 1992, 2009). First of all, it has been found that in humans with medial temporal lobe (MTL) lesion, anterograde amnesia does not affect all forms of memory. Declarative memory, which includes the ability to remember facts and events, is impaired by MTL lesion, while non-declarative memory, which encompasses learning skills and habits, is otherwise spared (Cohen and Squire, 1980; Squire et al., 2004). This result suggests that multiple memory systems exist, and MTL is only necessary for the formation of declarative memory. Moreover, it was also found that while MTL lesion patients such as H.M. suffer from anterograde amnesia, they also display temporally graded retrograde amnesia: they are unable to recall events years before the lesion, but are able to recall older memories (Marslen-Wilson and Teuber, 1975). This result suggests that MTL does not disengage once the memory forms, but performs an important role in a slow memory consolidation process, where memories are transformed into a more robust form and become resistant to disruption (Squire, 1992).

As a result, Squire (1992) proposes that for declarative memories, the hippocampus (and its surrounding regions in MTL) serves as a fast system to quickly encode the memory. Then over a period of time, hippocampus actively engages with cortical regions in the

process of memory consolidation, which allows a representation of the memory to gradually form in the neocortex and become independent of hippocampal activity. This model was proposed by Squire (1992) as the standard model of memory consolidation.

The standard model received support from a wide range of animal studies (Squire, 2009). First of all, the temporally graded role of hippocampus in memory formation has been consistently demonstrated in rodents and primates, as shown by more than 30 studies compiled by Frankland and Bontempi (2005) with a variety of lesion techniques and memory tests. Moreover, studies tracking the activity and structural change of hippocampus have supported the prediction that hippocampus gradually disengages after initial memory encoding. For example, it has been found that over time after memory encoding, hippocampus shows gradually decreased activity and the cortex shows increased activity (e.g., Bontempi et al., 1999; Frankland et al., 2004; Takehara-Nishiuchi et al., 2006), as well as a similar gradient of neuronal structural change (e.g. Routtenberg et al., 2000; Mavil et al., 2004; Restivo et al., 2009). Furthermore, there is also evidence that the transferring process occurs during sleep. For example, task-related coordinated activity between hippocampus and visual cortex has been found when rats are asleep (Ji and Wilson, 2007).

The standard model is not without criticism. As the standard model is similar to the original Marr (1971) model, the line of criticism involving place cells to Marr (1971)'s model also applies to the standard model, as the spatial orientation of the animal in an environment critically depends on hippocampus, even long after encoding when memory consolidation is thought to be complete (e.g. Mumby et al., 1999; Sutherland et al., 2001; Clark et al., 2005). Moreover, close examination of MTL lesion patients reveals that these patients have global deficits in recalling details of episodic memory, and this deficit is not temporally graded (Cipolotti et al., 2001; Viskontas et al., 2002). Other evidence suggests that for some more demanding memory tasks, the hippocampus is also active during memory recall after consolidation (Ryan et al., 2001; Wheeler et al., 2013). These criticisms of the standard model led to the development of multiple trace theory (discussed in 1.3.3).

### Multiple trace theory (memory transformation theory)

Multiple trace theory is an extension of the standard model. Similar to the standard model, multiple trace theory also acknowledges that the hippocampus automatically encodes all information during memory formation, and that the hippocampus initiates a representation of memory in the cortex (Nadel and Moscovitch, 1997). However multiple trace theory is different from the standard model on several accounts. First, multiple trace theory differentiates declarative memory into episodic memory (memory of events) and semantic memory (memory of facts), and states that the two kinds of memory are encoded differently. Multiple trace theory then proposes that for episodic memories, there is no consolidation process, and the memory is represented by both hippocampus and cortex. However, upon reactivation of an old episodic memory, a new hippocampal representation is formed to link part of the cortical representation of the memory. Multiple trace theory argues that the multiple hippocampal representations provide robustness to the underlying memory, so they are less likely to be disrupted (Nadel and Moscovitch, 1997).

Compared to the standard model, the multiple trace theory makes several different predictions, especially regarding to the encoding of episodic memory. First, it predicts that the reactivation of a memory, no matter how old the memory is, will depend on the hippocampus. Secondly, multiple trace theory predicts that as memories get older, hippocampal activation will be stronger and more distributed among to the multiple traces, while the standard model predicts the opposite. Thirdly, multiple trace theory suggests that reactivation of a memory as new traces are formed in hippocampus and cortex provides a window to update the memory, while in the standard model reactivation of the memory should not have any effects on the underlying neural representation.

The dissociation of semantic and episodic memories which multiple trace theory identified is well supported. For example in retrograde amnesia caused by MTL lesion, episodic memories are usually severely impaired, often dating back for decades or even lifetime, while semantic memories are less affected, and this impairment is temporally-graded (Kapur

et al., 1997; Vargha-Khadem et al., 1997; Moscovitch et al., 2005). Moreover, hippocampal activation has been consistently reported during recall of episodic memory (Maguire, 2001; Svoboda et al., 2006). In addition, it has been established that, both in animal models and humans, the reactivation of memory creates a window to alter the original memory representation (Wang and Morris, 2010; Dunbar and Taylor, 2016).

On the other hand, many predictions of multiple trace theory have not been validated. For example, hippocampal activation during the recall of a remote memory is at a level similar to that of a recent memory (Addis et al., 2004; Steinvorth et al., 2006; Wheeler et al., 2013), which stands in contrast to the predictions of multiple trace theory. Moreover, while multiple trace theory predicts that partial lesioning of hippocampus leads to temporal-graded amnesia, this is not found in rodent models (Sutherland et al., 2010), and inconsistently in humans (Yassa and Reagh, 2013). The biological relevance of multiple trace theory has also been questioned, as it seems to necessitate a huge amount of storage for the multiple traces, which the hippocampus may not be able to provide (Yassa and Reagh, 2013).

In conclusion, multiple trace theory has been influential in recent studies of reconsolidation, and could potentially provide novel treatments for many psychiatric conditions (Dunbar and Taylor, 2016), however evidence exists against many of its core predictions. Efforts are still being made to amend multiple trace theory to account for the available evidence (Moscovitch et al., 2005; Yassa and Reagh, 2013).

### Cognitive mapping theory

Cognitive mapping theory was proposed in response of the discovery of place cells in the hippocampus (O'Keefe and Dostrovsky, 1971; O'Keefe and Conway, 1978). Place cells are neurons that respond to the position of the animal in a certain environment, independent of the behavioural state of the animal (O'Keefe and Conway, 1978). In rats, it has been found that 20–30 % of CA1 cells show place preference, and the ensemble of place cells is able to accurately determine the position of the animal (Guzowski et al., 1999; O'Keefe and

Burgess, 2005; Ziv et al., 2013). Place cell responses form rapidly when the animals is in a novel environment, and the place representation of each place cell remains stable, at least over months (Wilson and McNaughton, 1993; Ziv et al., 2013). Place cells remain the most robust neural representation of higher cognitive function observed to date.

Based on the discovery of place cells, cognitive mapping theory proposes that the main function of hippocampus is to maintain a map of the environment, in order to allow navigation and the formation of spatial memory. Further research has revealed cells responding to different features of the spatial map in the hippocampus and the adjacent entorhinal cortex, supporting the idea that hippocampus is important in maintaining a spatial map. For example, cells in the EC have been found to encode a hexagonal lattice of the current environment at different frequencies, and have been proposed to be important for distance measurement (Fyhn et al., 2004; Hafting et al., 2005; Moser et al., 2015); cells encoding the border of the current environment are also reported (Solstad et al., 2008). In addition, cells in the hippocampus do not only respond to allocentric cues. For example, cells responding to the head direction of the animals are also reported, supporting the idea that the function of hippocampus is navigation (Sargolini et al., 2006).

Cognitive mapping theory also predicts that the hippocampus should be active during spatial navigation tasks, and that lesioning the hippocampus will result in a performance deficit in these tasks. These two predictions are supported by imaging and lesion studies. Functional neuroimaging studies have shown that hippocampal activity correlates with performance of spatial navigation tasks in humans (Burgess et al., 2002; Hartley et al., 2007). In addition, patients with hippocampal lesions have deficits in learning to navigate new environments (Hartley et al., 2007). These human studies are paralleled by animal studies, which have shown that rats with hippocampal lesions are unable to navigate the environment using allocentric cues, however are still able to utilize egocentric cues (Morris, 2006). There is also a correlation of hippocampal damage in AD with this symptom. While the hippocampus is one of the earliest brain structures affected in AD and its precursor MCI, at the same time one of the early symptoms of AD is the inability to learn and explore

new environments (Vlček and Laczó, 2014).

Cognitive mapping theory, although having received wide support, also has several weaknesses. The first criticism is that only a small proportion of cells show properties of spatial coding in hippocampus, and in fact, cells may also encode time (Hampson et al., 1993), odour (Wood et al., 1999), tactile input (Young et al., 1994), or reward and punishment (Moser et al., 2008), which have no relationship with space. Moreover, it is not clear how episodic memory is encoded by the spatial map (Konkel and Cohen, 2009). In response, proponents of the cognitive mapping theory suggest a generalization of the cognitive mapping theory, where the hippocampus not only encodes the three-dimensional space, but also dimensions along time, language, and other factors (Burgess et al., 2002). This generalization is similar to the relational theory, which will be discussed in the next section.

### **Relational theory**

Relational theory was proposed to reconcile two seemingly incompatible views of hippocampal function: episodic memory function and spatial navigation, and has aimed to provide an explanation of hippocampal function which applies both to animal models and to humans. First proposed by Eichenbaum (1993), relational theory states that the hippocampus is fundamentally a “relation processor”. Given that multimodal sensory information converges in hippocampus, the function of hippocampus is to represent the output of the sensory system in a common multi-dimensional space, and captures the relationship between items in these sensory experiences (Eichenbaum, 1993).

Relational theory, therefore, suggests that the hippocampus is not specialized in encoding episodic memory, nor does it support for spatial navigation. Both episodic memory and spatial information are just examples of “relationships” captured by hippocampus. Spatial memories are relational mappings of specific events and objects to a spatial context, and episodic memories are relationship of concepts, events, and objects to time and space. The hippocampus creates these relationships in dimensions of space, time and concepts, which underlie both spatial and episodic memory (Eichenbaum and Cohen, 2014).

This view of hippocampal function is able to explain the findings that hippocampus encodes time and sensory aspects of particular events other than space (Hampson et al., 1993; Young et al., 1994; Wood et al., 1999; Moser et al., 2008). Relational theory is also able to explain why the hippocampus is necessary for many memory tasks which do not involve encoding space, for example, object recognition (Eacott and Norman, 2004; Langston and Wood, 2010), trace fear conditioning (where animals associate a conditioned stimulus with a delayed unconditioned stimulus) (Crestani et al., 2002; McEchron et al., 1998) and taste aversion (where the animals associate a particular taste with a punishment) (Best and Orr, 1973; Gallo and Cândido, 1995), as these tasks can all be regarded as forming an association between specific sensory outcomes and either time or context.

There are also neural correlates of the relationship formed in the hippocampus. In animals, recalling a specific event also reactivates the representation of the place where the event occurred (Moita et al., 2003; Itskov et al., 2011), and new learning in hippocampus leads to reorganization of the cellular activity which was related to a previous, similar learning episode (McKenzie et al., 2013). In humans, hippocampal activation during sequential learning only carries information about objects in learnt temporal contexts, but not about objects in random contexts (Hsieh et al., 2014). And again, new learning of object pairings in humans activates hippocampal representations of related previously learnt pairings (Zeithamova et al., 2012). More recent studies of hippocampal lesion patients have also revealed that these patients' cognitive deficits are not limited to episodic memory and spatial navigation, but also language, imagination and creative thinking (Duff et al., 2009, 2013).

On the other hand, it is unclear why certain kinds of associations are mediated by hippocampus while others are not, especially given that many of these associative learning tasks involve very similar sensory and motivation pairings but do not require the hippocampus (e.g. auditory fear conditioning, (Phillips and LeDoux, 1992)). Relational theory also does not take the unique anatomical structure of hippocampus into account or explain how the anatomy of hippocampus gives rise to its function. Nevertheless, relational theory is able to explain a wide range of functions of hippocampus, and has the advantage of being applicable

across animals and humans.

## 1.4 Synaptic mechanisms for memory

### 1.4.1 Introduction

The brain's ability to learn and remember stems from its ability to change with experience. How do neurons change, and how do changes on the cellular level give rise to the ability to learn and remember? These questions were first comprehensively tackled by Donald Hebb in 1949, whose model is now famously paraphrased as "neurons that fire together, wire together". However, evidence for Hebb (1949)'s proposition only started to appear more than 20 years after its publication, when long-term potentiation (LTP) - where a high frequency stimulation results in a persistent strengthening of synapses, was discovered (Bliss and Lomo, 1973). After the discovery of LTP, a variety of mechanisms for neural plasticity were also found to be important for learning and memory. On the synaptic level, LTP and long-term depression (LTD), and more formally, spike-timing-dependent plasticity have been found to regulate strength of a single synapse. Moreover, synapses themselves are plastic, and synaptogenesis (the growth of new synapses) and synaptic elimination also contributes to neuroplasticity. The discovery of neurogenesis in DG and olfactory bulbs has also shed light on neural plasticity at the population level.

In this section, I will briefly review the evidence and mechanisms underlying LTP and LTD, as these mechanisms are important for synaptic plasticity (changes in synaptic strength), and critical for learning in the hippocampus. These mechanisms are also the first to be compromised in AD. How they are affected by AD is discussed in Section 1.5.2.

### 1.4.2 The $\alpha$ -amino-3-hydroxy-5-methyl-4-isoxazolepropionic acid (AMPA) receptor

AMPA receptors (AMPARs) mediate the majority of fast excitatory transmission in the brain. There are four types of subunits in the composition of AMPARs, namely GluA1–

GluA4. The AMPAR forms a heteromeric “dimer of dimers”, consisting of two pairs of different subunits (Ayalon and Stern-Bach, 2001). In hippocampus, the majority of AMPARs are composed of GluA1/2 or GluA2/3, and synaptic AMPARs are predominantly of type GluA1/2 (Wenthold et al., 1996; Lu et al., 2009). The GluA2 subunit undergoes post-transcriptional editing. Residue 607, which lies on the channel wall, is modified from glutamine to arginine in the majority of adult neurons (Greger et al., 2003). This change renders GluA2-containing AMPARs impermeable to  $\text{Ca}^{2+}$  ions, and predominantly mediates excitatory synaptic transmission (Sommer et al., 1991; Swanson et al., 1997). Although limited in expression, the GluA2-lacking, and therefore  $\text{Ca}^{2+}$ -permeable AMPARs are implicated in mediating excitotoxicity in neurological disorders such as ischemia and AD (Kwak and Weiss, 2006; Whitehead et al., 2017), however the exact role these receptors play in physiological conditions is still under research (Whitehead et al., 2017).

AMPARs are first synthesized in the endoplasmic reticulum (ER) of the cell as homo-dimers, and then these homo-dimers form tetramers. The teramerized receptors are then transported to the cell surface (Henley and Wilkinson, 2013). It is now widely acknowledged that the mobilized AMPARs are inserted near the synapse, but not directly onto the synapse, potentially due to inaccessibility of the post-synaptic density (PSD) to transport vesicles (Henley et al., 2011; Chater and Goda, 2014). Cell-surface AMPARs are highly mobile and diffuse along the cell membrane laterally. However, AMPARs, especially GluA2 containing ones, can become immobilized on the synaptic membrane (Borgdorff and Chouquet, 2002; Groc et al., 2004). The density of AMPARs on the synaptic membrane is highly correlated with the synaptic strength, and is under tight control with constant receptor exocytosis and endocytosis at extrasynaptic sites (Malinow and Malenka, 2002; Henley et al., 2011). Therefore, the strength of a synapse reflects the balance of receptor exocytosis and endocytosis processes.

### 1.4.3 LTP

First discovered by Bliss and Lomo (1973) in the rabbit hippocampus, LTP refers to the phenomenon of synaptic strengthening after a brief high-frequency stimulation. Since its initial discovery, LTP has been found not limited to hippocampus, but prevalent across the brain (e.g. Clugnet and LeDoux, 1990). LTP is therefore proposed to be a general phenomenon of neural plasticity (Malenka and Bear, 2004).

While early studies debated whether LTP was a pre-synaptic or post-synaptic phenomenon (Malinow and Tsien, 1990; Bekkers and Stevens, 1990; Isaac et al., 1995; Liao et al., 1995), more recent glutamate uncaging studies have shown that direct stimulation of dendritic spines with glutamate is sufficient to induce LTP, therefore establishing that LTP is primarily mediated by post-synaptic mechanisms (Kerchner and Nicoll, 2008). The post-synaptic molecular mechanisms of LTP have been extensively studied, especially in the Shaffer collateral – CA1 synapse. The initiation of LTP starts with the activation of NMDARs after high-frequency stimulation (Collingridge et al., 1983). The opening of NMDARs results in an influx of  $\text{Ca}^{2+}$  and activation of  $\text{Ca}^{2+}$ /calmodulin-dependent protein kinase II (CaMKII). While a rapid increase of synaptic AMPARs is observed after CaMKII activation (Patterson et al., 2010), the exact mechanism of how CaMKII activation leads to accumulation of AMPAR on the synapse is still under debate (Herring and Nicoll, 2016).

The currently accepted hypothesis is that CaMKII directly phosphorylates the GluA1 subunits of AMPARs or their associated proteins, transmembrane AMPAR regulatory proteins (TARPs), leading to their increased synaptic trafficking. It has been found that GluA1 is indeed phosphorylated by CaMKII after LTP induction (McGlade-McCulloch et al., 1993; Barria et al., 1997; Lee et al., 2003), and that GluA1 with a mutated C-terminal which blocks the CaMKII phosphorylation, failed to traffic to synapse, while mutation on other AMPAR subunits does not affect their synaptic trafficking (Hayashi et al., 2000; Shi et al., 2001). Moreover, LTP in GluA1 knockout mice is impaired, while unaffected in GluA2 or GluA3 knockout mice (Zamanillo et al., 1999; Meng et al., 2003). Similar results are also

found for TARPs, such that TARP is phosphorylated during LTP induction, and blocking the CaMKII-mediated phosphorylation of TARPs also prevents AMPAR translocation to the synapse (Tomita et al., 2005; Sumioka et al., 2010).

While ample evidence has indicated AMPAR/TARP as a central player in LTP and a direct downstream target of CaMKII, this view is not unchallenged. The main criticism of the AMPAR/TARP-centric hypothesis is that LTP is never completely blocked in the absence of AMPAR phosphorylation, only attenuated (Herring and Nicoll, 2016). This is further demonstrated by molecular replacement studies. Under strong stimulation, LTP is not affected by replacing endogenous AMPARs with either a mutant GluA1 subunit where all LTP-related residues are mutated, or even completely replaced by kainate receptors, which do not interact with TARP (Granger et al., 2013; Chen et al., 2003). These results suggest alternative mechanisms for LTP might exist. Other hypotheses have been proposed to explain these results. For example it has been hypothesized that CaMKII may create holes in the PSD which capture AMPARs, and CaMKII may phosphorylate recycling endosomes, which are responsible for inserting AMPARs onto synaptic membrane. Both of these hypotheses still require further evidence for validation (Herring and Nicoll, 2016).

#### 1.4.4 LTD

Opposite to LTP, LTD is a process whereby synaptic strength is persistently decreased after receiving low-frequency stimulation. There are several types of LTD, and they can be classified in different ways. First LTD can be either homosynaptic, and only acts in the synapse which receives low-frequency stimulation, or heterosynaptic, where LTD also affects synapses which are not stimulated. Second, both homo- and heterosynaptic LTD can then be classified into *de novo* LTD or depotentiation. In *de novo* LTD, baseline synaptic strength is persistently decreased, however in depotentiation, LTD only reduces the strength of a previously potentiated synapse (e.g. by LTP) to baseline, however does not affect the synaptic strength if it is already at baseline. (Collingridge et al., 2010). Different type of LTD may be mediated by different mechanisms, and can co-exist in the

same population of synapses (Collingridge et al., 2010). Here I will review the two best-studied LTD mechanisms in the hippocampus: NMDAR-dependent LTD and metabotropic glutamate receptor (mGluR)-dependent LTD.

*De novo* LTD and depotentiation at many synapses are dependent on NMDARs (Collingridge et al., 1983; Dudek and Bear, 1992). In NMDAR-dependent LTD, low levels of  $\text{Ca}^{2+}$  ions enter from NMDARs, and activate calcineurin. Calcineurin then disinhibits protein phosphatase 1 (PP1) by dephosphorylating inhibitor-1 (Mulkey et al., 1993). PP1 then dephosphorylates its target (such as GluA1), and facilitates the removal of the receptor from synaptic membrane (Collingridge et al., 2004). In addition, the low level of  $\text{Ca}^{2+}$  entry also activates  $\text{Ca}^{2+}$  sensors such as hippocalcin (Palmer et al., 2005). Hippocalcin, upon activation, translocates to the plasma membrane, then binds and activates the clathrin adaptor protein assembly polypeptide 2 (AP2). AP2 then replaces the N-ethylmaleimide-sensitive factor (NSF), de-stabilizes the AMPAR on the synaptic membrane, and initiates clathrin-mediated endocytosis of the AMPAR (Collingridge et al., 2004; Palmer et al., 2005). Another pathway involves a different low-affinity  $\text{Ca}^{2+}$  sensor, protein interacting with C Kinase - 1 (PICK1). PICK1 mediates the dephosphorylation of GluA2, and may also play a role in endocytosis by inducing membrane curvature (Collingridge et al., 2004; Lin and Huganir, 2007). However the exact role of PICK1 in AMPAR endocytosis is still under debate (Collingridge et al., 2010). As a result of multiple converging pathways, synaptic AMPAR density is reduced, and the result is a persistent decrease of synaptic strength.

LTD mediated by mGluRs recruits proteins in different pathways from NMDAR-dependent LTD (Gladding et al., 2009). While all types of mGluR can potentially mediate LTD, in CA1 hippocampus mGluR5, and to a small extent mGluR1, initiate most mGluR-mediated LTD (Lüscher and Huber, 2010). Both mGluR5 and mGluR1 activate the protein kinase C (PKC) pathway through inositol triphosphate (IP3) and diacylglycerol (DAG) (Oliet et al., 1997). PKC then recruits PICK1 and neuronal calcium sensor 1 (NCS-1), phosphorylates the C-terminal of GluA2, and mediates its endocytosis (Bellone and Lüscher, 2006; Jo et al., 2008). In addition, mGluR activation in LTD also enables rapid protein syn-

thesis through the activation of eukaryotic elongation factor 2 (eEF2) and the mechanistic target of rapamycin (mTor) pathway, which leads to the translation of proteins such as activity-regulated cytoskeleton-associated protein (arc) and protein tyrosine phosphatases (PTP) (Park et al., 2008; Zhang et al., 2008). These *de novo* synthesized proteins, again, are implicated in the process of AMPAR endocytosis (Collingridge et al., 2010).

#### 1.4.5 Homeostatic plasticity

Hebbian plasticity, while implicated in learning and memory, is computationally unstable. Cells undergoing LTP are involved in a positive feedback loop, and tend to become hyperactive, while cells under LTD are excessively silenced, leading to a pathological deletion of synaptic connections. It is therefore hypothesized that besides Hebbian plasticity, additional mechanisms exist in the cell to maintain overall synaptic strength within a physiological dynamic range (Bienenstock et al., 1982; Cooper and Bear, 2012). Indeed, a number of mechanisms, both pre-synaptic and post-synaptic, has been found to maintain either excitability of the cell or amplitude of excitatory postsynaptic current (EPSC) (Turrigiano et al., 1998; Frank et al., 2006; Collingridge et al., 2010; Chater and Goda, 2014; Wang et al., 2016).

One of the most studied mechanisms for homoeostatic plasticity is synaptic scaling, where global synaptic strength is regulated to control the excitability of cells. It was first found in rat cortical neuron cultures, where chronic inhibition of presynaptic terminals resulted in an increase of AMPAR-mediated post-synaptic currents, while chronic block of  $\gamma$ -aminobutyric acid (GABA)-mediated inhibition decreased post-synaptic currents (Turrigiano et al., 1998). This effect was later confirmed *in vivo* by several studies (Whitt et al., 2014). In synaptic scaling, the strength of synapses across the whole cell is scaled multiplicatively by a uniform amount, opposing the direction of external changes in neural activity. Importantly, relative strength between synapses is maintained in this process, and therefore information stored in individual synapse is not lost (Turrigiano, 2008).

The molecular pathway for synaptic scaling partially overlaps with those of LTP and

LTD. Not only are AMPARs central to both mechanisms, but regulatory pathways and proteins involved in LTP and LTD are also important for synaptic scaling. Blocking  $\text{Ca}^{2+}$ , CaMKII or protein kinase A (PKA) prevents synaptic upscaling, while blocking calcineurin or  $\text{Ca}^{2+}$ /calmodulin-dependent protein kinase IV (CaMKIV) pathway induces synaptic upscaling (Goel et al., 2011; Kim and Ziff, 2014; Ibata et al., 2008). Proteins important for modulating synaptic AMPAR density such as PICK1, glutamate receptor-interacting protein (GRIP-1) and the TARP protein stargazin, have all been shown to be necessary for synaptic upscaling (Anggono et al., 2011; Gainey et al., 2015; Louros et al., 2014). Moreover, immediate early genes such as *homer1a* or *arc*, which are responsive to LTP and LTD, are also necessary for synaptic scaling (Hu et al., 2010; Gao et al., 2010). The commonality between synaptic scaling and activity-dependent synaptic plasticity suggests that while conceptually separate, these regulatory processes are closely associated, and may fail or become compromised under similar pathological conditions (Fernandes and Carvalho, 2016).

#### 1.4.6 Synaptic plasticity and memory hypothesis

LTP and LTD, being consistent with the hebbian model, have been considered as mechanisms for learning and memory since they were discovered (Morris, 1990; Bliss and Collingridge, 1993; Shors and Matzel, 1997; Martin et al., 2000). Moreover, LTP and LTD are correlated with memory formation, and have similar time-scales: both have a early phase independent of protein synthesis, and a late phase dependent of protein synthesis (Abel and Lattal, 2001; Reymann and Frey, 2007). The molecular mechanisms of LTP and LTD also involve many key proteins necessary for memory formation, such as NMDARs and  $\text{Ca}^{2+}$  signaling pathways (Martin et al., 2000). This evidence has been formalized in the synaptic plasticity and memory hypothesis, which proposes that activity-dependent synaptic plasticity is induced during memory formation, and is both necessary and sufficient for information storage in the brain (Martin et al., 2000).

However, as critiqued by Neves et al. (2008), direct empirical evidence showing necessity

and sufficiency of synaptic plasticity in learning and memory is hard to obtain. To show necessity of, for example, LTP in memory, the ideal evidence would show the abolition of LTP, but nothing else, results in a learning and memory deficit (Neves et al., 2008). Since most findings are based on molecular manipulation of key proteins in synaptic plasticity, these results are often confounded by other synaptic and cellular functions of the targeting protein (Neves et al., 2008). However, further evidence can be obtained from occlusion studies, where necessity can be implied if saturation of either memory formation or LTP blocks the other. Indeed, it has been shown that watermaze training in rats results in a failure to induce certain forms of LTP in CA1 cells (Habib et al., 2014). Conversely, saturating LTP in DG prevents spatial learning (Moser et al., 1998). These results suggest at a minimum that LTP and memory formation share some necessary mechanisms (Takeuchi et al., 2014). The evidence however, is mixed. It is also reported that in some cases, abolishing LTP, for example by knocking-out GluA1 in hippocampus, does not affect spatial learning (Zamanillo et al., 1999). This discrepancy in evidence suggests that LTP many involve various different mechanisms, which may be specific to different induction protocols (Neves et al., 2008).

To show synaptic plasticity is sufficient for memory, one will need to show that activating synaptic plasticity mechanisms creates an artificial memory (Neves et al., 2008), and this has not been possible until recent development of optogenetics, which allows activation and deactivation of neural populations with light (Zhang et al., 2007; Rajasethupathy et al., 2016). In an auditory fear conditioning paradigm, Nabavi et al. (2014) trained rats to associate a foot shock with optogenetic stimulation of auditory thalamus and auditory cortex, hence creating an artificial memory. The authors further showed that optically induced LTD abolishes the fear memory, and subsequent LTP induction reactivates the fear memory (Nabavi et al., 2014). This result is the first direct evidence that LTP and LTD are sufficient to induce and inhibit memory, respectively.

In conclusion, the synaptic plasticity and memory hypothesis is well supported by empirical evidence. While the LTP and LTD are sometimes considered as an artificially

constructed experimental phenomena (Stevens, 1998), the mechanism underlying LTP and LTD are both necessary and sufficient to support memory formation.

## 1.5 Hippocampal deficits in AD

### 1.5.1 Initiation of AD pathology in hippocampus

Converging evidence suggests that the hippocampus and its surrounding brain areas in the MTL are the first brain areas compromised in the development AD (Palmer and Good, 2011; Zhou et al., 2016). For example, post-mortem studies of AD patients have reported initial NFTs and neuronal loss in the EC, which then spread to other regions of MTL in a predictable network-dependent manner (Braak and Braak, 1991; Van Hoesen and Solodkin, 1993; Zhan et al., 2009). In fact, longitudinal studies have shown significant neuronal loss and atrophy of EC in patients with MCI and early AD, and in addition, the degree of neurodegeneration in EC and hippocampus correlates with cognitive performance (Kordower et al., 2001; Jack et al., 2002; Pennanen et al., 2004). These results suggest that hippocampal neuronal degeneration is a sensitive biomarker for AD progression and cognitive outcome (Jack et al., 2002; Zhou et al., 2016).

While the AD pathology is consistently found to originate in the EC and hippocampus, it is still unclear why this circuit is particularly vulnerable to AD. Several hypotheses exists. It has been hypothesized that EC and hippocampal neurons are formed early in development, and the vulnerability is simply due to the neurons' old age (Rakic and Nowakowski, 1981). The complicated morphology, larger surface area, and higher energy consumption in the EC neurons may contribute to the vulnerability (Hevner and Wong-Riley, 1992; Buckmaster et al., 2004). Moreover, the specific molecular environment of EC neurons renders them with reduced neurotropic support (Narisawa-Saito et al., 1996; Peterson et al., 1996) and increased inflammation (Janelsins et al., 2005; Okun et al., 2010), both of which have been found to aggravate A $\beta$  toxicity (Tang et al., 2008; Stranahan and Mattson, 2010).

The neuronal degeneration of EC then propagates to the DG and CA3 through the

perforant pathway. Firstly, presynaptic markers are reduced at the perforant-DG synapse, correlating with a spatial learning deficit in animal models of AD (Smith et al., 2000). While initially the post-synaptic cells are unaffected, over time they show reduced amplitude of EPSCs, and an increase in LTP threshold (Calhoun et al., 2008; Barnes and McNaughton, 1980; Barnes et al., 2000). DG neurons then, in turn, show an increase of A $\beta$  deposition and synaptic degeneration (Reilly et al., 2003; Dong et al., 2007), leading to an imbalance of excitation and inhibition through the hippocampal network and reduction of both short-term and long-term plasticity (Palop et al., 2007). Changes in cytoskeletal architecture and atrophy of the hippocampus also potentially contribute by the prion-like axonal trafficking of *tau* protein (Clavaguera et al., 2009). However, as *tau* cannot cross the synapse, the mechanism of how it affects post-synaptic cells is still unclear (Stranahan and Mattson, 2010).

### 1.5.2 Synaptic deficits

There is converging evidence that the main pathological marker of AD, A $\beta$ , inhibits LTP and promotes LTD. In mouse models of AD where A $\beta$  production is transgenically enhanced, hippocampal LTP is severely impaired in advance of plaque formation and neural degeneration, and these LTP deficits are correlated with learning impairment in these mice (Hsia et al., 1999; Chapman et al., 1999; Roberson et al., 2011). Moreover, acute A $\beta$  induction leads to severe LTP impairment, both *in vitro* (Lambert et al., 1998; Shankar et al., 2008) and *in vivo* (Walsh et al., 2002; Hu et al., 2008). In human AD patients, similar impairment of LTP-like cortical plasticity is also observed (Inghilleri et al., 2006; Koch et al., 2012). On the other hand, the LTP impairment created by A $\beta$  is accompanied by an enhancement of LTD, such that sub-threshold stimulation which does not have an effect in wild-type mice can create LTD in mouse models of AD (Hsia et al., 1999; Fitzjohn et al., 2001; Jacobsen et al., 2006).

The molecular pathways by which A $\beta$  modulates LTP and LTD are still under investigation. Current evidence suggests that A $\beta$  leads to more excitable synapses, and that

attenuated LTP and enhanced LTD are a result of neuronal homeostasis processes trying to maintain overall cell activity (Guntupalli et al., 2016; Jang and Chung, 2016). For example, A $\beta$  blocks synaptic glutamate reuptake by astrocytes, and therefore lead to chronic increase of synaptic glutamate levels (Matos et al., 2008; Li et al., 2009). The increased amount of glutamate may spill over to the extra-synaptic membrane, and activates GluN2B-containing NMDARs, which are abundantly present at extra-synaptic sites in mature hippocampal neurons (Citri and Malenka, 2008; Li et al., 2011; Shipton and Paulsen, 2014). Activation of extra-synaptic NMDARs then leads to an excess influx of Ca<sup>2+</sup>, which activates PP1, calcineurin and MAPK pathway (Hsieh et al., 2006; Shankar et al., 2007; Zhao et al., 2010). As a result, synaptic AMPARs are dephosphorylated and endocytosed, and consequently synaptic strength is reduced (Hsieh et al., 2006; Liu et al., 2010; Miñano-Molina et al., 2011).

A $\beta$  also affects mGluR-dependent LTD. It has been found that A $\beta$  clusters and stabilizes membrane mGluR5s, potentially through the membrane protein cellular prion protein (PrP<sup>C</sup>), which upon A $\beta$  activation, binds to mGluR5 (Renner et al., 2010; Um et al., 2013). The activated PrP<sup>C</sup>-mGluR5 complex then interacts with homer1b/c, Fyn and CaMKII, all of which are implicated in hippocampal LTP and LTD (Raka et al., 2015; Haas et al., 2016). Moreover, inhibiting mGluR5s pharmacologically or genetically in mouse AD models rescues deficits in LTP, dendritic spine density and spatial learning (Rammes et al., 2011; Hu et al., 2014; Um et al., 2013; Hamilton et al., 2014). The mGluR- and NMDAR-mediated pathways of A $\beta$  are not independent. Activation of mGluR can lead to NMDAR activation through CaMKII and PKC pathways (Chen et al., 2011; Jin et al., 2015), and conversely NMDAR activation can enhance mGluR activity through calcineurin (Alagarsamy et al., 1999, 2005).

In conclusion, A $\beta$  has been consistently shown to shift hippocampal synaptic plasticity from LTP to LTD. Although further investigation is still required, multiple molecular pathways are implicated and converges on the dysregulation of synaptic AMPAR density.

### 1.5.3 Hyperexcitability

While individual hippocampal synapses shift from LTP to LTD in the presence of A $\beta$ , synaptic changes are not predictive to changes in neural networks. With degeneration of excitatory synapses, counter-intuitively a hyperactive hippocampus has been consistently found across animal models and human patients (Palop and Mucke, 2016). Mouse models of AD show larger discharges on electroencephalogram (EEG), increased hippocampal immediately-early gene (IEG) expression *in vivo*, paradoxically accompanied by decreased surface AMPARs (Palop et al., 2007; Harris et al., 2010; Born et al., 2014). Pharmacologically-induced hyperactivity *in vivo* in mouse hippocampus creates molecular, synaptic and anatomical deficits similar to that of mouse models of AD (Palop et al., 2007). This has also been confirmed by more recent *in vivo* calcium imaging studies, where hippocampal neurons in a mouse model of AD were found to have increased spontaneous activity, especially those neurons located close to plaques (Busche et al., 2012).

Similarly in humans, hyperactivation of hippocampus has been reported in asymptomatic individuals with high risk of developing AD, suggesting hippocampal hyperactivity is an alteration of neural networks early in the development of AD pathology (Sperling et al., 2009; Reiman et al., 2012). While A $\beta$  disrupts glutamate reuptake and may directly create hyperexcitability, it also promotes neural degradation (Spires and Hyman, 2004; Koffie et al., 2009). Neurons treated with A $\beta$  have shorter dendrites and lower dendritic spine density, and these morphological changes also promote hyperexcitability (Siskova et al., 2014).

Given the hyperexcitability of neural networks in AD, it is therefore not surprising that epilepsy often accompanies AD. Spontaneous epileptic activity has been reported in many mouse models of AD, and this is usually accompanied by behavioural seizures and a lower threshold for pharmacologically induced seizures (Palop et al., 2007; Ittner et al., 2010; Um et al., 2012). Incidences of epileptic seizures are also common in AD patients. While prevalence varies from study to study due to different detection methods and difficulty of

seizure assessment in AD patients, a recent review suggests that on average epileptic seizures affect 17% of late-onset AD patients, which is 7–8 times higher than the general incidental rate of epilepsy (Amatniek et al., 2006; Horváth et al., 2016). Moreover, populations with a genetic disposition toward AD have an even higher rate of epilepsy, and the epileptic episodes often precede any sign of cognitive decline (Moehlmann et al., 2002; Cabrejo et al., 2006; McNaughton et al., 2012).

Moreover, AD patients with concomitant epilepsy have faster progression of cognitive decline (Vossel et al., 2013; Bakker et al., 2015). Anti-epileptic treatment in MCI restores cognitive ability in the short-term (Bakker et al., 2015). In animal models of AD, anti-epileptic treatment restores synaptic function, long-range network coherence, as well as cognitive and behavioural deficits (Sanchez et al., 2012; Busche et al., 2015). These findings suggest that network hyperexcitability is not only a symptom of AD, but is also important in the initial development of AD progression, and can be a potential therapeutic target for AD.

#### 1.5.4 Circuit function deficits

##### Place encoding

Given the discovery of place encoding in hippocampus and the finding that deficits in spatial navigation are one of the first symptoms of AD, it is surprising that only a few studies have investigated how hippocampal place encoding is compromised in AD. This idea was first studied by Cacucci et al. (2008), where the authors recorded from both wild-type and an APP transgenic mouse model of AD, Tg2576. They have found that while at a young age the transgenic mice have similar place encoding, place fields in aged Tg2576 mice are less defined, as measured by a larger field size and less spatial information encoded by cells. The degradation of place fields also correlated with deficits in spatial memory and amyloid plaque burden in the hippocampus (Cacucci et al., 2008).

More recent studies suggest that the place field deficit in AD mouse models is a learning

deficit instead of an encoding deficit. Cheng and Ji (2013) recorded CA1 place cells in aged mice with *tau* pathology on a linear track. The authors found while the transgenic mice have degraded place fields, potentially due to the hyperexcitability of the CA1 neurons, on a familiar track these mice are still able to maintain the correct sequence of firing, from which the mice's position can be decoded. However, the transgenic mice failed to form new place cell trajectories when placed on a novel track (Cheng and Ji, 2013). In a later study, Zhao et al. (2014) investigated CA1 place encoding in an APP transgenic mouse model, and found the transgenic mice were able to initiate place fields in a novel environment, however over time, they were unable to refine these place fields. Furthermore this deficit correlated with a deficit in spatial memory performance; the transgenic mice learnt slower and less effectively than the wild-type mice. In a recent study, Mably et al. (2017) showed that in the 3x-Tg mice, not only the place fields are less accurate than the wild-type (WT) mice, they are also unstable, varies more in both the spatial representation and firing rate across trials.

While neuroimaging techniques in humans are unable to resolve single cells activity and identify place cells, the hexagonal symmetry of grid cells in EC creates a similarly symmetric blood-oxygen-level dependent (BOLD) signal, which can be detected under functional magnetic resonance imaging (fMRI) (Doeller et al., 2010). Kunz et al. (2015) recently investigated this grid-cell-like representation in individuals with genetic depositions for AD before cognitive decline. Similar to the place field results found in mouse models, Kunz et al. (2015) found while the spatial memory performance is similar between the AD-risk group and the control group, grid-cell-like representations in the AD-risk group were less stable over time, and the degradation of grid-cell-like representation was also correlated with hippocampal hyperactivation.

In conclusion, evidence from both mouse models and human studies suggests that the spatial encoding in hippocampus and EC is affected in AD, which potentially leads to cognitive deficits in spatial memory. However, future study is needed to understand the circuit mechanisms of this hippocampal spatial encoding deficit in AD.

### Pattern separation and completion

The two vital circuit mechanisms of hippocampus, as first predicted by the Marr model, are pattern separation and pattern completion (Discussed in 1.3.3). It is thought that the DG functions as a pattern separator, which involves pulling similar patterns apart to reduce memory interference, and that the role of CA1 is pattern completion, where noisy or incomplete patterns are mapped to the original, complete pattern (Rolls, 2013b). Given the hippocampal deficits seen in AD, it is hypothesized that the process of pattern separation and pattern completion are compromised. However, only a few studies have investigated this hypothesis explicitly (Maruszak and Thuret, 2014).

Palmer and Good (2011) used c-Fos expression to study hippocampal cell activity in the APP transgenic mice, Tg2576. Mice were exposed to either a familiar environment or a novel environment, and hippocampal cell activity was examined by analyzing the expression of the IEG, c-Fos. The authors found that while wild-type mice showed increased DG activation during novel environment exposure, potentially supporting a pattern separation process, transgenic mice showed similar DG activation, but an increased CA3 activation. The authors concluded that the Tg2576 mice have a deficit in pattern separation, and that this leads to an overactive pattern completion, resulting in memory deficits (Palmer and Good, 2011).

However, this theory was not supported by a later human study. Ally et al. (2013) studied behavioural pattern separation and pattern completion processes in human patients in MCI and mild AD. In their study, MCI patients, AD patients and age-matched controls were presented with a lag-based memory task, where the individuals were presented with a continuous list of pictures. The list of pictures contained repeated, similar, and novel items, and the participants were asked to label the items accordingly. The authors found that for similar items, the AD patients performed significantly worse in telling them apart during testing, and the performance of the MCI group was negatively correlated with the lag, with the performance of low-lag items similar to control group and that of high-lag compara-

ble to AD. In addition, Ally et al. (2013) also examined the pattern completion process. Interestingly, while the MCI patients showed intact behavioural pattern completion, the AD patients showed a significant deficit (Ally et al., 2013). These results suggest that in AD, both behavioural pattern completion and behavioural pattern separation are impaired, while in MCI, only behavioural pattern separation is impaired in a temporal-graded manner (Ally et al., 2013).

However, it is worth bearing in mind that neither the Palmer and Good (2011) nor Ally et al. (2013) studies directly address the pattern separation and pattern completion process originally defined computationally, and conflicting results are not uncommon once a definition is loosed. The findings of these studies may be influenced by processes other than pattern separation or pattern completion (Santoro, 2013). While computational studies have long proposed that pattern separation and pattern completion processes can be compromised in AD (Horn et al., 1993; Hasselmo, 1994, 1997), validating these hypothesis requires simultaneous recording of large ensemble of hippocampal neurons *in vivo* during behaviour, which has not been possible until recently (discussed in Section 1.6).

## 1.6 Methods and tools for investigating neural population activity

### 1.6.1 *In vivo* electrophysiological recording

*In vivo* electrophysiological recording is one of the oldest techniques for recording neural activity from a living brain. In electrophysiological recording, one or multiple fine-tipped microelectrodes are inserted into the brain region of interest. If the tips of the electrodes are placed close to or within the cell membrane of neurons, changes of the membrane potential when these neuron generate action potentials can be detected. The signal is then amplified, sampled and recorded.

Since the electrical activity of the cell is measured directly, cell activity can be measured in a time resolution of less than 1 ms, which allows the shape of the action potential to

be resolved (Lütcke et al., 2013). Moreover, since the insertion of microelectrodes induces minimal tissue damage, it is possible to reach deep in the brain, and therefore this method is preferred for recording in larger model animals such as cats and monkeys (Lütcke et al., 2013). A chronic implantation is stable for months, allowing repeated recordings from the same animal. With recent development of electrode array, it is possible to record more than a hundred units simultaneously from multiple brain regions (Berényi et al., 2014; Xie et al., 2016). Another unique advantage of single unit recording is the possibility to deliver electrical neural stimulation. A small electric current can be precisely delivered through the same recording electrode, which is useful for brain-computer interfaces (Hatsopoulos and Donoghue, 2009).

With the flexibility of single unit recording, however, comes less stability. Firstly, *in vivo* electrophysiological recording requires extraordinary mechanical stability, experimenters often need to wait for months before getting a stable recording, possibly because of the formation of scar tissue which de-stabilizes the electrodes (Jackson and Fetz, 2007). Secondly, while neuron identity across recording sessions can be inferred by the unique signature in the action potential waveform, this method cannot reliably distinguish whether the same neuron is recorded over time (Rousche and Normann, 1998; Schmitzer-Torbert and Redish, 2004; Tolias et al., 2007). In fact, recordings tend to become unstable quickly over time, such that half of the stable units can drop out in the first three days of recording (Fraser and Schwartz, 2012). Thirdly, while it is possible to cluster units into regular spiking (often representing excitatory cells) and fast spiking (often representing inhibitory cells), *in vivo* electrophysiological recording is otherwise unable to differentiate subpopulation of neurons (Connors and Gutnick, 1990). And lastly, recordings from single units are heavily biased towards neurons which fire across the whole experimental session, neurons which stay silent for long periods of time will be missed in the recording. Therefore the recorded population may not represent the true underlying neural population (Lütcke et al., 2013).

Many of the limitations of *in vivo* electrophysiological recording can be overcome by combination with the recent development of optogenetics, where light-sensitive ion channels

can be expressed in neurons, and allow neural activity to be controlled by light (Yizhar et al., 2011). Combined with molecular constructs, opsins can be expressed in specific neural subpopulations. A pattern of light stimulation can be used to identify opsin-expressing neurons during *in vivo* electrophysiological recording (Zhao et al., 2011).

In conclusion, *in vivo* recording is useful to identify circuit mechanisms which rely on the activity of individual neurons. In addition, *In vivo* electrophysiology also allows relatively easy neurostimulation as well as simultaneous recording from multiple brain regions, and with optogenetics, identification of neural subpopulations.

### 1.6.2 Immunohistochemistry and *in situ* hybridization against IEGs

Neuronal activity leads to *de novo* protein synthesis. IEGs are a group of genes that are immediately expressed after neural activity. For example, it has been shown that IEGs such as arc, c-fos, zif268 are selectively up-regulated after maximum electroconvulsive shock, LTP induction, and behavioural experiences (Guzowski et al., 1999; Vann et al., 2000; Hall et al., 2001). After exposure to a novel environment, the arc-expressing population of neurons is similar in size to electrophysiological estimates. Repeated exposure to the same environment reactivates similar populations of neurons (Guzowski et al., 2006; Niibori et al., 2012). Moreover, given many of the IEGs are crucially involved in the synaptic plasticity process, IEGs are widely used as a molecular marker of neural activity (Minatohara et al., 2015).

The crucial role of IEG-expressing neurons in learning and memory has been directly confirmed recently using optogenetic techniques. Inhibiting the hippocampal neural population that expresses c-fos or arc after contextual fear conditioning prevents the expression of the fear memory during memory recall (Denny et al., 2014; Tanaka et al., 2014). Moreover, reactivating the c-fos ensemble formed during contextual fear conditioning is able to reactivate memory response (Liu et al., 2012; Cowansage et al., 2014; Ohkawa et al., 2015), or even able to modify the original memory in a new environment (Ramirez et al., 2013; Redondo et al., 2014). These two lines of evidence confirm that the IEG-expressing neurons

are both necessary and sufficient for learning and memory.

The expression of IEGs is detected in *post mortem* tissue by immunohistochemistry (IHC) against proteins or fluorescent *in situ* hybridization (FISH) against messenger RNA (mRNA), and therefore the size of the neural population to be analyzed is theoretically unlimited. And in fact, IEGs staining allows neural activity across the whole-brain to be studied with cellular precision (Wheeler et al., 2013). Recent developments in tissue clearing and microscopy allow fast whole-brain imaging at the scale of a mouse brain (Chung and Deisseroth, 2013; Tomer et al., 2014), and combining this technique with the detection of IEGs, whole-brain analysis of active neural ensembles is much less labour intensive, and more accessible to researchers.

Recent developments have also allowed genetic access to active neurons by taking advantage of the molecular mechanisms of IEG expression. This idea was first developed and demonstrated by Reijmers et al. (2007), where the authors expressed the tetracycline-off transcriptional activator (tTA) under the Fos promoter. In their procedure, experimental mice are placed under a doxycycline diet, which suppresses the activation of tTA. During the experimental intervention, doxycycline is removed from the diet, allowing activation of tTA only in c-fos expressing neurons. The tTA then binds to a tetracycline operator for expression of the transgene of interest. A more recent, similar system, targeted recombination in active populations (TRAP), has been developed by Guenthner et al. (2013). In TRAP transgenic mice, the promoters of arc and c-fos drive a tamoxifen-dependent recombinase, CreER(T2). When tamoxifen is given, CreER(T2) is expressed only in active cells, allowing Cre-dependent recombination of any gene of interest (Guenthner et al., 2013). Both systems give genetic access to active neurons within a certain period of time, and can be combined with molecular tools for labelling, tracing and manipulating neurons. These tools provide powerful ways to understand circuitry mechanisms.

The major disadvantage of IEG-based studies is the time resolution. First, IEG expression needs to be examined *post mortem*, and can only represent neural activity at a single time point. However, several techniques exist allowing comparison of IEG-expression at two

time points. The cellular compartment analysis of temporal activity by fluorescent *in situ* hybridization (catFISH) method, developed by Guzowski et al. (1999), takes advantage of the temporally different cellular localization of arc mRNA. Arc mRNA can be detected in the nucleus 5 min after expression, and is transported into the cytoplasm after 30 min. If the two experimental procedures of interest are performed at 5 min and 30 min before the animal is sacrificed for arc detection, the cell population with cytoplasmic arc signal will represent the active ensemble during the first procedure, and the population with nuclear arc signal will represent the population active during the second (Guzowski et al., 1999). IEGs with different expression rates can be used to identify two active cell ensembles in a similar manner. For example, homer1a's signal cannot be detected in the cell nucleus until 30 min after cell activation, and it can be co-stained with arc nuclear signal to identify active ensembles from 5 min and 30 min prior (Vazdarjanova and Guzowski, 2004). Moreover, longer intervals between two procedures can be achieved by using the TRAP or Fos-tTA transgenic mice described above, in combination with a fluorescent marker which marks the first period of activation. The second period can be detected by IHC against IEG such as c-fos (Reijmers et al., 2007; Guenthner et al., 2013). However, in this procedure, temporal precision can be as long as 12 h compared to minutes for direct FISH against IEGs.

In conclusion, while IEG detection provides almost perfect spatial range and resolution and allows analysis of the activation pattern of the whole brain at a cellular level, it can only detect activation of a few time points imprecisely. While this prevents it being used for investigating fast dynamics of neural activity, the genetic access it provides nevertheless provides a powerful way for manipulating neuronal activity at the circuit level.

### 1.6.3 *In vivo* two-photon calcium imaging

*In vivo* imaging records neural activity using molecular sensors which convert physiological events in the neuron into detectable optical signals. While traditional imaging techniques use small-molecule dyes which respond to membrane potential, pH or  $\text{Ca}^{2+}$  concentration changes in the cell, recent development of genetically encoded calcium indicator (GECI)

$\text{Ca}^{2+}$  sensors have surpassed the performance of small-molecule  $\text{Ca}^{2+}$  dyes in both sensitivity and responsiveness (Lütcke et al., 2013). GECIs can be expressed in cell-type specific manner, non-invasively, and most importantly, allow long-term expression for weeks to months. Given this, GECIs have largely replaced traditional dyes.

In *in vivo* calcium imaging, fluorescent calcium sensors such as gCaMP are introduced to the neural population of interest, either by viral delivery or by a transgene. To allow optical access, a cranial window is created above the brain region of interest. During imaging, the animal's head is firmly fixed on the microscope stage, and fluorescence from the sensors are directly imaged through the cranial window (Lütcke et al., 2013; Yang and Yuste, 2017).

*In vivo* calcium imaging has overcome many of the shortcomings of electrical recording. First, cell identity can be defined. The unique distribution of neurons and blood vessels in the field of view allows the same population of neurons to be imaged (if chronically expressing a GECI) for weeks to months. Second, *in vivo* calcium imaging is able to capture a large and dense set of neurons, often able to record hundreds of neurons simultaneously. Thirdly, subpopulations of neurons are easily identifiable, either through the use of specific promoters which drive the expression of GECIs in specific neural populations, or by using fluorescent markers in a separate colour channel. These advantages make *in vivo* calcium imaging ideal for studying fast dynamics of neural ensembles (Lütcke et al., 2013).

Moreover, the spatial resolution of calcium imaging is only limited by that of the microscope, which can usually reach, or with recent development of super-resolution microscopy, surpass the diffraction limit (Dudok et al., 2015). This allows researchers to track subcellular features over time. Moreover, combined with optogenetics or caged glutamate, the excitation light from the microscope can also be used to induce activity, either at cellular or subcellular level (Kantvari et al., 2010; Noguchi et al., 2011; Prakash et al., 2012). These advantage of *in vivo* imaging also make it a powerful tool for the study of dynamic subcellular processes.

One of the major disadvantages of *in vivo* two-photon calcium imaging is limitation to the region of interest. Since the brain is opaque, excitation light and emission fluorescence can

only penetrate the surface of the tissue. Even with the recent development of multi-photon imaging, where short bursts of intense laser at long wavelengths are used to stimulate fluorescent molecules, the depth of imaging is often limited to about 1 mm from the top of the brain, restricting *in vivo* calcium imaging to cortical regions in small rodents (Horton et al., 2013; Yang and Yuste, 2017). This limitation can be overcome by physically inserting a gradient-index (GRIN) lens into the region of interest, which relays an image to the surface. This allows the imaging of deep brain regions such as hippocampus, thalamus and hypothalamus without significantly affecting imaging quality (Attardo et al., 2015).

A second disadvantage of *in vivo* two-photon calcium imaging technique is the requirement of firm head fixation of the animal, which limits the behavioural paradigms available to the animal, and may induce stress. To allow complex behavioural paradigms with *in vivo* imaging, the microscope stage can be modified to include a virtual environment setup (Harvey et al., 2009). The mouse is placed on a omni-direction treadmill, which measures the speed and direction of the mouse's movement. A toroidal screen occupying the entire visual field is used to display the virtual environment and update with the mouse's movement. This system allows tasks such as spatial exploration and decision making to be performed during *in vivo* imaging (Harvey et al., 2009, 2012).

In conclusion, *in vivo* calcium imaging is well-suited for studies of the dynamic neural circuit. However, the behavioural and spatial limitations of the microscope restricts its application to cortical activity with a few behavioural paradigms, and the result may not reflect that of a naturally behaving animal. In addition, setting up *in vivo* imaging system usually requires significant effort and time of the researchers, as well as a significant financial cost to the laboratory. These restrictions limit its application in neuroscience research.

#### 1.6.4 Fluorescent endoscopy

The fluorescent endoscopy approach allows *in vivo* imaging in freely behaving animals. In fluorescent endoscopy, a thin relay GRIN lens is inserted into the brain region of interest and fixed in this position. The relay lens forms an image of the targeted cells at the surface

of the brain. This image is then transferred away from the animal, while allowing the animal to behave freely. Two approaches are available to achieve the goal of recording at a cellular level. The advantages and disadvantages of each of approach are discussed below.

### Fiber bundle based fluorescence endoscopes

In the fiber bundle based fluorescence endoscopy, the GRIN lens is attached to an optic fiber bundle. The flexibility of the fiber bundle allows an animal to behave freely, while traditional fluorescence microscopy techniques can be used to capture the image of cells at the end of the fiber bundle (Flusberg et al., 2008).

The fiber bundle approach has several advantages. First, since it can be coupled with traditional microscopy techniques, strong stimulation light can be applied, and faint fluorescent signals can be detected. It is also easy to combine optogenetics with the fiber bundle approach. With an arbitrary-patterned illuminator, individual cells in the field of view can be selected and stimulated, at the same time as calcium imaging. This advantage allows traditional electrophysiology to be performed in freely-behaving animals, which can be very powerful for the observation and control of local neural circuits (Szabo et al., 2014).

The main disadvantages of the fiber bundle based approach are resolution and field-of-view. Currently single fibers in the fiber bundle can only be as small as  $4\text{ }\mu\text{m}$  in diameter, which is barely enough to resolve individual cells. As a result, multiple overlapping cells may be detected as a single cell, and strong fluorescence in neuronal processes can also be falsely detected as cellular signal. The field of view is determined by the diameter of the fiber bundle. However, thicker fiber bundles are also significantly more rigid, potentially limiting the behaviour of the animal (Yang and Yuste, 2017).

### Miniature integrated fluorescence endoscopes

A second approach to *in vivo* calcium imaging involves integrating all components of the fluorescent microscope, including light source, filters and sensors, on the animal's head, and only transmitting the image in electrical signals. Earlier attempts focused on minia-

ture two-photon microscopes with an external pulse laser source (Flusberg et al., 2005; Piyawattanametha et al., 2009). While these mini-microscopes were able to produce optical slices in freely behaving rats (Sawinski et al., 2009), their complexity in engineering and slow frame rates prevented their popularity in neuroscience laboratories (Hamel et al., 2015; Yang and Yuste, 2017).

Later development of miniature endoscopes used camera-based single-photon imaging, with an integrated high-intensity light-emitting diode (LED) as a light source (Ghosh et al., 2011). Single photon imaging provides a larger field of view (FOV) and faster frame rates than the two-photon approach. Even though it cannot provide optical slices, recent developments in calcium indicators make indicators that are sufficiently bright to provide a satisfying signal-to-noise ratio (SNR). The original development from Ghosh et al. (2011) was able to record calcium transients from hundreds of neurons in CA1 at more than 20 frames per second. A later paper demonstrated how this technique could be used to record brain activity in sensory, cognitive and motor tasks (Ziv et al., 2013).

The integrated single-photon endoscopes developed by Ghosh et al. (2011) is primarily designed to record the green fluorescence from gCaMP calcium indicators. It is therefore unable to detect a second image channel, which can be useful for distinguishing neural subpopulations. In addition, the design described by Ghosh et al. (2011) is still not accessible to the majority of neuroscience laboratories which have little expertise in microfabrication, optics and electronic engineering. I attempt to address these two limitations in Section 2 in this thesis.

### 1.6.5 Conclusion

In conclusion, the ideal tool for examining neural circuits needs to have high spatial resolution, a large field of view, good temporal resolution, and offers minimal disturbance to animal's natural behaviour. Table 1.1 provides a summary of the advantages and disadvantages of the technologies discussed in this section. The choice of technology to investigate neuronal activity depends on a trade-off between advantages and disadvantages. It can

be predicted that in the foreseeable future, studies of neural circuit mechanisms will continue to take a hybrid approach, where multiple techniques will be combined for the best performance.

	<i>In vivo</i> electro- physiological recording	IEG detection	<i>In vivo</i> two-photon imaging	Miniature microscopes
<b>Number of cells</b>	tens to hundreds	unlimited	hundreds	hundreds
<b>Distinguishing subpopulations</b>	possible with optogenetics	easy	easy	possible
<b>Temporal resolution</b>	<1 ms	minutes to hours	10–100 ms	10–100 ms
<b>Recording stability</b>	days	single time point	months	months
<b>Brain region</b>	unlimited	unlimited	surface	unlimited
<b>Behaviour compatibility</b>	unlimited	at most 2 events	head-fixed	unlimited

**Table 1.1** Comparison of techniques for studying neural activity at cellular level.

## 1.7 Hypothesis and research aims

The cognitive impairments seen in AD suggest that normal neural circuitry functions are compromised. The abnormal function of neural circuitry is potentially mediated by, and in turn aggravates, the underlying molecular and cellular pathophysiology of AD. The failure of current interventions targeting the removal of A $\beta$  suggests that the cognitive impairment in AD is a consequence of complex pathophysiology (Canter et al., 2016). Understanding the neural circuitry mechanisms that directly contribute to the cognitive symptoms in AD may yield novel treatment targets for preventing memory loss in AD.

In this thesis, I examined the hippocampal circuitry deficits that underlie memory loss

in AD. I focused on a mouse model of early AD, TgCRND8. TgCRND8 mice carry a double mutated human APP gene. A $\beta$  plaques are first observed at the age of 9–11 week, together with neurite dystrophy (Chishti et al., 2001). At this age, these mice display significant memory deficits in hippocampal-related memory tasks such as Morris watermaze and contextual fear conditioning (Hyde et al., 2005; Yiu et al., 2011). These cellular and cognitive symptoms parallel the early development of AD in human patients.

Early computational models of AD have suggested that while synaptic loss in AD creates memory deficits, enhancing the strength of the remaining synapses can compensate for this deficit (Horn et al., 1993). Considering that aberrant synaptic AMPA trafficking is a cardinal signal of synaptic degeneration in AD, I decided to use the well-characterized interference peptide TAT-GluA2<sub>3Y</sub> to rescue synaptic deficits, and investigate whether this rescue improves neural circuit functions and ultimately memory performance of TgCRND8 mice. TAT-GluA2<sub>3Y</sub> is a membrane permeable peptide which selectively inhibits activity-dependent AMPAR endocytosis (Ahmadian et al., 2004), and blocks AD-related CA1 LTD (Dong et al., 2015). Chronically infusing TAT-GluA2<sub>3Y</sub> in a mouse model of AD also prevents memory degradation (Dong et al., 2015). However, how hippocampal circuit function is affected by TAT-GluA2<sub>3Y</sub>-mediated synaptic strengthening is still unknown.

To investigate circuitry deficit in TgCRND8 mice, the first aim of this thesis is to design and assemble an integrated miniature microscope for imaging calcium transients in freely behaving mice. This approach allows us to record neural activity from hundreds of neurons at the cellular level while mice perform memory tasks. Compared to the original Ghosh et al. (2011) publication, I intended to create a version of miniature microscope which is readily available and can be easily produced in laboratories with little engineering expertise. At the same time, I attempt to add a separate colour channel, which potentially allows the identification of neural subpopulations using a separate fluorophore.

The second aim of this thesis is to use this tool to investigate the circuitry mechanisms of TgCRND8 mice in contextual fear conditioning, which is a memory task dependent on hippocampal function. My hypotheses are threefold. First, given that a hyperactive hip-

pocampus has been consistently found across mouse models of AD and human patients, I hypothesized that CA1 neurons in TgCRND8 mice would similarly display hyperactivity. Secondly, I hypothesized these transgenic (Tg) mice would show a deficit in memory encoding efficiency of hippocampal neurons. Previously it has been found in a taupathy mouse model, which is related to AD, hippocampal place cells are less efficient in encoding space (Cheng and Ji, 2013; Ciupek et al., 2015). Therefore, I hypothesized that CA1 hippocampal neurons in TgCRND8 mice are similarly affected in encoding a fear memory. Thirdly, I hypothesized that the pattern completion process, which is important for memory recall, is compromised in these mice. In addition, I also investigated whether TAT-GluA2<sub>3Y</sub> treatment affects the above mentioned circuit function. I hypothesized that TAT-GluA2<sub>3Y</sub> treatment would be able to rescue the circuit deficits in TgCRND8 mice, and as a consequence, also able to rescue behavioural deficit.

Through this study, I hope to highlight neural circuit deficits in AD, which is an under-studied area when compared with the cellular pathophysiology and behavioural symptoms of AD. I hope that this study, as well as future studies in this area, is able to create a necessary link between cellular pathology and the cognitive symptoms of AD, and make the tools for studying circuitry mechanisms more accessible to the neuroscience community. A better understanding of the circuitry deficits in AD will provide inspiration for novel AD treatment in the future.



# 2

## CONSTRUCTION OF A MINIATURE EPI-FLUORESCENCE MICROSCOPE

---

### 2.1 Introduction

One of the major technological limitations in neuroscience research is recording neural activity in model animals. Traditional techniques such multi-unit recordings give excellent temporal resolution, however the spatial resolution — as measured by the number of cells simultaneously recorded — is limited. Moreover, it is very hard to distinguish cell subpopulations within the same region from the recording. Neural activity can also be inferred by *post mortem* staining of neural activity markers, such as cFos or arc. This method gives excellent spatial resolution, however the temporal resolution is very poor, where the time window of neural activity lasts from minutes to hours.

Live calcium imaging combines the best of both methods. By labelling cells of interest with a calcium indicator, neural activity can be recorded with millisecond resolution. Hundreds of cells can be simultaneously recorded, and specific subpopulations can be distinguished by fluorescence in different colour channels. However, traditional live calcium imaging requires the animals' head to be firmly fixed under a microscope stage. This requirement is incompatible with most well established behaviour assays, and at the same

time introduces significant stress on the animal, potentially confounding behavioural results. Moreover, due to light scattering in opaque brain tissue, most of the studies have focused only on cortical areas, while techniques to image deep brain tissue on a standard two-photon microscope are still under development, and not widely adopted (Barreto and Schnitzer, 2012).

*In vivo* calcium imaging in behaving animals was first demonstrated by Mark Schnitzer's group at Stanford (Ghosh et al., 2011). The authors constructed a miniature epifluorescence microscope, and chronically implanted it in the brain to image fluorescence from region of interest. In a follow-up paper (Ziv et al., 2013), the authors demonstrated that their miniature microscope could image GCaMP3 calcium signals from hippocampal CA1 place cells for more than a month. However, there are several limitations to their design: first their design incorporates an objective lens 1 mm in diameter, which is impractical to reach deep brain tissue; second, their mini-microscope was only able to identify GCaMP signals, and therefore unable to distinguish different cell types within the population (Ghosh et al., 2011; Ziv et al., 2013).

In the current project, I tackled the above mentioned limitations by building a head-mounted miniature microscope which is able to image calcium signals in deep brain structures, and is also capable of imaging a separate fluorescence colour channel in order to distinguish different cell types. Moreover, I created an simple open design which requires little engineering experience to assemble, so it can be assembled and used cost-efficiently in most neuroscience laboratories.

## **2.2 Material and methods**

### **2.2.1 General design of the mini-microscope**

The mini-microscope follows the same design principle as an general single-photon epi-fluorescence microscope, except for size constraints. Excitation light is emitted from a high-intensity LED light source, filtered, and reflected by a dichroic mirror to illuminate

the sample. The fluorescent emission light from the sample is collected by the objective, passes through the dichroic mirror, and is filtered and focused on the camera. To fit the necessary size constraints, we chose a high-intensity LED as the light source, a GRIN lens as an objective, and a miniaturized complimentary metal-oxide-semiconductor (CMOS) camera to capture the image (Figure 2.2a).

The optical design of the microscope was accomplished using Zemax software (Zemax Development Corporation) to optimize the lens and filter configuration. The casing of the microscope was modelled using OpenSCAD software.

### Lens configuration

The lens configuration consists of a GRIN objective lens and a ocular barrel lens forming a “4F system”, where the distance between the thin-lens equivalent of the two lenses equals to the sum of the focal length. Potential lenses for emission light path were selected from modelling and calculation to give a working distance of 100 µm in water, a magnification of 6x and a back focal length of 6 cm. During prototyping, the lenses were purchased and installed into custom-made mounts on a two-arm stereotaxic frame. The distance between the lenses was then optimized against a fibre bundle light source close to the GRIN lens. A drum lens was used to collect light from the LED. The drum lens was tested in a similar manner and selected to produce diverging light after the GRIN lens. We chose to use an achromatic doublet as the barrel lens ( $F=15\text{ mm}$ , Edmund Optics). and a 1.8 mm diameter 0.25-pitch GRIN lens (64–537, Edmund Optics) as objective for hippocampus imaging. To minimize brain damage for deep brain imaging, the objective lens was a home-assembled doublet of a 0.5 mm diameter, 1-pitch GRIN relay lens (ILW-050-P050, GoFoton) and a 2 mm diameter 0.25-pitch GRIN lens (ILW-200-P025, GoFoton). The details of doublet assembly are described in section 2.2.1.

**Filter selection**

Filters were selected to cover the excitation and emission spectra of the genetically encoded calcium sensor GCaMP6f (Chen et al., 2013) and further screened for high bandwidth and low overlap. To fit the size constraints, the excitation and emission filters had dimensions of 4 mm × 4 mm × 1 mm, and the dichroic mirror was 5.6 mm × 4 mm × 1 mm. We chose to use a fluorescein isothiocyanate (FITC) filter set for gCaMP6 imaging (49002, Chroma). For dual colour imaging, we took advantage of broad excitation spectrum of the red retrobeads, and used the same blue light to excite the red fluorophore. In these experiments, a TRITC/FITC with single band exciter filter set was used (59204, Chroma).

**Electronics**

The image sensor was selected to have a package size of less than 1.5 cm × 1.5 cm. We used a commercially available analogue camera module (HD1313BW, Ruishibao) that gave satisfactory sensitivity and dynamic range. The camera board was connected to a 5 V power regulator. After the power regulator, the wires were connected through a slip ring (SRC012-C, Adafruit) to avoid tangling of the wires during animal behaviour. After the slip ring, the wires are connected to a 12 V direct current (DC) power source and a universal serial bus (USB) analogue video capture card (Capit, Mygica). The video capture card was controlled by custom software for synchronized video capture. Alternatively, a board-level miniature integrated digital camera (MU9PM-MBRD, XIMEA) could also be used. While the XIMEA camera adds significant cost to the miniature microscope, it allows custom control of camera parameters such as pixel binning, gain and exposure. The XIMEA camera also outputs in 12-bit per pixel, and gives a better overall SNR.

A monochrome, high-intensity blue LED (LXML-PB01-0023, Lumiled) was used as the light source. The wires providing power to the LED joined the video camera wires through the slip ring, and were then connected to a variable DC power source. During recording, the LED was driven at a current between 20 mA and 50 mA.

### Casing and assembly

The microscope casing was printed in black resin (GPBK02, Formlabs) using a Form 2 3D printer (Formlabs, Sommerville MA). This material renders a black, rigid and opaque casing with a feature resolution of 25 µm. The microscope body was screwed onto the camera holder via a printed M8 thread to allow easy change of the focal plane. A side-mounted M2×2 mm nylon set screw was used to lock the camera holder on the microscope body and fix the focus of the mini-microscope.

We used parts from a 2.5 mm phone jack for the connection between the microscope body and baseplate. The phone jack is widely available, and the low-profile fine thread interface allows easy and firm connection of the mini-microscope body to the baseplate. The threaded tube was sawed off from the phone jack and glued to the bottom the mini-microscope body, and the corresponding nut was glued to the 3D-printed baseplate. The objective GRIN lens was inserted vertically into the center of the baseplate, and fixed with optical adhesive (NOA61, Norland). The drum lens and filters were snugly fitted into corresponding slots in the filter box, and the LED was fixed onto the filter box with two-part epoxy adhesive.

### Objective lens assembly for deep brain imaging

For deep brain imaging, a 0.5 mm diameter, 1.0-pitch relay lens was connected to the center of a 2 mm diameter, 0.25-pitch GRIN lens using optical adhesive (NOA61, Norland). The setup was modified from Kim et al. (2012) to ensure concentricity and alignment. In the setup (Figure 2.1, a micro V-clamp (VK250, ThorLab) was used to hold the large GRIN lens in place vertically, and the thin relay lens was mounted on another V-groove clamp attached to a 3-axis manipulator (E.g., DT12XYZ, ThorLabs). The two micro V-clamps were leveled using a bull's eye spirit level. A lens and camera chip were mounted under the large GRIN lens, and were used to capture and display the image of the large GRIN lens on a monitor for monitoring the relative horizontal position of the two lenses. A dissection microscope was mounted horizontally for monitoring the vertical position of the two lenses.

During assembly, both lenses were mounted in the V-clamps respectively. A small drop of ultraviolet (UV) curing optical adhesive (NOA61, Norland) was added to the bottom surface of the relay lens using a 27-gauge needle. The relay lens was then lowered to just above the large GRIN lens, when an image of the relay lens became visible on the monitor. The relay lens was then moved to the center of the large GRIN lens according to the monitor display. Observed through the dissecting microscope, the relay lens was then lowered to touch the upper surface of the large GRIN lens. A 375 nm spot UV light source (Spotty-B, Fusionet) was used to cure the optical adhesive. The curing time is calculated to give at least  $3 \text{ J mm}^{-2}$  of UV light on the optical adhesive.

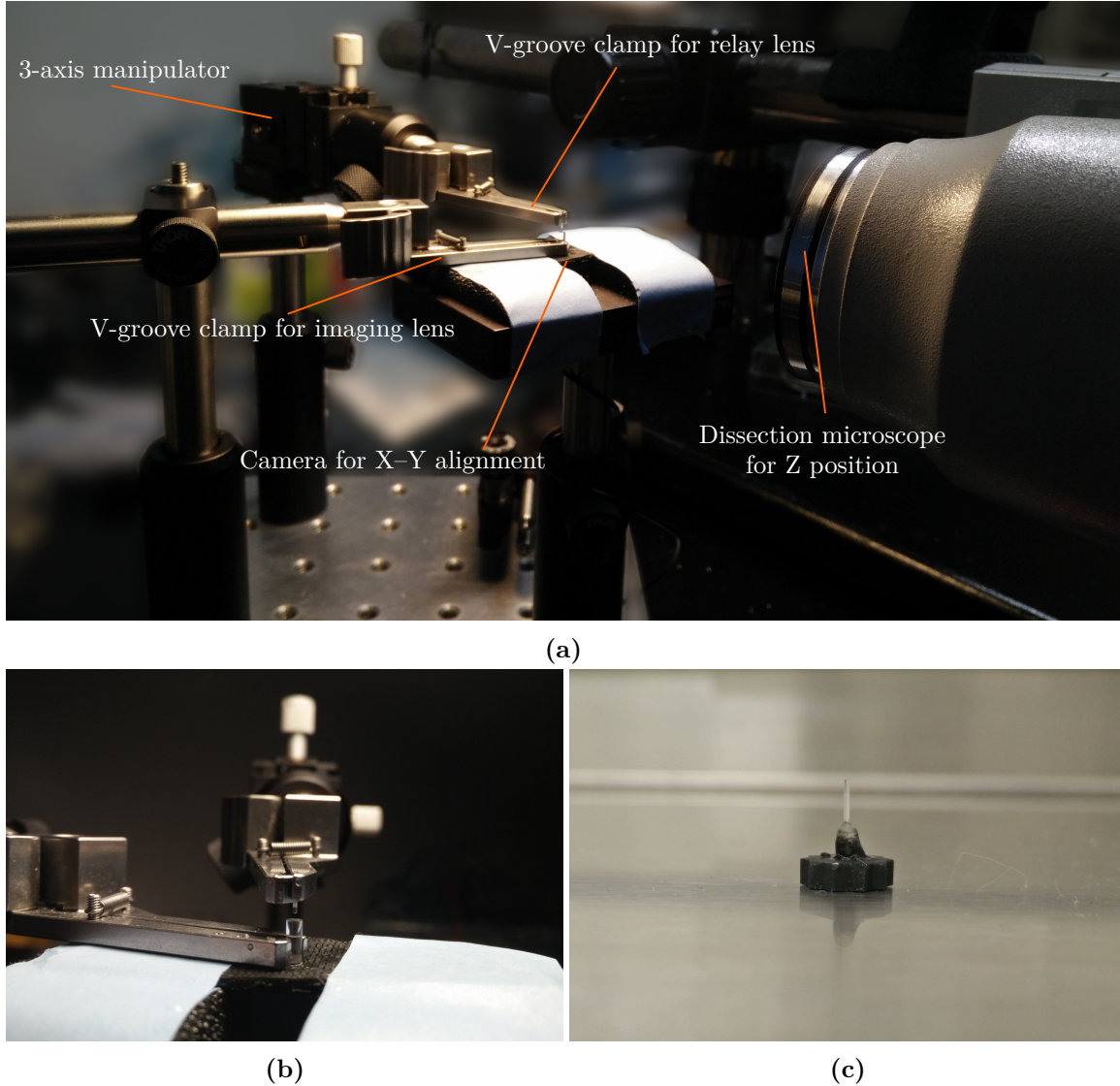


**Figure 2.1** Assembly of deep brain imaging lenses. The lenses were held by two leveled V-groove clamps. A camera was installed at the base of the large GRIN lens to monitor X–Y alignment of the two lenses. Translation of the top V-groove clamp was controlled by a 3-axis manipulator. A drop of optical adhesive was placed at the bottom of the thin lens. The thin lens was then moved downwards until two lenses touch. The optical adhesive was cured by illumination of a spot UV light source. (a) Set up for the doublet assembly. (b) Close up of the lenses in X–Y alignment. (c) Doublet assembled in a mini-microscope baseplate.

### **2.2.2 Viral infusion**

Each mouse received intraperitoneal (i.p.) injection of atropine ( $0.1\text{ mg kg}^{-1}$ ) and chloro-hydrate ( $400\text{ mg kg}^{-1}$ ) before being secured on a stereotaxic frame. An incision was made on the scalp and the skin was pulled to the side to reveal the skull. Holes were drilled above the brain region of interest on the skull for micropipette injection.  $1.0\text{ }\mu\text{l}$  AAV-syn-GCaMP6 virus was loaded into a glass micropipette and gradually lowered to target coordinate (CA1: anteroposterior (A/P)  $-1.8\text{ mm}$ , mediolateral (M/L)  $1.5\text{ mm}$ , dorsoventral (D/V)  $-1.5\text{ mm}$  from Bregma; lateral amygdala (LA): A/P  $-1.4\text{ mm}$ , M/L  $3.5\text{ mm}$ , D/V  $5.0\text{ mm}$  from Bregma), and injected at a rate of  $0.12\text{ }\mu\text{l/min}$ . The micropipette was left in the brain for an extra  $10\text{ min}$  before slowly retracted. The incision was sutured and treated with antibiotics. Each mouse then received subcutaneous injection of analgesic (ketoprofen,  $5\text{ mg kg}^{-1}$ ) before returned to a partially heated clean cage for recovery.

### **2.2.3 Implantation of the mini-microscope**

Mice with viral expression of gCaMP6 were anesthetized and head-fixed in a stereotaxic frame as described in Section 2.2.2. Three screws were placed around the viral injection site for anchoring of the microscope. For implantation targeting CA1, a circular craniology of  $2\text{ mm}$  was performed above the viral injection site. The dura was pierced and lifted with fine tweezers to expose the brain. The brain was then continually irrigated with artificial cerebral-spinal fluid to remove the blood. A 27-gauge aspiration needle was used to remove cortex and expose CA1. For implantation targeting LA, after anchoring the screws, a 27-gauge needle was lowered to the target coordinate, left for  $5\text{ min}$ , and slowly retracted to create a canal for the thin lens to implant.

The mini-microscope was then fixed on the stereotaxic frame and gradually lowered to  $0.2\text{ mm}$  above the target coordinates (CA1: A/P  $-1.8\text{ mm}$ , M/L  $1.5\text{ mm}$ , D/V  $-1.3\text{ mm}$  from Bregma; LA: A/P  $-1.4\text{ mm}$ , M/L  $3.4\text{ mm}$ , D/V  $-4.8\text{ mm}$  from Bregma). Opaque black dental acrylic was applied to secure the microscope baseplate to the skull. Once

the dental acrylic was cured, the microscope body was detached from the baseplate and replaced with a cap. Mice were given  $5 \text{ mg kg}^{-1}$  ketoprofen for analgesia before returned to a clean cage for recovery.

#### 2.2.4 *In vivo* mini-microscope testing

After lens implantation, the mice were kept in the home cage for at least two weeks before the first image session. This time allows the optical window to clear. Following this recovery, the mice were handled and the cap was removed and replaced with the microscope body. A typical imaging session lasted for at least 5 min. After the imaging session, the microscope body was removed, the mice were recapped and returned to their home cage.

#### 2.2.5 Image analysis

##### Extracting cells from calcium imaging videos

Before processing, the raw videos were corrected for uneven illumination by applying a high-pass Gaussian filter ( $20 \mu\text{m} \times 20 \mu\text{m}$  kernel) to each frame. To reduce computation time, the videos were down-sampled to 5 fps for processing. Individual cell calcium signals were extracted from the video similarly to previously described (Mukamel et al., 2009). First, the illumination-corrected down-sampled video was regarded as a matrix of pixels by time, and principle component analysis (PCA) was applied to reduce the temporal dimension to 300–500 components. The principal components were then regarded as mixtures of individual cells, and separated by independent component analysis (ICA). ICA components with a single mode and 90% peak width of less than  $30 \mu\text{m}$  were classified as cells. The time-course of cell components were calculated by multiplying the inverse of ICA component matrix with the corresponding illumination-corrected raw video.

All calcium activity traces were normalized to have zero median and unit noise standard deviation. The noise standard deviation was estimated from median absolute deviation of the trace. The signal to noise ratio (SNR) was calculated as the ratio of maximum signal

intensity and noise standard deviation. Only traces with more than 10 SNR and animals with more than 20 cells were included in the analysis. The average activity of a cell was calculated by the area under the calcium trace above 3 standard deviation of the noise divided by duration.

### **Mapping cells across session**

Cells were extracted from the recordings for both the training and test session respectively. The position of each cell was calculated as the center of mass of pixels above the 90 percentile intensity in the extracted ICA components. The position of cells for each recording were approximately aligned to have overlapping centers of mass, then rotated to have overlapping principle component vectors. The two point clouds were then precisely aligned using a manual approximation and finally the trimmed iterative closest point algorithm (TrICP) (Chetverikov et al., 2002). TrICP is robust against outliers, which allows accurate alignment even when cells were observed in one session but were missing in another. TrICP was performed using a 40 % outlier ratio, optimizing both translation and rotation. After alignment, cells that shifted less than  $2\text{ }\mu\text{m}$  from one session to another were marked as the same cell.

## **2.3 Results**

### **2.3.1 Capability and *in vitro* testing of the mini-microscope**

The mini-microscope provides an easy and inexpensive tool for neuroscience laboratories to measure calcium activity in freely behaving animals. Our completely assembled mini-microscope costs less than \$ 1000, weighs less than 3g, and can be bounded in a  $25\text{ mm} \times 16\text{ mm} \times 11\text{ mm}$  box (Figure 2.2b). Adult mice with the mini-microscope attached are able to rear, groom, and freely explore environment with no noticeable change from their natural behaviour.

The theoretical optical resolution of the mini-microscope is  $1\text{ }\mu\text{m}$ . To measure the reso-

lution empirically, we tested the mini-microscope against United States Air Force (USAF) resolution target (38-257, Edmund Optics). As shown in Figure 2.3a, the thinnest lines (group 7 element 6, 2.07  $\mu\text{m}$  width) are clearly distinguishable. This suggests that the empirical resolution of the microscope is smaller than 2  $\mu\text{m}$ . With this resolution, the mini-microscope is able to resolve cell bodies and capillary blood vessels.

We first tested the mini-microscope in a perfused brain. We virally expressed green fluorescence protein (GFP) in the LA of a mice using herpes simplex virus (HSV), and perfused and harvested the brain 3 days later when the GFP expression had peaked. The brain was sliced coronally on a vibratome until fluorescence was detectable on the cutting surface. The trunk of the brain was then imaged under the mini-microscope. As seen in Figure 2.3b, the GFP cell bodies and the apical dendrites could be resolved from the mini-microscope image. This result confirms that the fluorescence under LED illumination can be reliably detected by the CMOS camera.

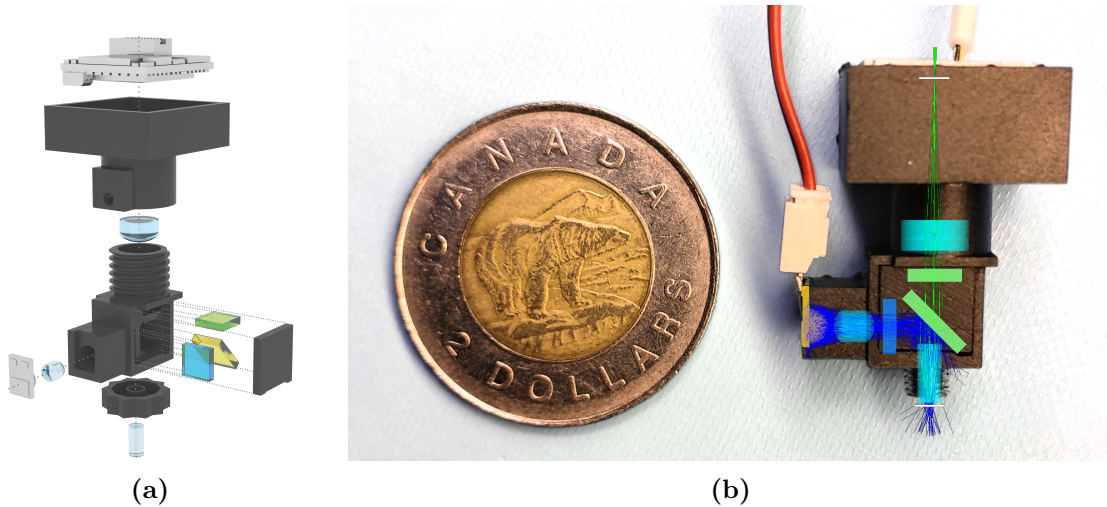


**Figure 2.2** (a) Schematic of the miniature microscope. Excitation light is emitted from a high-intensity blue LED, filtered and reflected to the sample by a dichroic mirror. GCaMP6 emission are collected by the gradient-index (GRIN) lens, filtered and focused onto a CMOS camera chip, where the images are sent to a computer and recorded. (b) Assembled mini-microscope with optic path overlay. The complete mini-microscope weights less than 3 g and can be bounded in a 25 mm  $\times$  16 mm  $\times$  11 mm box.

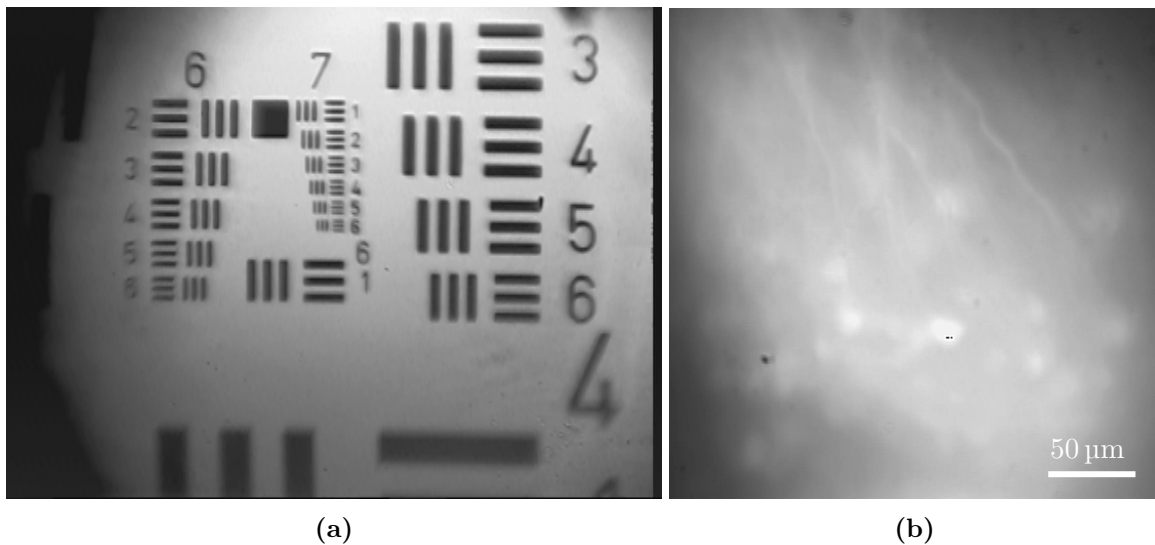


**Figure 2.3** Resolution test for the mini-microscope. The mini-microscope has a resolution of less than 2 μm, and can resolve cell bodies and apical dendrites in the perfused brain sample. (a) USAF resolution test target. (b) GFP-expressing cells in perfused brain.

### 2.3.2 Measuring blood flow with mini-microscope

To test the *in vivo* imaging capabilities of the microscope, we first implanted the mini-microscope above the cortex, and injected 150 μl of fluorescein-dextran (molecular weight 150 kDa; FD150, Sigma) in the mouse tail vein. Fluorescein-dextran fills the blood vessels, and fluoresces with similar excitation and emission wavelengths to GCaMP. As expected, after fluorescein-dextran injection, the blood vessels were clearly visible when the microscope is implanted (Figure 2.4). The resolution of the mini-microscope allows identification of individual erythrocytes in the capillaries, and therefore the erythrocyte flow rate can be calculated and shown in Figure 2.4b. This measurement allows using the mini-microscope to study haemodynamic responses in the capillaries in freely behaving mice.

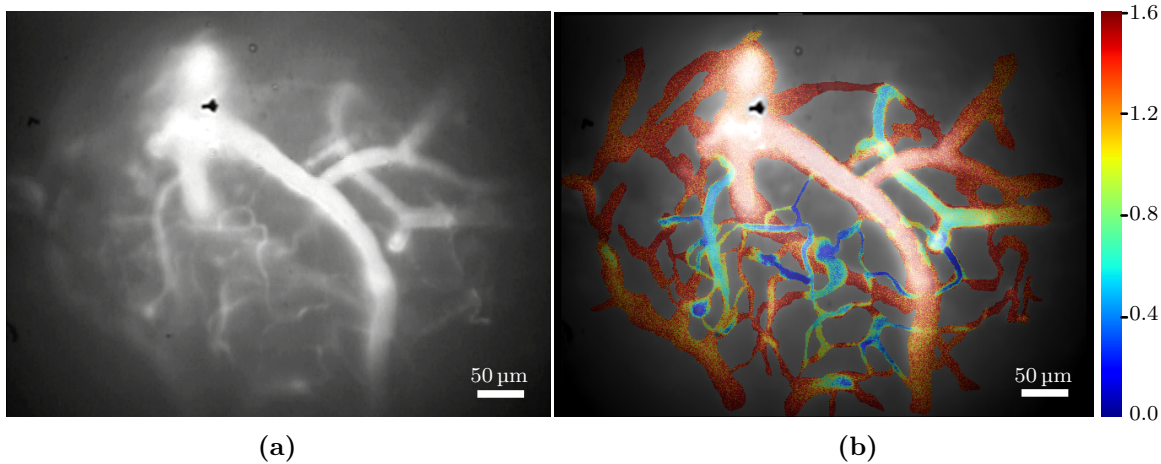


**Figure 2.4** *In vivo* image of blood vessel. The mouse received 10 mg kg<sup>-1</sup> fluorescein-dextran in tail vein. The mini-microscope was placed at cortex when the mouse was under anaesthesia. (a) Mean fluorescent image of blood vessels under mini-microscope. (b) Heatmap of erythrocyte flow speed overlaid on the mean fluorescent image. Erythrocyte flow speed is measured in mm s<sup>-1</sup>.

### 2.3.3 Recording calcium transients in CA1

To test GCaMP6s expression *in vivo*, we infused adeno-associated virus (AAV) expressing GCaMP6s into CA1 hippocampus and implanted the mini-microscope above the injection site. During the behavioural session, the mouse was placed in a novel environment to explore for 5 min, during which GCaMP6 fluorescence was recorded by the mini-microscope. The maximum projection of the GCaMP6 fluorescence in a 5-minute session is shown in Figure 2.5. We were able to extract 200 cells and their corresponding Ca<sup>2+</sup> transients from the recording (Figure 2.6, 2.7).

The positions of the mouse was traced out in the behaviour video. The time-course of the identified cells was mapped back onto the behaviour of the mouse. Figure 2.8 shows Ca<sup>2+</sup> activity of potential place cells as they responded to specific locations in the environment the mouse was in.

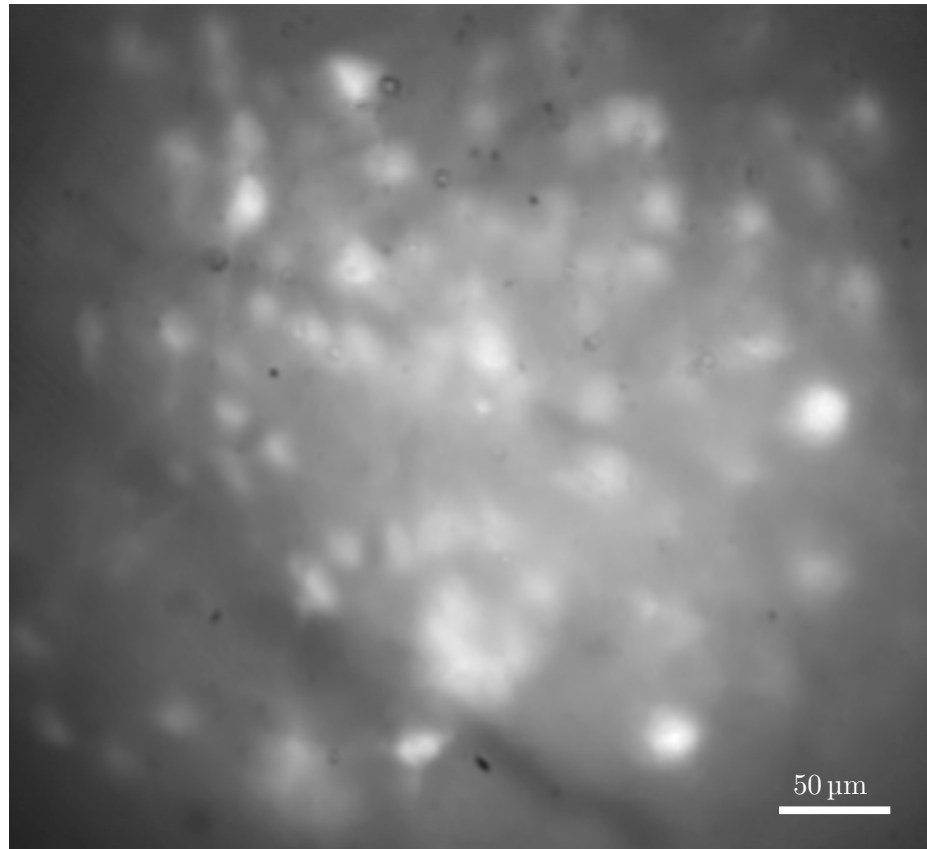


**Figure 2.5** Cells in CA1 captured by the mini-microscope in a freely behaving mouse. Two weeks after AAV infusion and microscope implantation, the animal was allowed to freely explore a novel environment. The picture is a maximum projection of all frames captured in a 5-minute session.

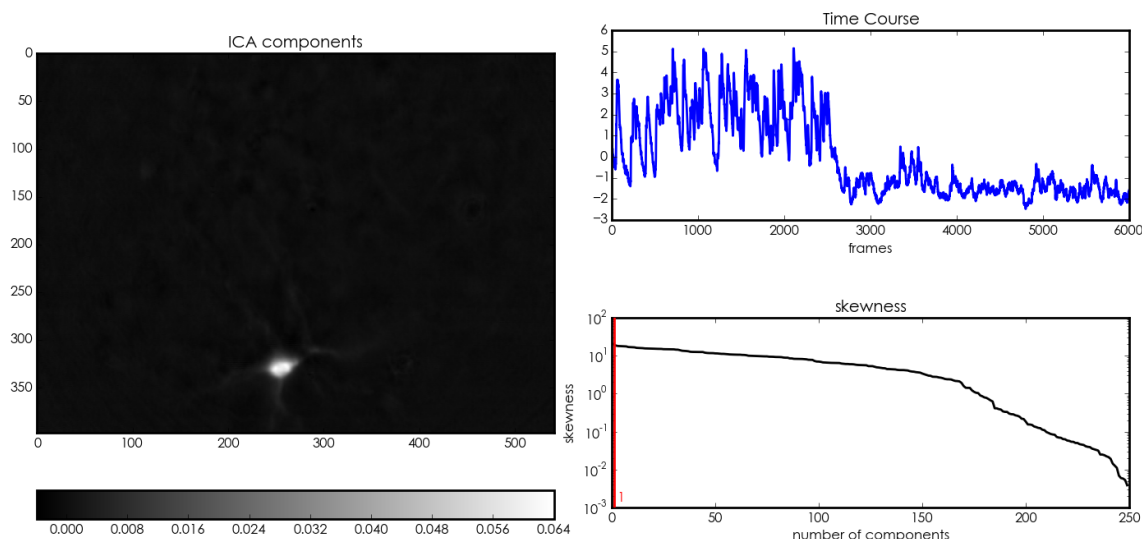


**Figure 2.6** Example of an independent component of the video after analysis, showing both the extracted spatial location of the cell (left) and the un-normalized activity (top right).

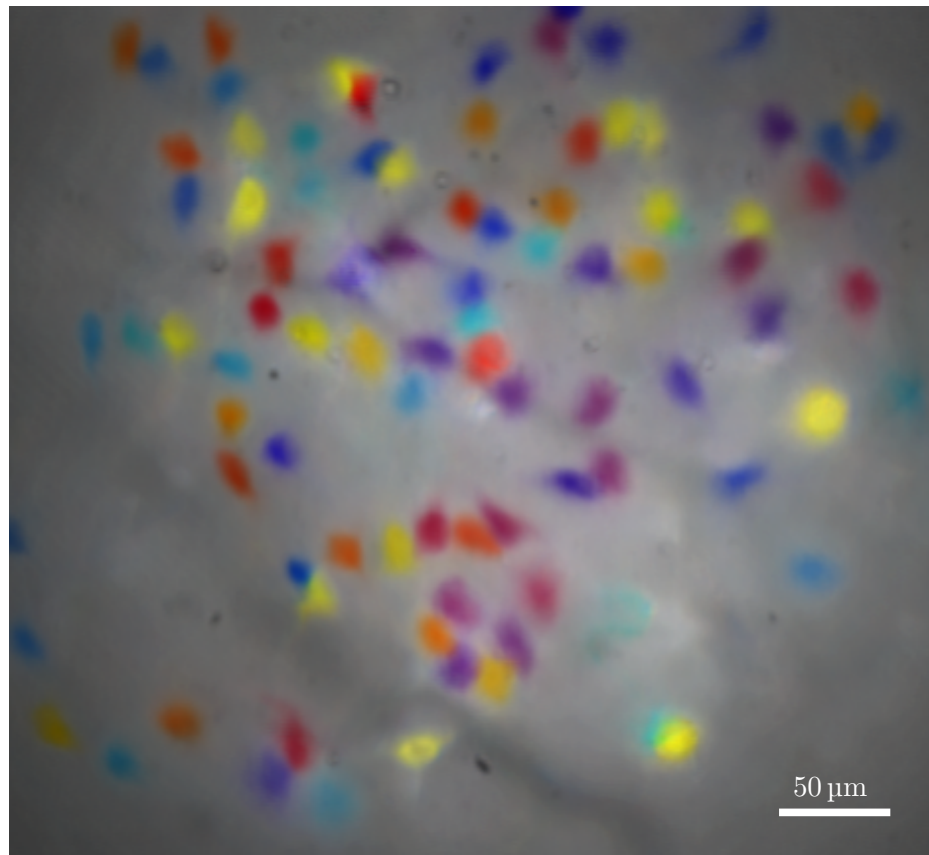


**Figure 2.7** More than 100 cells are identified in a single imaging session. The identified cells are randomly coloured.

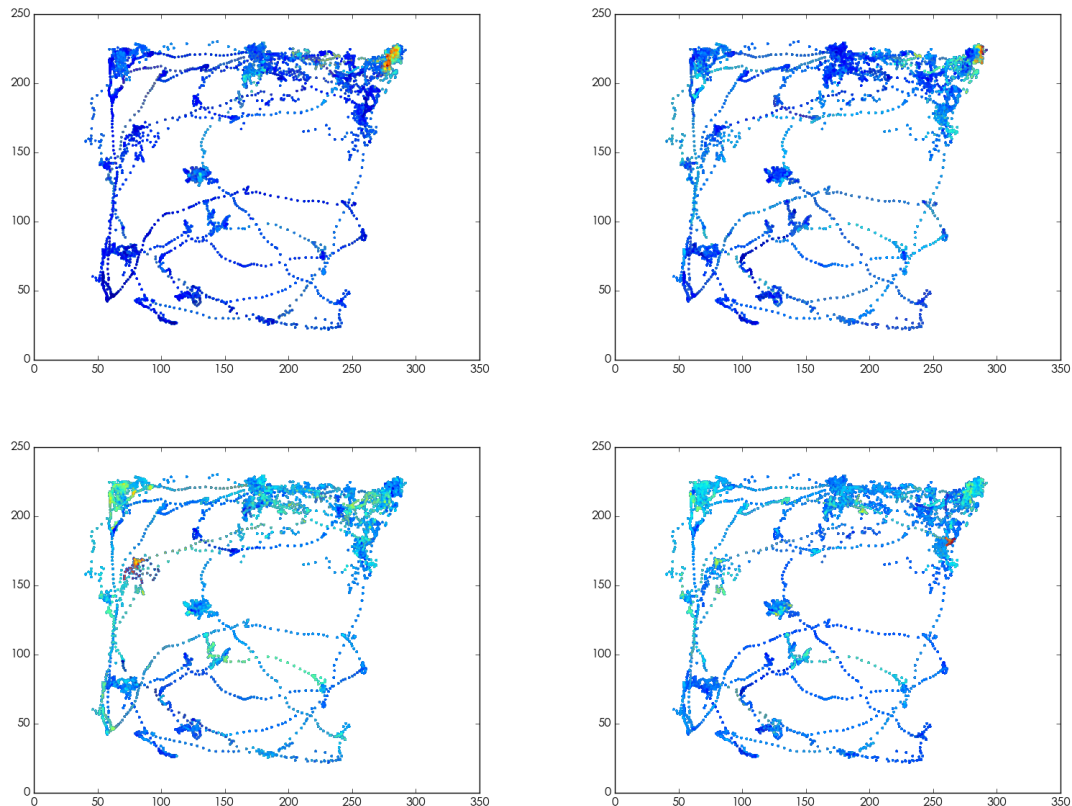


**Figure 2.8** Activity of 4 sample cells plotted against location of the mouse. The colour represents the  $\text{Ca}^{2+}$  activity. The cellular activity is specific to the mouse's location in the environment.

### 2.3.4 Video preprocessing

#### Illumination correction

The size of the mini-microscope limits its illumination pathway, and as a result the illumination in the FOV is uneven. Uneven illumination not only affects the calcium signal and cell detection, but also adds difficulty to the motion correction step, since the uneven illumination pattern appears stable even when there is relative movement between the mini-microscope and the target. To correct this, a 2D Gaussian filter with large window ( $20\text{ }\mu\text{m} \times 20\text{ }\mu\text{m}$ ) was convolved with each frame to extract the lower frequency components of the image as the illumination pattern. The illumination pattern was then subtracted from the frame. Figure 2.9 shows the maximum projection of an *in vivo* video recording of CA1 cells expressing gCaMP6f before and after illumination correction. Cells under intense illumination in the center can be clearly visualized after illumination correction.

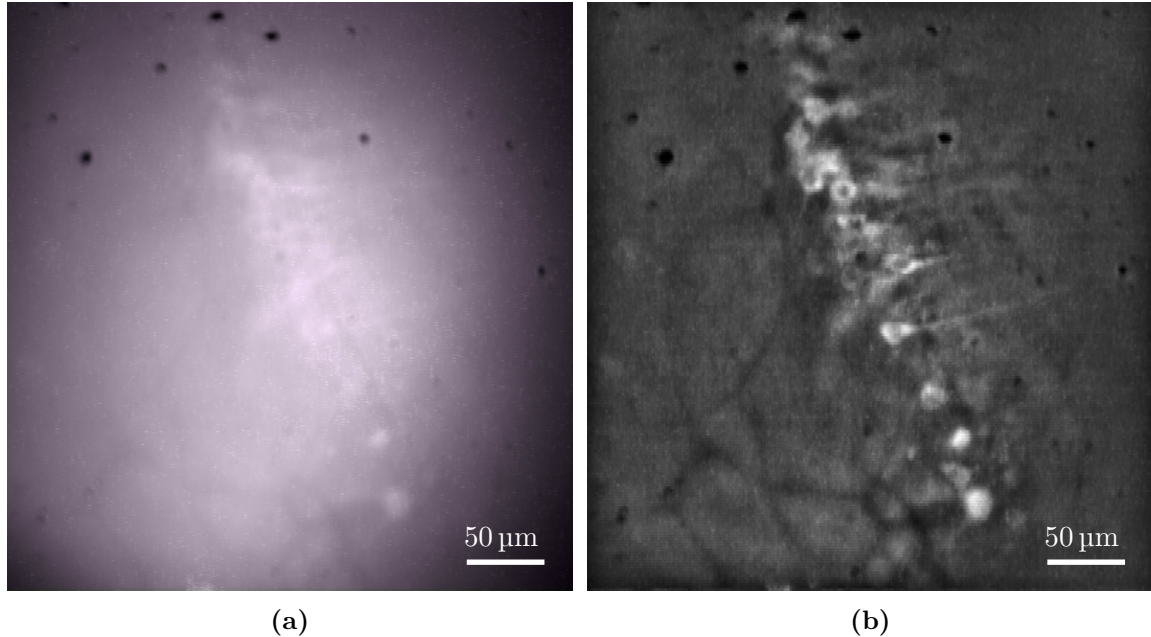


**Figure 2.9** Illumination correction allows better detection of cells. This is a maximum projection of a video taken by the mini-microscope, before (a) and after (b) illumination correction. Cells in the center of the FOV are clearly visible after illumination correction.

### Motion correction

After illumination correction, the video was then de-dusted and corrected for motion. Occasional dust speckles on the camera appear as stationary small dark objects in the video, and interfere with motion detection. To remove the dust speckles, pixels two standard deviation darker than mean intensity were labelled for each frame. The labelled pixels were morphologically eroded and dilated to remove labelling noise, and then inpainted using Navier-Stokes based methods (Bertalmio et al., 2001).

As camera motion is almost entirely translational, after dust removal we used phase correlation algorithm to achieve motion correction at sub-pixel level (Guizar-Sicairos et al., 2008). The reference frame was initialized to be the first frame. A moving average of 25 registered frames was generated, and the reference frame was updated by maximum projection of the moving average frame to the reference frame. To test the efficacy of the motion correction algorithm, we generated a recording with significant motion artifacts by losing the connection of the mini-microscope to the baseplate during recording. As can be seen from the maximum projection of the original recording and stabilized recording (Figure 2.10), we are able to obtain a stable image of cells significant motion artifacts in the original video.

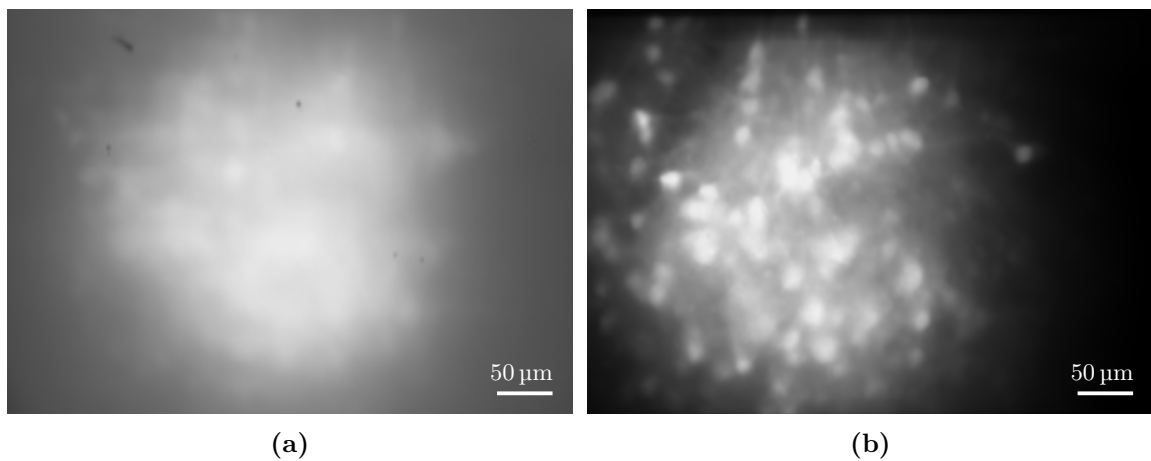


**Figure 2.10** Average video frame before and after motion correction.

### 2.3.5 Between session stability

To measure the stability of the imaging field between sessions, animals with gCaMP6 infused in CA1 underwent contextual fear conditioning, and 24 h later, were placed back in the same context for testing. The mini-microscope was attached during both imaging sessions, and the recordings are aligned as shown in Figure 2.11. In this mouse, we are able to detect 88 active cells from day 1 and 70 active cells from day 2. We were able to align videos from both sessions and found 57 cells active for both sessions. This result is similar to previously reported results (Ziv et al., 2013), and validates our method to map cells between sessions.

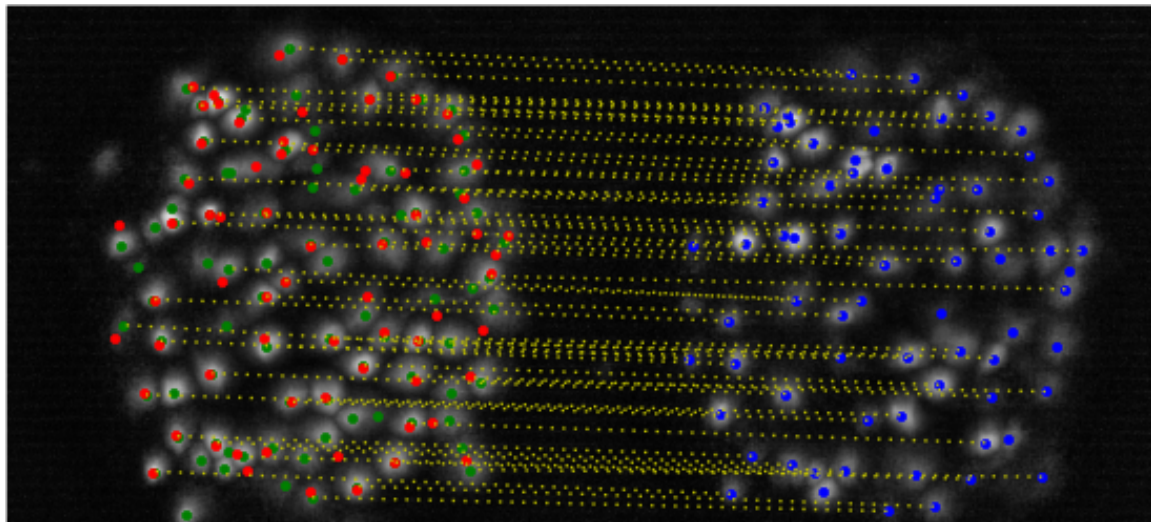


**Figure 2.11** Recorded active cells in CA1 when the mouse is exposed to the same context between two days. Red and blue dots represent centroid of each recorded cell in day 1 and day 2, respectively. Yellow dotted lines shows mapping from a day 2 cell to its image in day 1 (represented with green dots).

### 2.3.6 Deep brain imaging

The original design of the miniature microscope incorporated an objective lens of 1.8 mm in diameter. This lens is both too thick and too short to reach deep brain structures such as LA. We modified the design and attached a 4.8 mm long 0.5 mm diameter relay GRIN lens (ILW-050-P100, GoFoton) to the objective lens. Attaching the relay lens does not significantly alter the imaging ability of the mini-microscope, but allows the lens to reach

deep brain regions without extensive damage. With this configuration, we were able to record neural activity from more than 40 cells in LA and track them over time (Figure 2.12).

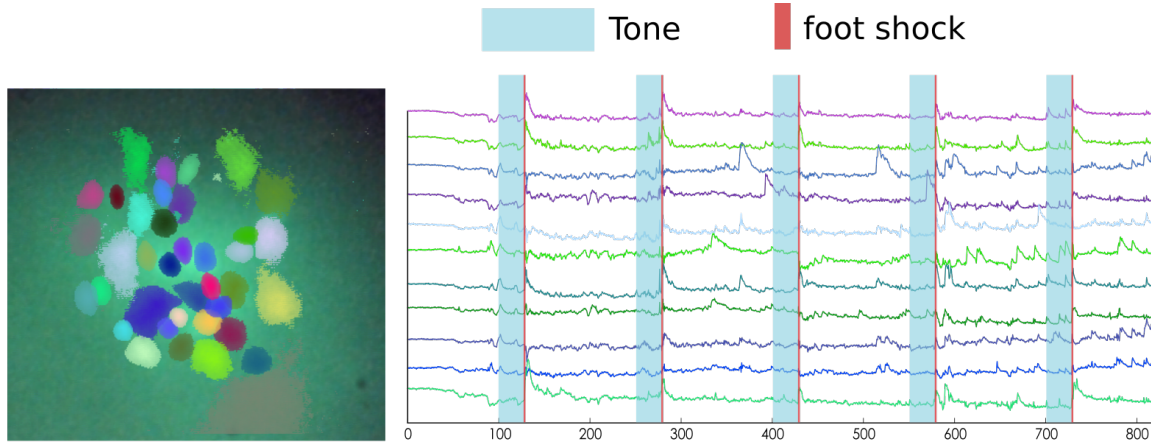


**Figure 2.12** Raw calcium signals of LA neurons during fear conditioning. Left: extracted map of neurons, randomly coloured. Right: Sample calcium signals over time.

### 2.3.7 Two colour

To test the two-colour version of the mini-microscope, we infused red retrobeads (Lumafluor) into the nucleus accumbens (NAc) bilaterally and gCaMP6-expressing AAV in LA. The retrobeads were trafficked retrogradely along axons, and labelled LA neurons that project to NAc. The images acquired from both the green and red channel are shown in Figure 2.13c and 2.13d. Importantly, there is no interference between the two channels, suggesting that the two-colour mini-microscope is able to image two colour channels independently.

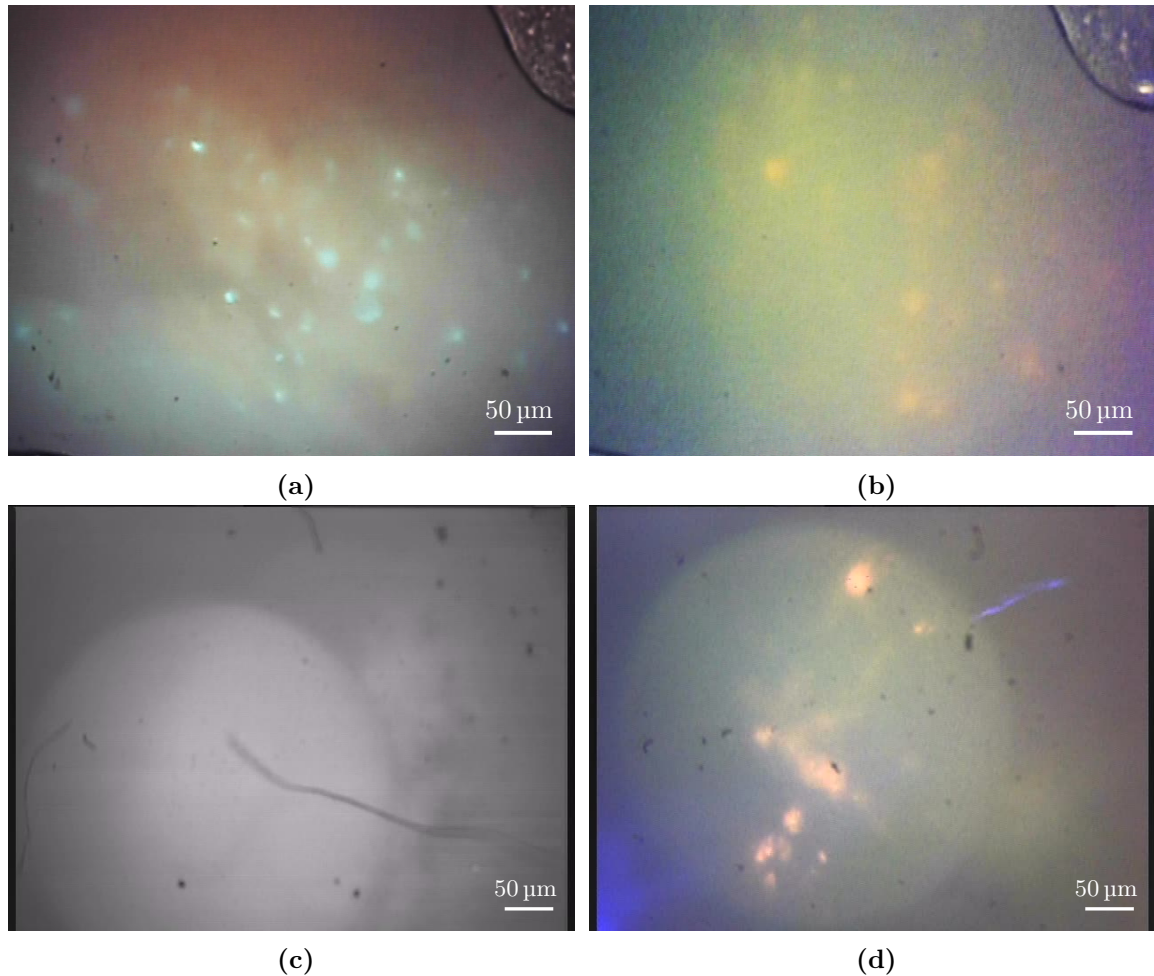


**Figure 2.13** Images of cells with different fluorescent proteins using the two-colour mini-microscope prototype. (a) HSV-GFP in perfused brain. (b) HSV-tdTomato in perfused brain. (c) Red retrobeads *in vivo* in green channel. (d) Red retrobeads *in vivo* in red channel.

## 2.4 Discussion

In the current project, we developed a miniature integrated microscope for calcium imaging in freely behaving mice. The mini-microscope weighs less than 3 g, and can be implanted on a mouse's head without altering the mouse's natural behaviour. We successfully used this microscope to record calcium transients both from CA1 in dorsal hippocampus and LA. Moreover, we added an additional red colour channel for subpopulation identification. With the additional colour channel, we have shown that it is possible to identify cells with specific projection targets by retrograde tracing using fluorescent retrobeads.

Compared to previously designed mini-microscopes, our design is simple to build and cost efficient. All optical and electronic parts are commercially available, and the casing can be 3D-printed. The mini-microscope is designed to be easily assembled with minimal tools. Our design allows biology researchers with minimal engineering experience to build the mini-microscope and use it for biological research. Moreover, the full cost a single mini-microscope is between \$300 and \$1000, and will not represent a significant expense to most biology laboratories.

Here we used PCA–ICA for sorting the cells from videos. It is worth noting that although this method can extract cells and traces reliably, it is not optimal: the PCA–ICA method can only catch statistical regularities in the cell activity, but any spatial information is ignored. As a result, if the statistical distribution of cell activity is similar between some cells, for example if the duration of the video is relatively short or there are cells fire in synchrony, the PCA–ICA is unable to extract individual cells correctly. In addition, the results of PCA–ICA may include negative values in cell activity, which should be limited to only positive values. Recently, Pnevmatikakis et al. (2016) used a constrained non-negative matrix factorization (CNMF) approach for cell sorting from calcium imaging videos. This method took into consideration of the spatial information of each cell, as well as the activity signature of the calcium indicators, and has been shown to be more accurate than PCA–ICA in videos acquired from two-photon microscopes. It is promising that a similar CNMF

approach can be applied to the mini-microscope dataset for cell sorting.

Comparing to *in vivo* two-photon calcium imaging, our mini-microscope lacks the advantage of focusing deeper from the GRIN lens surface, as well as providing an optical slicing of the volume. The latter generates a challenge especially in cell sorting, as overlapping cells in the mini-microscope image may not be separated easily. While the PCA–ICA methods is able to resolve and distinguish partially overlapped cells Mukamel et al. (2009), it is unable to distinguish two completely overlapped cells.

Again, this limitation is can be largely resolved by Pnevmatikakis et al. (2016)’s CNMF approach. They have shown that with their approach, they are able to correctly segregate and recover two overlapping cells (Pnevmatikakis et al., 2016). Moreover, Yang et al. (2016) showed that they are able to recover calcium activity recorded from simultaneous multi-plane two-photon imaging, where the cells from different z-planes are mixed together. The ability to separate overlapping cells make the CNMF especially attractive for the mini-microscope recordings, especially in brain regions where cell density is high, and a significant portion of recorded cells overlap with each other.

In the two-colour version of the mini-microscope, colour aberration still exists, such that the alignment of the red and green channels is not perfect. However, the colour aberration is not significant, and will only result in a theoretical shift of 2  $\mu\text{m}$  in the field of view. Given that the diameter of a neuron is usually more than 10  $\mu\text{m}$ , this misalignment will not significantly affect the identification of neural subpopulations in the red channel. The colour aberration is primarily introduced by the GRIN lens, and can be corrected by using a GRIN lens with an optimal radial refractory index profile. However although technically possible, such GRIN lens is not currently available commercially.

# 3

## MEMORY FORMATION IN ALZHEIMER'S DISEASE

---

### 3.1 Introduction

Progressive memory loss is the defining feature of Alzheimer's disease (AD). The early stages of AD are characterized by the inability to acquire new memories, often observed as difficulty in recalling recent events (Wilson et al., 1983; Storandt and Hill, 1989; Albert, 1996). Over time, memory loss gradually worsens and additional cognitive symptoms (including aphasia, apraxia, agnosia, dyscalculia, executive function impairment) develop (Shah and Reichman, 2006). Although the precise cause(s) of AD remain elusive, A $\beta$ , derived from APP, is widely implicated (Tanzi and Bertram, 2001; Selkoe, 2002). Mutations in APP cause FAD (Price and Sisodia, 1998; Hardy and Selkoe, 2002) and increase A $\beta$  levels (Citron et al., 1992; Cai et al., 1993). While high A $\beta$  may eventually trigger cell death, memory deficits are observed in AD patients before extensive neurodegeneration (Selkoe, 2002), suggesting that A $\beta$  itself interferes with the ability to acquire memories, at least in the early stages of the disease.

Memory formation is thought to be mediated by the strengthening of excitatory synaptic transmission between neurons (Bailey and Kandel, 1993; Lamprecht and LeDoux, 2004). The majority of fast excitatory neurotransmission is mediated by AMPARs. AMPARs

are localized in dendritic spines and composed of four types of subunits (GluA1-4), which combine to form tetramers (Hollmann and Heinemann, 1994). In mature hippocampal pyramidal neurons, most AMPARs consist of two identical heterodimers comprised of GluA1/2 and GluA2/3 dimers (Wenthold et al., 1996). AMPARs are highly dynamic and undergo rapid shuttling between the plasma membrane and internal recycling pools. For instance, the activity-dependent removal of AMPAR from the synapse (endocytosis) rapidly and persistently reduces surface expression of GluA2-containing AMPARs. This endocytosis is critical for the expression of some forms of LTD, a type of synaptic plasticity that is characterized by a decrease in synaptic strength and dendritic spine size/density (Malinow and Malenka, 2002; Collingridge et al., 2004; Zhou et al., 2004). In addition, endocytosis of GluA2-containing AMPAR is implicated in homeostatic synaptic scaling (Gainey et al., 2009). Therefore, changes in surface expression of GluA2s may critically modulate memory formation.

Intriguingly, a recent finding shows that A $\beta$  potentiates endocytosis of GluA2-containing AMPARs in hippocampal organotypic slice cultures. Hsieh and colleagues showed that high levels of A $\beta$  (produced by transiently expressing human APP or incubating slices directly in synthetic A $\beta$ ) decreases both synaptic strength and spine density by internalizing GluA2-containing AMPARs (Hsieh et al., 2006). This finding was replicated by applying synthetic A $\beta$  peptides to neuroblastoma N2A cells (Zhao et al., 2010) or dissociated hippocampal neurons (Liu et al., 2010; Zhao et al., 2010). However, whether a decrease in synaptic GluA2 levels is responsible for the memory deficits observed in AD patients or even in mice designed to model AD is not known. Here using a mini-microscope, we directly investigated whether interfering with GluA2-containing AMPAR endocytosis is sufficient to reverse the circuitry and memory deficits observed in a mouse models of early AD.

## 3.2 Material and methods

### 3.2.1 Animals and vectors

All mice were housed in groups of 3–5 on a 12-hour light/dark cycle. Food and water were provided *ad libitum* to all mice. Experiments were performed during the light phase of the circadian cycle. Mice were at least 8 weeks old at the beginning of all experiments. All experiments were conducted in accordance to the Hospital for Sick Children Animal Care and Use Committee.

#### TgCRND8 mice

TgCRND8 mice were developed at the Centre of Research for Neurodegenerative Diseases (CRND), carrying a human APP695 transgene with both the Swedish (K670N-M671L) and Indiana (V717F) FAD mutations under the regulation of the Syrian hamster prion promoter (Chishti et al., 2001). Transgenic mice were maintained on a 129S6/SvEvTac background. TgCRND8s were then crossed with either WT C57BL/6NTac or GP5.17. Tg and WT litter-mates of F1 generation were used in the experiments.

#### GP5.17 mice

GP5.17 mice transgenically express the fluorescent calcium indicator GCaMP6f under the Thy1 promoter (Dana et al., 2014). Offspring of TgCRND8 × GP5.17 positive for GCaMP6f and negative for APP were included in the WT group. Double positive offspring were included in the Tg group.

#### Viral vectors

In some TgCRND8 mice, GCaMP6f was delivered using AAV. GCaMP6f expression was controlled by the human synapsin (hSyn) promoter. AAV-DJ-syn-GCaMP6f virus was purchased from Stanford University Gene and Viral Vector Core and used undiluted.

**TAT-GluA2<sub>3Y</sub> peptide**

To deliver the GluA2<sub>3Y</sub> construct (YKEGYNVYG) to our target region, we attached it to the protein transduction domain of the Human Immunodeficiency Virus (HIV) *tat* gene (TAT peptide). The TAT peptide is able to be transported across cell membrane and blood brain barrier (BBB). TAT-GluA2<sub>3Y</sub> was synthesized from the sequence YGRKKRRQRRRYKEGYNVYG. Injection solution is prepared as 15 mmol TAT-GluA2<sub>3Y</sub> in saline solution.

**3.2.2 Viral infusion**

Each mouse received i.p. injection of atropine ( $0.1 \text{ mg kg}^{-1}$ ) and chloral hydrate ( $400 \text{ mg kg}^{-1}$ ) before being secured on a stereotaxic frame. An incision was made on the scalp and the skin was pulled to the side to reveal the skull. Holes were drilled in the skull above CA1 for micropipette injection. Virus was loaded into a glass micropipette and gradually lowered to target coordinates. 1.5  $\mu\text{l}$  of virus was injected on each side at a rate of 0.12  $\mu\text{l}/\text{min}$ , targeting CA1 (A/P  $-1.8 \text{ mm}$ , M/L  $1.5 \text{ mm}$ , D/V  $3.5 \text{ mm}$  from Bregma). The micropipette was left in the brain for an additional 10 min before slowly retracted. The incision was sutured and treated with antibiotics. Each mouse then received subcutaneous injection of analgesic (ketoprofen,  $5 \text{ mg kg}^{-1}$ ) before returned to a partially heated clean cage for recovery.

**3.2.3 Histology**

Placement of lens implants and extent of viral infection was determined by gCaMP6f fluorescence expression *post-mortem*. After all experiments, mice were transcardially perfused with first phosphate-buffered saline (PBS) then 4% paraformaldehyde (PFA). The brains were dissected, kept in 4% PFA overnight, and washed with PBS. The brains were then sliced coronally on a vibratome (VT1200S, Leica) to  $50 \mu\text{m}$  thickness. Slices containing LA were then mounted on gelatin-coated glass slides with a hardening mounting media (Permaflour, ThermoScientific). The mounted brain slices were assessed under an epi-fluorescence microscope (Eclipse 80i, Nikon) for histology.

### 3.2.4 Contextual fear conditioning

Fear conditioning chambers (31 cm × 24 cm × 21 cm; MED Associates, St. Albans, VT) consisted of 2 stainless steel and 2 clear acrylic walls with a stainless steel shock-grid floor (bars 3.2 mm diameter, spaced 7.9 mm apart). A plastic drop-pan containing a 70% ethanol solution was placed below the grid floor. A fan provided low-level white noise during training and testing in the context. Behaviour was monitored by overhead cameras, which recorded video images of the chambers at 15 Hz.

Mice underwent contextual fear conditioning three weeks after mini-microscope base-plate implantation. One hour before training, mice received either TAT-GluA<sub>2</sub>Y peptide (15 mmol kg<sup>-1</sup>, i.p.) or vehicle injection. A mini-microscope was attached to the mouse to record calcium transients during both training and testing of contextual fear conditioning.

During training, mice were confined in the chamber for 5 min. A 2-second foot-shock of 0.5 mA was delivered at 4 min time point. During testing session 24 h later, mice were placed back in the training environment for 10 min.

### 3.2.5 Motion tracking

Videos of mouse behaviour were encoded as grey-scale images. Due to a dark background, occlusion by mini-microscope wires and commutators, and changing shadows, no simple feature was able to reliably identify the mouse from the background. Instead, we calculated the distribution of multiple features from a training set of videos where mice were correctly tracked, and used all the features together to estimate the position of the mouse for each frame in a new video. During model fitting, distribution of every feature was estimated with a Gaussian kernel with a bandwidth calculated using Silverman's rule of thumb (Silverman, 1986):  $1.06\sigma n^{-\frac{1}{5}}$ , where  $\sigma$  is the standard deviation of the samples, and  $n$  is the number of samples.

## Features

**Pixel intensity.** Pixel intensity at mouse's position. This feature tries to capture the mouse's fur colour.

**Normalized pixel intensity.** Normalized pixel intensity of mouse's position, where the frame is normalized to a zero mean and unit standard deviation. This feature tries to capture mouse's fur colour when the illumination in the chamber varies across frames.

**Foreground pixel intensity.** Pixel intensity difference between foreground and background images at the mouse's position. The background image of the environment was generated by taking the mean pixel density across time. This feature tries to separate mice from any background pixels with similar colour.

**Difference to low pass intensity.** Pixel intensity difference between foreground image and low-pass filtered foreground image (10 mm window) at the mouse's position. This feature tries to capture the fact that the mouse's colour is close to uniform, therefore eliminates sporadic noise pixels with similar colour.

**Speed.** Distance between the mouse's positions in two consecutive frames.

**Change in intensity.** Difference of pixel intensity at the mouse's positions in two consecutive frames. This feature captures the fact that the mouse's colour is relative consistent between frames.

**Change in intensity (blurred).** Similar to change in intensity, but using Gaussian blurred images (10 mm window) to remove effect of random noise.

**Magnitude of acceleration.** Magnitude of acceleration vector, which is calculated as the vector difference of two consecutive velocity calculations.

**Segmentation area.** Edges in the frame are detected (Canny, lower threshold=100, higher threshold=200). The resulting image is then morphologically closed (6 iterations) to remove sporadic edges. The area enclosing the position of the mouse is then calculated. This feature tries to capture the size of the mouse.

## Tracking

The mouse's position over time was modelled as a hidden Markov chain (HMM), as shown in Figure 3.1. The mouse's true position at time  $i$  was represented by the latent variables  $z_i$ . At each time point, the value of all the feature measurements were represented as  $x_i$ . Under this model, the goal of tracking the mice is equivalent to estimating the latent variables  $z_i$  using  $x_i$ .

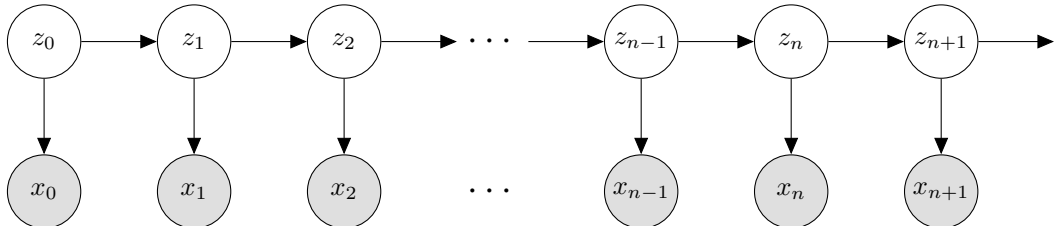


**Figure 3.1** HMM model for tracking mice. The mouse's true position at time  $i$  is represented by the latent variables  $z_i$ , measurements of the mouse's position is represented by  $x_i$ .

We used particle filter to estimate the position of the mice. Specifically, we approximated the posterior distribution  $f_{z_n}(z_n|X_n)$  with  $L$  particles at  $\{a_n^i\}_{i=1}^L$  with weights  $\{w_n^i\}_{i=1}^L$ , such that the posterior distribution can be approximated with a mixture of Dirac delta function:

$$f_{z_n}(z_n|X_n) \approx \sum_{i=1}^L w_n^i \delta(z_n - a_n^i) \quad (3.1)$$

On the other hand, using Bayes' rule and the HMM structure, we have:

$$\begin{aligned}
f_{z_n}(z_n|X_n) &\propto f_{x_n}(x_n|z_n, X_{n-1}) \cdot f_{z_n}(z_n|X_{n-1}) \\
&= f_{x_n}(x_n|z_n) \int f_{z_n}(z_n|z_{n-1}) f_{z_{n-1}}(z_{n-1}|X_{n-1}) dz_{n-1} \\
&\approx f_{x_n}(x_n|z_n) \int f_{z_n}(z_n|z_{n-1}) \cdot \sum_{i=1}^L w_{n-1}^i \delta(z_{n-1} - a_{n-1}^i) dz_{n-1} \\
&= f_{x_n}(x_n|z_n) \sum_{i=1}^L w_{n-1}^i \int f_{z_n}(z_n|z_{n-1}) \delta(z_{n-1} - a_{n-1}^i) dz_{n-1} \\
&= f_{x_n}(x_n|z_n) \sum_{i=1}^L w_{n-1}^i f_{z_n}(z_n|a_{n-1}^i)
\end{aligned}$$

where the probability distribution  $f_{x_n}(x_n|z_n)$  is the measurement model, which we approximated with the normalized product of all feature distributions. The motion model  $f_{z_n}(z_n|z_{n-1})$  was approximated with the distribution of speed at all directions. Combined with (3.1), we can find  $\{a_n^i\}_{i=1}^L$  by sampling from the mixture  $\sum_{i=1}^L w_{n-1}^i f_{z_n}(z_n|a_{n-1}^i)$ , and calculate  $w_n^i = f_{x_n}(x_n|a_n^i)$ . The centre of mass of all particles was used as an estimate of the mouse's position  $z_n$ . This process was then iterated for all frames to track the mouse's position in one behavioural video.

### 3.2.6 Analysis

#### Freezing behaviour

Freezing behaviour of the mice during first 10 min of contextual fear memory testing was assessed by an experimenter blind to the genotype and treatment of the mice. Frame-to-frame timestamps for the beginning and end of freezing bouts were recorded.

#### Preprocessing for calcium transients

All calcium transients were normalized to have zero median and unit noise standard deviation. The noise standard deviation was estimated from the median absolute deviation of the transient. The SNR was calculated as the ratio of maximum signal intensity and noise

standard deviation. Only transients with more than 10 SNR and mice with more than 20 cells were included in the analysis. The average activity of a cell was calculated by the area under the calcium transients above 3 standard deviation of the noise divided by duration.

### Mutual information

The mutual information measurement of two random variables represents the degree of relatedness between them. The mutual information between the calcium transient for each cell  $C$ , a continuous random variable and the freezing state of the mouse  $F$ , a discrete random variable, is defined as:

$$I(C, F) = \int_{c \in C} \sum_{f \in F} P(c, f) \log \frac{P(c, f)}{P(c)P(f)} dc \quad (3.2)$$

Here we chose the Kozachenko–Leonenko entropy estimator (KLE) to estimate the mutual information. While electrophysiological studies have commonly adapted from Skaggs et al. (1993) to calculate mutual information between cell activity and position of the animal for characterization of spatial encoding in hippocampus (e.g., Knierim et al., 1995; Skaggs and McNaughton, 1996; Ji and Wilson, 2007; Cheng and Ji, 2013; Roux et al., 2017), unfortunately this method is not applicable to raw calcium imaging traces. Skaggs et al. (1993)'s method made an important assumption: that during a sufficient short time, the electrophysiological recording of a neuron is essentially binary, with the neuron either firing or not. With this assumption, the firing rate of a single neuron can be modelled as a Poisson distribution, and the integral in Formula 3.2 is then tractable.

Unfortunately, the calcium trace we have collected is a continuous variable which violate Skaggs et al. (1993)'s assumption. A different way to estimate the mutual information then is to quantize the cell activity into finite bins. Mutual information between the binned cell activity and behavioural states can then be calculated, as the integral of Formula 3.2 is then replaced by a summation over all bins of cell activity. This binning method is however negatively biased, and only represents a lower bound of the actual information content

measurement. Correction methods exists, however they tend to be sensitive to specific distributions of data (Paninski, 2003).

Another method for entropy estimation exploits the nearest neighbour distance within the dataset, which contains information about the underlying probability distribution of the continuous variable. Kozachenko and Leonenko (1987) first showed that entropy estimation using nearest neighbour distance is unbiased, under the mild assumption that the probabilistic density function of the continuous random variable is smooth. Here we preferred KLE for mutual information measurement, as it is non-parametric and robust, while estimates from binning-based methods, even with correction for their asymptotic bias, is sensitively dependent on the choice of binning size and method to correct bias (Victor, 2002; Ross, 2014).

To estimate the mutual information between freezing and calcium transients, we used the KLE twice to estimate the entropy of calcium transient  $H(C)$  and its conditional entropy on freezing  $H(C|F)$  (Victor, 2002; Ross, 2014). The mutual information was then calculated using the identity:

$$I(C, F) = H(C) - H(C|F) \quad (3.3)$$

The KLE is a nearest-neighbour entropy estimator. Given a data point  $C_{i,0}$  from a continuous random variable and its  $m^{\text{th}}$  nearest neighbour  $C_{i,m}$ , we define  $V_{i,m}$  as the volume of sphere centred at  $C_{i,0}$  with a radius equal to the distance between  $C_{i,0}$  and  $C_{i,m}$ . The entropy of  $C$  can be estimated as:

$$H(C) \approx \langle \log V_{i,m}^F \rangle + \varphi(N) - \varphi(m) \quad (3.4)$$

where  $N$  is the number of samples, and  $\langle \cdot \rangle$  denotes the average over  $1 \dots N$ , and  $\varphi$  is the digamma function. Similarly, we can calculate the entropy for the conditional entropy  $H(C|F)$ :

$$H(C|F) \approx \langle \log V_{i,k}^{F_i} \rangle + \langle \varphi(N_{F_i}) \rangle - \varphi(k) \quad (3.5)$$

where  $N_{F_i}$  is the number of samples in the freezing state of  $i^{\text{th}}$  sample, and here we use the  $k^{\text{th}}$  nearest neighbour conditioned on  $F_i$  for the calculation.

To avoid sampling error, we fixed  $k$  for each sample, but changed  $m$  to the total number of samples between the sample  $C_{i,0}$  and its  $k^{\text{th}}$  nearest neighbour conditioned on  $F_i$ ,  $C_{i,k}^{F_i}$ . Therefore we have:

$$\log V_{i,m_i} = \log V_{i,k}^{F_i}, \forall i$$

Plug (3.4) and (3.5) to (3.3), we have:

$$I(C, F) \approx \varphi(N) - \langle \varphi(m_i) \rangle - \langle \varphi(N_{F_i}) \rangle + \varphi(k)$$

### Machine learning

Time-course data for the calcium transients and mouse behavioural states were paired and shuffled across time. The calcium transient for each cell was regarded as a single feature. Classifiers were then trained and validated using 5-fold cross validation. Specifically, the shuffled data was divided into 5 equal blocks. Each block was presented one at a time, and the classifier was trained using the remaining 4 blocks. The presented block was then used to test the performance of the classifier. The classifier prediction from each block was then concatenated and sorted into the original order. In the analysis, we used two classifiers, a naive Bayes classifier (NBC) and a Gaussian support vector machine (gSVM).

**Naive Bayes classifier (NBC).** In an NBC, the classifier tries to infer the likelihood of the  $i^{\text{th}}$  target class  $T_i$  given the features  $\mathbf{x} = (x_1, x_2, \dots, x_n)$ . Therefore, we have:

$$P(T_i|\mathbf{x}) = \frac{P(T_i, \mathbf{x})}{P(\mathbf{x})}$$

The denominator is not relevant for classification purposes, since it does not depend on the target class  $T_i$ . Therefore, repeatedly applying the chain rule, we have:

$$\begin{aligned}
 P(T_i|x_1, \dots, x_n) &\propto P(x_1, \dots, x_n, T_i) \\
 &= P(x_1|x_2, \dots, x_n, T_i)P(x_2, \dots, x_n, T_i) \\
 &\quad \vdots \\
 &= P(x_1|x_2, \dots, x_n, T_i)P(x_2|x_3, \dots, x_n, T_i) \dots P(x_{n-1}|x_n, T_i)P(x_n|T_i)P(T_i) \\
 &= P(T_i) \prod_{k=1}^{n-1} P(x_k|x_{k+1}, \dots, x_n, T_i)
 \end{aligned}$$

To make the product tractable, NBC discards the interaction between all the features, and assumes the features are conditionally independent. Therefore, each of the terms in the product can be reduced to:

$$P(x_k|x_{k+1}, \dots, x_n, T_i) = P(x_k|T_i)$$

Therefore:

$$P(T_i|\mathbf{x}) = C \cdot P(T_i) \cdot \prod_{k=1}^n P(x_k|T_i)$$

where  $C$  is a constant independent of  $T_i$ . The conditional probability for each feature  $P(x_k|T_i)$  is estimated from the training data assuming a Gaussian distribution. During testing, the target class with maximum likelihood  $\hat{T} = \arg \max_i P(T_i|\mathbf{x})$  is predicted.

**Gaussian support vector machine (gSVM).** A support vector machine (SVM) aims to find a hyperplane  $\mathbf{w}^T \mathbf{x} + b = 0$  which separates the target classes with maximum margin. Concretely, for features  $\mathbf{x}$  and targets  $y$ , the SVM aims to maximize the minimum distance for each data point, transformed by a function  $\phi$ , to the classifying hyperplane:

$$\arg \max_{\mathbf{w}, b} \left( \min_{i=1}^n \frac{y_i(\mathbf{w}^T \phi(\mathbf{x}_i) + b)}{|\mathbf{w}|} \right) \quad (3.6)$$

Given that  $\mathbf{w}$  and  $b$  can be scaled without changing the value of this term, we scale  $\mathbf{w}$  and  $b$  such that the minimum distance to classifying plane  $\min_{i=1}^n (y_i(\mathbf{w}^T \phi(\mathbf{x}_i) + b))$  is equal to 1. The original objective function therefore becomes:

$$\begin{aligned} & \arg \max_{\mathbf{w}, b} \left( \min_{i=1}^n \frac{y_i(\mathbf{w}^T \phi(\mathbf{x}_i) + b)}{|\mathbf{w}|} \right) \\ &= \arg \max_{\mathbf{w}, b} \frac{1}{|\mathbf{w}|} \min_{i=1}^n (y_i(\mathbf{w}^T \phi(\mathbf{x}_i) + b)) \\ &= \arg \max_{\mathbf{w}, b} \frac{1}{|\mathbf{w}|} \cdot 1 \\ &= \arg \min_{\mathbf{w}, b} \frac{|\mathbf{w}|^2}{2} \end{aligned}$$

To allow the classifier to perform with data sets that are not linearly separable, an error term can be added for each data point  $\varepsilon_i$ . If the distance from the data point to the classifying hyperplane is at least 1, the value of  $\varepsilon_i$  will be 0. If the data point lies within the margin but is still correctly classified,  $\varepsilon_i$  represents the distance from the data point to the boundary of its correct class, and will have a value between 0 and 1. If the data point is incorrectly classified,  $\varepsilon_i$  will have a value greater than 1. The error is controlled by a parameter  $C$ , which dictates how relaxed the classifying boundary is. Therefore the objective function becomes:

$$\arg \min_{\mathbf{w}, b} \left( \frac{|\mathbf{w}|^2}{2} + C \sum_{i=1}^n \varepsilon_i \right)$$

under the constraints that data are classified for all  $i$ :

$$y_i(\mathbf{w}^T \phi(\mathbf{x}_i) + b) \geq 1 - \varepsilon_i$$

$$\varepsilon_i \geq 0$$

To find the extrema of the objective function under these constraints, we create the Lagrangian:

$$\mathcal{L}(\mathbf{w}, b, \lambda, \mu) = \frac{|\mathbf{w}|^2}{2} + C \sum_{i=1}^n \varepsilon_i - \sum_{i=1}^n \lambda_i (y_i(\mathbf{w}^T \phi(\mathbf{x}_i) + b) - 1 + \varepsilon_i) - \sum_{i=1}^n \mu_i \varepsilon_i \quad (3.7)$$

where  $\lambda = (\lambda_1, \lambda_2, \dots, \lambda_n)$ , and  $\mu = (\mu_1, \mu_2, \dots, \mu_n)$ . We can optimize it by setting its partial derivatives regarding to  $\mathbf{w}$ ,  $b$ ,  $\varepsilon$  to 0:

$$\begin{aligned}\frac{\partial \mathcal{L}}{\partial \mathbf{w}} &= \mathbf{w} - \sum_{i=1}^n \lambda_i y_i \phi(\mathbf{x}_i) = 0 \\ \frac{\partial \mathcal{L}}{\partial b} &= - \sum_{i=1}^n \lambda_i y_i = 0 \\ \frac{\partial \mathcal{L}}{\partial \varepsilon_i} &= C - \lambda_i - \mu_i = 0, \forall i\end{aligned}\tag{3.8}$$

Using (3.8) to eliminate  $\mathbf{w}$ ,  $b$ ,  $\varepsilon$  from the Lagrangian (3.7), equivalently we aim to minimize the Lagrangian of  $\lambda$ :

$$\mathcal{L}^*(\lambda) = \sum_{i=1}^n \lambda_i - \frac{1}{2} \sum_{i=1}^n \sum_{j=1}^n \lambda_i \lambda_j y_i y_j \phi(\mathbf{x}_i)^T \phi(\mathbf{x}_j)\tag{3.9}$$

subject to:

$$0 \leq \lambda_i \leq C, i = 1, \dots, n$$

$$\sum_{i=1}^n \lambda_i y_i = 0$$

The parameters  $\lambda_i$  can then be solved numerically through quadratic programming. Since Equation 3.9 does not depend on  $\phi$ , but only the inner product  $\phi(\mathbf{x}_i)^T \phi(\mathbf{x}_j)$ , we can replace the term with a function  $K(\chi, \chi) \rightarrow \mathbb{R}$ , which represents a measure of similarity between  $\mathbf{x}_i$  and  $\mathbf{x}_j$ . In this way, the data  $\mathbf{x}$  can be projected into a high dimensional space (or even infinite-dimension space) to allow a linear separation between the classes. Particularly, here we used the Gaussian kernel:

$$K(\mathbf{x}_i, \mathbf{x}_j) = e^{-\frac{|\mathbf{x}_i - \mathbf{x}_j|^2}{2\sigma^2}}$$

The Gaussian kernel is a universal kernel (Park and Sandberg, 1991), meaning that with proper regulation, an SVM with it can create a classification boundary approaching any function at arbitrary precision. Therefore using a Gaussian kernel, we would be able to

capture any structure present in the training data which helps in prediction.

The parameters of the model,  $\lambda_i$  and  $\mu_i$  are fitted with training data. To predict a new data point  $\mathbf{x}'$ , we calculate the sign of the distance from it to the classification boundary (3.6), using (3.8) to eliminate  $\mathbf{w}$ , and  $b$ :

$$\text{sgn} \left( \sum_{i=1}^n \lambda_i y_i K(\mathbf{x}', \mathbf{x}_i) + b \right)$$

as the prediction of whether the mouse is freezing or not freezing.

We used the `SVC` module from `scikit-learn` Python package for gSVM classification. The regularization hyperparameter  $C = 100$  and Gaussian kernel variance hyperparameter  $2\sigma^2 = \dim(\mathbf{x})$  were set to the default provided by the Python package `scikit-learn`. Hyper-parameters were scanned with a grid search on log scale. The hyper-parameters giving the best classifier performance were selected.

## Statistics

Influence of *Genotype* (Tg, WT) and *Treatment* (Vehicle, TAT-GluA2<sub>3Y</sub>) was evaluated with two-way analysis of variance (ANOVA). Covariates were controlled with general linear model (GLM). Comparisons between single levels were contrasted with T-tests, and multiple levels with F-tests. Bonferroni correction was performed for multiple comparisons. For analysis where the number of samples was large, if comparison of means was not significant, a two-sample Kolmogorov-Smirnov test (KS test) was performed to detect any difference in the distributions of the two samples. All statistical tests were performed using `statsmodels` package in the Python programming language.

## Bayesian modelling

Monte-Carlo Markov chain (MCMC) sampling was performed on `pymc` package in Python. Samples were drawn using Metropolis-Hastings steps. 540 000 samples were drawn with 40 000 in the burn-in period. The rest were thinned 10 times, resulting in 50 000 total

samples for each model. Bayes factors of alternative hypothesis versus null hypothesis ( $BF_{10}$ ) were calculated. Interpretation of Bayes factors is reported according to Kass and Raftery (1995), where there is positive evidence if the Bayes factor is between 3 and 20, strong evidence if it is between 20 and 150, and very strong evidence if it is greater than 150.

### 3.3 Results

#### 3.3.1 TAT-GluA<sub>2</sub><sub>3Y</sub> rescues memory deficits in Tg mice

To record CA1 activity, we first expressed the GECI GCaMP6f in WT and Tg mice. GCaMP6f was expressed by crossing the TgCRND8 mouse line with a GP5.17 mouse line. F1 offspring positive for GCaMP6f were used in the experiment ( $N = 17$ ). We also crossed TgCRND8 mice with a background C57BL/6 line, and infused an AAV in the CA1 of dorsal hippocampus to express GCaMP6f ( $N = 14$ ). We then implanted the mini-microscope above CA1 for recording of calcium activity. We found no difference between the two groups of mice, and pooled results from both groups.

First, we examined the behavioural performance between the WT and the Tg mice. We hypothesized that the Tg mice would have deficits in contextual fear memory, and that this deficit could be rescued by TAT-GluA<sub>2</sub><sub>3Y</sub> treatment before training. The experimental paradigm is summarized in Figure 3.2. Mini-microscope base-plates were surgically implanted unilaterally in the CA1 of dorsal hippocampus in gCaMP6f expressing WT and TgCRND8 (Tg) mice. The mice received either vehicle (Veh) or TAT-GluA<sub>2</sub><sub>3Y</sub> (Glu) peptide one hour before training. Twenty-four hours later, the mice were put back into the training chamber for the memory test of contextual fear conditioning. Figure 3.3 shows cells recorded from a single mouse and calcium transients from a sample of cells.

Figure 3.4 shows the percent of time spent freezing during the memory test. A two-way ANOVA revealed a significant interaction between *Genotype* and *Treatment* ( $F_{1,27}=5.45$ ,

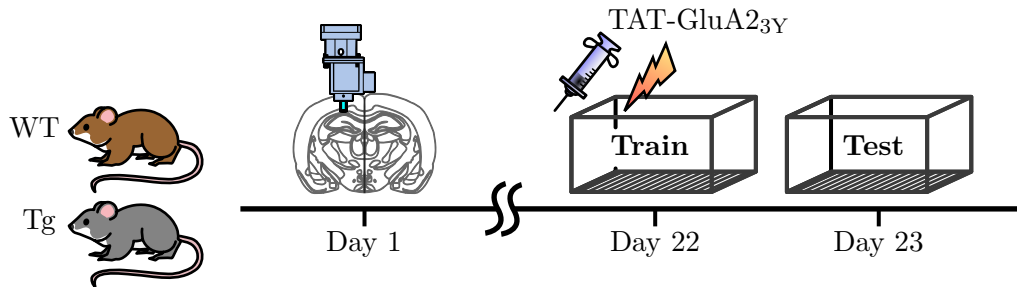


**Figure 3.2** Experimental paradigm. Adult WT and Tg mice (with gCaMP6f expression) were implanted with a mini-microscope base-plate targeting CA1 hippocampus on day 0. Fluorescent cells were visible three weeks later. Mice received TAT-GluA<sub>23Y</sub> peptide or vehicle (i.p.) 1 h before contextual fear conditioning. Mice were tested 24 h later for freezing behaviour. Calcium transients were recorded for both training and testing session.

$p=0.027$ ) as well as a significant main effect in *Genotype* ( $F_{1,27}=12.79$ ,  $p=0.001$ ). *Post hoc* tests showed that Tg-Veh mice had significantly lower freezing than WT mice (WT-Veh vs Tg-Veh,  $T=4.21$ ,  $p<0.001$ ), and this effect was rescued by TAT-GluA<sub>23Y</sub> treatment (Tg-GluA<sub>23Y</sub> vs Tg-Veh,  $T=2.85$ ,  $p=0.008$ ; WT-Veh vs Tg-GluA<sub>23Y</sub>,  $T=1.12$ ,  $p=0.27$ ). TAT-GluA<sub>23Y</sub> had no significant effect on WT mice (WT-Veh vs WT-GluA<sub>23Y</sub>,  $T=0.355$ ,  $p=0.72$ ).

This result is consistent with previous reports (Palmer and Good, 2011; Zhou et al., 2016) that Tg mice have deficits in hippocampal-related memory tasks. It also confirms our hypothesis that the memory deficit of Tg mice can be rescued by TAT-GluA<sub>23Y</sub> treatment.

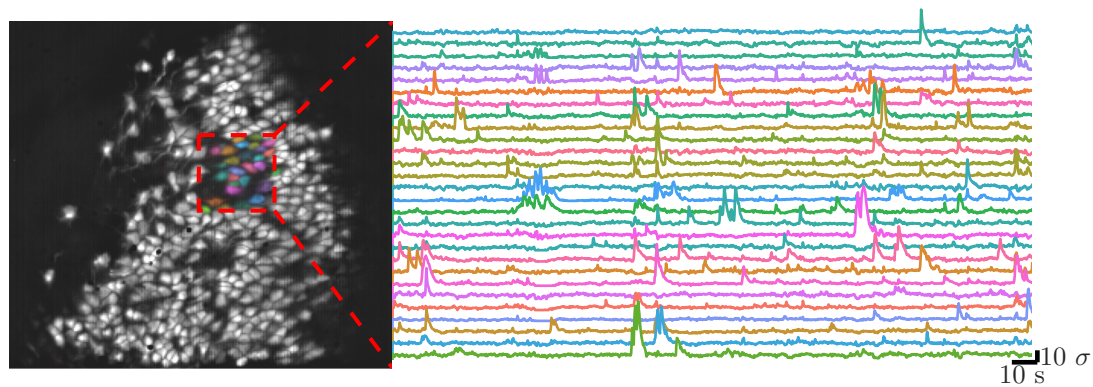


**Figure 3.3** Sample cell image and calcium transients. Transients are randomly coloured and correspond to cells of the same colour.

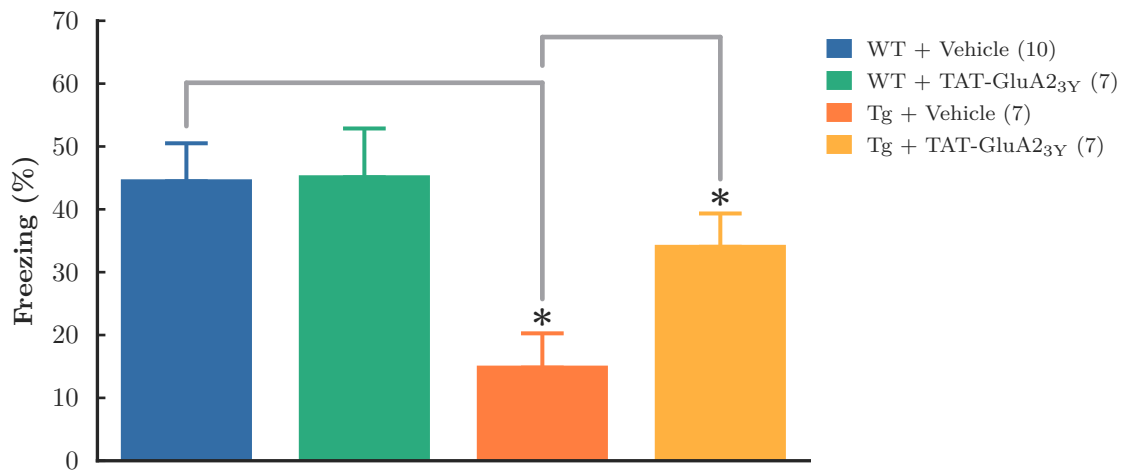


**Figure 3.4** Percent freezing during memory test. Tg mice have significant lower freezing, and TAT-GluA<sub>23Y</sub> treatment returns the freezing to wild-type level.

### 3.3.2 Tg mice can initiate freezing

We then investigated whether the deficits in Tg mice were due to less freezing initiation or freezing maintenance. Previous reports suggested that in a mouse model of AD, place cells in AD are unstable (Cheng and Ji, 2013), and it is possible that a similar deficit is present in memory encoding. Here we analyzed the freezing bout length and freezing bout number, where a freezing bout was defined as a continuous period of freezing. We hypothesized that if AD mice had a deficit in memory maintenance, the mice would show significantly reduced freezing bout length. However if the AD mice had no deficit in initiating freezing, the mice would have a similar number of freezing bouts.

Figure 3.5 summarizes the number and length of freezing bouts in each group. There is no significant difference between groups in the number of freezing bouts (Figure 3.5a, omnibus  $F_{3,27}=0.84$ ,  $p=0.48$ ). We then examined the average length of freezing bouts per mouse, and found a significant interaction between *Genotype* and *Treatment* ( $F_{1,27}=6.5$ ,  $p=0.01$ ) and a significant main effect of *genotype* ( $F_{1,27}=17.7$ ,  $p<0.001$ ). *Post hoc* tests showed Tg-Veh mice to have significantly shorter freezing bouts (WT-Veh vs Tg-Veh,  $T=4.75$ ,  $p<0.001$ ), and this deficit was fully rescued by TAT-GluA2<sub>3Y</sub> treatment (Tg-GluA2<sub>3Y</sub> vs Tg-Veh,  $T=3.10$ ,  $p=0.002$ ; WT-Veh vs Tg-GluA2<sub>3Y</sub>,  $T=1.66$ ,  $p=0.10$ ). There was no effect of TAT-GluA2<sub>3Y</sub> on WT mice ( $T=0.22$ ,  $p=0.83$ ). This result suggests that the vehicle treated Tg mice do not have a deficit in initiating freezing behaviour, however they are unable to maintain this freezing for an extended period.

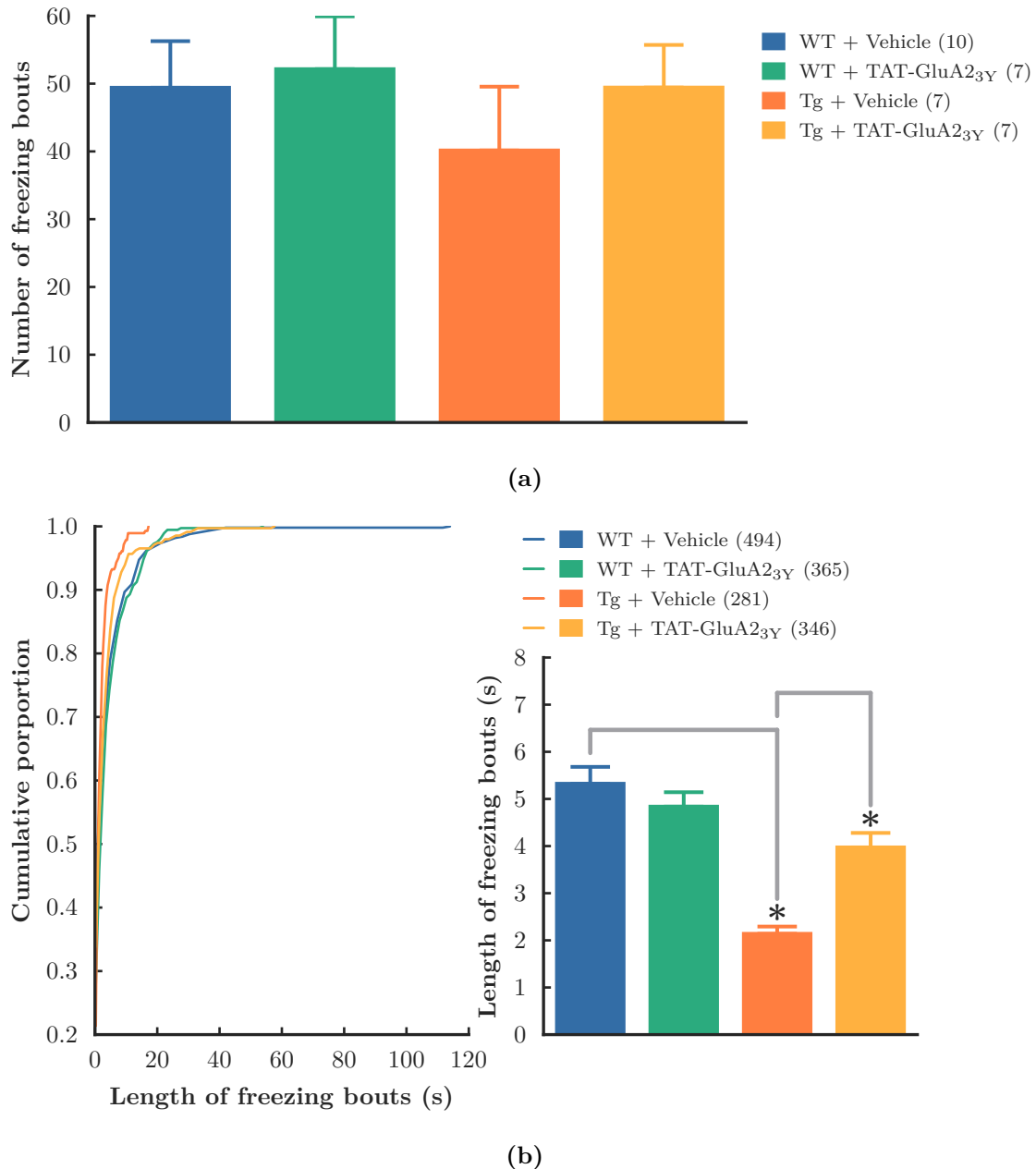


**Figure 3.5** Average number of freezing bouts (a) and length of freezing bouts (b). Tg mice freeze as often as WT mice, but with shorter duration. This is rescued by TAT-GluA<sub>2</sub><sub>3Y</sub> treatment.

### 3.3.3 TAT-GluA<sub>2</sub><sub>3Y</sub> rescues hyperactivity in Tg cells

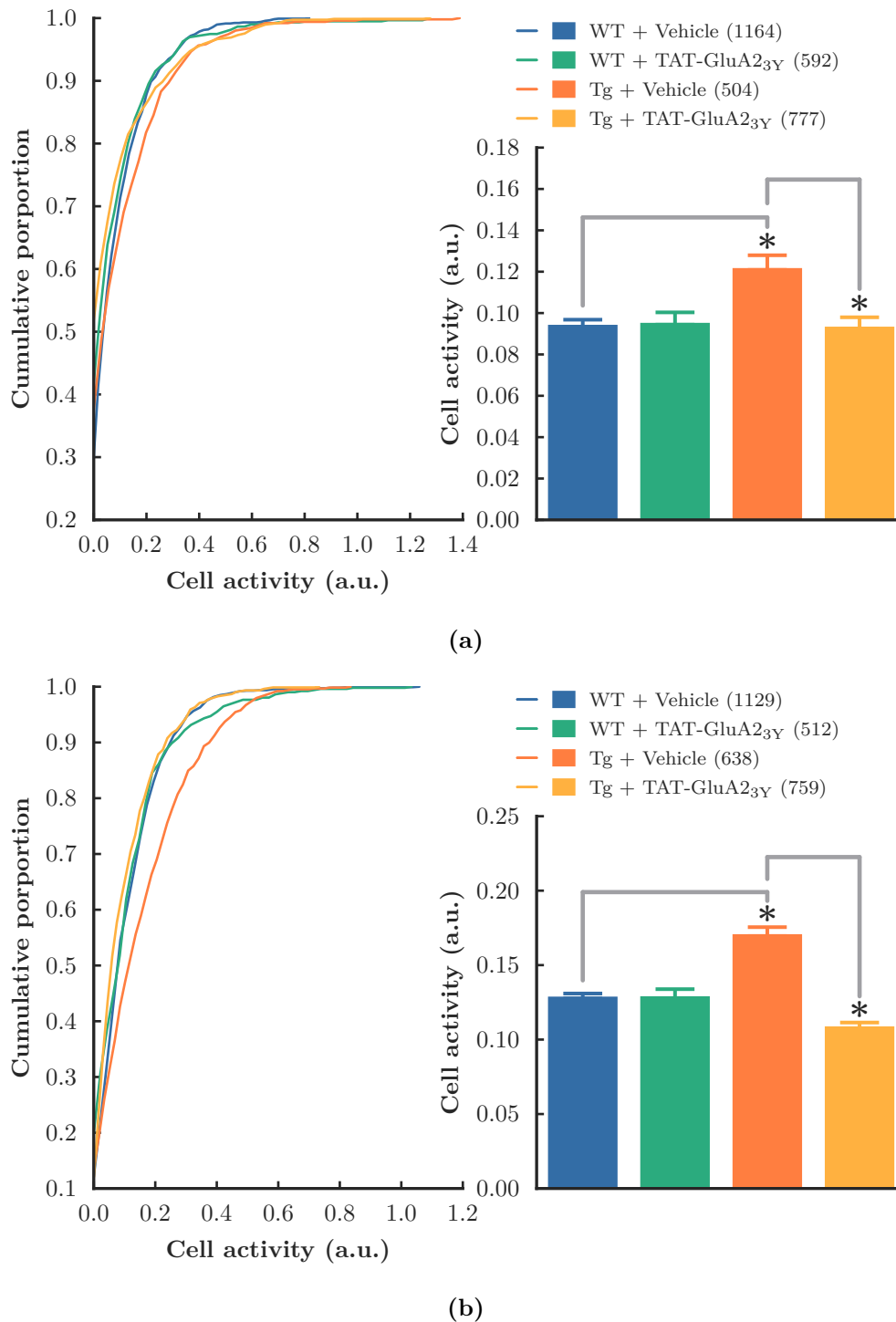
It has been previously shown that amyloid plaques in Tg mice disturb the excitatory-inhibitory balance of cells (Palop and Mucke, 2016). In the CA1, previous reports have found cells to be hyperactive in mouse models of AD. Here we asked whether CA1 cells in Tg mice show hyperactivity, and hypothesized that TAT-GluA<sub>2</sub><sub>3Y</sub> treatment would be able to rescue a hyper-excitable phenotype.

Figure 3.6a shows average cell activity during the training session before foot-shock. During training, two-way ANOVA revealed a significant interaction between *Genotype* and *Treatment* ( $F_{1,3033}=7.7$ ,  $p=0.006$ ), as well as significant main effects of *Genotype* ( $F_{1,3033}=6.2$ ,  $p=0.01$ ) and *Treatment* ( $F_{1,3033}=5.1$ ,  $p=0.02$ ). *Post hoc* tests showed that Tg-Veh animals had significantly higher cell activity (WT-Veh vs Tg-Veh,  $T=-3.72$ ,  $p<0.001$ ), and TAT-GluA<sub>2</sub><sub>3Y</sub> treatment was able to restore average cell activity to WT level. (Tg-GluA<sub>2</sub><sub>3Y</sub> vs Tg-Veh,  $T=-3.58$ ,  $p<0.001$ ; WT-Veh vs Tg-GluA<sub>2</sub><sub>3Y</sub>,  $T=0.14$ ,  $p=0.89$ ). TAT-GluA<sub>2</sub><sub>3Y</sub> did not have any effect on WT mice (WT-Veh vs WT-GluA<sub>2</sub><sub>3Y</sub>,  $T=-0.137$ ,  $p=0.89$ ). This result is consistent with previous reports in the literature (Verret et al., 2012), showing cells in Tg mice have increased overall cell activity. Interestingly, while TAT-GluA<sub>2</sub><sub>3Y</sub> treatment restored the mean cell activity during training, the distribution of cell activity was significantly different from WT (WT-Veh vs Tg-GluA<sub>2</sub><sub>3Y</sub>,  $K=0.16$ ,  $p<0.001$ ). As is shown in the cumulative distribution plot, Tg mice with TAT-GluA<sub>2</sub><sub>3Y</sub> treatment still had a higher proportion of highly active cells.

Similar effect were found during testing (Figure 3.6b). Two-way ANOVA revealed significant interaction of *Genotype* and *Treatment* ( $F_{1,3029}=78.4$ ,  $p<0.001$ ), as well as major effects of *Genotype* ( $F_{1,3029}=32.7$ ,  $p<0.001$ ) and *Treatment* ( $F_{1,3029}=27.4$ ,  $p<0.001$ ). *Post hoc* tests showed a significant increase of cell activity in the Tg-Veh group (WT-Veh vs Tg-Veh,  $T=-10.1$ ,  $p<0.001$ ), and this effect was corrected by TAT-GluA<sub>2</sub><sub>3Y</sub> treatment (WT-Veh vs Tg-GluA<sub>2</sub><sub>3Y</sub>,  $T=0.73$ ,  $p=0.47$ ; Tg-GluA<sub>2</sub><sub>3Y</sub> vs Tg-Veh,  $T=-9.97$ ,  $p<0.001$ ). There was also a trend of increased cell activity after TAT-GluA<sub>2</sub><sub>3Y</sub> treatment in the WT group,

however the p-value is close to threshold after correction for multiple comparisons (WT-Veh vs WT-GluA<sub>2</sub>Y, T=-2.53, p=0.012, threshold = 0.013). Interestingly during testing, TAT-GluA<sub>2</sub>Y was able to fully rescue the hyper-activity in the Tg group (KS test: Veh-WT vs Tg-GluA<sub>2</sub>Y, K=0.06, p=0.07; Tg-Veh vs Tg-GluA<sub>2</sub>Y, K=2.29, p<0.001). These results suggest that the effect TAT-GluA<sub>2</sub>Y treatment is long-lasting: treatment during memory encoding is also able to rescue CA1 hyperactivity in Tg mice during memory testing 24 h later.

Comparing the cell activity between testing and training, we found that Tg mice have significantly increased cell activity during testing, which was not found in WT mice (Figure 3.7; Two-way ANOVA, *Genotype* × *Treatment* interaction  $F_{1,4380}=32.4$ , p<0.001, *Genotype* main effect  $F_{1,4380}=23.0$ , p<0.001, *Treatment* main effect  $F_{1,4380}=23.6$ , p<0.001; *post hoc* test WT-Veh vs Tg-Veh, T=-7.4, p<0.001, WT-Veh vs WT-GluA<sub>2</sub>Y, T=-0.487, p=0.63). TAT-GluA<sub>2</sub>Y treatment blocked increases in cell activity during testing (Tg-GluA<sub>2</sub>Y vs Tg-Veh, T=-7.5, p<0.001). The cumulative plot suggests that Tg mice had similar proportions of cells with increased activity, however in Tg mice the cells increased more than those in WT mice. This result confirms previous reports that mouse models of AD show disrupted excitation-inhibition balance in CA1 (Palop and Mucke, 2016).



**Figure 3.6** Distribution and mean of average cell activity during (a) training before foot shock and (b) memory test. Cells in the Tg mice are significantly more active, and this is rescued by TAT-GluA<sub>2</sub>Y treatment. Cell numbers are listed in the legend with parenthesis. The cell activity are measured in arbitrary units (a.u.).

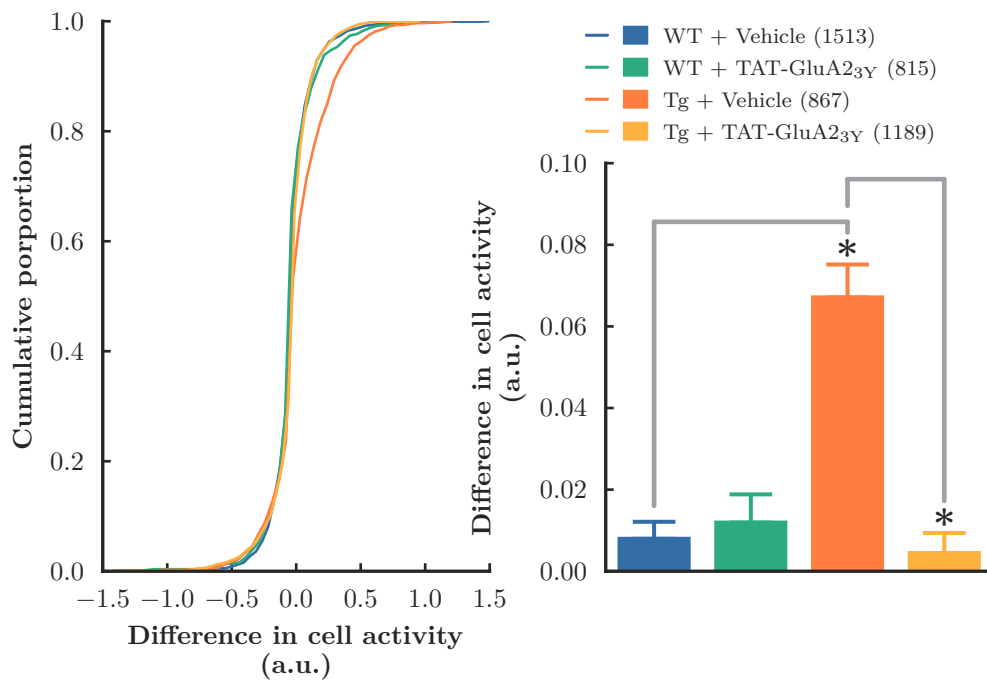


**Figure 3.7** Cell activity difference between training and testing sessions. Tg mice significantly increased their cell activity during testing session, and this is blocked by TAT-GluA23Y treatment.

### 3.3.4 TAT-GluA<sub>2</sub><sub>3Y</sub> rescues contextual fear memory recall by decreasing activity

Given that the Tg mice and WT mice showed different amounts of freezing, it is possible that the observed hyperactivity is a result of these behavioural differences. To control for behavioural state, we investigated the average cell activity when the mice were freezing or not freezing during the 5-min context memory test. The results are summarized in figure 3.8.

A two-way ANOVA on the average activity when mice are freezing showed an insignificant interaction between *Genotype* and *Treatment* ( $F_{1,3034}=-0.03$ ,  $p=0.97$ ). There was a significant main effect of both *Genotype* ( $F_{1,3034}=6.9$ ,  $p=0.008$ ) and *Treatment* ( $F_{1,3034}=18.7$ ,  $p<0.001$ ). *Post hoc* tests showed that cells in the vehicle-treated Tg mice had significantly higher activity than those in WT mice (WT-Veh vs Tg-Veh,  $T=-2.0$ ,  $p=0.04$ ), and this deficit was fully rescued by TAT-GluA<sub>2</sub><sub>3Y</sub> treatment (Tg-GluA<sub>2</sub><sub>3Y</sub> vs Tg-Veh,  $T=-3.1$ ,  $p=0.002$ ; WT-Veh vs Tg-GluA<sub>2</sub><sub>3Y</sub>,  $T=1.4$ ,  $p=0.16$ ). Moreover, TAT-GluA<sub>2</sub><sub>3Y</sub> treatment also significantly decreased cell activity in WT mice (WT-Veh vs WT-GluA<sub>2</sub><sub>3Y</sub>,  $T=3.0$ ,  $p=0.002$ ). These results show that neurons in Tg mice have significantly increased activity during freezing, and TAT-GluA<sub>2</sub><sub>3Y</sub> treatment has a significant inhibitory effect on cell activity both in WT and Tg mice.

For the cell activity when the mice did not show freezing behaviour, we performed a two-way ANOVA, and found a significant *Genotype*  $\times$  *Treatment* interaction ( $F_{1,3029}=13.6$ ,  $p<0.001$ ), as well as a significant main effect of *Treatment* ( $F_{1,3029}=12.3$ ,  $p<0.001$ ). TAT-GluA<sub>2</sub><sub>3Y</sub> treatment only significantly decreased activity in the Tg mice (Tg-GluA<sub>2</sub><sub>3Y</sub> vs Tg-Veh,  $T=-5.4$ ,  $p<0.001$ ), and had no effect on WT mice (WT-GluA<sub>2</sub><sub>3Y</sub> vs WT-Veh,  $T=-0.56$ ,  $p=0.58$ ). These results suggest TAT-GluA<sub>2</sub><sub>3Y</sub> may rescue the Tg phenotype by globally decreasing background cell activity. These results suggest TAT-GluA<sub>2</sub><sub>3Y</sub> treatment is able to decrease cell activity during freezing for both Tg and WT mice, however it also decrease cell activity in Tg when the mouse is not freezing.

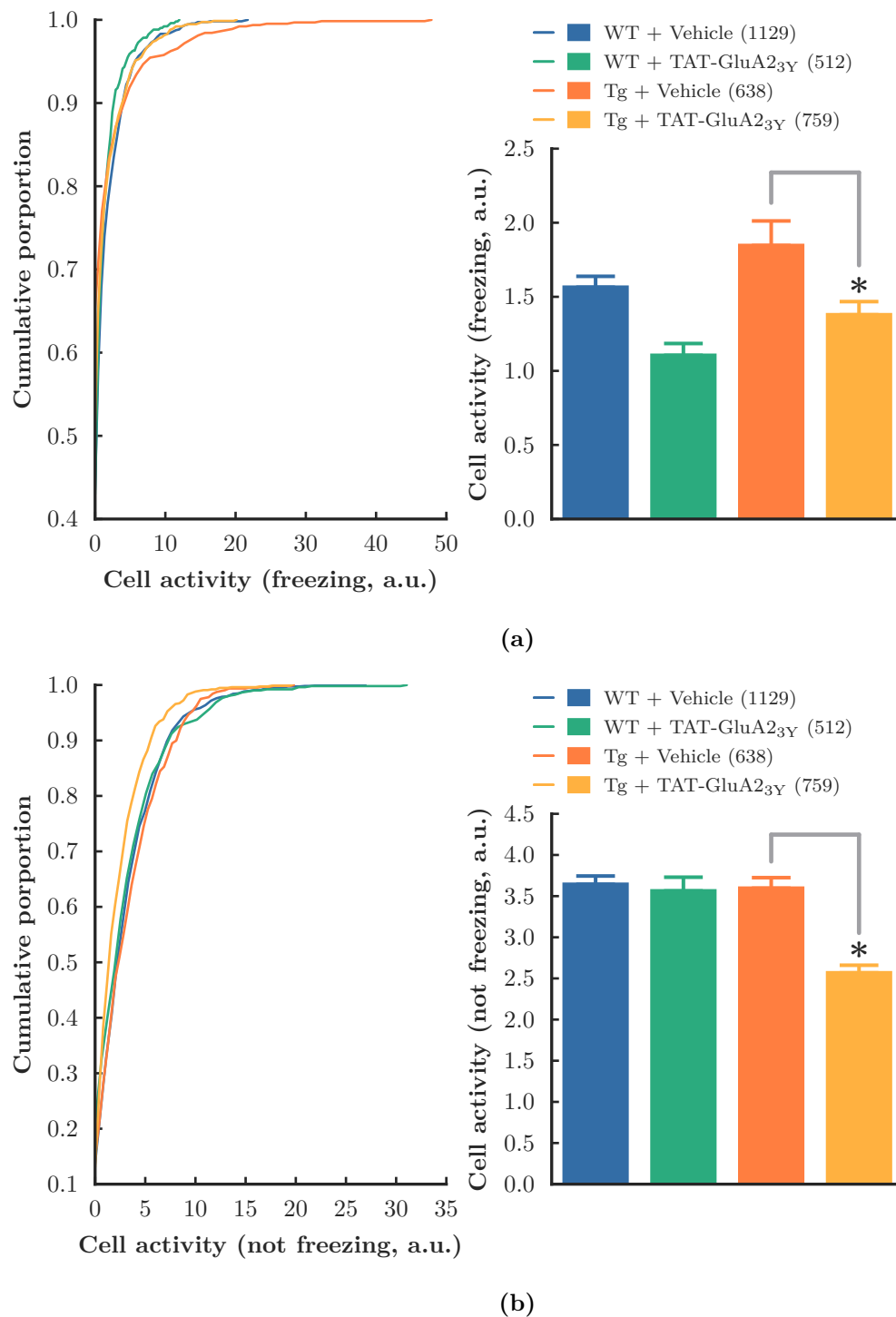


**Figure 3.8** Average cell activity when mice were (a) freezing and (b) not freezing during the 5-min contextual memory test. Cells in Tg mice have significantly higher activity during freezing, and TAT-GluA<sub>2</sub>Y treatment decreases cell activity in both WT and Tg groups. When the mice were not freezing, TAT-GluA<sub>2</sub>Y treatment decreases cell activity only in Tg mice, but has no effect in WT mice. This result suggests that the effect of TAT-GluA<sub>2</sub>Y in Tg mice is a global decrease of cell activity.

### 3.3.5 TAT-GluA2<sub>3Y</sub> rescues freezing encoding deficit in Tg cells

Previous reports have suggested that CA1 neurons in Tg mice have deficits in encoding spatial information (Cheng and Ji, 2013). It is possible that such encoding deficits in AD is a general phenomenon, and also affects contextual fear memory. Therefore we investigated how WT and Tg cells encode freezing.

First we examined cells individually, and calculated the mutual information between the calcium transients and freezing behaviour (Victor, 2002; Ross, 2014). Mutual information captures both linear and non-linear relationships between two random variables and reflects how much predictive power one variable has for another. Following the naming from Skaggs et al. (1993), where the mutual information between cell activity and animal's position is dubbed “spatial information”, here we refer to the mutual information between cell activity and mouse's freezing behaviour as “freezing information”.

The group differences in freezing information were compared using a two-way ANOVA. There was a significant *Genotype*  $\times$  *Treatment* interaction ( $F_{1,4380}=126.7$ ,  $p<0.001$ ), as well as main effects in both *Genotype* ( $F_{1,4380}=254.0$ ,  $p<0.001$ ) and *Treatment* ( $F_{1,4380}=54.7$ ,  $p<0.001$ ). *Post hoc* tests showed the Tg-Veh group to have significantly less freezing information (WT-Veh vs Tg-Veh,  $T=19.3$ ,  $p<0.001$ ), and that this deficit was partially rescued by TAT-GluA2<sub>3Y</sub> treatment (Tg-GluA2<sub>3Y</sub> vs Tg-Veh,  $T=13.2$ ,  $p<0.001$ ), as the Tg-GluA2<sub>3Y</sub> group had significantly less freezing information than WT-Veh group (WT-Veh vs Tg-GluA2<sub>3Y</sub>,  $T=6.0$ ,  $p<0.001$ ; Figure 3.9). WT-GluA2<sub>3Y</sub> had significantly less freezing information than WT-Veh, although the significance was close to threshold (WT-Veh vs WT-GluA2<sub>3Y</sub>,  $T=2.5$ ,  $p=0.011$ , threshold=0.013). This result suggests that in the Tg group, individual cell activity in hippocampus CA1 is not a good predictor of the mouse's freezing behaviour. This is partially recovered by TAT-GluA2<sub>3Y</sub> treatment.

Given that CA1 cells are known to encode place, and Tg mice have deficits in spatial encoding, it is possible the differences in spatial encoding confounded the freezing information measurement. Moreover, Tg mice have low levels of freezing during the memory

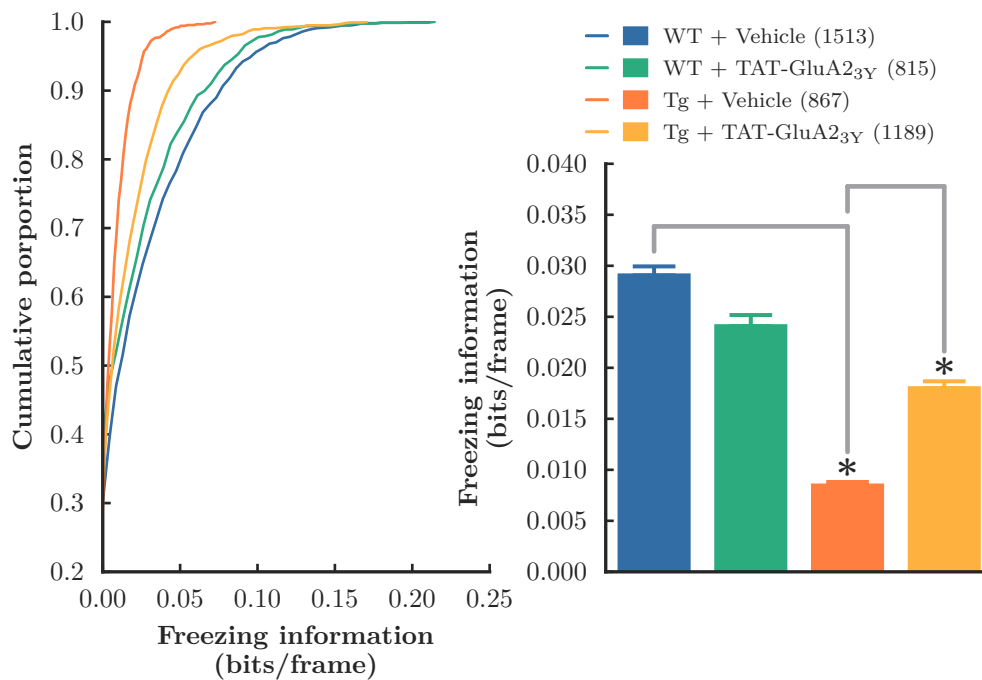


**Figure 3.9** Freezing information during the context memory test. This measurement represents how much information a particular cell has in a period of time about whether the mouse is freezing. Cells in Tg mice encode significantly less freezing information than the WT groups, and TAT-GluA23Y treatment can only partially rescue the effect.

test. It is possible that mice with low levels of freezing, therefore weaker memory, have deficits in freezing encoding in the cells. That is, the difference of freezing information in Tg may be the result of weaker memory instead of a specific deficit due to the expression of the transgene. To eliminate the effect of the mouse's position, we calculated the average freezing information for all mouse positions, therefore eliminating the contribution of place. To control for the potential effect of freezing level, we have included it as a covariate in the two-way ANOVA.

The result is similar to the freezing information observed in Figure 3.9 (Figure 3.10). There was a significant interaction between *Genotype* and *Treatment* ( $F_{1,4380}=97.9$ ,  $p<0.001$ ), as well as significant main effects in *Genotype* ( $F_{1,4380}=139.4$ ,  $p<0.001$ ) and *Treatment* ( $F_{1,4380}=100.3$ ,  $p<0.001$ ). Furthermore, this test revealed that the freezing level was not a significant confounding factor ( $T=-0.65$ ,  $p=0.50$ ) for freezing information. Again, *post hoc*

tests showed that Tg-Veh cells had significantly lower freezing information with position controlled (WT-Veh vs Tg-Veh,  $T=15.1$ ,  $p<0.001$ ), and this deficit was fully rescued by TAT-GluA2<sub>3Y</sub> (Tg-GluA2<sub>3Y</sub> vs Tg-Veh,  $t=13.9$ ,  $p<0.001$ ; WT-Veh vs Tg-GluA2<sub>3Y</sub>,  $t=1.9$ ,  $p=0.06$ , threshold=0.013). This result suggests that the deficit of freezing encoding in Tg mice is independent of the mouse's position in space and freezing levels during the memory test session.

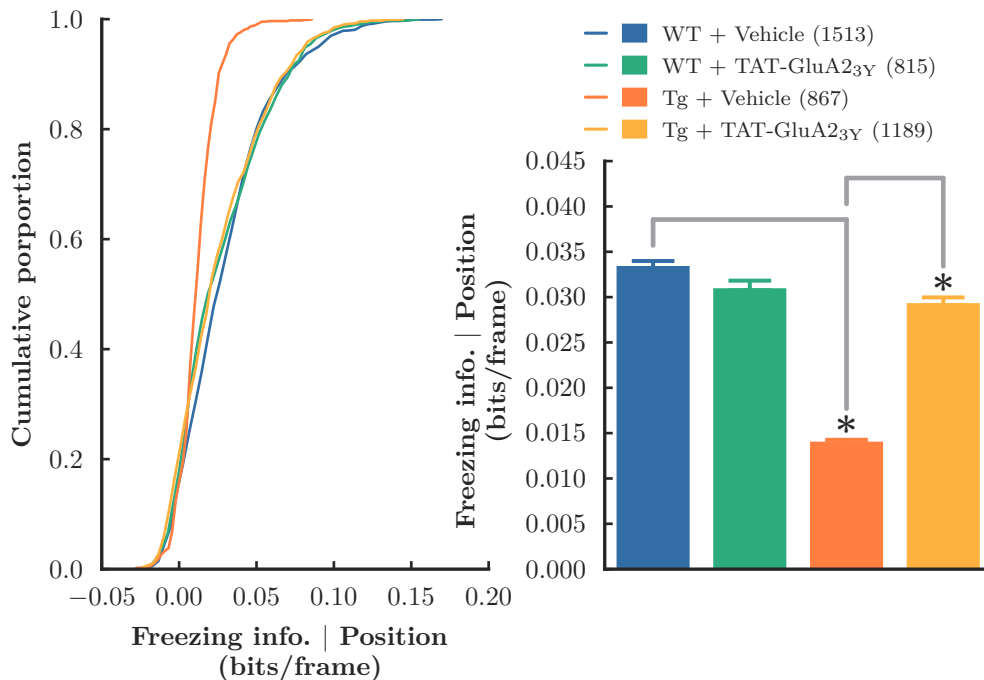


**Figure 3.10** Freezing information encoded in cells is not reliant on mouse position or freezing level. This measurement removes the effect of position from our freezing information measurement. This result is similar to Figure 3.9. This suggests that the position of the mouse is not a confounding factor for our freezing information measurement.

### 3.3.6 Network encoding of freezing behaviour

While all the measurements we have performed thus far consider each cell individually, we must also ask whether the activity of these cells are independent of each other, or if some degree of information is encoded in the coordination between them. To answer this question, we took advantage of machine learning algorithms. A NBC models the cells as

independent of each other, and therefore uses the neural signatures in individual cells for prediction. A universal classifier such as gSVM on the other hand, is able to take advantage of information encoded by individual cells as well as the ensemble of cells. To investigate whether the neural signature of recalling a contextual fear memory (as measured by freezing behaviour) is encoded by the cells individually or at the network, we trained both an NBC and a gSVM to predict freezing behaviour from calcium transients at each time point. The performance of NBC represents the prediction power encoded independently in cells, and the performance of gSVM represents total prediction power of the network.

The result is shown in Figure 3.11. A three-way ANOVA of *Genotype*  $\times$  *Treatment*  $\times$  *Classifier* was carried out. We found a significant main effect of *Classifier* ( $F_{1,51}=60.8$ ,  $p<0.001$ ), and no other significant interactions or main effects. This result shows that gSVM significantly outperforms the NBC classifier across all treatment groups, suggesting that the network encodes more information about freezing than the cells individually. Moreover, unlike the information content for individual cells, both NBC and gSVM have the same performance across all genotype and treatment groups. This suggests that with the activity of multiple cells, the deficits in information content in Tg mice are compensated.

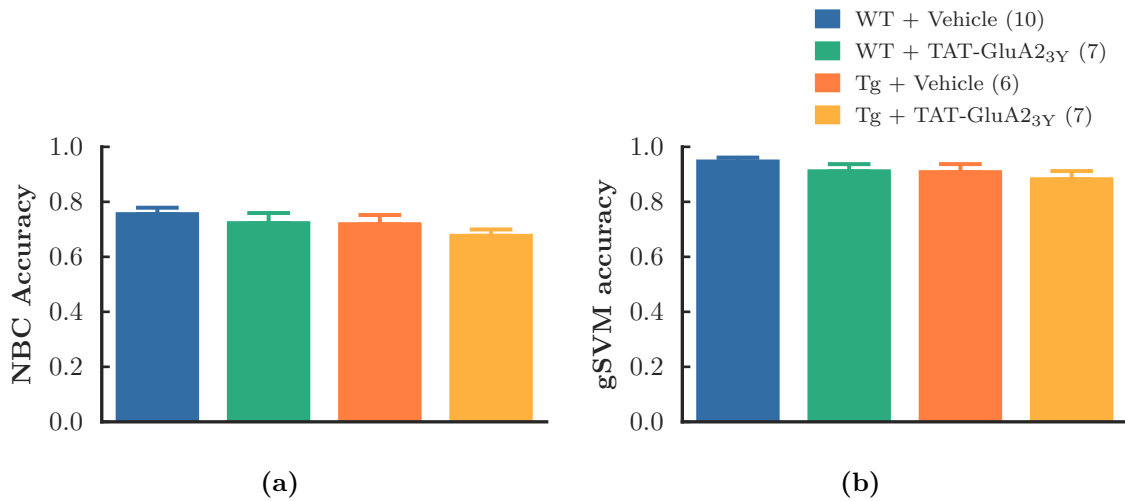


**Figure 3.11** Performance of (a) NBC and (b) gSVM in predicting freezing from cell activity. Since NBC assumes the cells are independent and gSVM is more general, the performance difference between the two suggests a portion of freezing information is encoded at the network level. Both NBC and gSVM perform similarly across all groups, suggesting that the deficit in information content in Tg mice can be compensated by the network activity.

### 3.3.7 Freezing encoding precedes freezing behaviour

We next examined whether freezing encoding in the network precedes freezing onset. We plotted average prediction accuracy for the classifiers at the time mice transition into freezing. We hypothesized that if the neural signature for freezing behaviour in the network precedes the behaviour, the classifiers will predict freezing earlier than behavioural onset, which will result in a reduction in prediction accuracy before behavioural onset.

We used Bayes modeling (Figure 3.12) to detect whether the prediction accuracy changes before behaviour change, and compared change points between groups. The result is summarized in Figure 3.13. We found very strong evidence for a change point in NBC performance in every group (all Bayes factors  $BF_{10} > 5 \times 10^4$ ). The change point appeared  $3.4^{+0.1}_{-0.1}$ s in WT-Veh,  $2.8^{+0.1}_{-0.1}$ s in WT-GluA23Y,  $2.8^{+0.2}_{-0.3}$ s in Tg-Veh, and  $2.6^{+0.1}_{-0.1}$ s in Tg-GluA23Y before freezing onset (uncertainties are 95 % credible intervals). Pairwise comparisons showed very strong evidence that the change point in WT-Veh occurred earlier than

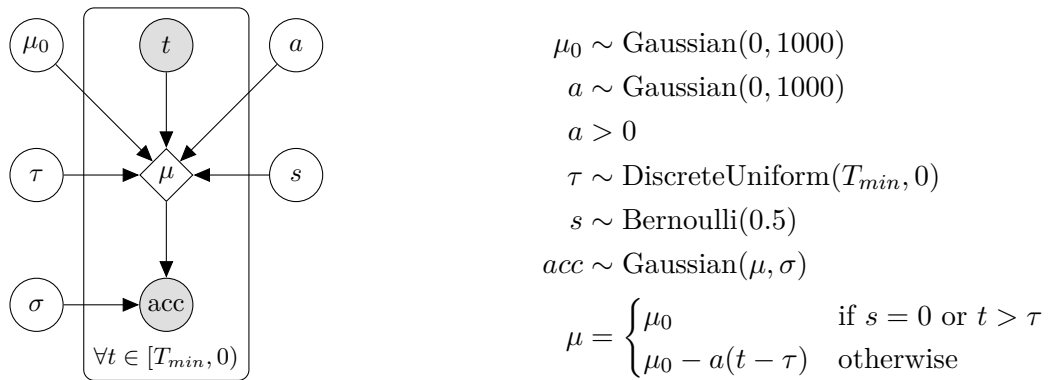


**Figure 3.12** Bayes model for change point detection. The accuracy is modelled as a Gaussian distribution with mean as a function of time and constant variance. In the null hypothesis, the mean is constant and estimated from the data. In the alternative hypothesis, the mean is modelled as constant up to the change point, then as a linear function of time with a negative slope. A Bernoulli variable *selector* is estimated to choose from each of the hypothesis. All variables have non-informative priors

the other three groups, while the other three groups occurred at the same time (WT-Veh vs WT-GluA<sub>2</sub>Y,  $BF_{10} > 250$ ; WT-Veh vs Tg-Veh,  $BF_{10} = 7.5$ ; WT-Veh vs Tg-GluA<sub>2</sub>Y,  $BF_{10} > 250$ ; all other comparisons  $BF_{10} < 0.2$ ). Since NBC regards each cell independently, this result suggests that the freezing signal in individual cells occurs earlier than the onset of freezing behaviour.

On the other hand, we found very strong evidence for a change point in gSVM performance in WT-Veh ( $BF_{10} > 5 \times 10^4$ ), WT-GluA<sub>2</sub>Y ( $BF_{10} > 5 \times 10^4$ ) and Tg-GluA<sub>2</sub>Y ( $BF_{10} > 5 \times 10^4$ ), and also strong evidence for the lack of a change point in Tg-Veh mice ( $BF_{10} < 0.02$ ). The change points were estimated to be  $0.6^{+0.0}_{-0.1}$ s in WT-Veh,  $2.6^{+0.2}_{-0.3}$ s in WT-GluA<sub>2</sub>Y, and  $0.3^{+0.1}_{-0.2}$ s in Tg-GluA<sub>2</sub>Y, before the freezing onset. Pairwise comparisons showed very strong evidence of an earlier change point in WT-GluA<sub>2</sub>Y than the other groups (WT-GluA<sub>2</sub>Y vs WT-Veh,  $BF_{10} > 250$ ; WT-GluA<sub>2</sub>Y vs Tg-GluA<sub>2</sub>Y,  $BF_{10} > 250$ ). There is minimal evidence that the change point in WT-Veh was earlier than Tg-GluA<sub>2</sub>Y ( $BF_{10} = 2.5$ ). These results suggest that the network neural signature for freezing occurs earlier than freezing behaviour in WT groups. However this neural code is not detected in the Tg group. TAT-GluA<sub>2</sub>Y treatment of the Tg mice is able to partially rescue

this effect. In addition, the network freezing signal occurs earlier in WT-GluA<sub>2</sub>Y than the other groups. These results suggest that TAT-GluA<sub>2</sub>Y treatment helps strengthen the network signal, both in WT and Tg mice.

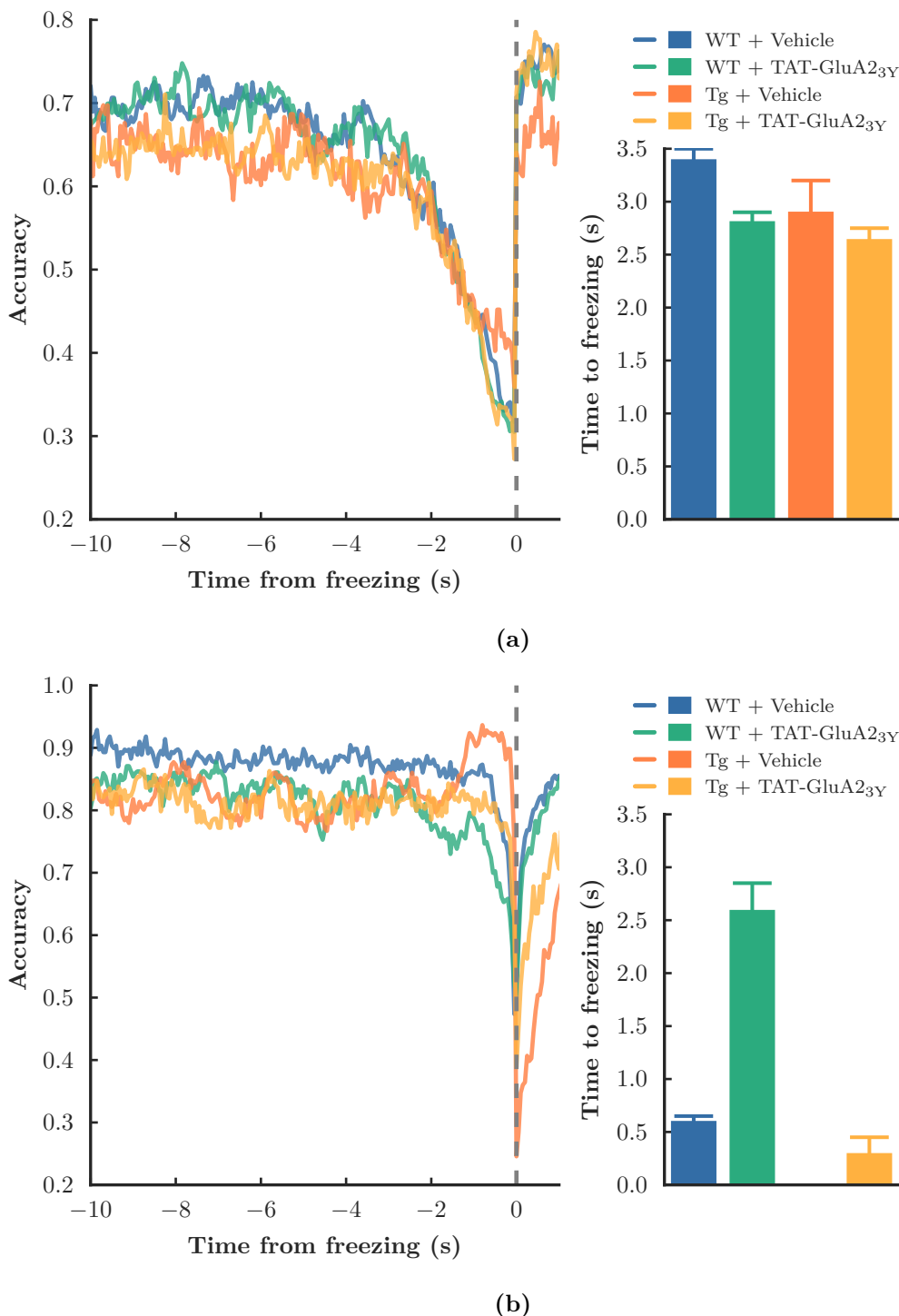


**Figure 3.13** Average accuracy of classifiers at the beginning of freezing behaviour in mice during the context memory test. For WT and Tg-GluA2<sub>3Y</sub> groups, both NBC and gSVM shows significantly decreased performance just before the mice show freezing behaviour. This suggests that CA1 neural activity drives freezing behaviour. The error bars on the top shows 95 % credible interval of the change point, if the alternative hypothesis is favoured.

### 3.3.8 Memory recall in Tg mice is unstable

Our results show that Tg mice have shorter freezing bouts, and suggest that Tg mice may have an unstable representation of contextual fear memory, and may be unable to maintain the expression of this fear memory. Here we directly tested the robustness of the representation of fear memory expression in CA1. Using the gSVM classifier, we calculated the distance of the brain state to the gSVM classification boundary. We hypothesized that if Tg mice have an unstable representation of fear memory, their brain state during freezing will be closer to the classification boundary than the WT mice.

The result is shown in Figure 3.14. We found at the initiation of freezing behaviour, the neural state of WT mice fell into the freezing classification boundary, as is shown with a significant negative distance. However in the Tg mice, the network state stayed close to the classification boundary. This result suggests that a small perturbation is more likely to shift the Tg mouse network state out of freezing, and this may result in a corresponding change of behavioural state from freezing to not freezing. This result suggests that the CA1 network state in Tg mice is unstable. TAT-GluA2<sub>3Y</sub> treatment is able to rescue this deficit.

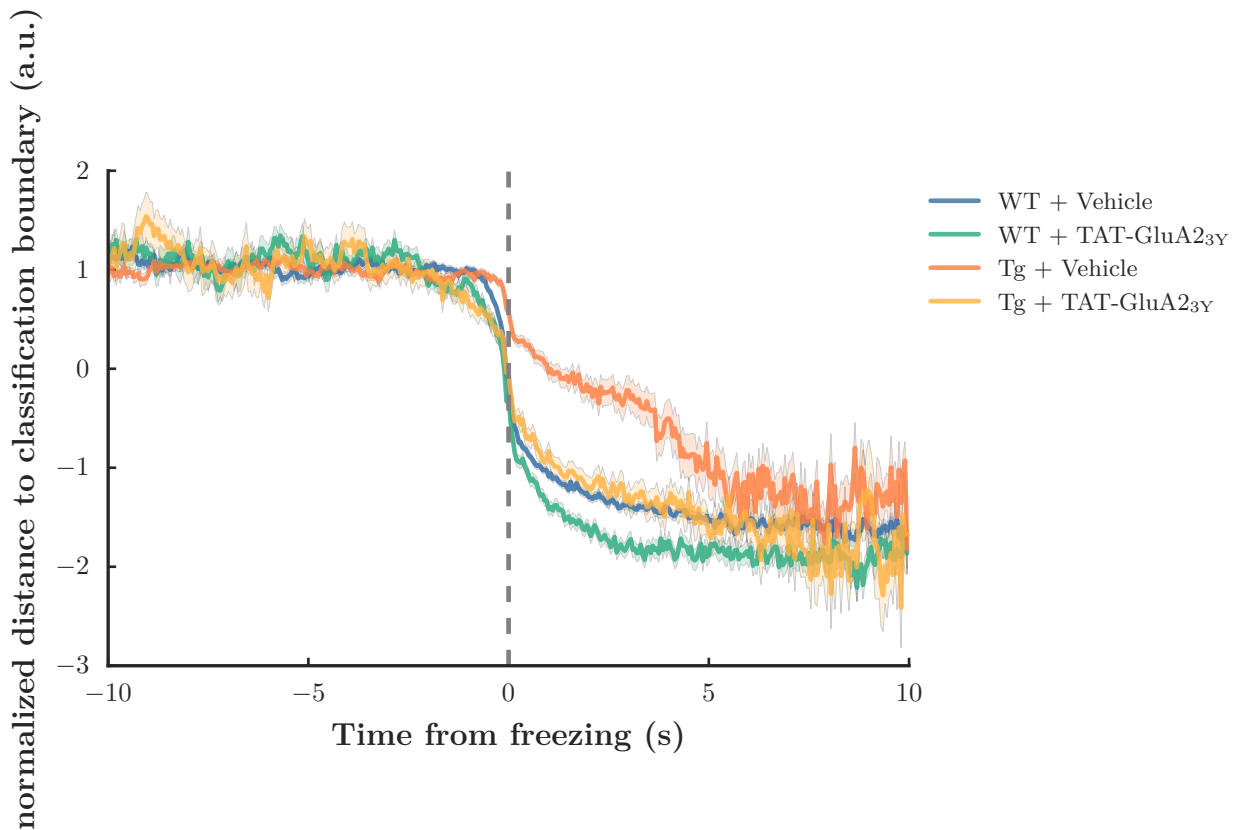


**Figure 3.14** The normalized distance to the gSVM classification boundary. A positive distance represents the network state of not freezing, and a negative distance represent the network state of freezing. We found during freezing, the network state of the WT groups are deep in the freezing state, while the Tg mice show a network state close to the classification boundary. This suggests that the freezing state in the Tg CA1 network is more likely to be disrupted by small perturbations in the network. TAT-GluA2<sub>3Y</sub> treatment during training is able to rescue this deficit in Tg mice.

### 3.3.9 Memory deficits in Tg mice are not a result of forgetting

Recent studies have suggested that the memory deficit in early AD may not be a result of forgetting, as a previously learned memory in a mouse model of AD can be artificially reactivated (Roy et al., 2016). Given that we are able to detect a neuronal signature for freezing in our Tg mice, and they are able to initiate freezing as often as WT mice, we hypothesized that they still retain a representation of the fear memory, and their memory deficit is not a result of forgetting.

To test this hypothesis, we trained WT and Tg mice treatment-free, and 3 d later, treated mice with TAT-GluA<sub>2</sub>Y or saline vehicle when they were briefly exposed to the training context as a reminder. The memory test occurred 24 h later. The result is summarized in Figure 3.15. We found no significant interaction between *Genotype* and *Treatment* ( $F_{1,43}=1.3$ ,  $p=0.2$ ), but significant main effects of *Genotype* ( $F_{1,43}=9.02$ ,  $p=0.004$ ) and *Treatment* ( $F_{1,55}=7.3$ ,  $p=0.010$ ). *Post hoc* tests showed that Tg-Veh had a significant memory deficit (Tg-Veh vs WT-Veh,  $T=2.92$ ,  $p=0.006$ ), however this deficit was fully rescued by TAT-GluA<sub>2</sub>Y treatment (Tg-GluA<sub>2</sub>Y vs Tg-Veh,  $T=2.61$ ,  $p=0.012$ ; WT-Veh vs Tg-GluA<sub>2</sub>Y,  $T=0.11$ ,  $p=0.91$ ). This result suggests that Tg mice retain a neural representation of the fear memory for at least 3 days, therefore the memory deficit 1 day after training is not a result of forgetting. In addition, the memory deficit can also be rescued with TAT-GluA<sub>2</sub>Y treatment if the mouse is exposed to a reminder.

We then investigated whether the effect of the TAT-GluA<sub>2</sub>Y was memory specific. In a separate cohort of mice, we used a protocol similar to Figure 3.15, except the mice received TAT-GluA<sub>2</sub>Y in their home-cage instead of the reminder context (Figure 3.16). In this case, the TAT-GluA<sub>2</sub>Y treatment did not have any effect on memory recall. There was no significant interaction between *Genotype* and *Treatment* ( $F_{1,43}=0.2$ ,  $p=0.66$ ), however there was a significant main effect of *Genotype* ( $F_{1,43}=45.1$ ,  $p<0.001$ ), but no significant effect of *Treatment* ( $F_{1,43}=0.11$ ,  $p=0.74$ ). This suggests that TAT-GluA<sub>2</sub>Y treatment has no effect without the presence of the reminder. Together, these two results suggest that Tg mice can

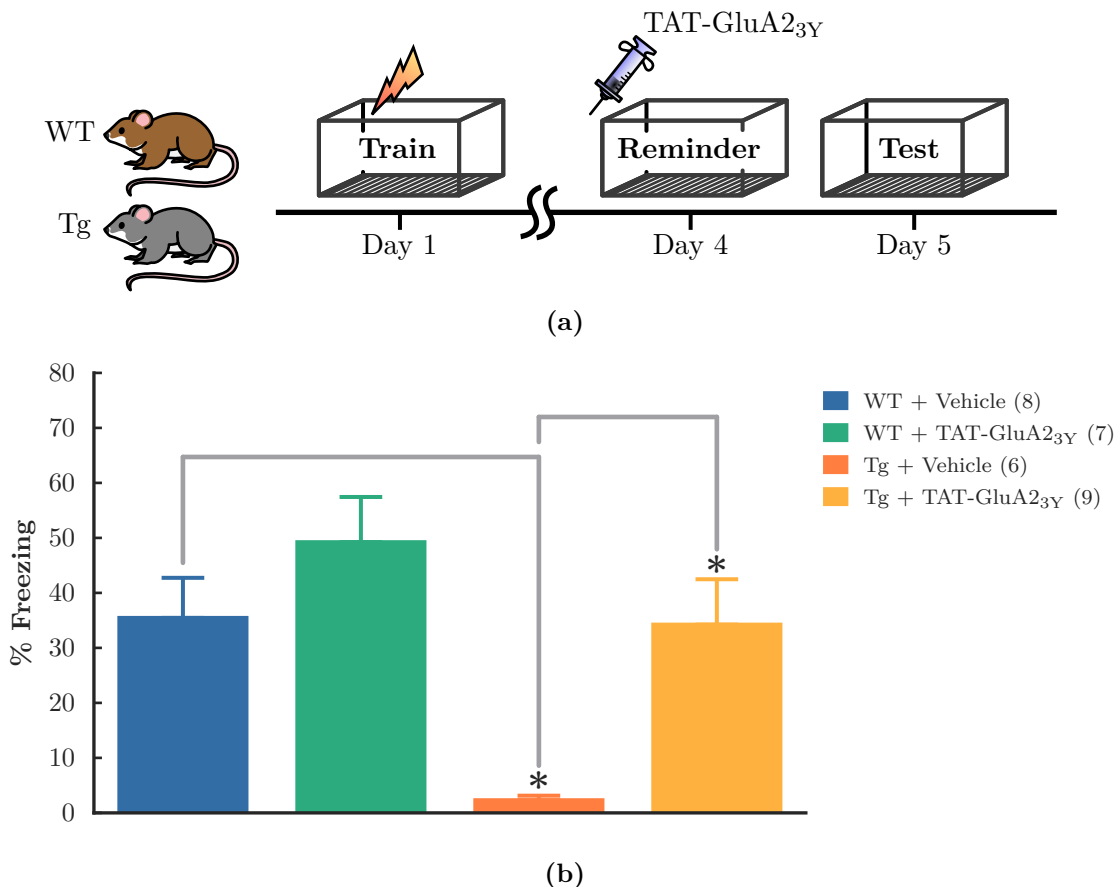


**Figure 3.15** Tg mice retained a representation of fear memory for at least 3 days. WT and Tg mice were contextual fear conditioned, given a reminder 3 days later with treatment and tested on the following day. Tg mice showed significantly less freezing. This effect was rescued by TAT-GluA2<sub>3Y</sub> treatment.

retain a neural representation of the fear memory, can therefore the memory deficit is not due to forgetting. The TAT-GluA2<sub>3Y</sub> treatment during exposure to a reminder can rescue this deficit.

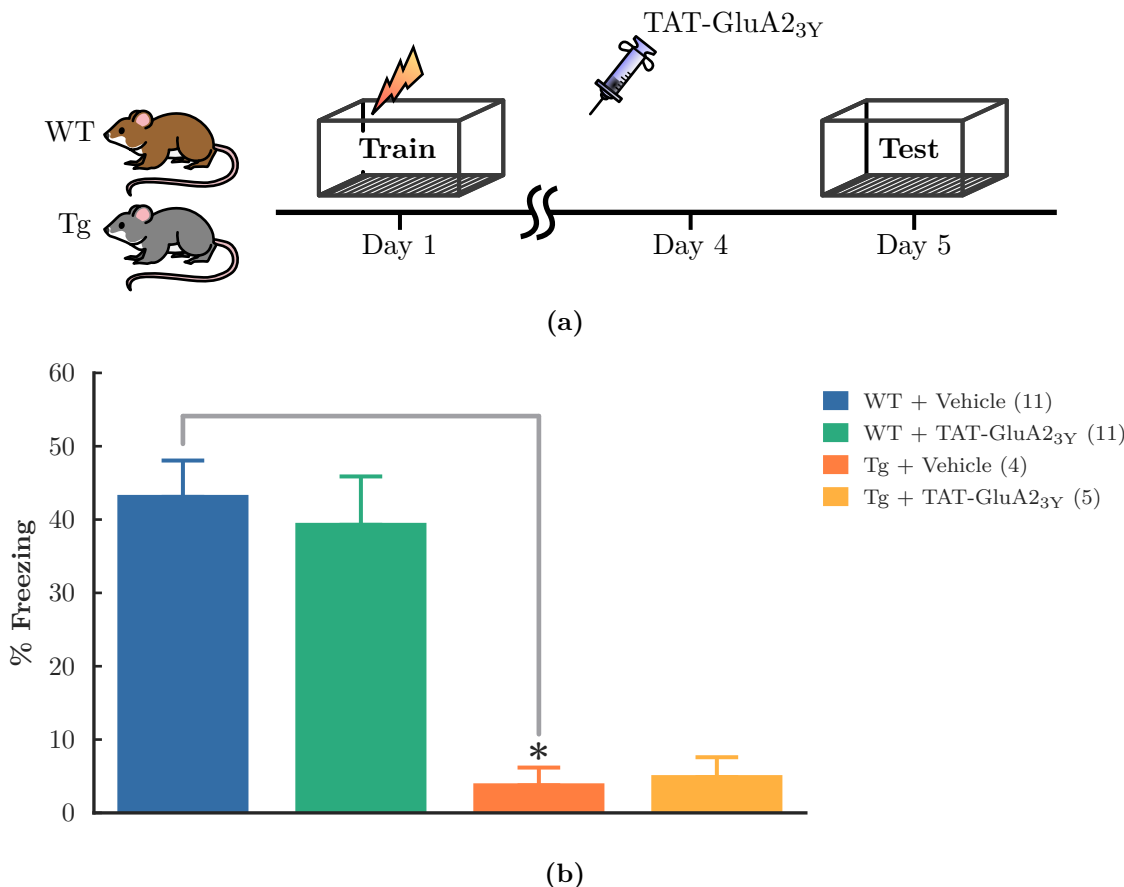


**Figure 3.16** TAT-GluA<sub>23Y</sub> does not rescue memory recall without reminder. WT and Tg mice were contextual fear conditioned, given treatment 3 d later in their home cages and tested on the following day. TAT-GluA<sub>23Y</sub> treatment without reminder is unable to rescue recall deficit in Tg mice.

### 3.4 Discussion

In the current project, we took advantage of our custom built miniature microscope to record CA1 cells in WT and a mouse model of early AD, TgCRND8 mice, during contextual fear conditioning. We found a significant memory deficit in TgCRND8 mice. Correlated with the memory deficit, we also discovered that the TgCRND8 mice have hyperactive CA1 neurons. Compared to the WT mice, the CA1 neurons in TgCRND8 mice contain reduced information content about the mouse's behavioural state of memory recall. This reduction of information content was independent of spatial encoding and the strength of memory (as

measured by proportion of time the mouse spent freezing), suggesting that the reduction in information content is related to the specific fear memory deficit in the TgCRND8 mice.

To investigate ensemble encoding of the fear memory, we trained machine learning classifiers to predict, at each time point, the behavioural state of memory recall using the calcium activity of the neurons. To differentiate the cellular and network activity, we used NBC and gSVM and compared results obtained from both classifiers. NBC is only able to detect signals when each neuron is treated as independent from others, while gSVM, being a general classifier, is able to utilize all available information, including those both at the individual cell level, and also information stored in the higher order relationship between the activity of cells.

The first finding from the prediction accuracy of the classifiers is that the classifiers were able to decode at similar accuracy level between TgCRND8 and WT mice. This is in contrast of our mutual information content result, which suggests that individual cells in the Tg mice have a deficit in encoding memory recall. These two results suggest that although the physiology of individual cells are significantly impacted by the TgCRND8 phenotype, neurons as a network can largely compensate and perform information encoding. This is also supported by the finding that the gSVM performs significantly better than the NBC, suggesting that a significant portion of the information for memory recall is stored in the cooperative activity of neurons.

Previous studies have established that the neural activity in CA1 is both necessary and sufficient for contextual fear conditioning. Early studies has shown that inhibition or lesion CA1 hippocampus, either before or after training, is detrimental for contextual fear conditioning (Maren, 2001). The sufficiency of CA1 activity in contextual fear conditioning has recently been demonstrated (Ryan et al., 2015; Roy et al., 2016), where the authors labelled CA1 neurons active during contextual fear conditioning, and shows that reactivating the same set of neurons is able to reactivate the contextual fear memory. These results suggest that a neural signature for the fear memory is present in the CA1 neural activity, and therefore can be detected by a universal classifier.

However while the NBC and gSVM are able to detect neural signature of the fear memory, the neural signature the classifiers learned may not be exclusively represent the contextual fear memory. Neural activity which correlates to physiological and other undetected behavioural processes, as long as it is predictive to the freezing behaviour of the mice, may also be learned by the classifiers. Inclusion of these extra patterns does not affect our conclusion, since these patterns are still results of fear memory recall, and just like freezing behaviour, can be regarded as part of the neural signature for the *expression* of fear memory.

To investigate how the degradation of cell firing in CA1 neurons of TgCRND8 mice contributes to their memory deficit, we then investigated whether the important circuit function of hippocampus, pattern completion, which is necessary for memory recall, is affected in the TgCRND8 mice. The Marr model and more recent empirical evidence (Rolls, 2013b; Neunuebel and Knierim, 2014) suggest that while CA3 is the major site in hippocampus where pattern completion occurs, however the input–output difference in CA1 is relatively linear (Neunuebel and Knierim, 2014; Knierim and Neunuebel, 2016). Therefore, the pattern completion process should also be reflected in CA1 activity, and can be detected in our recording.

To observe the pattern completion process, we have aligned the classifier performances to the time when mice begin to freeze. In NBC, we observed a decrease in prediction accuracy just before the mice start to freeze. The decrease of prediction accuracy is a result of the classifier misclassifying non-freezing to freezing. This shows that the classifier starts to predict the mice freezing just before the behavioural change. There is no between-group difference in the NBC prediction accuracy, however while the WT group shows similar prediction precedence in gSVM, this precedence is missing for gSVM prediction in the TgCRND8 mice.

It is worth noting that, here we used trained classifiers as detectors for the freezing neural signature, and our goal was to investigate whether neural signature of freezing appears before behaviour onset. Although we have found that the machine learning classifiers predict freezing ahead of time, we have not investigated whether the neural signature lead any

other behavioural changes such as exiting freezing state. This is primarily because the mice showed a range of different behaviour upon the end of freezing period, including moving, grooming, rearing and sniffing, and these different behaviours may have different dynamics in the CA1 neural activity. However, if there was a global precedence of CA1 activity on behaviour change, it could be detected by training and testing the machine learning classifier with different time lags. The distribution of classifier accuracy across different time lags can reveal information of any global precedence of neural activity signature for behaviour.

Since the classifiers were trained to recognize specific neural activity patterns for the fear memory, the precedence of classifier prediction to behaviour suggest that the CA1 activity pattern for the fear memory leads behaviour. The gradual rise of the classifier's prediction before freezing also suggests that patterns of fear memory arise dynamically: the fear memory pattern starts as a partial pattern which can only barely detected by the classifier, and this gradually develops into a full pattern which biases the prediction of the classifier.

The difference of temporal dynamics of the "pattern completion" process also hints at the underlying dynamic mechanism of the process. Since the NBC is only able to detect activity patterns at the individual cell level, the rise of fear prediction in NBC suggests that individual cells start show the firing pattern of the fear memory. On the other hand, the gSVM detects network pattern, which is composed of synchronized activity of individual cells. We have found the NBC prediction precedes the gSVM prediction, suggesting that the fear memory pattern in the CA1 starts as an incomplete pattern composed of unsynchronized individual cell activity, and as the cellular pattern completes, it leads to synchronized network activity, and is detected by the gSVM later on.

The difference between the TgCRND8 and WT mice can also be interpreted in this framework. The TgCRND8 mice displayed similar dynamics in NBC, suggesting that the cellular signals are not affected. However, the absence of a dynamic pattern completion process in the gSVM suggests that while individual cells are able to respond to the initiation of a fear memory, the cells are unable to coordinate to form a network pattern.

The inability of the TgCRND8 mice to coordinate and form a network pattern is better shown in Figure 3.14, where we investigated the relative distance of network state to the gSVM classifier boundary. Given the high accuracy of the gSVM prediction, the gSVM classifier boundary can approximate the actual behaviour state transition boundary. We found that TgCRND8 mice approached the fear memory state boundary later, and also more shallowly than WT mice, further confirming a deficit in the pattern completion process.

Interestingly, treating the TgCRND8 mice with TAT-GluA<sub>2</sub><sub>3Y</sub> during memory formation was able to rescue the cellular, network, and behavioural deficits we have found. TgCRND8 mice with TAT-GluA<sub>2</sub><sub>3Y</sub> treatment were able to show normal expression of fear memory. The TAT-GluA<sub>2</sub><sub>3Y</sub> treatment was able to decrease the cell excitability of TgCRND8 mice, and allow the activity of the cells to be as informative as WT mice about the behavioural state of the memory recall. Moreover, the TAT-GluA<sub>2</sub><sub>3Y</sub> treatment was also able to rescue the pattern completion deficit.

Some of the effects of the TAT-GluA<sub>2</sub><sub>3Y</sub> treatment were also observed on WT mice. While the TAT-GluA<sub>2</sub><sub>3Y</sub> treatment had no effect on the overall cell activity in WT mice, when we control movement of the mice and only compare cell activity during freezing, we found TAT-GluA<sub>2</sub><sub>3Y</sub> decreases cell activity even in WT mice. Moreover, TAT-GluA<sub>2</sub><sub>3Y</sub> treatment in WT mice also led the classifier to predict freezing earlier than vehicle-treated WT mice, which is evidence for an enhancement of the pattern completion process.

The deficits seen in TgCRND8 mice could be the result of a deficit in memory, or a pathologically enhanced forgetting. To test this hypothesis, we trained WT and TgCRND8 mice, and only treated the mice with vehicle or TAT-GluA<sub>2</sub><sub>3Y</sub> three days later when mice were briefly exposed to a reminder. The memory was tested on the following day. We found that while TgCRND8 mice show a memory deficit, TAT-GluA<sub>2</sub><sub>3Y</sub> treatment during reminder is able to completely rescue the memory deficit. However interestingly, the presence of the reminder is crucial for the rescuing effect of TAT-GluA<sub>2</sub><sub>3Y</sub>, as TAT-GluA<sub>2</sub><sub>3Y</sub> treatment when mice are in their home cage does not have an effect on memory recall.

These two results suggest that first, TgCRND8 mice are still able to form a stable rep-

resentation of the contextual fear memory which last for at least 3 days. Since if this was not the case, TAT-GluA2<sub>3Y</sub> treatment with reminder should not have any rescuing effect, as the memory would not be present at that time point. Therefore, these results suggest that the memory deficit in the TgCRND8 mice is not a result of pathologically enhanced forgetting, but that they were unable to recall the encoded memory representation.

This conclusion suggests two possibilities. First, it is possible that the TgCRND8 mice has a deficit in memory encoding. These mice may only be able to encode a memory representation which is too weak to be recalled. TAT-GluA2<sub>3Y</sub> treatment during training or reminder strengthens this memory representation, and therefore rescues the deficit. A second possibility is that the TgCRND8 mice has a deficit in memory recall. In this case, even if they are able to encode memory unaffected by AD, they may not be able to recall them, potentially due to a deficit in the pattern completion process. In this case, TAT-GluA2<sub>3Y</sub> treatment during training and reminder sessions makes the memory representation even stronger, and this additional strength of memory representation in CA1 compensates for a lack of pattern completion process.

An acute mouse model of AD will be required to tease these two possibilities out, for example, by viral expression or direct infusion of A $\beta$  in CA1. If the mice can recall any memory formed before A $\beta$  infusion, it suggests that the memory deficit in AD is due to memory encoding deficit. On the other hand if there is a deficit in recalling a normally encoded memory, it suggests that the disruption of memory recall process leads to the memory deficit in AD.

In conclusion, we have found that TgCRND8 mice were able to form a contextual fear memory, however were unable to recall it. This deficit was accompanied by a hyperactive CA1 and decreased information content in CA1 cells. While behavioural information could still be decoded using activity of a neural population, cells in TgCRND8 mice were unable to pattern complete a contextual fear memory. This deficit may explain the recall deficit in these mice. Moreover, all deficits could be rescued by TAT-GluA2<sub>3Y</sub> treatment during training. Given the effect of TAT-GluA2<sub>3Y</sub> on synaptic strengthening, the current study

is able to link synaptic functions to neural circuits in CA1, and ultimately behaviour. While the mechanism by which synaptic function creates changes in CA1 neural circuit function is still unclear, this study creates a potential link of between circuit function and analysis at the molecular and behavioural scale. It further demonstrates the importance of understanding circuit function in the study of AD, and suggests a potential novel treatment target for AD at a neural circuit level.



# 4

## GENERAL DISCUSSION

---

### 4.1 Construction of the mini-microscope

#### 4.1.1 Advantages of the current mini-microscope

In the current project, we have constructed a miniature microscope which weighs less than 3 g. The light weight of the mini-microscope allows for its implantation on mice without causing significant alterations to their natural behaviour. This miniature microscope is able to image green fluorescence at a resolution of at less 2  $\mu\text{m}$ . Using a tail vein injection of the fluorescent dye dextran-fluorescein, we are able to resolve individual red blood cells in capillary blood vessels, and measure the flow rate of the blood in the capillaries.

Moreover, we have shown that the mini-microscope is able to record calcium transients from GCaMP-expressing neurons. Using the mini-microscope, we are able to image more than 200 CA1 neurons simultaneously, and identify potential place cells from the recording. Furthermore, with the addition of a thin relay GRIN lens, we are able to extend the imaging capability of the mini-microscope to deep brain regions with minimal damage to the tissue. Here we have demonstrated simultaneous recording of more than 40 neurons in LA while a mouse undergoes auditory fear conditioning.

In this project, we recorded calcium transients at a rate of 20 frames per second, but this does not represent a limit in the frame rate. With the XIMEA camera (MU9PM),

the recoding rate can reach up to 200 frames per second at shorter exposure and a cost of spatial resolution. A higher frame rate will allow identification of fast brain oscillations such as the 7–11 Hz theta oscillation and potentially the fast 40–100 Hz gamma oscillation, both of which have been shown to be important in learning and memory. Calcium imaging is especially suited for detection of brain oscillations, as these oscillation may not lead to action potentials, but create sub-threshold changes of membrane potential which would be reflected by a fluctuation of internal calcium concentrations. The ability to simultaneously image a dense ensemble of neurons allows brain oscillations to be measured in each cell, and the SNR in detecting these oscillations can be increased by averaging signals from all cells and even background fluorescence. The brain oscillation signal can then be related to neural activities to study how local neural circuits respond to the brain oscillation.

In the current project, we have also demonstrated the ability of the mini-microscope to image in both red and green channels. The extra colour channel can be used for the identification of neural subpopulations or for gathering extra information from the brain. In our prototype we used blue light to stimulate red retrobeads and the fluorescent protein tdTomato, both of which have a broad excitation spectrum. However, this requirement is usually not necessary. If the red channel is static, it can be captured by a separate mini-microscope with an efficient excitation LED and corresponding filters just for the red fluorophore. The resulting image can be later aligned with recording of calcium transients for cell identification.

Our design of mini-microscope costs \$300–\$1000 for each unit, which will not represent a significant expense in most neuroscience laboratories. Moreover, all components of the mini-microscope are commercially available and can be assembled with minimal tools, providing access to neuroscientists with no requirement of engineering experience. The microscope casing is 3D printable. We will make both the 3D models and relevant analysis code freely available in order to open this work to the neuroscience community.

#### 4.1.2 Advantages of using the mini-microscope to study AD

As a test of the usefulness of the miniature microscope, we used it to image CA1 neurons in a transgenic mouse model of AD, TgCRND8, while the mice encoded and recalled a contextual fear memory. On average, we were able to image more than 100 neurons simultaneously for each mouse, and this data enabled us to investigate hippocampal circuitry mechanisms in AD.

The importance of the mini-microscope in understanding neural circuitry mechanisms is particularly reflected in the classifier prediction results. We have found that the NBC, which predicts mouse behaviour by considering individual neurons, is unable to reveal the pattern completion deficit in TgCRND8 mice. This result suggests that a significant amount of information about the mice's behavioural states is contained in the synergy between activity of neurons. This information cannot be revealed using traditional methods such as *in vivo* electrophysiological recording, where only a handful neurons can be recorded at the same time. To compensate for the scarcity of simultaneously recorded neurons, electrophysiological recordings often require experimenters to repeat the same behaviour trial many times, which may lead to changes in the animal's behaviour, which potentially confounds the interpretation of the data. However in the current study, the mini-microscope has given us the freedom to choose an experimental paradigm which is well-established in the field of behavioural neuroscience. This freedom allowed us to connect the findings from the neural activity recordings to the rich findings of behavioural neuroscience. This stands in contrast to *in vivo* 2-photon imaging, where due to the requirement of head fixation, only specifically designed behavioural paradigms are compatible, whose neural mechanisms are less well understood.

## 4.2 Examining circuitry deficits in a mouse model of AD

### 4.2.1 CA1 hyperexcitability

We found that in TgCRND8 mice, CA1 neurons are more active than those in WT mice, both during context exposure and during contextual memory recall. TAT-GluA2<sub>3Y</sub> treatment during training is able to reduce the overall cell activity to WT level. Moreover, to control for the behavioural state of the mice, we investigated cell activity when the mice were both freezing and active. We found the TgCRND8 genotype has a significant effect on increasing cell activity during freezing, and TAT-GluA2<sub>3Y</sub> treatment reduces cell activity in both WT and TgCRND8 mice. When mice were not freezing during the memory test, only TgCRND8 mice treated with TAT-GluA2<sub>3Y</sub> has a significant decrease in cell activity compared to the other three groups.

Our results confirm previous findings that CA1 cells in AD are hyperactive (Palop and Mucke, 2016). We have also found that while during memory test, the average cell activity in WT mice is at the same level as it is during contextual exposure, cell activity in the TgCRND8 mice increases during memory testing compared to the memory encoding session (Figure 3.7). This result suggests that in addition to the hyperactivity introduced by AD pathology, the TgCRND8 mice show additional activity in response to the memory recall task. This finding parallels evidence from human patients with early AD, where fMRI studies have found hyperactivity in the hippocampus only during memory recall, and that this negatively correlates with memory performance (Sperling et al., 2009; Reiman et al., 2012; Kunz et al., 2015). It has been hypothesized that this task-dependent increase of hippocampal cell activity may be a compensatory mechanism in response of degraded hippocampal function in AD (Kunz et al., 2015).

While hyperexcitability in AD mice is present when the mouse is freezing, cell activity when the mouse is not freezing does not differ between groups. Considering that the majority of CA1 cells lower their activity during freezing, it is possible that the hyperactivity

of CA1 neurons is caused by an inability to keep silent. This is congruent with the NMDAR pathology seen in AD, where NMDARs are found to spontaneously activate in AD, and cause excitation in the neuron (Danysz and Parsons, 2012). This result is also hinted at by Cheng and Ji (2013), who investigated spatial encoding in another mouse model of AD. In their study, when a mouse was in the receptive field of a place cell, the cell was normally active. However when the mouse was outside the receptive field of the place cell, the cell was unable to stop firing, leading to enlarged place fields (Cheng and Ji, 2013).

It is somewhat counter-intuitive that the TAT-GluA2<sub>3Y</sub> treatment, which increases synaptic AMPAR density and therefore strengthens excitatory synapses, results in a decrease of overall neural activity in CA1. However, considering that the hyperexcitability in AD is hypothesized to be the result of increased LTD and decreased LTP in the synapse (discussed in Section 1.5.2), and TAT-GluA2<sub>3Y</sub> has been shown to block LTD, it is possible that TAT-GluA2<sub>3Y</sub> treatment rescues excitability by reversing the LTP–LTD imbalance. It is still unclear how an LTP–LTD imbalance leads to hyperexcitability. Computational models of AD neurons suggest this may be caused by a loss of synaptic spines in hippocampal neurons. This morphological change of neuronal dendrites in AD creates less hindrance for the transmission of incoming excitatory postsynaptic potentials (EPSPs), therefore allowing the neurons to be more excitable (Siskova et al., 2014). It is possible that TAT-GluA2<sub>3Y</sub> rescues hyperexcitability by restoring the morphology of the neurons. There is a close correlation between synaptic AMPAR density and spine size, and endocytosis of GluA2-containing AMPARs can trigger changes in dendritic spine size (Hanley, 2008). Indeed, in unpublished data from this project, we have found TAT-GluA2<sub>3Y</sub> treatment protects from spine density decreases in both CA1 and DG after an acute expression of APP, supporting the possibility that TAT-GluA2<sub>3Y</sub> rescues hyperexcitability by restoring normal neuronal morphology in AD.

The TAT-GluA2<sub>3Y</sub> treatment was applied to TgCRND8 mice only 1 h before contextual fear training, however the effect of TAT-GluA2<sub>3Y</sub> was present both during contextual fear training and during memory testing. This suggests that TAT-GluA2<sub>3Y</sub> starts to affect cell

excitability within 1 h, and has long-term effects. A closer investigation of cell activity during training shows that, while TAT-GluA<sub>2</sub>Y is able to correct average cell activity in TgCRND8 mice to WT level, the distribution of cell activity between Tg-TAT-GluA<sub>2</sub>Y and WT-Veh is still significantly different. From the cumulative plot (Figure 3.6a), the distribution of the lower 90 % of cell activity in Tg-TAT-GluA<sub>2</sub>Y is similar to WT-Veh, however activity of the most active 10 % of cells are similar to Tg-Veh. This difference is not present 24 h later during memory testing. This suggests that the rescuing effect of TAT-GluA<sub>2</sub>Y is a gradual process which take hours to complete. Cells that are less hyperactive are first rescued, and cells with very high activity require longer time for the effect of TAT-GluA<sub>2</sub>Y to appear. Given that cells close to amyloid plaques are more excitable (Busche et al., 2012), it is possible these cells with very high activity are located near amyloid plaques, have more damage from the AD pathology, and require longer time for the pathological process to reverse.

#### **4.2.2 Contextual fear memory**

In this project, we subjected WT and TgCRND8 mice to contextual fear conditioning, and found that while the TgCRND8 mice show inferior memory during testing, this memory deficit can be rescued by TAT-GluA<sub>2</sub>Y treatment either during training, or during exposure to a brief reminder. This result suggests that TgCRND8 mice are still able to encode the memory during training, however have deficits in recalling the memory during testing. Similar results have been reported previously. In another mouse model of early AD, APP/PS1, Roy et al. (2016) tagged cells activated during contextual fear conditioning, and optically activated these cells during memory recall. They found that while the APP/PS1 mice showed a memory deficit during memory recall, light stimulation of the contextual fear memory trace was able to induce memory expression.

In order to distinguish whether the memory recall deficit is due to initiation or maintenance of memory expression, we have also analyzed the number of freezing bouts and duration of freezing bouts in TgCRND8 and WT mice. We found that while the TgCRND8

mice do not show a significant difference in number of freezing bouts during memory test, the duration of these freezing bouts are significantly shorter than those of the WT mice. This result suggests that the TgCRND8 mice are still able initiate the memory recall, however are unable to maintain it. This result, however, does not pinpoint whether the deficit is in memory encoding or memory recall. It is likely that during training, the TgCRND8 mice encoded the fear memory in a abnormal form which prevents normal recall. Further experiments are still required to investigate this.

#### 4.2.3 Encoding

In the current study, we found that cell activity in TgCRND8 mice is not as predictive of fear memory expression as that in WT mice. On the other hand, this deficit is not reflected in the prediction accuracy of the machine learning classifiers: both NBC and gSVM are able to predict freezing from cell activity in TgCRND8 mice as well as in WT mice. This discrepancy of the prediction power suggests that the hippocampal neural circuit is highly redundant, such that even when the prediction power of individual neurons is negatively affected by AD, there is no significant information loss if multiple neurons are combined to make a prediction. Similar results are found in place encoding, where while individual neurons in a AD mouse model have degraded spatial encoding (Cacucci et al., 2008; Cheng and Ji, 2013; Mably et al., 2017), the ensemble is still able to accurately represent the mouse's position (Cheng and Ji, 2013).

In this study, we only recorded close to one hundred cells in CA1 for each mouse on average, and the information in the activity of these neurons is enough for an accurate prediction of the mouse's fear memory recall. There are more than  $1 \times 10^4$  neurons in CA1: therefore even if under AD pathology where individual cells' firing patterns are degraded, any downstream brain structure should still able to decode the information. This then suggests that the degradation of individual cell activity in AD is secondary to the cognitive deficit, since to an efficient downstream brain structure, redundancy in the brain can protect information loss due to the degradation of cell activity.

This conclusion also explains why in the preclinical population, significant AD pathology often does not impact cognitive performance (Discussed in Section 1.1.2). Another important implication of this conclusion is that treatment of the AD pathology alone, without any restoration of the neural network structure, will not result in a significant improvement in cognitive symptoms. This may explain the failure of recent attempts at treating AD with A $\beta$  clearance: it is possible that even with the successful A $\beta$  removal, additional intervention is still required to restore the neural network at a circuitry level.

The importance of neural network structure is also reflected in the difference of gSVM and NBC performance. The significantly improved performance of the gSVM suggests that the network encodes more information than individual cells. This may be a universal phenomenon across the brain, as it has also recently been found in other brain regions such as basolateral amygdala (BLA) during auditory fear conditioning (Grewe et al., 2017). Moreover, we find the accuracy of the gSVM, which predicts freezing based on the cell ensemble as whole, is again similar to WT mice. This suggests that when a mouse is freezing, the information contained in the activity of the neural network in AD mice is unaffected.

#### **4.2.4 Pattern completion**

Given that the neural network contains can accurately predict freezing in AD mice, it is intriguing how the AD mice have a memory deficit at all. During memory expression, the information content for the cell ensemble in AD is not different from that of the WT mice, and it is therefore possible the memory deficit can be detected outside of the duration where the memory is expressed. Given that these AD mice have deficit in recalling the fear memory, and that the process of pattern completion in hippocampus is theorized to be important in memory recall, we investigated whether this process is affected in the TgCRND8 mice.

To detect the pattern completion process, we aligned classifier prediction accuracy to the time point when the mice show behavioural change (Figure 3.13). We found a significant

drop of prediction accuracy just prior to freezing, both in the NBC and gSVM. Since the drop in accuracy happens at a time where mice are predominantly not freezing, the accuracy drop suggests that the classifiers are (inaccurately) predicting freezing, before mice start to freeze.

Since the classifiers are trained on each time point shuffled, they are agnostic to the temporal dynamics of cell activity. Therefore, the significant change of prediction accuracy before freezing must reflect changes in the pattern of neural activity itself. Moreover, the fact that the change of neural activity in CA1 is present before behaviour onset is very important in interpreting findings of this study. Given that nature of the study is correlational, the causal relationship between neural activity and behaviour is unclear. However, the temporal precedence of CA1 activity suggests that the neural activity pattern is not a result of the mouse's behaviour, but likely involved in initiating the behaviour. This confirms that the neural activity difference we have found between treatment and genotype groups is a result of circuitry deficit, instead of a consequence of different behaviour between mice.

We have found in the NBC prediction, the temporal signature of freezing behaviour in WT mice precedes the other three groups. Given that the NBC considers each cell individually, this result suggests that the activity of individual cells start to form a “cellular signal” for freezing, which is a measurement of the contextual fear memory recall. The findings that all groups in NBC predict freezing before behaviour, and that they have similar temporal precedence over behaviour suggest that in Tg mice, the “cellular signal” for contextual fear memory recall is unaffected.

On the other hand, we found that the gSVM prediction precedes freezing in WT mice, however this is not present in the vehicle-treated AD mice. Again, given that the gSVM detects a network pattern of cell activity, this result suggests that in WT mice, a “network signal” of freezing appears in the CA1 network, however this signal is missing from the AD mice before freezing.

As the gSVM can accurately classify the behavioural state of mice based on their neural

activity, we can use the gSVM to approximate the neural activity pattern of recalling a contextual fear memory (considering each freezing bout as an episode of memory recall). The gradual rise of freezing prediction before the freezing behaviour therefore represents the process of pattern completion: where an incomplete freezing pattern first appears in the network and confuses the classifier’s attempt to predict freezing. Over time, the pattern gets more complete, which leads to increased classifier prediction of freezing.

We found that the “cellular signal”, as detected by the NBC, appears significantly earlier than the “network signal” from the gSVM. This result reveals some details about the pattern completion process. The pattern completion process starts with individual cells changing their firing rate to that representing their activity distribution during memory expression, potentially guided by feed-forward input. However, as the memory pattern is a collection of patterns, at any single point each cell may have the activity from different patterns. Therefore at this time point, NBC, which only classifies by examining whether the activity of individual neurons represents *any* single contextual fear memory pattern, is able to detect a pattern for fear memory recall. However as the cell activities are not synchronized, no significant global pattern can be detected by gSVM.

However, as the “cellular signal” grows stronger, some cell activities become synchronized, and form a partial global pattern. This global pattern then, potentially through recurrent connections, recruits more cells to join the pattern. At this time, the partial global pattern can be detected by the gSVM, and this positive feedback loop continues until the pattern is complete. This pattern then forms an attractor of brain states, which maintains itself despite small fluctuation in the feed-forward input, and only disappears when there is a large shift of the feed-forward input which significantly deviates the neural activity pattern from the contextual memory pattern (Rolls, 2013b).

It is easy to fit the specific deficit of AD mice within this interpretation. AD mice show normal dynamic of “cellular signal”, however they are missing the “network signal”. It is therefore possible that the AD mice have a deficit in pattern completion: that the positive feedback force of converting an asynchronous “cellular signal” to a “network signal” is

degraded. The lack of a gradual network signal suggests that the “network signal” in the AD mice is likely formed by chance, that at some point, a global pattern appears from the asynchronous activity of individual cells.

This result is also supported by reports of neural oscillation deficits in AD. In hippocampus, the 3–12 Hz theta oscillation and the faster 25–120 Hz gamma oscillation are considered important for learning and memory, and are critically dependent on the integrity of hippocampal neural networks (Buzsáki, 2002; Colgin et al., 2009). However, both theta and gamma oscillations have been shown to be altered in rodent models of AD. It has been reported that the progression of plaque deposition is correlated with a decrease of theta power and frequency in both mouse models of AD, and acute A $\beta$  treatment in rats (Scott et al., 2012; Villette et al., 2010). A decreased oscillation power is also found in the gamma frequency, and removal of A $\beta$  plaques is able to block the deficit (Driver et al., 2007; Kuruodenkandy et al., 2014). The coupling of theta and gamma oscillations has also been reported to be affected in AD (Goutagny et al., 2013).

Similar oscillation deficits are also found in the human patients. EEG recordings in early AD patients have shown a decreased coupling between parietal alpha and prefrontal theta oscillations, and event-related delta, theta and alpha coherences are also significantly decreased (Güntekin et al., 2008; Montez et al., 2009). Moreover, the prefrontal theta coherence increases in AD patients treated with AChE inhibitors (Yener et al., 2007), suggesting a close relationship between brain oscillations and AD. More recent studies aim to enhance brain oscillations in AD, and suggest a causal relationship between the two. It has been found that deep brain stimulation at gamma frequency, both in rodent models and AD patients, is able to improve cognitive function (Suthana and Fried, 2014). A recent study also showed that in a mouse model of early AD, induction of gamma oscillation also reverses A $\beta$  deposition (Iaccarino et al., 2016).

These results suggest that the pattern completion deficit in AD may be closely related to the brain oscillation deficit reported in the literature. However in the current study the cell activity is recorded at 20 Hz. The sampling frequency is unfortunately too slow to allow

detection of any brain oscillations above 10 Hz. How a deficit in brain oscillation affects the pattern completion process in AD is an important topic for future research.

Secondly, this interpretation suggests that AD mice may still be able to initiate freezing, however due to degraded attractor functions, they are unable to maintain the state of memory recall. This is supported by our findings that the Tg mice have similar number of freezing bouts, however a significantly shortened bout duration, showing a deficit in maintaining the expression of the memory but not initiating the memory.

Moreover, the instability of the memory state in AD can be inferred from the distance to the boundary of memory states. We measured the signed distance to the gSVM classification boundary when the mouse's behaviour transitioned into freezing (Figure 3.14). We have found that while WT mice show an acceleration over and away from the boundary, the Tg mice only barely cross the boundary, and stay close to it during freezing. Therefore, a small perturbation in the brain state is more likely to shift the Tg mice out of freezing. The freezing state in the WT mice, on the other hand, is more robust to small perturbations.

While the current study is the first to suggest that neural attractor states for memory recall are unstable in AD, evidence from human behavioural studies suggest that similar dynamics may exist in AD patients for other cognitive functions. Attention has long been considered computationally as a result of neural attractor states, and the strength of the attractor is important for maintaining attention (Desimone and Duncan, 1995; Rolls, 2008, 2013a). Interestingly, early AD patients have no deficits in focusing the attention, however, their attention is more likely to be disrupted by distractors, and less likely to be maintained over time (Perry and Hodges, 1999). This result is similar to the memory recall deficit we have found in the current study, suggesting that it is possible that the deficit in attractor state in early AD is global, affecting many brain areas' cognitive functions.

The fragility of the memory attractor in AD may also implicate another curious deficit of AD called subjective memory impairment (Jahn, 2013). Subjective memory impairment is defined as a sense of memory deterioration with no objective impairment in cognitive test. Subjective memory impairment is correlated with hyperactivation of the MTL during

memory tasks, and predictive of hippocampal atrophy as well as later development of cognitive impairment and AD (Jahn, 2013). It is possible the subjective memory impairment arises from our finding that during memory recall, the network state in AD tends to stay close to the boundary of the attractor state. This close distance can be detected by other brain regions, and reduce the confidence of those brain regions in predicting the patient's behaviour, creating a sense of unsureness without a degradation of performance.

The deterioration of the attractor state in AD can be caused by several factors. First, we showed that the deficit in AD mice can be rescued by TAT-GluA2<sub>3Y</sub> treatment with a reminder. From this we concluded that the AD mice have encoded the contextual fear memory during training, but that this memory may not be encoded in the same way as in WT mice. Therefore, the attractor state deficit can be a result of the formation of a weak attractor for the memory. Given that the neurons in AD have impaired LTP, and the normal memory encoding process may be interfered with by hyperactive neurons, it is unlikely that the memory encoding process is completely spared.

Secondly, it is also possible that interference exists during the memory recall. The hyperactivity observed in the AD mice may generate noise in the network state, so even with a functional memory attractor, the network state is more likely to spontaneously shift out of the attractor field due to noise. In addition, it is also possible that in AD, other attractor states exist, and these sporadic attractors may actively pull the network state toward their own center of attraction, and away from that of the memory recall. This is hinted at both by animal and human studies. In a mouse model of taupathy, Cheng and Ji (2013) have found that the CA1 place cells displayed rigid firing, such that the firing pattern of a familiar environment lingers even when the mice is placed in a novel environment. In humans, MCI and early AD patients have deficits in shifting attention, and often maintain focus on an initial item even when it is no longer relevant (Perry and Hodges, 1999). These studies suggest that if the memory recall deficit is a result of competing attractor fields, it is possible that the competing attractor represents a strong, familiar memory formed previously. This hypothesis can be tested by artificially creating a strong attractor state,

for example, using repeated optical activation of a selected neural ensemble (Carrillo-Reid et al., 2016), before contextual fear conditioning. The hypothesis will be supported if a future experiment shows the similar pattern reappeared during contextual fear memory recall in AD and correlates with the memory deficit.

#### **4.2.5 TAT-GluA<sub>2</sub><sub>3Y</sub> treatment is able to rescue circuitry deficits in AD**

In the current project, we gave TgCRND8 mice an acute treatment of TAT-GluA<sub>2</sub><sub>3Y</sub> during memory formation. This treatment is able to rescue information content in CA1 neural activity as well as the presence of a network pattern just before memory recall, and rescues the pattern completion deficit in the TgCRND8 mice. Interestingly, while behaviourally TAT-GluA<sub>2</sub><sub>3Y</sub> had no effect on WT mice, TAT-GluA<sub>2</sub><sub>3Y</sub>-treated WT mice showed an earlier presence of network pattern before memory recall compared to vehicle-treated WT mice.

These results suggest that TAT-GluA<sub>2</sub><sub>3Y</sub> treatment during memory formation has a long-lasting effect. Moreover, given that the effect of TAT-GluA<sub>2</sub><sub>3Y</sub> treatment is present only when the memory is activated, either during formation or a reminder, these results suggest that the TAT-GluA<sub>2</sub><sub>3Y</sub> treatment potentially affects memory by strengthening the underlying neural representation. A robustly-connected memory trace allows it to be reactivated with a degraded pattern, so that a small number of neurons showing the activity of a memory are able to synchronize the network. In fact this is what we have found: at the same level of cellular memory signalling, TAT-GluA<sub>2</sub><sub>3Y</sub> treatment, both in WT and Tg mice, forms a network pattern with a smaller cellular signal. This suggests that on a circuit level, the TAT-GluA<sub>2</sub><sub>3Y</sub> treatment results in an enhanced pattern completion process.

Our finding that TAT-GluA<sub>2</sub><sub>3Y</sub> treatment strengthens the memory network is congruent with the literature, where the TAT-GluA<sub>2</sub><sub>3Y</sub> treatment has been shown to make the memory more resilient. For example, chronic TAT-GluA<sub>2</sub><sub>3Y</sub> treatment prevents forgetting of contextual fear memory, conditioned place preference, and novel object recognition (Dong et al., 2015; Migues et al., 2016). Treatment of TAT-GluA<sub>2</sub><sub>3Y</sub> also protects memory recall from protein synthesis inhibitors in auditory fear memory (Lopez et al., 2015).

Our results, together with many other previous studies, found that in WT mice, TAT-GluA<sub>2,3Y</sub> treatment does not affect the magnitude of the memory (Dias et al., 2012; Dong et al., 2015; Migues et al., 2016). This suggests that the magnitude of memory, especially several days after memory formation, is not encoded in the strength of functional connections within an engram.

Given that the TAT-GluA<sub>2,3Y</sub> blocks synaptic AMPAR endocytosis and therefore prevents LTD (Ahmadian et al., 2004), it is likely that the rescuing effect of TAT-GluA<sub>2,3Y</sub> is mediated through synaptic plasticity. Dong et al. (2015) showed that TAT-GluA<sub>2,3Y</sub> treatment prevented LTP from decay, and was able to rescue memory deficits in the APP23/PS45 mouse model of AD. Moreover, it has been shown that LTP may be sufficient to rescue memory recall. Roy et al. (2016) also found while the optogenetic reactivation of contextual fear memory does not have long-term effect, a train of fast, LTP-inducing stimulations of the memory trace is able to rescue the memory deficit in APP/PS1 mice. Our findings that the effect of TAT-GluA<sub>2,3Y</sub> requires a reminder of the original memory is consistent with these results: in the short-term, the activity of the original memory trace needs to be reactivated by the reminder in order for the associations to be strengthened, and without activation of the original memory, our no-reminder controls did not benefit from the TAT-GluA<sub>2,3Y</sub>-mediated rescuing of memory recall.

The long term effect of TAT-GluA<sub>2,3Y</sub> is in accordance with the idea that AD pathology forms a positive feedback loop, that the effect of AD pathology including synaptic degeneration and aberrant neural activity in turn accelerates the signature pathology. In the current study, we show that an acute TAT-GluA<sub>2,3Y</sub> treatment is able to have lasting effects at least 24 h later when the TAT-GluA<sub>2,3Y</sub> is not longer present. This result suggests that in TgCRND8 mice, correcting the synaptic pathology is not only able to rescue cognitive ability, but may also prevent feedback loop of AD pathology in the short term. Previous reports of chronic TAT-GluA<sub>2,3Y</sub> treatment in a mouse model of AD showed a reduction of neuritic plaques, supporting the hypothesis that rescuing circuit function in AD can protect neurons from the AD pathology (Dong et al., 2015). While more research is required

to investigate long-term effect and outcome of TAT-GluA2<sub>3Y</sub> treatment in AD, our result and previous studies (Roy et al., 2016; Miguez et al., 2016; Dong et al., 2015) suggest that interventions that restore network circuit functions in AD can enhance cognitive function and potentially protect neurons from AD pathology.

# 5

## CONCLUSIONS AND FUTURE DIRECTIONS

---

### 5.1 Conclusion

In the current project, we sought to explore the circuit mechanisms of hippocampal function, and how deficits in this functioning contribute to the cognitive symptoms of AD. To investigate neural circuitry functions, we first designed and built a miniature fluorescent microscope for recording of neural activity in freely behaving mice. The mini-microscope is implantable on a mouse's head, and combined with the expression of a calcium indicator such as gCaMP6f, we have shown that the mini-microscope is able to record hundreds of neurons in CA1, and tens of neurons in LA simultaneously in freely behaving mice. In addition, we have extended the ability of mini-microscope to include a second colour channel, which can be potentially used to identify neural subpopulations and other brain structures concurrently with neural activity recording.

In the second part of this project, we used our mini-microscope to investigate circuitry deficits in a mouse model of early AD, TgCRND8. We recorded from CA1 as mice learned and recalled a contextual fear memory. We have found that TgCRND8 mice have a significant memory deficit, showing less freezing during contextual memory test. This deficit

is the result of significantly shorter freezing bouts, but not a reduced number of freezing bouts, suggesting the memory deficit may be the result of an inability to maintain the expression of a fear memory.

From the calcium recordings, we have found that CA1 neurons in TgCRND8 mice are hyperactive, and the cell activity of TgCRND8 mice contains less information about the behavioural state of mice during memory recall. This effect is independent of spatial location of the mice, suggesting that the deficit reflects impaired recall of the fear memory.

Next, we took advantage of machine learning methods to investigate how memory information is recalled in the CA1 circuitry. We differentiated the cellular signal, where individual neurons were independently considered, and a network signal, where the activity of all neurons was considered using a NBC and gSVM, respectively. The two classifiers were trained on the ensemble neural activity to predict the behaviour of the mice at each time point. We have found that even though individual neurons in CA1 contained less information about the behavioural state of the mice, the ensemble of neurons was still able to create an accurate prediction of when the mice were freezing. Moreover, we have found that the gSVM showed significantly better performance than the NBC, suggesting that a significant amount of information is encoded in the synergy between activity of single neurons.

The performance of NBC and gSVM suggests that these classifiers are able to recognize a neural activity pattern for fear memory recall. We then investigated how this pattern emerged at the beginning of memory recall. We aligned the classifier predictions to the time when the mice started to freeze, and found a gradual decrease of prediction accuracy before the mice froze, where the classifiers started to falsely predict freezing before the behaviour occurs. This result shows that the fear memory pattern emerges gradually before the behavioural change. This process corresponds to the pattern completion process in hippocampus. We found that in the NBC, all groups showed similar timing in the pattern completion, suggesting that in the TgCRND8 mice, the cellular signal for pattern completion is not impaired. However in gSVM, TgCRND8 mice showed no pattern completion,

suggesting that in TgCRND8 mice, even though individual cells show activity patterns of freezing, these activity are not synchronized, and cannot form a pattern across the network.

In addition, we found that in TgCRND8 mice, the network state tended to linger at the classification boundary during freezing, while the other groups were able to dip into the freezing attractor state. This result suggests that in TgCRND8 mice, the attractor state for the expression of the memory is not robust, and is susceptible to interruption from minor deviation. This result explains the behavioural findings that the TgCRND8 mice are unable to maintain freezing, and more likely to be distracted.

AD is characterized by significant synaptic loss, and a bias away from LTP toward LTD. Here we investigated whether rescuing synaptic function in AD is able to restore hippocampal circuit function and consequently behaviour. We used the well-characterized peptide TAT-GluA2<sub>3Y</sub>: TAT-GluA2<sub>3Y</sub> blocks AMPAR endocytosis, therefore increases synaptic strength, and shifts synaptic plasticity towards LTP. We found that TAT-GluA2<sub>3Y</sub> treatment before contextual fear memory training was able to rescue the hyperactivity phenotype found in TgCRND8 mice. Moreover, this rescuing effect was long lasting: during memory testing the treated TgCRND8 mice showed normal cell activity levels, better information content for behaviour, and also a pattern completion processes similar to WT mice. Interestingly, we found that TAT-GluA2<sub>3Y</sub> treated WT mice showed an earlier pattern completion process, suggesting that effect of TAT-GluA2<sub>3Y</sub> may promote LTP, and this leads to a strengthening of the memory network, allowing the network pattern to be retrieved with a smaller cellular signal.

We then investigated whether the memory deficit in TgCRND8 mice is due to forgetting. We trained mice with contextual fear conditioning, gave the mice a brief reminder with TAT-GluA2<sub>3Y</sub> treatment 3 days later, then tested their fear memory on the following day. We found TAT-GluA2<sub>3Y</sub> treatment during a brief reminder is able to rescue the fear memory in TgCRND8 mice, while vehicle treated TgCRND8 mice still show the memory deficit. This result suggests that the contextual fear memory is at least encoded one day after training, and the memory deficit is not caused by forgetting. Moreover, we found that a

memory reminder was necessary for the rescuing effect of TAT-GluA<sub>2</sub><sub>3Y</sub>. This supports our calcium imaging result that TAT-GluA<sub>2</sub><sub>3Y</sub> rescues memory recall by strengthening the active memory trace.

In conclusion, in this project we have developed a miniature fluorescent microscope for calcium imaging in freely behaving mice, and used it to image CA1 neural activity in WT and AD model TgCRND8 mice. We found the TgCRND8 mice have contextual fear memory deficits, hyperactive CA1 neurons, and less information content about behaviour. We found the memory recalled by TgCRND8 mice was unstable, both at the neural circuit level and behavioural level. TAT-GluA<sub>2</sub><sub>3Y</sub> treatment which potentially enhances LTP can rescue both circuitry dysfunction and behaviour in TgCRND8 mice, suggesting the importance of restoring circuitry function as a potential treatment in restoring cognitive functions in AD.

## **5.2 Future directions for mini-microscope development**

### **5.2.1 Technical improvement for the mini-microscope**

The focus mechanism in the mini-microscope can be improved in the future. In the current project, the focus of our mini-microscope is manually adjusted and fixed during the whole imaging session. This only allows us to image a 400 μm × 400 μm × 50 μm rectangular box 50–150 μm below the lens. If the focus can be adjusted fast enough during recording, it may be possible to provide a scan across the z-axis, and allow recording of more neurons in a 3D volume. In addition, in cases where neurons are heterogeneous across the z-axis such as cortex, a fine-adjustment of focal plane can give the experimenter more control to image specific subpopulations.

One way to improve the focus mechanism is to, instead of manually turning the camera up and down, control movement using a miniature motor. While this can provide an easy auto-focus mechanism, it will not be fast enough to give z-scan during recording. Moreover, the addition of an extra motor on the mini-microscope can add significant weight, making it too heavy for small rodents such as mice.

Alternatively, a liquid lens can be used to replace the barrel lens we currently use to focus light to the camera. A liquid lens contains two immiscible liquids, and the curved interface between the two liquids provides the function of a lens. The focus of a liquid lens can be changed by applying voltage across the two liquids, which will bend the meniscus of the two liquids accordingly (Kuiper and Hendriks, 2004). A liquid lens allows focus change in several milliseconds, and is fast enough to provide a real time z-scan with the mini-microscope. However, current commercially available liquid lenses are still too large to be implemented on a mini-microscope. Future miniaturized liquid lens can be a great improvement for the mini-microscope.

In the current project, the mini-microscope is connected to a computer through a cable. Although the mini-microscope is compatible with the majority of behavioural paradigms, a connection cable can make some paradigms hard to perform, especially in environments with overhead structures, or during long-term recording sessions. Efforts can be made to create a wireless version of the mini-microscope. Again, the size and weight of the transmitting circuit and battery could be prohibitive on small rodents. However, recent developments have shown that in a resonant cavity, electrical power can be delivered wirelessly using radio frequency and a minimal implant weighing 20 mg (Montgomery et al., 2015). This could potentially provide the means for a wireless power source, and if combined with minimal transmission circuitry, it would be possible to allow wireless long-term calcium imaging in freely behaving animals. A wireless mini-microscope would be very useful for investigating neural circuitry for slower neural circuitry process such as consolidation and circadian rhythms.

### 5.2.2 Combining mini-microscope with other techniques for investigating circuitry function

One important future improvement for the construction of the mini-microscope is to combine it with other methods for investigating neural circuitry mechanisms. This will allow cross-referencing the neural activity to other physiological, anatomical and molecular in-

formation to provide a whole picture of the function of neural circuits under investigation.

First, efforts can be made to allow *post mortem* identification of the field of view from the mini-microscope. This would allow the mini-microscope data to be enriched with information from IHC or FISH, which could potentially provide detailed molecular and cellular information about neurons, and offer an explanation of how subpopulations of neurons with different molecular markers coordinate circuitry behaviour.

However in order to reach this goal, the optical properties of the mini-microscope will have to be accurately characterized. Efforts will need to be made in quantification of the curvature, range, and depth of the field of view. Measurement of these parameters allows mapping the cells identified in the mini-microscope to their original x–y plane, and also give constraints to the position of z-axis. The next step is to construct a 3D image of the *post mortem* tissue, potentially using tissue clearing techniques such as clear lipid-exchanged anatomically rigid imaging/immunostaining-compatible tissue hydrogel (CLARITY). The reconstructed calcium imaging cells can then be mapped to the 3D image of the *post mortem* tissue, allowing further molecular characterization of the recorded neurons.

Secondly, it is also possible to combine mini-microscope recording with local field potential (LFP) measurement for concurrent identification of brain oscillations. This addition does not pose any theoretical challenge, as LFP measurements only require several extracellular metal electrodes, and LFP recording techniques are well established. However to shield potential interference from the camera chip, the LFP signals may need to be amplified and digitized on the headset before the signal is transmitted. This may require extra electronic circuitry, and may be challenging in small rodents such as mice, where both the weight and size of the implant are restricted.

Our investigation of pattern completion in AD can greatly benefit from a potential combination of LFP and mini-microscope. Since we have found that the network signal, not individual cellular signals, are important in mediating the memory recall deficit, it suggests that the neurons in AD are not synchronized to form a pattern. In the hippocampus, oscillations in theta and gamma frequency has been implicated in learning and memory, and are

hypothesized to provide a reference frame to which neurons can align their activity. Given previous reports that in other mouse models of AD, both theta and gamma oscillation are degraded (Driver et al., 2007; Villette et al., 2010; Scott et al., 2012; Goutagny et al., 2013), it is possible that the pattern completion deficit is a consequence of degraded oscillation. And if so, artificially restoring the oscillation by stimulation of the neurons, either electrically or optogenetically, could potentially restore the pattern completion process in AD mice.

### 5.3 Effect of TAT-GluA<sub>2</sub><sub>3Y</sub> in strengthening memory trace

We hypothesized that TAT-GluA<sub>2</sub><sub>3Y</sub> rescues the circuitry deficits in AD by strengthening of the memory trace, however direct evidence is still required to show that the connection of neurons involved in the contextual fear memory are strengthened after TAT-GluA<sub>2</sub><sub>3Y</sub> treatment. This hypothesis can be directly tested by combining the mini-microscope recording with two-photon imaging. Carrillo-Reid et al. (2016) have shown that a strong, optogenetically imprinted neural ensemble can be recalled by reactivated by stimulating a single neuron in the ensemble. A similar experiment can be conducted for evaluation of the fear memory ensemble. First, an excitatory opsin can be introduced to the cells of interest. After mini-microscope recording of contextual fear conditioning, the mice can be head-fixed on the stage of two-photon microscope, where the same cells can be imaged through the GRIN lens, and neurons involved in the memory trace can be identified. Part of the memory trace can then be optically stimulated, and if the connections between neurons of the fear memory ensemble are strong, a partial activation of the ensemble should be able to activate the rest of the ensemble. Therefore we predict in TAT-GluA<sub>2</sub><sub>3Y</sub>-treated mice, activation of a smaller part of the ensemble should be able to reactivate the whole memory trace.

## 5.4 Pattern completion and pattern separation

In the current project, we recorded from CA1, which is considered an output of the hippocampus circuit, after both pattern separation process in DG and pattern completion process in CA3 (Rolls, 2013b). We have only tested contextual fear memory using the same context, which would primarily involve the pattern completion process. However, it would also be interesting to see, whether the TAT-GluA2<sub>3Y</sub> treatment also improves the pattern-separation process.

If the pattern completion process is enhanced by the TAT-GluA2<sub>3Y</sub> treatment without affecting the pattern separation process, it follows that the patterns are likely able to complete with a smaller partial activation. This suggests that the memory strengthened by TAT-GluA2<sub>3Y</sub> treatment is more generalized: since a similar environment may activate part of the trace, and this leads to completion of the fear memory pattern and generates corresponding behaviour. However, this hypothesis is not supported by previous studies. Migues et al. (2016) gave chronic TAT-GluA2<sub>3Y</sub>-treatment in dorsal hippocampus after mice were trained with object recognition, conditioned place preference, or contextual fear conditioning. Interestingly, the authors found TAT-GluA2<sub>3Y</sub> treatment not only prevents generalization, but in fact allowed the mice to distinguish different memory testing environment more than the vehicle treated group (Migues et al., 2016).

Migues et al. (2016)'s result may not be surprising, given that TAT-GluA2<sub>3Y</sub> treatment improves LTP, which has also been shown to be important for the pattern separation process in DG (Rolls, 2013b). However, neither Migues et al. (2016) nor our current experiment distinguished CA3 and DG in the TAT-GluA2<sub>3Y</sub> treatment, and therefore are unable to tease out the effects of TAT-GluA2<sub>3Y</sub> on pattern separation and pattern completion separately. A future experiment could limit the effect of TAT-GluA2<sub>3Y</sub> to either CA3 or DG, and observe both the CA1 activity and the mouse's behaviour. We hypothesize that TAT-GluA2<sub>3Y</sub> treatment in CA3 will result in an enhancement of pattern completion as well as behavioural generalization, and treatment in DG will result in an enhancement pattern

separation and behavioural discrimination.

A more direct way, but technically more difficult approach is to investigate the involvement of the pattern separation process using the mini-microscope to image CA3 and DG simultaneously, and observe the pattern completion and pattern separation process directly. This potentially could be done using a doublet GRIN lens, where a small, thin relay GRIN lens is glued to a large GRIN lens. With proper placement, it allows imaging CA3 using the rest of the surface of the large GRIN lens, and the thin GRIN lens could be inserted above DG to relay an image to the large GRIN lens. If combined with connectivity studies, data from this approach could allow direct validation of the computational model of hippocampus. Furthermore, in a disease model having information from both DG and CA3 cell activity as well as their connectivity could enable researchers to pinpoint the functional impairment in the hippocampus circuitry.

## 5.5 Effect of TAT-GluA<sub>2</sub><sub>3Y</sub> in correcting AD pathology

In the current project, we have shown that the TAT-GluA<sub>2</sub><sub>3Y</sub> treatment was not only able to rescue the behavioural deficits seen in TgCRND8 mice, but was also able to rescue circuitry function in these mice. Given that the aberrant circuitry activity in AD promotes AD pathology, it is worth investigating whether TAT-GluA<sub>2</sub><sub>3Y</sub>, and its target of AMPAR endocytosis, can be targeted to alleviate AD pathology. Results from Dong et al. (2015) show that chronically TAT-GluA<sub>2</sub><sub>3Y</sub>-treated AD mice have fewer amyloid plaques compared to vehicle treated mice after memory training. However, it is still unknown whether TAT-GluA<sub>2</sub><sub>3Y</sub> treatment can lead to a reversal of AD pathology. Instead of comparing to vehicle-treated controls, chronically treated AD mice can be longitudinally compared to mice before treatment to characterize the effect of TAT-GluA<sub>2</sub><sub>3Y</sub> on AD progression.

In addition with the mini-microscope, it may be possible to chronically image both the neural activity changes during the chronic treatment of TAT-GluA<sub>2</sub><sub>3Y</sub>, as well as simultaneous imaging of amyloid plaques (Zhang et al., 2015). Data from such experiments can

provide details on how plaque deposition affects circuit activity, as well as conversely, how circuit activity can affect AD progression. Moreover, TAT-GluA<sub>2</sub>Y, being an interference peptide, is not a good candidate for drug treatment because of its chemical instability, short half life, and inability to be administered orally (Fosgerau and Hoffmann, 2015). Future studies can also focus on small molecules which have similar circuitry effects as TAT-GluA<sub>2</sub>Y with better pharmacological properties.

In conclusion, the aims the current project have been two-fold: **a)** improve the current tools available for neuroscientists to investigate neural circuitry mechanisms, and **b)** contribute to the understanding of circuitry mechanisms underlying the cognitive deficits in AD. In the end, I hope through this thesis, I help to provide a potential link between studies at cellular level and behavioural level, and contribute to the understanding, and potential treatment of AD. In the future, I predict advances in neural recording technology will reveal detailed mechanisms of neural circuitry, and inspire novel treatments for neurological disorders such as AD.

## BIBLIOGRAPHY

---

- Abel, T. and Lattal, K. M. (2001). Molecular mechanisms of memory acquisition, consolidation and retrieval. *Current Opinion In Neurobiology*, 11(2):180–7.
- Addis, D. R., Moscovitch, M., Crawley, A. P., and McAndrews, M. P. (2004). Recollective qualities modulate hippocampal activation during autobiographical memory retrieval. *Hippocampus*, 14(6):752–62.
- Ahmadian, G., Ju, W., Liu, L., Wyszynski, M., Lee, S. H., Dunah, A. W., Taghibiglou, C., Wang, Y., Lu, J., Wong, T. P., Sheng, M., and Wang, Y. T. (2004). Tyrosine phosphorylation of glur2 is required for insulin-stimulated ampa receptor endocytosis and ltd. *The Embo Journal*, 23(5):1040–50.
- Alagarsamy, S., Marino, M. J., Rouse, S. T., Gereau, R. W., Heinemann, S. F., and Conn, P. J. (1999). Activation of nmda receptors reverses desensitization of mglur5 in native and recombinant systems. *Nature Neuroscience*, 2(3):234–40.
- Alagarsamy, S., Saugstad, J., Warren, L., Mansuy, I. M., Gereau, R. W., and Conn, P. J. (2005). Nmda-induced potentiation of mglur5 is mediated by activation of protein phosphatase 2b/calcineurin. *Neuropharmacology*, 49 Suppl 1:135–45.
- Albert, M. S. (1996). Cognitive and neurobiologic markers of early alzheimer disease. *Proceedings Of The National Academy Of Sciences Of The United States Of America*, 93(24):13547–51.
- Ally, B. A., Hussey, E. P., Ko, P. C., and Molitor, R. J. (2013). Pattern separation and

- pattern completion in alzheimer's disease: evidence of rapid forgetting in amnestic mild cognitive impairment. *Hippocampus*, 23(12):1246–58.
- Alonso, A. C., Zaidi, T., Grundke-Iqbali, I., and Iqbal, K. (1994). Role of abnormally phosphorylated tau in the breakdown of microtubules in alzheimer disease. *Proceedings Of The National Academy Of Sciences Of The United States Of America*, 91(12):5562–6.
- Alzheimer's Association (2016). 2016 alzheimer's disease facts and figures. *Alzheimer'S & Dementia : The Journal Of The Alzheimer'S Association*, 12(4):459–509.
- Alzheimer's Society of Canada (2010). Rising tide: the impact of dementia on canadian society. [Online; accessed 15-February-2017].
- Amatniek, J. C., Hauser, W. A., DelCastillo-Castaneda, C., Jacobs, D. M., Marder, K., Bell, K., Albert, M., Brandt, J., and Stern, Y. (2006). Incidence and predictors of seizures in patients with alzheimer's disease. *Epilepsia*, 47(5):867–72.
- Anggono, V., Clem, R. L., and Huganir, R. L. (2011). Pick1 loss of function occludes homeostatic synaptic scaling. *The Journal Of Neuroscience : The Official Journal Of The Society For Neuroscience*, 31(6):2188–96.
- Arrighi, H. M., Neumann, P. J., Lieberburg, I. M., and Townsend, R. J. (2010). Lethality of alzheimer disease and its impact on nursing home placement. *Alzheimer Disease And Associated Disorders*, 24(1):90–5.
- Attardo, A., Fitzgerald, J. E., and Schnitzer, M. J. (2015). Impermanence of dendritic spines in live adult ca1 hippocampus. *Nature*, 523(7562):592–6.
- Ayalon, G. and Stern-Bach, Y. (2001). Functional assembly of ampa and kainate receptors is mediated by several discrete protein-protein interactions. *Neuron*, 31(1):103–13.
- Bailey, C. H. and Kandel, E. R. (1993). Structural changes accompanying memory storage. *Annual Review Of Physiology*, 55:397–426.

- Bakker, A., Albert, M. S., Krauss, G., Speck, C. L., and Gallagher, M. (2015). Response of the medial temporal lobe network in amnestic mild cognitive impairment to therapeutic intervention assessed by fmri and memory task performance. *Neuroimage. Clinical*, 7:688–98.
- Barage, S. H. and Sonawane, K. D. (2015). Amyloid cascade hypothesis: Pathogenesis and therapeutic strategies in alzheimer's disease. *Neuropeptides*, 52:1–18.
- Barnes, C. A. and McNaughton, B. L. (1980). Physiological compensation for loss of afferent synapses in rat hippocampal granule cells during senescence. *The Journal Of Physiology*, 309:473–85.
- Barnes, C. A., Rao, G., and Houston, F. P. (2000). Ltp induction threshold change in old rats at the perforant path–granule cell synapse. *Neurobiology Of Aging*, 21(5):613–20.
- Barrett, A. M., Orange, W., Keller, M., Damgaard, P., and Swerdlow, R. H. (2006). Short-term effect of dementia disclosure: how patients and families describe the diagnosis. *Journal Of The American Geriatrics Society*, 54(12):1968–70.
- Barreto, R. P. J. and Schnitzer, M. J. (2012). In vivo optical microendoscopy for imaging cells lying deep within live tissue. *Cold Spring Harbor Protocols*, 2012(10):1029–34.
- Barria, A., Muller, D., Derkach, V., Griffith, L. C., and Soderling, T. R. (1997). Regulatory phosphorylation of ampa-type glutamate receptors by cam-kii during long-term potentiation. *Science (New York, N.Y.)*, 276(5321):2042–5.
- Bartus, R. T. (2000). On neurodegenerative diseases, models, and treatment strategies: lessons learned and lessons forgotten a generation following the cholinergic hypothesis. *Experimental Neurology*, 163(2):495–529.
- Bartus, R. T., Dean, R. L., Beer, B., and Lippa, A. S. (1982). The cholinergic hypothesis of geriatric memory dysfunction. *Science (New York, N.Y.)*, 217(4558):408–14.

- Bassil, N. and Grossberg, G. T. (2009). Novel regimens and delivery systems in the pharmacological treatment of alzheimer's disease. *Cns Drugs*, 23(4):293–307.
- Bateman, R. J., Xiong, C., Benzinger, T. L. S., Fagan, A. M., Goate, A., Fox, N. C., Marcus, D. S., Cairns, N. J., Xie, X., Blazey, T. M., Holtzman, D. M., Santacruz, A., Buckles, V., Oliver, A., Moulder, K., Aisen, P. S., Ghetti, B., Klunk, W. E., McDade, E., Martins, R. N., Masters, C. L., Mayeux, R., Ringman, J. M., Rossor, M. N., Schofield, P. R., Sperling, R. A., Salloway, S., and Morris, J. C. (2012). Clinical and biomarker changes in dominantly inherited alzheimer's disease. *The New England Journal Of Medicine*, 367(9):795–804.
- Bekkers, J. M. and Stevens, C. F. (1990). Presynaptic mechanism for long-term potentiation in the hippocampus. *Nature*, 346(6286):724–9.
- Bellone, C. and Lüscher, C. (2006). Cocaine triggered ampa receptor redistribution is reversed in vivo by mglur-dependent long-term depression. *Nature Neuroscience*, 9(5):636–41.
- Berényi, A., Somogyvári, Z., Nagy, A. J., Roux, L., Long, J. D., Fujisawa, S., Stark, E., Leonardo, A., Harris, T. D., and Buzsáki, G. (2014). Large-scale, high-density (up to 512 channels) recording of local circuits in behaving animals. *Journal of neurophysiology*, 111(5):1132–1149.
- Bertalmio, M., Bertozzi, A. L., and Sapiro, G. (2001). Navier-stokes, fluid dynamics, and image and video inpainting. In *Computer Vision and Pattern Recognition, 2001. CVPR 2001. Proceedings of the 2001 IEEE Computer Society Conference on*, volume 1, pages I–I. IEEE.
- Best, P. J. and Orr, J. (1973). Effects of hippocampal lesions on passive avoidance and taste aversion conditioning. *Physiology & Behavior*, 10(2):193–196.
- Bienenstock, E. L., Cooper, L. N., and Munro, P. W. (1982). Theory for the development of neuron selectivity: orientation specificity and binocular interaction in visual cortex.

- The Journal Of Neuroscience : The Official Journal Of The Society For Neuroscience*, 2(1):32–48.
- Blennow, K., Hampel, H., Weiner, M., and Zetterberg, H. (2010). Cerebrospinal fluid and plasma biomarkers in alzheimer disease. *Nature Reviews. Neurology*, 6(3):131–44.
- Bliss, T. V. and Collingridge, G. L. (1993). A synaptic model of memory: long-term potentiation in the hippocampus. *Nature*, 361(6407):31–9.
- Bliss, T. V. and Lomo, T. (1973). Long-lasting potentiation of synaptic transmission in the dentate area of the anaesthetized rabbit following stimulation of the perforant path. *The Journal Of Physiology*, 232(2):331–56.
- Bond, M., Rogers, G., Peters, J., Anderson, R., Hoyle, M., Miners, A., Moxham, T., Davis, S., Thokala, P., Wailoo, A., Jeffreys, M., and Hyde, C. (2012). The effectiveness and cost-effectiveness of donepezil, galantamine, rivastigmine and memantine for the treatment of alzheimer's disease (review of technology appraisal no. 111): a systematic review and economic model. *Health Technology Assessment (Winchester, England)*, 16(21):1–470.
- Bontempi, B., Laurent-Demir, C., Destrade, C., and Jaffard, R. (1999). Time-dependent reorganization of brain circuitry underlying long-term memory storage. *Nature*, 400(6745):671–5.
- Borgdorff, A. J. and Choquet, D. (2002). Regulation of ampa receptor lateral movements. *Nature*, 417(6889):649–53.
- Born, H. A., Kim, J.-Y., Savjani, R. R., Das, P., Dabaghian, Y. A., Guo, Q., Yoo, J. W., Schuler, D. R., Cirrito, J. R., Zheng, H., Golde, T. E., Noebels, J. L., and Jankowsky, J. L. (2014). Genetic suppression of transgenic app rescues hypersynchronous network activity in a mouse model of alzheimer's disease. *The Journal Of Neuroscience : The Official Journal Of The Society For Neuroscience*, 34(11):3826–40.

- Braak, H. and Braak, E. (1991). Demonstration of amyloid deposits and neurofibrillary changes in whole brain sections. *Brain Pathology (Zurich, Switzerland)*, 1(3):213–6.
- Bramblett, G. T., Goedert, M., Jakes, R., Merrick, S. E., Trojanowski, J. Q., and Lee, V. M. (1993). Abnormal tau phosphorylation at ser396 in alzheimer's disease recapitulates development and contributes to reduced microtubule binding. *Neuron*, 10(6):1089–99.
- Bruce, D. (2001). Fifty years since lashley's in search of the engram: refutations and conjectures. *Journal Of The History Of The Neurosciences*, 10(3):308–18.
- Buchhave, P., Minthon, L., Zetterberg, H., Wallin, A. K., Blennow, K., and Hansson, O. (2012). Cerebrospinal fluid levels of  $\beta$ -amyloid 1-42, but not of tau, are fully changed already 5 to 10 years before the onset of alzheimer dementia. *Archives Of General Psychiatry*, 69(1):98–106.
- Buckmaster, P. S., Alonso, A., Canfield, D. R., and Amaral, D. G. (2004). Dendritic morphology, local circuitry, and intrinsic electrophysiology of principal neurons in the entorhinal cortex of macaque monkeys. *The Journal Of Comparative Neurology*, 470(3):317–29.
- Buckmaster, P. S., Strowbridge, B. W., and Schwartzkroin, P. A. (1993). A comparison of rat hippocampal mossy cells and ca3c pyramidal cells. *Journal Of Neurophysiology*, 70(4):1281–99.
- Burgess, N., Maguire, E. A., and O'Keefe, J. (2002). The human hippocampus and spatial and episodic memory. *Neuron*, 35(4):625–41.
- Burghaus, L., Schütz, U., Krempel, U., de Vos, R. A., Jansen Steur, E. N., Wevers, A., Lindstrom, J., and Schröder, H. (2000). Quantitative assessment of nicotinic acetylcholine receptor proteins in the cerebral cortex of alzheimer patients. *Brain Research. Molecular Brain Research*, 76(2):385–8.
- Busche, M. A., Chen, X., Henning, H. A., Reichwald, J., Staufenbiel, M., Sakmann, B., and Konnerth, A. (2012). Critical role of soluble amyloid- $\beta$  for early hippocampal hyper-

- activity in a mouse model of alzheimer's disease. *Proceedings Of The National Academy Of Sciences Of The United States Of America*, 109(22):8740–5.
- Busche, M. A., Kekuš, M., Adelsberger, H., Noda, T., Förstl, H., Nelken, I., and Konnerth, A. (2015). Rescue of long-range circuit dysfunction in alzheimer's disease models. *Nature Neuroscience*, 18(11):1623–30.
- Buzsáki, G. (2002). Theta oscillations in the hippocampus. *Neuron*, 33(3):325–40.
- Cabrejo, L., Guyant-Maréchal, L., Laquerrière, A., Vercelletto, M., De la Fournière, F., Thomas-Antérion, C., Verny, C., Letourneau, F., Pasquier, F., Vital, A., Checler, F., Frebourg, T., Campion, D., and Hannequin, D. (2006). Phenotype associated with app duplication in five families. *Brain : A Journal Of Neurology*, 129(Pt 11):2966–76.
- Cacucci, F., Yi, M., Wills, T. J., Chapman, P., and O'Keefe, J. (2008). Place cell firing correlates with memory deficits and amyloid plaque burden in tg2576 alzheimer mouse model. *Proceedings Of The National Academy Of Sciences Of The United States Of America*, 105(22):7863–8.
- Cai, X. D., Golde, T. E., and Younkin, S. G. (1993). Release of excess amyloid beta protein from a mutant amyloid beta protein precursor. *Science (New York, N.Y.)*, 259(5094):514–6.
- Cajal, S. R. (1893). *Estructura del asta de ammon y fascia dentata*. tip. de Fortanet.
- Calhoun, M. E., Fletcher, B. R., Yi, S., Zentko, D. C., Gallagher, M., and Rapp, P. R. (2008). Age-related spatial learning impairment is unrelated to spinophilin immunoreactive spine number and protein levels in rat hippocampus. *Neurobiology Of Aging*, 29(8):1256–64.
- Canter, R. G., Penney, J., and Tsai, L.-H. (2016). The road to restoring neural circuits for the treatment of alzheimer's disease. *Nature*, 539(7628):187–196.

- Carrillo-Reid, L., Yang, W., Bando, Y., Peterka, D. S., and Yuste, R. (2016). Imprinting and recalling cortical ensembles. *Science (New York, N.Y.)*, 353(6300):691–4.
- Chapman, P. F., White, G. L., Jones, M. W., Cooper-Blacketer, D., Marshall, V. J., Irizarry, M., Younkin, L., Good, M. A., Bliss, T. V., Hyman, B. T., Younkin, S. G., and Hsiao, K. K. (1999). Impaired synaptic plasticity and learning in aged amyloid precursor protein transgenic mice. *Nature Neuroscience*, 2(3):271–6.
- Chater, T. E. and Goda, Y. (2014). The role of ampa receptors in postsynaptic mechanisms of synaptic plasticity. *Frontiers In Cellular Neuroscience*, 8:401.
- Chen, H.-H., Liao, P.-F., and Chan, M.-H. (2011). mglur5 positive modulators both potentiate activation and restore inhibition in nmda receptors by pkc dependent pathway. *Journal Of Biomedical Science*, 18:19.
- Chen, L., El-Husseini, A., Tomita, S., Bredt, D. S., and Nicoll, R. A. (2003). Stargazin differentially controls the trafficking of alpha-amino-3-hydroxyl-5-methyl-4-isoxazolepropionate and kainate receptors. *Molecular Pharmacology*, 64(3):703–6.
- Chen, T.-W., Wardill, T. J., Sun, Y., Pulver, S. R., Renninger, S. L., Baohan, A., Schreiter, E. R., Kerr, R. A., Orger, M. B., Jayaraman, V., Looger, L. L., Svoboda, K., and Kim, D. S. (2013). Ultrasensitive fluorescent proteins for imaging neuronal activity. *Nature*, 499(7458):295–300.
- Chen, X., Li, M., Wang, S., Zhu, H., Xiong, Y., and Liu, X. (2014). Pittsburgh compound b retention and progression of cognitive status—a meta-analysis. *European Journal Of Neurology*, 21(8):1060–7.
- Cheng, J. and Ji, D. (2013). Rigid firing sequences undermine spatial memory codes in a neurodegenerative mouse model. *Elife*, 2:e00647.
- Chetelat, G. and Baron, J.-C. (2003). Early diagnosis of alzheimer's disease: contribution of structural neuroimaging. *Neuroimage*, 18(2):525–41.

- Chetverikov, D., Svirko, D., Stepanov, D., and Krsek, P. (2002). The trimmed iterative closest point algorithm. In *Pattern Recognition, 2002. Proceedings. 16th International Conference on*, volume 3, pages 545–548. IEEE.
- Chevaleyre, V. and Piskorowski, R. A. (2016). Hippocampal area ca2: An overlooked but promising therapeutic target. *Trends In Molecular Medicine*, 22(8):645–55.
- Chien, D. T., Szardenings, A. K., Bahri, S., Walsh, J. C., Mu, F., Xia, C., Shankle, W. R., Lerner, A. J., Su, M.-Y., Elizarov, A., and Kolb, H. C. (2014). Early clinical pet imaging results with the novel phf-tau radioligand [f18]-t808. *Journal Of Alzheimer'S Disease : Jad*, 38(1):171–84.
- Chishti, M. A., Yang, D. S., Janus, C., Phinney, A. L., Horne, P., Pearson, J., Strome, R., Zuker, N., Loukides, J., French, J., Turner, S., Lozza, G., Grilli, M., Kunicki, S., Morissette, C., Paquette, J., Gervais, F., Bergeron, C., Fraser, P. E., Carlson, G. A., George-Hyslop, P. S., and Westaway, D. (2001). Early-onset amyloid deposition and cognitive deficits in transgenic mice expressing a double mutant form of amyloid precursor protein 695. *The Journal Of Biological Chemistry*, 276(24):21562–70.
- Chung, K. and Deisseroth, K. (2013). Clarity for mapping the nervous system. *Nature Methods*, 10(6):508–13.
- Cipolotti, L., Shallice, T., Chan, D., Fox, N., Scahill, R., Harrison, G., Stevens, J., and Rudge, P. (2001). Long-term retrograde amnesia...the crucial role of the hippocampus. *Neuropsychologia*, 39(2):151–72.
- Citri, A. and Malenka, R. C. (2008). Synaptic plasticity: multiple forms, functions, and mechanisms. *Neuropsychopharmacology : Official Publication Of The American College Of Neuropsychopharmacology*, 33(1):18–41.
- Citron, M., Oltersdorf, T., Haass, C., McConlogue, L., Hung, A. Y., Seubert, P., Vigo-Pelfrey, C., Lieberburg, I., and Selkoe, D. J. (1992). Mutation of the beta-amyloid pre-

- cursor protein in familial alzheimer's disease increases beta-protein production. *Nature*, 360(6405):672–4.
- Ciupek, S. M., Cheng, J., Ali, Y. O., Lu, H.-C., and Ji, D. (2015). Progressive functional impairments of hippocampal neurons in a tauopathy mouse model. *The Journal Of Neuroscience : The Official Journal Of The Society For Neuroscience*, 35(21):8118–31.
- Clark, R. E., Broadbent, N. J., and Squire, L. R. (2005). Impaired remote spatial memory after hippocampal lesions despite extensive training beginning early in life. *Hippocampus*, 15(3):340–6.
- Clark, R. E. and Squire, L. R. (2013). Similarity in form and function of the hippocampus in rodents, monkeys, and humans. *Proceedings Of The National Academy Of Sciences Of The United States Of America*, 110 Suppl 2:10365–70.
- Clavaguera, F., Bolmont, T., Crowther, R. A., Abramowski, D., Frank, S., Probst, A., Fraser, G., Stalder, A. K., Beibel, M., Staufenbiel, M., Jucker, M., Goedert, M., and Tolnay, M. (2009). Transmission and spreading of tauopathy in transgenic mouse brain. *Nature Cell Biology*, 11(7):909–13.
- Clugnet, M. C. and LeDoux, J. E. (1990). Synaptic plasticity in fear conditioning circuits: induction of ltp in the lateral nucleus of the amygdala by stimulation of the medial geniculate body. *The Journal Of Neuroscience : The Official Journal Of The Society For Neuroscience*, 10(8):2818–24.
- Cohen, N. J. and Squire, L. R. (1980). Preserved learning and retention of pattern-analyzing skill in amnesia: dissociation of knowing how and knowing that. *Science (New York, N.Y.)*, 210(4466):207–10.
- Coleman, P., Federoff, H., and Kurlan, R. (2004). A focus on the synapse for neuroprotection in alzheimer disease and other dementias. *Neurology*, 63(7):1155–62.

- Colgin, L. L., Denninger, T., Fyhn, M., Hafting, T., Bonnevie, T., Jensen, O., Moser, M.-B., and Moser, E. I. (2009). Frequency of gamma oscillations routes flow of information in the hippocampus. *Nature*, 462(7271):353–7.
- Collingridge, G. L., Isaac, J. T. R., and Wang, Y. T. (2004). Receptor trafficking and synaptic plasticity. *Nature Reviews. Neuroscience*, 5(12):952–62.
- Collingridge, G. L., Kehl, S. J., and McLennan, H. (1983). Excitatory amino acids in synaptic transmission in the schaffer collateral-commissural pathway of the rat hippocampus. *The Journal Of Physiology*, 334:33–46.
- Collingridge, G. L., Peineau, S., Howland, J. G., and Wang, Y. T. (2010). Long-term depression in the cns. *Nature Reviews. Neuroscience*, 11(7):459–73.
- Connors, B. W. and Gutnick, M. J. (1990). Intrinsic firing patterns of diverse neocortical neurons. *Trends In Neurosciences*, 13(3):99–104.
- Contestabile, A. (2011). The history of the cholinergic hypothesis. *Behavioural Brain Research*, 221(2):334–40.
- Cooper, L. N. and Bear, M. F. (2012). The bcm theory of synapse modification at 30: interaction of theory with experiment. *Nature Reviews. Neuroscience*, 13(11):798–810.
- Cowansage, K. K., Shuman, T., Dillingham, B. C., Chang, A., Golshani, P., and Mayford, M. (2014). Direct reactivation of a coherent neocortical memory of context. *Neuron*, 84(2):432–41.
- Crestani, F., Keist, R., Fritschy, J.-M., Benke, D., Vogt, K., Prut, L., Blüthmann, H., Möhler, H., and Rudolph, U. (2002). Trace fear conditioning involves hippocampal alpha<sub>5</sub> gaba(a) receptors. *Proceedings Of The National Academy Of Sciences Of The United States Of America*, 99(13):8980–5.
- Dana, H., Chen, T.-W., Hu, A., Shields, B. C., Guo, C., Looger, L. L., Kim, D. S., and

- Svoboda, K. (2014). Thy1-gcamp6 transgenic mice for neuronal population imaging in vivo. *Plos One*, 9(9):e108697.
- Danysz, W. and Parsons, C. G. (2012). Alzheimer's disease,  $\beta$ -amyloid, glutamate, nmda receptors and memantine—searching for the connections. *British Journal Of Pharmacology*, 167(2):324–52.
- Davis, K. L., Mohs, R. C., Marin, D., Purohit, D. P., Perl, D. P., Lantz, M., Austin, G., and Haroutunian, V. (1999). Cholinergic markers in elderly patients with early signs of alzheimer disease. *Jama*, 281(15):1401–6.
- DeKosky, S. T., Ikonomovic, M. D., Styren, S. D., Beckett, L., Wisniewski, S., Bennett, D. A., Cochran, E. J., Kordower, J. H., and Mufson, E. J. (2002). Upregulation of choline acetyltransferase activity in hippocampus and frontal cortex of elderly subjects with mild cognitive impairment. *Annals Of Neurology*, 51(2):145–55.
- Denny, C. A., Kheirbek, M. A., Alba, E. L., Tanaka, K. F., Brachman, R. A., Laughman, K. B., Tomm, N. K., Turi, G. F., Losonczy, A., and Hen, R. (2014). Hippocampal memory traces are differentially modulated by experience, time, and adult neurogenesis. *Neuron*, 83(1):189–201.
- Desimone, R. and Duncan, J. (1995). Neural mechanisms of selective visual attention. *Annual Review Of Neuroscience*, 18:193–222.
- Deutsch, J. A. (1971). The cholinergic synapse and the site of memory. *Science (New York, N.Y.)*, 174(4011):788–94.
- Dias, C., Wang, Y. T., and Phillips, A. G. (2012). Facilitated extinction of morphine conditioned place preference with tat-glua2(3y) interference peptide. *Behavioural Brain Research*, 233(2):389–97.
- Dodart, J. C., Meziane, H., Mathis, C., Bales, K. R., Paul, S. M., and Ungerer, A. (1999).

- Behavioral disturbances in transgenic mice overexpressing the v717f beta-amyloid precursor protein. *Behavioral Neuroscience*, 113(5):982–90.
- Doeller, C. F., Barry, C., and Burgess, N. (2010). Evidence for grid cells in a human memory network. *Nature*, 463(7281):657–61.
- Dong, H., Martin, M. V., Chambers, S., and Csernansky, J. G. (2007). Spatial relationship between synapse loss and beta-amyloid deposition in tg2576 mice. *The Journal Of Comparative Neurology*, 500(2):311–21.
- Dong, Z., Han, H., Li, H., Bai, Y., Wang, W., Tu, M., Peng, Y., Zhou, L., He, W., Wu, X., Tan, T., Liu, M., Wu, X., Zhou, W., Jin, W., Zhang, S., Sacktor, T. C., Li, T., Song, W., and Wang, Y. T. (2015). Long-term potentiation decay and memory loss are mediated by ampar endocytosis. *The Journal Of Clinical Investigation*, 125(1):234–47.
- Drachman, D. A. and Leavitt, J. (1974). Human memory and the cholinergic system. a relationship to aging? *Archives Of Neurology*, 30(2):113–21.
- Driver, J. E., Racca, C., Cunningham, M. O., Towers, S. K., Davies, C. H., Whittington, M. A., and LeBeau, F. E. N. (2007). Impairment of hippocampal gamma-frequency oscillations in vitro in mice overexpressing human amyloid precursor protein (app). *The European Journal Of Neuroscience*, 26(5):1280–8.
- Dubois, B., Hampel, H., Feldman, H. H., Scheltens, P., Aisen, P., Andrieu, S., Bakardjian, H., Benali, H., Bertram, L., Blennow, K., Broich, K., Cavedo, E., Crutch, S., Dartigues, J.-F., Duyckaerts, C., Epelbaum, S., Frisoni, G. B., Gauthier, S., Genthon, R., Gouw, A. A., Habert, M.-O., Holtzman, D. M., Kivipelto, M., Lista, S., Molinuevo, J.-L., O'Bryant, S. E., Rabinovici, G. D., Rowe, C., Salloway, S., Schneider, L. S., Sperling, R., Teichmann, M., Carrillo, M. C., Cummings, J., and Jack, C. R. (2016). Preclinical alzheimer's disease: Definition, natural history, and diagnostic criteria. *Alzheimer'S & Dementia : The Journal Of The Alzheimer'S Association*, 12(3):292–323.

- Dudek, S. M. and Bear, M. F. (1992). Homosynaptic long-term depression in area ca1 of hippocampus and effects of n-methyl-d-aspartate receptor blockade. *Proceedings Of The National Academy Of Sciences Of The United States Of America*, 89(10):4363–7.
- Dudok, B., Barna, L., Ledri, M., Szabó, S. I., Szabadits, E., Pintér, B., Woodhams, S. G., Henstridge, C. M., Balla, G. Y., Nyilas, R., Varga, C., Lee, S.-H., Matolcsi, M., Cervenak, J., Kacskovics, I., Watanabe, M., Sagheddu, C., Melis, M., Pistis, M., Soltesz, I., and Katona, I. (2015). Cell-specific storm super-resolution imaging reveals nanoscale organization of cannabinoid signaling. *Nature Neuroscience*, 18(1):75–86.
- Duff, M. C., Hengst, J. A., Tranel, D., and Cohen, N. J. (2009). Hippocampal amnesia disrupts verbal play and the creative use of language in social interaction. *Aphasiology*, 23(7-8):926–939.
- Duff, M. C., Kurczek, J., Rubin, R., Cohen, N. J., and Tranel, D. (2013). Hippocampal amnesia disrupts creative thinking. *Hippocampus*, 23(12):1143–9.
- Dunbar, A. B. and Taylor, J. R. (2016). Reconsolidation and psychopathology: Moving towards reconsolidation-based treatments. *Neurobiology of Learning and Memory*.
- Eacott, M. J. and Norman, G. (2004). Integrated memory for object, place, and context in rats: a possible model of episodic-like memory? *The Journal Of Neuroscience : The Official Journal Of The Society For Neuroscience*, 24(8):1948–53.
- Eichenbaum, H. (1993). *Memory, amnesia, and the hippocampal system*. MIT press.
- Eichenbaum, H. and Cohen, N. J. (2014). Can we reconcile the declarative memory and spatial navigation views on hippocampal function? *Neuron*, 83(4):764–70.
- Fagan, A. M., Xiong, C., Jasielec, M. S., Bateman, R. J., Goate, A. M., Benzinger, T. L. S., Ghetti, B., Martins, R. N., Masters, C. L., Mayeux, R., Ringman, J. M., Rossor, M. N., Salloway, S., Schofield, P. R., Sperling, R. A., Marcus, D., Cairns, N. J., Buckles, V. D., Ladenson, J. H., Morris, J. C., and Holtzman, D. M. (2014). Longitudinal change in csf

- biomarkers in autosomal-dominant alzheimer's disease. *Science Translational Medicine*, 6(226):226ra30.
- Fanselow, M. S. and Dong, H.-W. (2010). Are the dorsal and ventral hippocampus functionally distinct structures? *Neuron*, 65(1):7–19.
- Farlow, M., Anand, R., Messina, J., Hartman, R., and Veach, J. (2000). A 52-week study of the efficacy of rivastigmine in patients with mild to moderately severe alzheimer's disease. *European Neurology*, 44(4):236–41.
- Farlow, M. R., Andreasen, N., Riviere, M.-E., Vostiar, I., Vitaliti, A., Sovago, J., Caputo, A., Winblad, B., and Graf, A. (2015). Long-term treatment with active  $\alpha\beta$  immunotherapy with cad106 in mild alzheimer's disease. *Alzheimer's Research & Therapy*, 7(1):23.
- Fernandes, D. and Carvalho, A. L. (2016). Mechanisms of homeostatic plasticity in the excitatory synapse. *Journal Of Neurochemistry*, 139(6):973–996.
- Ferreira, S. T., Lourenco, M. V., Oliveira, M. M., and De Felice, F. G. (2015). Soluble amyloid- $\beta$  oligomers as synaptotoxins leading to cognitive impairment in alzheimer's disease. *Frontiers In Cellular Neuroscience*, 9:191.
- Finch, D. M., Nowlin, N. L., and Babb, T. L. (1983). Demonstration of axonal projections of neurons in the rat hippocampus and subiculum by intracellular injection of hrp. *Brain Research*, 271(2):201–16.
- Fitzjohn, S. M., Morton, R. A., Kuenzi, F., Rosahl, T. W., Shearman, M., Lewis, H., Smith, D., Reynolds, D. S., Davies, C. H., Collingridge, G. L., and Seabrook, G. R. (2001). Age-related impairment of synaptic transmission but normal long-term potentiation in transgenic mice that overexpress the human app695swe mutant form of amyloid precursor protein. *The Journal Of Neuroscience : The Official Journal Of The Society For Neuroscience*, 21(13):4691–8.

- Flusberg, B. A., Jung, J. C., Cocker, E. D., Anderson, E. P., and Schnitzer, M. J. (2005). In vivo brain imaging using a portable 3.9 gram two-photon fluorescence microendoscope. *Optics Letters*, 30(17):2272–4.
- Flusberg, B. A., Nimmerjahn, A., Cocker, E. D., Mukamel, E. A., Barretto, R. P. J., Ko, T. H., Burns, L. D., Jung, J. C., and Schnitzer, M. J. (2008). High-speed, miniaturized fluorescence microscopy in freely moving mice. *Nature Methods*, 5(11):935–8.
- Fosgerau, K. and Hoffmann, T. (2015). Peptide therapeutics: current status and future directions. *Drug Discovery Today*, 20(1):122–8.
- Frank, C. A., Kennedy, M. J., Goold, C. P., Marek, K. W., and Davis, G. W. (2006). Mechanisms underlying the rapid induction and sustained expression of synaptic homeostasis. *Neuron*, 52(4):663–77.
- Frankland, P. W. and Bontempi, B. (2005). The organization of recent and remote memories. *Nature Reviews. Neuroscience*, 6(2):119–30.
- Frankland, P. W., Bontempi, B., Talton, L. E., Kaczmarek, L., and Silva, A. J. (2004). The involvement of the anterior cingulate cortex in remote contextual fear memory. *Science (New York, N.Y.)*, 304(5672):881–3.
- Fraser, G. W. and Schwartz, A. B. (2012). Recording from the same neurons chronically in motor cortex. *Journal Of Neurophysiology*, 107(7):1970–8.
- Fyhn, M., Molden, S., Witter, M. P., Moser, E. I., and Moser, M.-B. (2004). Spatial representation in the entorhinal cortex. *Science (New York, N.Y.)*, 305(5688):1258–64.
- Gainey, M. A., Hurvitz-Wolff, J. R., Lambo, M. E., and Turrigiano, G. G. (2009). Synaptic scaling requires the glur2 subunit of the ampa receptor. *The Journal Of Neuroscience : The Official Journal Of The Society For Neuroscience*, 29(20):6479–89.
- Gainey, M. A., Tatavarty, V., Nahmani, M., Lin, H., and Turrigiano, G. G. (2015). Activity-dependent synaptic grip1 accumulation drives synaptic scaling up in response to action

- potential blockade. *Proceedings Of The National Academy Of Sciences Of The United States Of America*, 112(27):E3590–9.
- Gallo, M. and Cândido, A. (1995). Dorsal hippocampal lesions impair blocking but not latent inhibition of taste aversion learning in rats. *Behavioral neuroscience*, 109(3):413.
- Gao, M., Sossa, K., Song, L., Errington, L., Cummings, L., Hwang, H., Kuhl, D., Worley, P., and Lee, H.-K. (2010). A specific requirement of arc/arg3.1 for visual experience-induced homeostatic synaptic plasticity in mouse primary visual cortex. *The Journal Of Neuroscience : The Official Journal Of The Society For Neuroscience*, 30(21):7168–78.
- Geula, C. and Mesulam, M. M. (1996). Systematic regional variations in the loss of cortical cholinergic fibers in alzheimer's disease. *Cerebral Cortex (New York, N.Y. : 1991)*, 6(2):165–77.
- Ghosh, K. K., Burns, L. D., Cocker, E. D., Nimmerjahn, A., Ziv, Y., Gamal, A. E., and Schnitzer, M. J. (2011). Miniaturized integration of a fluorescence microscope. *Nature Methods*, 8(10):871–8.
- Gillette-Guyonnet, S., Andrieu, S., Nourhashemi, F., Gardette, V., Coley, N., Cantet, C., Gauthier, S., Ousset, P.-J., and Vellas, B. (2011). Long-term progression of alzheimer's disease in patients under antidementia drugs. *Alzheimer'S & Dementia : The Journal Of The Alzheimer'S Association*, 7(6):579–92.
- Gladding, C. M., Fitzjohn, S. M., and Molnár, E. (2009). Metabotropic glutamate receptor-mediated long-term depression: molecular mechanisms. *Pharmacological Reviews*, 61(4):395–412.
- Goedert, M. and Spillantini, M. G. (2006). A century of alzheimer's disease. *Science (New York, N.Y.)*, 314(5800):777–81.
- Goedert, M. and Spillantini, M. G. (2011). Pathogenesis of the tauopathies. *Journal Of Molecular Neuroscience : Mn*, 45(3):425–31.

- Goel, A., Xu, L. W., Snyder, K. P., Song, L., Goenaga-Vazquez, Y., Megill, A., Takamiya, K., Huganir, R. L., and Lee, H.-K. (2011). Phosphorylation of ampa receptors is required for sensory deprivation-induced homeostatic synaptic plasticity. *Plos One*, 6(3):e18264.
- Goutagny, R., Gu, N., Cavanagh, C., Jackson, J., Chabot, J.-G., Quirion, R., Krantic, S., and Williams, S. (2013). Alterations in hippocampal network oscillations and theta-gamma coupling arise before  $\alpha\beta$  overproduction in a mouse model of alzheimer's disease. *The European Journal Of Neuroscience*, 37(12):1896–902.
- Granger, A. J., Shi, Y., Lu, W., Cerpas, M., and Nicoll, R. A. (2013). Ltp requires a reserve pool of glutamate receptors independent of subunit type. *Nature*, 493(7433):495–500.
- Greenamyre, J. T., Maragos, W. F., Albin, R. L., Penney, J. B., and Young, A. B. (1988). Glutamate transmission and toxicity in alzheimer's disease. *Progress In Neuro-Psychopharmacology & Biological Psychiatry*, 12(4):421–30.
- Greger, I. H., Khatri, L., Kong, X., and Ziff, E. B. (2003). Ampa receptor tetramerization is mediated by q/r editing. *Neuron*, 40(4):763–74.
- Grewé, B. F., Gründemann, J., Kitch, L. J., Lecoq, J. A., Parker, J. G., Marshall, J. D., Larkin, M. C., Jercog, P. E., Grenier, F., Li, J. Z., Lüthi, A., and Schnitzer, M. J. (2017). Neural ensemble dynamics underlying a long-term associative memory. *Nature*, 543(7647):670–675.
- Groc, L., Heine, M., Cognet, L., Brickley, K., Stephenson, F. A., Lounis, B., and Choquet, D. (2004). Differential activity-dependent regulation of the lateral mobilities of ampa and nmda receptors. *Nature Neuroscience*, 7(7):695–6.
- Grundke-Iqbali, I., Iqbal, K., Tung, Y. C., Quinlan, M., Wisniewski, H. M., and Binder, L. I. (1986). Abnormal phosphorylation of the microtubule-associated protein tau (tau) in alzheimer cytoskeletal pathology. *Proceedings Of The National Academy Of Sciences Of The United States Of America*, 83(13):4913–7.

- Guenthner, C. J., Miyamichi, K., Yang, H. H., Heller, H. C., and Luo, L. (2013). Permanent genetic access to transiently active neurons via trap: targeted recombination in active populations. *Neuron*, 78(5):773–84.
- Guizar-Sicairos, M., Thurman, S. T., and Fienup, J. R. (2008). Efficient subpixel image registration algorithms. *Optics letters*, 33(2):156–158.
- Guntupalli, S., Widagdo, J., and Anggono, V. (2016). Amyloid- $\beta$ -induced dysregulation of ampa receptor trafficking. *Neural Plasticity*, 2016:3204519.
- Guo, J.-P., Arai, T., Miklossy, J., and McGeer, P. L. (2006). Abeta and tau form soluble complexes that may promote self aggregation of both into the insoluble forms observed in alzheimer's disease. *Proceedings Of The National Academy Of Sciences Of The United States Of America*, 103(6):1953–8.
- Guzowski, J. F., McNaughton, B. L., Barnes, C. A., and Worley, P. F. (1999). Environment-specific expression of the immediate-early gene arc in hippocampal neuronal ensembles. *Nature Neuroscience*, 2(12):1120–4.
- Guzowski, J. F., Miyashita, T., Chawla, M. K., Sanderson, J., Maes, L. I., Houston, F. P., Lipa, P., McNaughton, B. L., Worley, P. F., and Barnes, C. A. (2006). Recent behavioral history modifies coupling between cell activity and arc gene transcription in hippocampal ca1 neurons. *Proceedings Of The National Academy Of Sciences Of The United States Of America*, 103(4):1077–82.
- Götz, J., Streffer, J. R., David, D., Schild, A., Hoerndl, F., Pennanen, L., Kurosinski, P., and Chen, F. (2004). Transgenic animal models of alzheimer's disease and related disorders: histopathology, behavior and therapy. *Molecular Psychiatry*, 9(7):664–83.
- Güntekin, B., Saatçi, E., and Yener, G. (2008). Decrease of evoked delta, theta and alpha coherences in alzheimer patients during a visual oddball paradigm. *Brain Research*, 1235:109–16.

- Haas, L. T., Salazar, S. V., Kostylev, M. A., Um, J. W., Kaufman, A. C., and Strittmatter, S. M. (2016). Metabotropic glutamate receptor 5 couples cellular prion protein to intracellular signalling in alzheimer's disease. *Brain : A Journal Of Neurology*, 139(Pt 2):526–46.
- Habib, D., Tsui, C. K. Y., Rosen, L. G., and Dringenberg, H. C. (2014). Occlusion of low-frequency-induced, heterosynaptic long-term potentiation in the rat hippocampus in vivo following spatial training. *Cerebral Cortex (New York, N.Y. : 1991)*, 24(11):3090–6.
- Hafting, T., Fyhn, M., Molden, S., Moser, M.-B., and Moser, E. I. (2005). Microstructure of a spatial map in the entorhinal cortex. *Nature*, 436(7052):801–6.
- Hall, J., Thomas, K. L., and Everitt, B. J. (2001). Cellular imaging of zif268 expression in the hippocampus and amygdala during contextual and cued fear memory retrieval: selective activation of hippocampal ca1 neurons during the recall of contextual memories. *The Journal Of Neuroscience : The Official Journal Of The Society For Neuroscience*, 21(6):2186–93.
- Hamel, E. J. O., Grewe, B. F., Parker, J. G., and Schnitzer, M. J. (2015). Cellular level brain imaging in behaving mammals: an engineering approach. *Neuron*, 86(1):140–59.
- Hamilton, A., Esseltine, J. L., DeVries, R. A., Cregan, S. P., and Ferguson, S. S. G. (2014). Metabotropic glutamate receptor 5 knockout reduces cognitive impairment and pathogenesis in a mouse model of alzheimer's disease. *Molecular Brain*, 7:40.
- Hampson, R. E., Heyser, C. J., and Deadwyler, S. A. (1993). Hippocampal cell firing correlates of delayed-match-to-sample performance in the rat. *Behavioral Neuroscience*, 107(5):715–39.
- Hanley, J. G. (2008). Ampa receptor trafficking pathways and links to dendritic spine morphogenesis. *Cell Adhesion & Migration*, 2(4):276–82.

- Hardy, J. and Selkoe, D. J. (2002). The amyloid hypothesis of alzheimer's disease: progress and problems on the road to therapeutics. *Science (New York, N.Y.)*, 297(5580):353–6.
- Hardy, J. A. and Higgins, G. A. (1992). Alzheimer's disease: the amyloid cascade hypothesis. *Science (New York, N.Y.)*, 256(5054):184–5.
- Harris, J. A., Devidze, N., Verret, L., Ho, K., Halabisky, B., Thwin, M. T., Kim, D., Hamto, P., Lo, I., Yu, G.-Q., Palop, J. J., Masliah, E., and Mucke, L. (2010). Transsynaptic progression of amyloid- $\beta$ -induced neuronal dysfunction within the entorhinal-hippocampal network. *Neuron*, 68(3):428–41.
- Hartley, T., Bird, C. M., Chan, D., Cipolotti, L., Husain, M., Vargha-Khadem, F., and Burgess, N. (2007). The hippocampus is required for short-term topographical memory in humans. *Hippocampus*, 17(1):34–48.
- Harvey, C. D., Coen, P., and Tank, D. W. (2012). Choice-specific sequences in parietal cortex during a virtual-navigation decision task. *Nature*, 484(7392):62–8.
- Harvey, C. D., Collman, F., Dombeck, D. A., and Tank, D. W. (2009). Intracellular dynamics of hippocampal place cells during virtual navigation. *Nature*, 461(7266):941–6.
- Hasselmo, M. E. (1994). Runaway synaptic modification in models of cortex: Implications for alzheimer's disease. *Neural Networks*, 7(1):13–40.
- Hasselmo, M. E. (1997). A computational model of the progression of alzheimer's disease. *M.D. Computing : Computers In Medical Practice*, 14(3):181–91.
- Hatsopoulos, N. G. and Donoghue, J. P. (2009). The science of neural interface systems. *Annual Review Of Neuroscience*, 32:249–66.
- Hayashi, Y., Shi, S. H., Esteban, J. A., Piccini, A., Poncer, J. C., and Malinow, R. (2000). Driving ampa receptors into synapses by ltp and camkii: requirement for glur1 and pdz domain interaction. *Science (New York, N.Y.)*, 287(5461):2262–7.

- Hebb, D. O. (1949). *The Organization of Behavior*. Wiley, New York.
- Hebert, L. E., Weuve, J., Scherr, P. A., and Evans, D. A. (2013). Alzheimer disease in the united states (2010-2050) estimated using the 2010 census. *Neurology*, 80(19):1778–83.
- Helzner, E. P., Scarmeas, N., Cosentino, S., Tang, M. X., Schupf, N., and Stern, Y. (2008). Survival in alzheimer disease: a multiethnic, population-based study of incident cases. *Neurology*, 71(19):1489–95.
- Henley, J. M., Barker, E. A., and Glebov, O. O. (2011). Routes, destinations and delays: recent advances in ampa receptor trafficking. *Trends In Neurosciences*, 34(5):258–68.
- Henley, J. M. and Wilkinson, K. A. (2013). Ampa receptor trafficking and the mechanisms underlying synaptic plasticity and cognitive aging. *Dialogues In Clinical Neuroscience*, 15(1):11–27.
- Herring, B. E. and Nicoll, R. A. (2016). Long-term potentiation: From camkii to ampa receptor trafficking. *Annual Review Of Physiology*, 78:351–65.
- Hevner, R. F. and Wong-Riley, M. T. (1992). Entorhinal cortex of the human, monkey, and rat: metabolic map as revealed by cytochrome oxidase. *The Journal Of Comparative Neurology*, 326(3):451–69.
- Hollmann, M. and Heinemann, S. (1994). Cloned glutamate receptors. *Annual Review Of Neuroscience*, 17:31–108.
- Horn, D., Ruppin, E., Usher, M., and Herrmann, M. (1993). Neural network modeling of memory deterioration in alzheimer's disease. *Neural Computation*, 5(5):736–749.
- Horton, N. G., Wang, K., Kobat, D., Clark, C. G., Wise, F. W., Schaffer, C. B., and Xu, C. (2013). In vivo three-photon microscopy of subcortical structures within an intact mouse brain. *Nature photonics*, 7(3):205–209.

- Horváth, A., Szűcs, A., Barcs, G., Noebels, J. L., and Kamondi, A. (2016). Epileptic seizures in alzheimer disease: A review. *Alzheimer Disease And Associated Disorders*, 30(2):186–92.
- Hsia, A. Y., Masliah, E., McConlogue, L., Yu, G. Q., Tatsuno, G., Hu, K., Kholodenko, D., Malenka, R. C., Nicoll, R. A., and Mucke, L. (1999). Plaque-independent disruption of neural circuits in alzheimer's disease mouse models. *Proceedings Of The National Academy Of Sciences Of The United States Of America*, 96(6):3228–33.
- Hsiao, K., Chapman, P., Nilsen, S., Eckman, C., Harigaya, Y., Younkin, S., Yang, F., and Cole, G. (1996). Correlative memory deficits, abeta elevation, and amyloid plaques in transgenic mice. *Science (New York, N.Y.)*, 274(5284):99–102.
- Hsieh, H., Boehm, J., Sato, C., Iwatsubo, T., Tomita, T., Sisodia, S., and Malinow, R. (2006). Ampar removal underlies abeta-induced synaptic depression and dendritic spine loss. *Neuron*, 52(5):831–43.
- Hsieh, L.-T., Gruber, M. J., Jenkins, L. J., and Ranganath, C. (2014). Hippocampal activity patterns carry information about objects in temporal context. *Neuron*, 81(5):1165–78.
- Hu, J.-H., Park, J. M., Park, S., Xiao, B., Dehoff, M. H., Kim, S., Hayashi, T., Schwarz, M. K., Huganir, R. L., Seburg, P. H., Linden, D. J., and Worley, P. F. (2010). Homeostatic scaling requires group i mglur activation mediated by homer1a. *Neuron*, 68(6):1128–42.
- Hu, N.-W., Nicoll, A. J., Zhang, D., Mably, A. J., O'Malley, T., Purro, S. A., Terry, C., Collinge, J., Walsh, D. M., and Rowan, M. J. (2014). mglu5 receptors and cellular prion protein mediate amyloid- $\beta$ -facilitated synaptic long-term depression in vivo. *Nature Communications*, 5:3374.
- Hu, N.-W., Smith, I. M., Walsh, D. M., and Rowan, M. J. (2008). Soluble amyloid-beta peptides potently disrupt hippocampal synaptic plasticity in the absence of cerebrovascular dysfunction in vivo. *Brain : A Journal Of Neurology*, 131(Pt 9):2414–24.

- Hutton, M., Lendon, C. L., Rizzu, P., Baker, M., Froelich, S., Houlden, H., Pickering-Brown, S., Chakraverty, S., Isaacs, A., Grover, A., Hackett, J., Adamson, J., Lincoln, S., Dickson, D., Davies, P., Petersen, R. C., Stevens, M., de Graaff, E., Wauters, E., van Baren, J., Hillebrand, M., Joosse, M., Kwon, J. M., Nowotny, P., Che, L. K., Norton, J., Morris, J. C., Reed, L. A., Trojanowski, J., Basun, H., Lannfelt, L., Neystat, M., Fahn, S., Dark, F., Tannenberg, T., Dodd, P. R., Hayward, N., Kwok, J. B., Schofield, P. R., Andreadis, A., Snowden, J., Craufurd, D., Neary, D., Owen, F., Oostra, B. A., Hardy, J., Goate, A., van Swieten, J., Mann, D., Lynch, T., and Heutink, P. (1998). Association of missense and 5'-splice-site mutations in tau with the inherited dementia ftdp-17. *Nature*, 393(6686):702–5.
- Hyde, L. A., Kazdoba, T. M., Grilli, M., Lozza, G., Brusa, R., Brussa, R., Zhang, Q., Wong, G. T., McCool, M. F., Zhang, L., Parker, E. M., and Higgins, G. A. (2005). Age-progressing cognitive impairments and neuropathology in transgenic crnd8 mice. *Behavioural Brain Research*, 160(2):344–55.
- Hyman, B. T., Phelps, C. H., Beach, T. G., Bigio, E. H., Cairns, N. J., Carrillo, M. C., Dickson, D. W., Duyckaerts, C., Frosch, M. P., Masliah, E., Mirra, S. S., Nelson, P. T., Schneider, J. A., Thal, D. R., Thies, B., Trojanowski, J. Q., Vinters, H. V., and Montine, T. J. (2012). National institute on aging-alzheimer's association guidelines for the neuropathologic assessment of alzheimer's disease. *Alzheimer'S & Dementia : The Journal Of The Alzheimer'S Association*, 8(1):1–13.
- Iaccarino, H. F., Singer, A. C., Martorell, A. J., Rudenko, A., Gao, F., Gillingham, T. Z., Mathys, H., Seo, J., Kritskiy, O., Abdurrob, F., Adaikkan, C., Canter, R. G., Rueda, R., Brown, E. N., Boyden, E. S., and Tsai, L.-H. (2016). Gamma frequency entrainment attenuates amyloid load and modifies microglia. *Nature*, 540(7632):230–235.
- Ibata, K., Sun, Q., and Turrigiano, G. G. (2008). Rapid synaptic scaling induced by changes in postsynaptic firing. *Neuron*, 57(6):819–26.

- Inghilleri, M., Conte, A., Frasca, V., Scaldaferrri, N., Gilio, F., Santini, M., Fabbrini, G., Prencipe, M., and Berardelli, A. (2006). Altered response to rtms in patients with alzheimer's disease. *Clinical Neurophysiology : Official Journal Of The International Federation Of Clinical Neurophysiology*, 117(1):103–9.
- Isaac, J. T., Nicoll, R. A., and Malenka, R. C. (1995). Evidence for silent synapses: implications for the expression of ltp. *Neuron*, 15(2):427–34.
- Ishizuka, N., Weber, J., and Amaral, D. G. (1990). Organization of intrahippocampal projections originating from ca3 pyramidal cells in the rat. *The Journal Of Comparative Neurology*, 295(4):580–623.
- Itskov, P. M., Vinnik, E., and Diamond, M. E. (2011). Hippocampal representation of touch-guided behavior in rats: persistent and independent traces of stimulus and reward location. *Plos One*, 6(1):e16462.
- Ittner, L. M., Ke, Y. D., Delerue, F., Bi, M., Gladbach, A., van Eersel, J., Wölfling, H., Chieng, B. C., Christie, M. J., Napier, I. A., Eckert, A., Staufenbiel, M., Hardeman, E., and Götz, J. (2010). Dendritic function of tau mediates amyloid-beta toxicity in alzheimer's disease mouse models. *Cell*, 142(3):387–97.
- Jack, C. R., Dickson, D. W., Parisi, J. E., Xu, Y. C., Cha, R. H., O'Brien, P. C., Edland, S. D., Smith, G. E., Boeve, B. F., Tangalos, E. G., Kokmen, E., and Petersen, R. C. (2002). Antemortem mri findings correlate with hippocampal neuropathology in typical aging and dementia. *Neurology*, 58(5):750–7.
- Jack, C. R., Petersen, R. C., O'Brien, P. C., and Tangalos, E. G. (1992). Mr-based hippocampal volumetry in the diagnosis of alzheimer's disease. *Neurology*, 42(1):183–8.
- Jack, C. R., Petersen, R. C., Xu, Y. C., O'Brien, P. C., Smith, G. E., Ivnik, R. J., Boeve, B. F., Waring, S. C., Tangalos, E. G., and Kokmen, E. (1999). Prediction of ad with mri-based hippocampal volume in mild cognitive impairment. *Neurology*, 52(7):1397–403.

- Jackson, A. and Fetz, E. E. (2007). Compact movable microwire array for long-term chronic unit recording in cerebral cortex of primates. *Journal Of Neurophysiology*, 98(5):3109–18.
- Jacobsen, J. S., Wu, C.-C., Redwine, J. M., Comery, T. A., Arias, R., Bowlby, M., Martone, R., Morrison, J. H., Pangalos, M. N., Reinhart, P. H., and Bloom, F. E. (2006). Early-onset behavioral and synaptic deficits in a mouse model of alzheimer’s disease. *Proceedings Of The National Academy Of Sciences Of The United States Of America*, 103(13):5161–6.
- Jahn, H. (2013). Memory loss in alzheimer’s disease. *Dialogues In Clinical Neuroscience*, 15(4):445–54.
- Janelsins, M. C., Mastrangelo, M. A., Oddo, S., LaFerla, F. M., Federoff, H. J., and Bowers, W. J. (2005). Early correlation of microglial activation with enhanced tumor necrosis factor-alpha and monocyte chemoattractant protein-1 expression specifically within the entorhinal cortex of triple transgenic alzheimer’s disease mice. *Journal Of Neuroinflammation*, 2:23.
- Jang, S.-S. and Chung, H. J. (2016). Emerging link between alzheimer’s disease and homeostatic synaptic plasticity. *Neural Plasticity*, 2016:7969272.
- Ji, D. and Wilson, M. A. (2007). Coordinated memory replay in the visual cortex and hippocampus during sleep. *Nature Neuroscience*, 10(1):100–7.
- Jin, D.-Z., Xue, B., Mao, L.-M., and Wang, J. Q. (2015). Metabotropic glutamate receptor 5 upregulates surface nmda receptor expression in striatal neurons via camkii. *Brain Research*, 1624:414–23.
- Jo, J., Heon, S., Kim, M. J., Son, G. H., Park, Y., Henley, J. M., Weiss, J. L., Sheng, M., Collingridge, G. L., and Cho, K. (2008). Metabotropic glutamate receptor-mediated ltd involves two interacting ca(2+) sensors, ncs-1 and pick1. *Neuron*, 60(6):1095–111.
- Kantevari, S., Matsuzaki, M., Kanemoto, Y., Kasai, H., and Ellis-Davies, G. C. R. (2010). Two-color, two-photon uncaging of glutamate and gaba. *Nature Methods*, 7(2):123–5.

- Kapur, N., Millar, J., Colbourn, C., Abbott, P., Kennedy, P., and Docherty, T. (1997). Very long-term amnesia in association with temporal lobe epilepsy: evidence for multiple-stage consolidation processes. *Brain And Cognition*, 35(1):58–70.
- Kass, R. E. and Raftery, A. E. (1995). Bayes factors. *Journal of the american statistical association*, 90(430):773–795.
- Kehoe, P., Wavrant-De Vrieze, F., Crook, R., Wu, W. S., Holmans, P., Fenton, I., Spurlock, G., Norton, N., Williams, H., Williams, N., Lovestone, S., Perez-Tur, J., Hutton, M., Chartier-Harlin, M. C., Shears, S., Roehl, K., Booth, J., Van Voorst, W., Ramic, D., Williams, J., Goate, A., Hardy, J., and Owen, M. J. (1999). A full genome scan for late onset alzheimer's disease. *Human Molecular Genetics*, 8(2):237–45.
- Kerchner, G. A. and Nicoll, R. A. (2008). Silent synapses and the emergence of a postsynaptic mechanism for ltp. *Nature Reviews. Neuroscience*, 9(11):813–25.
- Kidd, M. (1963). Paired helical filaments in electron microscopy of alzheimer's disease. *Nature*, 197:192–3.
- Kim, J. K., Lee, W. M., Kim, P., Choi, M., Jung, K., Kim, S., and Yun, S. H. (2012). Fabrication and operation of grin probes for in vivo fluorescence cellular imaging of internal organs in small animals. *Nature protocols*, 7(8):1456–69.
- Kim, S. and Ziff, E. B. (2014). Calcineurin mediates synaptic scaling via synaptic trafficking of ca<sup>2+</sup>-permeable ampa receptors. *Plos Biology*, 12(7):e1001900.
- Klunk, W. E., Engler, H., Nordberg, A., Wang, Y., Blomqvist, G., Holt, D. P., Bergström, M., Savitcheva, I., Huang, G.-f., Estrada, S., Ausén, B., Debnath, M. L., Barletta, J., Price, J. C., Sandell, J., Lopresti, B. J., Wall, A., Koivisto, P., Antoni, G., Mathis, C. A., and Långström, B. (2004). Imaging brain amyloid in alzheimer's disease with pittsburgh compound-b. *Annals Of Neurology*, 55(3):306–19.

- Knierim, J. J., Kudrimoti, H. S., and McNaughton, B. L. (1995). Place cells, head direction cells, and the learning of landmark stability. *Journal of Neuroscience*, 15(3):1648–1659.
- Knierim, J. J. and Neunuebel, J. P. (2016). Tracking the flow of hippocampal computation: Pattern separation, pattern completion, and attractor dynamics. *Neurobiology Of Learning And Memory*, 129:38–49.
- Koch, G., Di Lorenzo, F., Bonnì, S., Ponzo, V., Caltagirone, C., and Martorana, A. (2012). Impaired ltp- but not ltd-like cortical plasticity in alzheimer’s disease patients. *Journal Of Alzheimer’S Disease : Jad*, 31(3):593–9.
- Koffie, R. M., Meyer-Luehmann, M., Hashimoto, T., Adams, K. W., Mielke, M. L., Garcia-Alloza, M., Micheva, K. D., Smith, S. J., Kim, M. L., Lee, V. M., Hyman, B. T., and Spires-Jones, T. L. (2009). Oligomeric amyloid beta associates with postsynaptic densities and correlates with excitatory synapse loss near senile plaques. *Proceedings Of The National Academy Of Sciences Of The United States Of America*, 106(10):4012–7.
- Komarova, N. L. and Thalhauser, C. J. (2011). High degree of heterogeneity in alzheimer’s disease progression patterns. *Plos Computational Biology*, 7(11):e1002251.
- Konkel, A. and Cohen, N. J. (2009). Relational memory and the hippocampus: representations and methods. *Frontiers In Neuroscience*, 3(2):166–74.
- Kordower, J. H., Chu, Y., Stebbins, G. T., DeKosky, S. T., Cochran, E. J., Bennett, D., and Mufson, E. J. (2001). Loss and atrophy of layer ii entorhinal cortex neurons in elderly people with mild cognitive impairment. *Annals Of Neurology*, 49(2):202–13.
- Kozachenko, L. and Leonenko, N. N. (1987). Sample estimate of the entropy of a random vector. *Problemy Peredachi Informatsii*, 23(2):9–16.
- Krstic, D. and Knuesel, I. (2013). Deciphering the mechanism underlying late-onset alzheimer disease. *Nature Reviews. Neurology*, 9(1):25–34.

- Kuiper, S. and Hendriks, B. (2004). Variable-focus liquid lens for miniature cameras. *Applied physics letters*, 85(7):1128–1130.
- Kunz, L., Schröder, T. N., Lee, H., Montag, C., Lachmann, B., Sariyska, R., Reuter, M., Stirnberg, R., Stöcker, T., Messing-Floeter, P. C., Fell, J., Doeller, C. F., and Axmacher, N. (2015). Reduced grid-cell-like representations in adults at genetic risk for alzheimer’s disease. *Science (New York, N.Y.)*, 350(6259):430–3.
- Kuret, J., Chirita, C. N., Congdon, E. E., Kannanayakal, T., Li, G., Necula, M., Yin, H., and Zhong, Q. (2005). Pathways of tau fibrillization. *Biochimica Et Biophysica Acta*, 1739(2-3):167–78.
- Kurudenkandy, F. R., Zilberter, M., Biverstål, H., Presto, J., Honcharenko, D., Strömberg, R., Johansson, J., Winblad, B., and Fisahn, A. (2014). Amyloid- $\beta$ -induced action potential desynchronization and degradation of hippocampal gamma oscillations is prevented by interference with peptide conformation change and aggregation. *The Journal Of Neuroscience : The Official Journal Of The Society For Neuroscience*, 34(34):11416–25.
- Kwak, S. and Weiss, J. H. (2006). Calcium-permeable ampa channels in neurodegenerative disease and ischemia. *Current Opinion In Neurobiology*, 16(3):281–7.
- Lacor, P. N., Buniel, M. C., Chang, L., Fernandez, S. J., Gong, Y., Viola, K. L., Lambert, M. P., Velasco, P. T., Bigio, E. H., Finch, C. E., Krafft, G. A., and Klein, W. L. (2004). Synaptic targeting by alzheimer’s-related amyloid beta oligomers. *The Journal Of Neuroscience : The Official Journal Of The Society For Neuroscience*, 24(45):10191–200.
- Lambert, M. P., Barlow, A. K., Chromy, B. A., Edwards, C., Freed, R., Liosatos, M., Morgan, T. E., Rozovsky, I., Trommer, B., Viola, K. L., Wals, P., Zhang, C., Finch, C. E., Krafft, G. A., and Klein, W. L. (1998). Diffusible, nonfibrillar ligands derived from abeta1-42 are potent central nervous system neurotoxins. *Proceedings Of The National Academy Of Sciences Of The United States Of America*, 95(11):6448–53.

- Lamprecht, R. and LeDoux, J. (2004). Structural plasticity and memory. *Nature Reviews Neuroscience*, 5(1):45–54.
- Langston, R. F. and Wood, E. R. (2010). Associative recognition and the hippocampus: differential effects of hippocampal lesions on object-place, object-context and object-place-context memory. *Hippocampus*, 20(10):1139–53.
- Larson, E. B., Shadlen, M.-F., Wang, L., McCormick, W. C., Bowen, J. D., Teri, L., and Kukull, W. A. (2004). Survival after initial diagnosis of alzheimer disease. *Annals Of Internal Medicine*, 140(7):501–9.
- Lee, H.-K., Takamiya, K., Han, J.-S., Man, H., Kim, C.-H., Rumbaugh, G., Yu, S., Ding, L., He, C., Petralia, R. S., Wenthold, R. J., Gallagher, M., and Huganir, R. L. (2003). Phosphorylation of the ampa receptor glur1 subunit is required for synaptic plasticity and retention of spatial memory. *Cell*, 112(5):631–43.
- Leoutsakos, J.-M. S., Han, D., Mielke, M. M., Forrester, S. N., Tschanz, J. T., Corcoran, C. D., Green, R. C., Norton, M. C., Welsh-Bohmer, K. A., and Lyketsos, C. G. (2012). Effects of general medical health on alzheimer’s progression: the cache county dementia progression study. *International Psychogeriatrics*, 24(10):1561–70.
- Levy-Lahad, E., Wasco, W., Poorkaj, P., Romano, D. M., Oshima, J., Pettingell, W. H., Yu, C. E., Jondro, P. D., Schmidt, S. D., and Wang, K. (1995). Candidate gene for the chromosome 1 familial alzheimer’s disease locus. *Science (New York, N.Y.)*, 269(5226):973–7.
- Lewis, J., Dickson, D. W., Lin, W. L., Chisholm, L., Corral, A., Jones, G., Yen, S. H., Sahara, N., Skipper, L., Yager, D., Eckman, C., Hardy, J., Hutton, M., and McGowan, E. (2001). Enhanced neurofibrillary degeneration in transgenic mice expressing mutant tau and app. *Science (New York, N.Y.)*, 293(5534):1487–91.
- Li, S., Hong, S., Shepardson, N. E., Walsh, D. M., Shankar, G. M., and Selkoe, D. (2009). Soluble oligomers of amyloid beta protein facilitate hippocampal long-term depression by disrupting neuronal glutamate uptake. *Neuron*, 62(6):788–801.

- Li, S., Jin, M., Koeglsperger, T., Shepardson, N. E., Shankar, G. M., and Selkoe, D. J. (2011). Soluble  $\alpha\beta$  oligomers inhibit long-term potentiation through a mechanism involving excessive activation of extrasynaptic nr2b-containing nmda receptors. *The Journal Of Neuroscience : The Official Journal Of The Society For Neuroscience*, 31(18):6627–38.
- Li, X. G., Somogyi, P., Ylinen, A., and Buzsáki, G. (1994). The hippocampal ca3 network: an in vivo intracellular labeling study. *The Journal Of Comparative Neurology*, 339(2):181–208.
- Liao, D., Hessler, N. A., and Malinow, R. (1995). Activation of postsynaptically silent synapses during pairing-induced ltp in ca1 region of hippocampal slice. *Nature*, 375(6530):400–4.
- Lin, D.-T. and Huganir, R. L. (2007). Pick1 and phosphorylation of the glutamate receptor 2 (glur2) ampa receptor subunit regulates glur2 recycling after nmda receptor-induced internalization. *The Journal Of Neuroscience : The Official Journal Of The Society For Neuroscience*, 27(50):13903–8.
- Lin, J., O'Connor, E., Rossom, R., Perdue, L., Burda, B., Thompson, M., et al. (2013). Screening for cognitive impairment in older adults: An evidence update for the us preventive services task force [internet]. *US Preventive Services Task Force Evidence Syntheses, formerly Systematic Evidence Reviews. Rockville, MD: Agency for Healthcare Research and Quality (US)*.
- Liu, S.-J., Gasperini, R., Foa, L., and Small, D. H. (2010). Amyloid-beta decreases cell-surface ampa receptors by increasing intracellular calcium and phosphorylation of glur2. *Journal Of Alzheimer's Disease : Jad*, 21(2):655–66.
- Liu, X., Ramirez, S., Pang, P. T., Puryear, C. B., Govindarajan, A., Deisseroth, K., and Tonegawa, S. (2012). Optogenetic stimulation of a hippocampal engram activates fear memory recall. *Nature*, 484(7394):381–5.

- Lopez, J., Gamache, K., Schneider, R., and Nader, K. (2015). Memory retrieval requires ongoing protein synthesis and nmda receptor activity-mediated ampa receptor trafficking. *The Journal Of Neuroscience : The Official Journal Of The Society For Neuroscience*, 35(6):2465–75.
- Louros, S. R., Hooks, B. M., Litvina, L., Carvalho, A. L., and Chen, C. (2014). A role for stargazin in experience-dependent plasticity. *Cell Reports*, 7(5):1614–25.
- Lu, W., Shi, Y., Jackson, A. C., Bjorgan, K., During, M. J., Sprengel, R., Seuberg, P. H., and Nicoll, R. A. (2009). Subunit composition of synaptic ampa receptors revealed by a single-cell genetic approach. *Neuron*, 62(2):254–68.
- Luchsinger, J. A., Reitz, C., Honig, L. S., Tang, M. X., Shea, S., and Mayeux, R. (2005). Aggregation of vascular risk factors and risk of incident alzheimer disease. *Neurology*, 65(4):545–51.
- Lüscher, C. and Huber, K. M. (2010). Group 1 mglur-dependent synaptic long-term depression: mechanisms and implications for circuitry and disease. *Neuron*, 65(4):445–59.
- Lütcke, H., Margolis, D. J., and Helmchen, F. (2013). Steady or changing? long-term monitoring of neuronal population activity. *Trends In Neurosciences*, 36(7):375–84.
- Mably, A. J., Gereke, B. J., Jones, D. T., and Colgin, L. L. (2017). Impairments in spatial representations and rhythmic coordination of place cells in the 3xtg mouse model of alzheimer’s disease. *Hippocampus*, 27(4):378–392.
- Maguire, E. A. (2001). Neuroimaging studies of autobiographical event memory. *Philosophical Transactions Of The Royal Society Of London. Series B, Biological Sciences*, 356(1413):1441–51.
- Malenka, R. C. and Bear, M. F. (2004). Ltp and ltd: an embarrassment of riches. *Neuron*, 44(1):5–21.

- Malinow, R. and Malenka, R. C. (2002). Ampa receptor trafficking and synaptic plasticity. *Annual Review Of Neuroscience*, 25:103–26.
- Malinow, R. and Tsien, R. W. (1990). Presynaptic enhancement shown by whole-cell recordings of long-term potentiation in hippocampal slices. *Nature*, 346(6280):177–80.
- Mamelak, M. (2017). Energy and the alzheimer brain. *Neuroscience And Biobehavioral Reviews*, 75:297–313.
- Maren, S. (2001). Neurobiology of pavlovian fear conditioning. *Annual review of neuroscience*, 24(1):897–931.
- Markesberry, W. R. (1997). Oxidative stress hypothesis in alzheimer’s disease. *Free Radical Biology & Medicine*, 23(1):134–47.
- Marr, D. (1971). Simple memory: a theory for archicortex. *Philosophical Transactions Of The Royal Society Of London. Series B, Biological Sciences*, 262(841):23–81.
- Marslen-Wilson, W. D. and Teuber, H. L. (1975). Memory for remote events in anterograde amnesia: recognition of public figures from newsphotographs. *Neuropsychologia*, 13(3):353–64.
- Martin, S. J., Grimwood, P. D., and Morris, R. G. (2000). Synaptic plasticity and memory: an evaluation of the hypothesis. *Annual Review Of Neuroscience*, 23:649–711.
- Maruszak, A. and Thuret, S. (2014). Why looking at the whole hippocampus is not enough-a critical role for anteroposterior axis, subfield and activation analyses to enhance predictive value of hippocampal changes for alzheimer’s disease diagnosis. *Frontiers In Cellular Neuroscience*, 8:95.
- Maruyama, M., Shimada, H., Suhara, T., Shinotoh, H., Ji, B., Maeda, J., Zhang, M.-R., Trojanowski, J. Q., Lee, V. M.-Y., Ono, M., Masamoto, K., Takano, H., Sahara, N., Iwata, N., Okamura, N., Furumoto, S., Kudo, Y., Chang, Q., Saido, T. C., Takashima, A., Lewis, J., Jang, M.-K., Aoki, I., Ito, H., and Higuchi, M. (2013). Imaging of tau

- pathology in a tauopathy mouse model and in alzheimer patients compared to normal controls. *Neuron*, 79(6):1094–108.
- Masters, C. L., Simms, G., Weinman, N. A., Multhaup, G., McDonald, B. L., and Beyreuther, K. (1985). Amyloid plaque core protein in alzheimer disease and down syndrome. *Proceedings Of The National Academy Of Sciences Of The United States Of America*, 82(12):4245–9.
- Mathis, C. A., Wang, Y., Holt, D. P., Huang, G.-F., Debnath, M. L., and Klunk, W. E. (2003). Synthesis and evaluation of 11c-labeled 6-substituted 2-arylbenzothiazoles as amyloid imaging agents. *Journal Of Medicinal Chemistry*, 46(13):2740–54.
- Matos, M., Augusto, E., Oliveira, C. R., and Agostinho, P. (2008). Amyloid-beta peptide decreases glutamate uptake in cultured astrocytes: involvement of oxidative stress and mitogen-activated protein kinase cascades. *Neuroscience*, 156(4):898–910.
- Maviel, T., Durkin, T. P., Menzaghi, F., and Bontempi, B. (2004). Sites of neocortical reorganization critical for remote spatial memory. *Science (New York, N.Y.)*, 305(5680):96–9.
- McClelland, J. L. (2013). Incorporating rapid neocortical learning of new schema-consistent information into complementary learning systems theory. *Journal Of Experimental Psychology. General*, 142(4):1190–210.
- McEchron, M. D., Bouwmeester, H., Tseng, W., Weiss, C., and Disterhoft, J. F. (1998). Hippocampectomy disrupts auditory trace fear conditioning and contextual fear conditioning in the rat. *Hippocampus*, 8(6):638–646.
- McGlade-McCulloh, E., Yamamoto, H., Tan, S. E., Brickey, D. A., and Soderling, T. R. (1993). Phosphorylation and regulation of glutamate receptors by calcium/calmodulin-dependent protein kinase ii. *Nature*, 362(6421):640–2.
- McKee, A. C., Cairns, N. J., Dickson, D. W., Folkerth, R. D., Keene, C. D., Litvan, I., Perl, D. P., Stein, T. D., Vonsattel, J.-P., Stewart, W., Tripodis, Y., Crary, J. F.,

- Bieniek, K. F., Dams-O'Connor, K., Alvarez, V. E., and Gordon, W. A. (2016). The first ninds/nibib consensus meeting to define neuropathological criteria for the diagnosis of chronic traumatic encephalopathy. *Acta Neuropathologica*, 131(1):75–86.
- McKenzie, S., Robinson, N. T. M., Herrera, L., Churchill, J. C., and Eichenbaum, H. (2013). Learning causes reorganization of neuronal firing patterns to represent related experiences within a hippocampal schema. *The Journal Of Neuroscience : The Official Journal Of The Society For Neuroscience*, 33(25):10243–56.
- McKhann, G. M., Knopman, D. S., Chertkow, H., Hyman, B. T., Jack, C. R., Kawas, C. H., Klunk, W. E., Koroshetz, W. J., Manly, J. J., Mayeux, R., Mohs, R. C., Morris, J. C., Rossor, M. N., Scheltens, P., Carrillo, M. C., Thies, B., Weintraub, S., and Phelps, C. H. (2011). The diagnosis of dementia due to alzheimer's disease: recommendations from the national institute on aging-alzheimer's association workgroups on diagnostic guidelines for alzheimer's disease. *Alzheimer'S & Dementia : The Journal Of The Alzheimer'S Association*, 7(3):263–9.
- McNaughton, D., Knight, W., Guerreiro, R., Ryan, N., Lowe, J., Poulter, M., Nicholl, D. J., Hardy, J., Revesz, T., Lowe, J., Rossor, M., Collinge, J., and Mead, S. (2012). Duplication of amyloid precursor protein (app), but not prion protein (prnp) gene is a significant cause of early onset dementia in a large uk series. *Neurobiology Of Aging*, 33(2):426.e13–21.
- Meng, Y., Zhang, Y., and Jia, Z. (2003). Synaptic transmission and plasticity in the absence of ampa glutamate receptor glur2 and glur3. *Neuron*, 39(1):163–76.
- Mielke, M. M., Rosenberg, P. B., Tschanz, J., Cook, L., Corcoran, C., Hayden, K. M., Norton, M., Rabins, P. V., Green, R. C., Welsh-Bohmer, K. A., Breitner, J. C. S., Munger, R., and Lyketsos, C. G. (2007). Vascular factors predict rate of progression in alzheimer disease. *Neurology*, 69(19):1850–8.
- Migues, P. V., Liu, L., Archbold, G. E. B., Einarsson, E. O., Wong, J., Bonasia, K., Ko,

- S. H., Wang, Y. T., and Hardt, O. (2016). Blocking synaptic removal of glua2-containing ampa receptors prevents the natural forgetting of long-term memories. *The Journal Of Neuroscience : The Official Journal Of The Society For Neuroscience*, 36(12):3481–94.
- Milner, T. A., Aoki, C., Sheu, K. F., Blass, J. P., and Pickel, V. M. (1987). Light microscopic immunocytochemical localization of pyruvate dehydrogenase complex in rat brain: topographical distribution and relation to cholinergic and catecholaminergic nuclei. *The Journal Of Neuroscience : The Official Journal Of The Society For Neuroscience*, 7(10):3171–90.
- Minatohara, K., Akiyoshi, M., and Okuno, H. (2015). Role of immediate-early genes in synaptic plasticity and neuronal ensembles underlying the memory trace. *Frontiers In Molecular Neuroscience*, 8:78.
- Miñano-Molina, A. J., España, J., Martín, E., Barneda-Zahonero, B., Fadó, R., Solé, M., Trullás, R., Saura, C. A., and Rodríguez-Alvarez, J. (2011). Soluble oligomers of amyloid- $\beta$  peptide disrupt membrane trafficking of  $\alpha$ -amino-3-hydroxy-5-methylisoxazole-4-propionic acid receptor contributing to early synapse dysfunction. *The Journal Of Biological Chemistry*, 286(31):27311–21.
- Moehlmann, T., Winkler, E., Xia, X., Edbauer, D., Murrell, J., Capell, A., Kaether, C., Zheng, H., Ghetti, B., Haass, C., and Steiner, H. (2002). Presenilin-1 mutations of leucine 166 equally affect the generation of the notch and app intracellular domains independent of their effect on abeta 42 production. *Proceedings Of The National Academy Of Sciences Of The United States Of America*, 99(12):8025–30.
- Moita, M. A. P., Rosis, S., Zhou, Y., LeDoux, J. E., and Blair, H. T. (2003). Hippocampal place cells acquire location-specific responses to the conditioned stimulus during auditory fear conditioning. *Neuron*, 37(3):485–97.
- Montez, T., Poil, S.-S., Jones, B. F., Manshanden, I., Verbunt, J. P. A., van Dijk, B. W., Brussaard, A. B., van Ooyen, A., Stam, C. J., Scheltens, P., and Linkenkaer-Hansen, K.

- (2009). Altered temporal correlations in parietal alpha and prefrontal theta oscillations in early-stage alzheimer disease. *Proceedings Of The National Academy Of Sciences Of The United States Of America*, 106(5):1614–9.
- Montgomery, K. L., Yeh, A. J., Ho, J. S., Tsao, V., Mohan Iyer, S., Grosenick, L., Ferenczi, E. A., Tanabe, Y., Deisseroth, K., Delp, S. L., and Poon, A. S. Y. (2015). Wirelessly powered, fully internal optogenetics for brain, spinal and peripheral circuits in mice. *Nature Methods*, 12(10):969–74.
- Morris, R. G. (1990). Toward a representational hypothesis of the role of hippocampal synaptic plasticity in spatial and other forms of learning. *Cold Spring Harbor Symposia On Quantitative Biology*, 55:161–73.
- Morris, R. G. M. (2006). Elements of a neurobiological theory of hippocampal function: the role of synaptic plasticity, synaptic tagging and schemas. *The European Journal Of Neuroscience*, 23(11):2829–46.
- Moscovitch, M., Rosenbaum, R. S., Gilboa, A., Addis, D. R., Westmacott, R., Grady, C., McAndrews, M. P., Levine, B., Black, S., Winocur, G., and Nadel, L. (2005). Functional neuroanatomy of remote episodic, semantic and spatial memory: a unified account based on multiple trace theory. *Journal Of Anatomy*, 207(1):35–66.
- Moser, E. I., Krobert, K. A., Moser, M. B., and Morris, R. G. (1998). Impaired spatial learning after saturation of long-term potentiation. *Science (New York, N.Y.)*, 281(5385):2038–42.
- Moser, E. I., Kropff, E., and Moser, M.-B. (2008). Place cells, grid cells, and the brain’s spatial representation system. *Annual Review Of Neuroscience*, 31:69–89.
- Moser, M.-B., Rowland, D. C., and Moser, E. I. (2015). Place cells, grid cells, and memory. *Cold Spring Harbor Perspectives In Biology*, 7(2):a021808.

- Mukamel, E. A., Nimmerjahn, A., and Schnitzer, M. J. (2009). Automated analysis of cellular signals from large-scale calcium imaging data. *Neuron*, 63(6):747–60.
- Mulkey, R. M., Herron, C. E., and Malenka, R. C. (1993). An essential role for protein phosphatases in hippocampal long-term depression. *Science (New York, N.Y.)*, 261(5124):1051–5.
- Mumby, D. G., Astur, R. S., Weisend, M. P., and Sutherland, R. J. (1999). Retrograde amnesia and selective damage to the hippocampal formation: memory for places and object discriminations. *Behavioural Brain Research*, 106(1-2):97–107.
- Myers, A., Holmans, P., Marshall, H., Kwon, J., Meyer, D., Ramic, D., Shears, S., Booth, J., DeVrieze, F. W., Crook, R., Hamshere, M., Abraham, R., Tunstall, N., Rice, F., Carty, S., Lillystone, S., Kehoe, P., Rudrasingham, V., Jones, L., Lovestone, S., Perez-Tur, J., Williams, J., Owen, M. J., Hardy, J., and Goate, A. M. (2000). Susceptibility locus for alzheimer's disease on chromosome 10. *Science (New York, N.Y.)*, 290(5500):2304–5.
- Nabavi, S., Fox, R., Proulx, C. D., Lin, J. Y., Tsien, R. Y., and Malinow, R. (2014). Engineering a memory with ltd and ltp. *Nature*, 511(7509):348–52.
- Nadel, L. and Moscovitch, M. (1997). Memory consolidation, retrograde amnesia and the hippocampal complex. *Current Opinion In Neurobiology*, 7(2):217–27.
- Nakazawa, K., Quirk, M. C., Chitwood, R. A., Watanabe, M., Yeckel, M. F., Sun, L. D., Kato, A., Carr, C. A., Johnston, D., Wilson, M. A., and Tonegawa, S. (2002). Requirement for hippocampal ca3 nmda receptors in associative memory recall. *Science (New York, N.Y.)*, 297(5579):211–8.
- Narisawa-Saito, M., Wakabayashi, K., Tsuji, S., Takahashi, H., and Nawa, H. (1996). Regional specificity of alterations in ngf, bdnf and nt-3 levels in alzheimer's disease. *Neuroreport*, 7(18):2925–8.

- Nelson, L. and Tabet, N. (2015). Slowing the progression of alzheimer's disease; what works? *Ageing Research Reviews*, 23(Pt B):193–209.
- Neunuebel, J. P. and Knierim, J. J. (2014). Ca3 retrieves coherent representations from degraded input: direct evidence for ca3 pattern completion and dentate gyrus pattern separation. *Neuron*, 81(2):416–27.
- Neves, G., Cooke, S. F., and Bliss, T. V. P. (2008). Synaptic plasticity, memory and the hippocampus: a neural network approach to causality. *Nature Reviews Neuroscience*, 9(1):65–75.
- Niibori, Y., Yu, T.-S., Epp, J. R., Akers, K. G., Josselyn, S. A., and Frankland, P. W. (2012). Suppression of adult neurogenesis impairs population coding of similar contexts in hippocampal ca3 region. *Nature Communications*, 3:1253.
- Noguchi, J., Nagaoka, A., Watanabe, S., Ellis-Davies, G. C. R., Kitamura, K., Kano, M., Matsuzaki, M., and Kasai, H. (2011). In vivo two-photon uncaging of glutamate revealing the structure-function relationships of dendritic spines in the neocortex of adult mice. *The Journal Of Physiology*, 589(Pt 10):2447–57.
- Nordberg, A., Alafuzoff, I., and Winblad, B. (1992). Nicotinic and muscarinic subtypes in the human brain: changes with aging and dementia. *Journal Of Neuroscience Research*, 31(1):103–11.
- Norton, M. C., Piercy, K. W., Rabins, P. V., Green, R. C., Breitner, J. C. S., Ostbye, T., Corcoran, C., Welsh-Bohmer, K. A., Lyketsos, C. G., and Tschanz, J. T. (2009). Caregiver-recipient closeness and symptom progression in alzheimer disease. the cache county dementia progression study. *The Journals Of Gerontology. Series B, Psychological Sciences And Social Sciences*, 64(5):560–8.
- Ohkawa, N., Saitoh, Y., Suzuki, A., Tsujimura, S., Murayama, E., Kosugi, S., Nishizono, H., Matsuo, M., Takahashi, Y., Nagase, M., Sugimura, Y. K., Watabe, A. M., Kato, F.,

- and Inokuchi, K. (2015). Artificial association of pre-stored information to generate a qualitatively new memory. *Cell Reports*, 11(2):261–9.
- Okamura, N., Furumoto, S., Harada, R., Tago, T., Yoshikawa, T., Fodero-Tavoletti, M., Mulligan, R. S., Villemagne, V. L., Akatsu, H., Yamamoto, T., Arai, H., Iwata, R., Yanai, K., and Kudo, Y. (2013). Novel 18f-labeled arylquinoline derivatives for noninvasive imaging of tau pathology in alzheimer disease. *Journal Of Nuclear Medicine : Official Publication, Society Of Nuclear Medicine*, 54(8):1420–7.
- O’Keefe, J. (1976). Place units in the hippocampus of the freely moving rat. *Experimental Neurology*, 51(1):78–109.
- O’Keefe, J. and Burgess, N. (2005). Dual phase and rate coding in hippocampal place cells: theoretical significance and relationship to entorhinal grid cells. *Hippocampus*, 15(7):853–66.
- O’Keefe, J. and Conway, D. H. (1978). Hippocampal place units in the freely moving rat: why they fire where they fire. *Experimental Brain Research*, 31(4):573–90.
- O’Keefe, J. and Dostrovsky, J. (1971). The hippocampus as a spatial map. preliminary evidence from unit activity in the freely-moving rat. *Brain Research*, 34(1):171–5.
- Okun, E., Griffioen, K., Barak, B., Roberts, N. J., Castro, K., Pita, M. A., Cheng, A., Mughal, M. R., Wan, R., Ashery, U., and Mattson, M. P. (2010). Toll-like receptor 3 inhibits memory retention and constrains adult hippocampal neurogenesis. *Proceedings Of The National Academy Of Sciences Of The United States Of America*, 107(35):15625–30.
- Oliet, S. H., Malenka, R. C., and Nicoll, R. A. (1997). Two distinct forms of long-term depression coexist in ca1 hippocampal pyramidal cells. *Neuron*, 18(6):969–82.
- Ossenkoppele, R., Schonhaut, D. R., Schöll, M., Lockhart, S. N., Ayakta, N., Baker, S. L., O’Neil, J. P., Janabi, M., Lazaris, A., Cantwell, A., Vogel, J., Santos, M., Miller, Z. A.,

- Bettcher, B. M., Vossel, K. A., Kramer, J. H., Gorno-Tempini, M. L., Miller, B. L., Jagust, W. J., and Rabinovici, G. D. (2016). Tau pet patterns mirror clinical and neuroanatomical variability in alzheimer's disease. *Brain : A Journal Of Neurology*, 139(Pt 5):1551–67.
- Palmer, A. and Good, M. (2011). Hippocampal synaptic activity, pattern separation and episodic-like memory: implications for mouse models of alzheimer's disease pathology. *Biochemical Society Transactions*, 39(4):902–9.
- Palmer, C. L., Lim, W., Hastie, P. G. R., Toward, M., Korolchuk, V. I., Burbidge, S. A., Banting, G., Collingridge, G. L., Isaac, J. T. R., and Henley, J. M. (2005). Hippocalcin functions as a calcium sensor in hippocampal ltd. *Neuron*, 47(4):487–94.
- Palop, J. J., Chin, J., Roberson, E. D., Wang, J., Thwin, M. T., Bien-Ly, N., Yoo, J., Ho, K. O., Yu, G.-Q., Kreitzer, A., Finkbeiner, S., Noebels, J. L., and Mucke, L. (2007). Aberrant excitatory neuronal activity and compensatory remodeling of inhibitory hippocampal circuits in mouse models of alzheimer's disease. *Neuron*, 55(5):697–711.
- Palop, J. J. and Mucke, L. (2016). Network abnormalities and interneuron dysfunction in alzheimer disease. *Nature Reviews. Neuroscience*, 17(12):777–792.
- Paninski, L. (2003). Estimation of entropy and mutual information. *Neural computation*, 15(6):1191–1253.
- Park, J. and Sandberg, I. W. (1991). Universal approximation using radial-basis-function networks. *Neural computation*, 3(2):246–257.
- Park, S., Park, J. M., Kim, S., Kim, J.-A., Shepherd, J. D., Smith-Hicks, C. L., Chowdhury, S., Kaufmann, W., Kuhl, D., Ryazanov, A. G., Huganir, R. L., Linden, D. J., and Worley, P. F. (2008). Elongation factor 2 and fragile x mental retardation protein control the dynamic translation of arc/arg3.1 essential for mglur-ltd. *Neuron*, 59(1):70–83.

- Parsons, C. G., Stöffler, A., and Danysz, W. (2007). Memantine: a nmda receptor antagonist that improves memory by restoration of homeostasis in the glutamatergic system—too little activation is bad, too much is even worse. *Neuropharmacology*, 53(6):699–723.
- Patterson, M. A., Szatmari, E. M., and Yasuda, R. (2010). Ampa receptors are exocytosed in stimulated spines and adjacent dendrites in a ras-erk-dependent manner during long-term potentiation. *Proceedings Of The National Academy Of Sciences Of The United States Of America*, 107(36):15951–6.
- Pennanen, C., Kivipelto, M., Tuomainen, S., Hartikainen, P., Hänninen, T., Laakso, M. P., Hallikainen, M., Vanhanen, M., Nissinen, A., Helkala, E.-L., Vainio, P., Vanninen, R., Partanen, K., and Soininen, H. (2004). Hippocampus and entorhinal cortex in mild cognitive impairment and early ad. *Neurobiology Of Aging*, 25(3):303–10.
- Perry, R. J. and Hodges, J. R. (1999). Attention and executive deficits in alzheimer's disease. a critical review. *Brain : A Journal Of Neurology*, 122 ( Pt 3):383–404.
- Peterson, D. A., Lucidi-Phillipi, C. A., Murphy, D. P., Ray, J., and Gage, F. H. (1996). Fibroblast growth factor-2 protects entorhinal layer ii glutamatergic neurons from axotomy-induced death. *The Journal Of Neuroscience : The Official Journal Of The Society For Neuroscience*, 16(3):886–98.
- Phillips, R. and LeDoux, J. (1992). Differential contribution of amygdala and hippocampus to cued and contextual fear conditioning. *Behavioral neuroscience*, 106(2):274.
- Piyawattanametha, W., Cocker, E. D., Burns, L. D., Barretto, R. P., Jung, J. C., Ra, H., Solgaard, O., and Schnitzer, M. J. (2009). In vivo brain imaging using a portable 2.9 g two-photon microscope based on a microelectromechanical systems scanning mirror. *Optics Letters*, 34(15):2309–11.
- Pnevmatikakis, E. A., Soudry, D., Gao, Y., Machado, T. A., Merel, J., Pfau, D., Reardon, T., Mu, Y., Lacefield, C., Yang, W., Ahrens, M., Bruno, R., Jessell, T. M., Peterka,

- D. S., Yuste, R., and Paninski, L. (2016). Simultaneous denoising, deconvolution, and demixing of calcium imaging data. *Neuron*, 89(2):285–99.
- Poorkaj, P., Bird, T. D., Wijsman, E., Nemens, E., Garruto, R. M., Anderson, L., Andreasidis, A., Wiederholt, W. C., Raskind, M., and Schellenberg, G. D. (1998). Tau is a candidate gene for chromosome 17 frontotemporal dementia. *Annals Of Neurology*, 43(6):815–25.
- Porsteinsson, A. P., Grossberg, G. T., Mintzer, J., and Olin, J. T. (2008). Memantine treatment in patients with mild to moderate alzheimer's disease already receiving a cholinesterase inhibitor: a randomized, double-blind, placebo-controlled trial. *Current Alzheimer Research*, 5(1):83–9.
- Prakash, R., Yizhar, O., Grewe, B., Ramakrishnan, C., Wang, N., Goshen, I., Packer, A. M., Peterka, D. S., Yuste, R., Schnitzer, M. J., and Deisseroth, K. (2012). Two-photon optogenetic toolbox for fast inhibition, excitation and bistable modulation. *Nature Methods*, 9(12):1171–9.
- Price, D. L. and Sisodia, S. S. (1998). Mutant genes in familial alzheimer's disease and transgenic models. *Annual Review Of Neuroscience*, 21:479–505.
- Price, J. L. and Morris, J. C. (1999). Tangles and plaques in nondemented aging and "preclinical" alzheimer's disease. *Annals Of Neurology*, 45(3):358–68.
- Rajasethupathy, P., Ferenczi, E., and Deisseroth, K. (2016). Targeting neural circuits. *Cell*, 165(3):524–34.
- Raka, F., Di Sebastiano, A. R., Kulhawy, S. C., Ribeiro, F. M., Godin, C. M., Caetano, F. A., Angers, S., and Ferguson, S. S. G. (2015). Ca(2+)/calmodulin-dependent protein kinase ii interacts with group i metabotropic glutamate and facilitates receptor endocytosis and erk1/2 signaling: role of β-amyloid. *Molecular Brain*, 8:21.

- Rakic, P. and Nowakowski, R. S. (1981). The time of origin of neurons in the hippocampal region of the rhesus monkey. *The Journal Of Comparative Neurology*, 196(1):99–128.
- Ramirez, S., Liu, X., Lin, P.-A., Suh, J., Pignatelli, M., Redondo, R. L., Ryan, T. J., and Tonegawa, S. (2013). Creating a false memory in the hippocampus. *Science (New York, N.Y.)*, 341(6144):387–91.
- Ramme, G., Hasenjäger, A., Sroka-Saidi, K., Deussing, J. M., and Parsons, C. G. (2011). Therapeutic significance of nr2b-containing nmda receptors and mglur5 metabotropic glutamate receptors in mediating the synaptotoxic effects of  $\beta$ -amyloid oligomers on long-term potentiation (ltp) in murine hippocampal slices. *Neuropharmacology*, 60(6):982–90.
- Redondo, R. L., Kim, J., Arons, A. L., Ramirez, S., Liu, X., and Tonegawa, S. (2014). Bidirectional switch of the valence associated with a hippocampal contextual memory engram. *Nature*, 513(7518):426–30.
- Reijmers, L. G., Perkins, B. L., Matsuo, N., and Mayford, M. (2007). Localization of a stable neural correlate of associative memory. *Science (New York, N.Y.)*, 317(5842):1230–3.
- Reilly, J. F., Games, D., Rydel, R. E., Freedman, S., Schenk, D., Young, W. G., Morrison, J. H., and Bloom, F. E. (2003). Amyloid deposition in the hippocampus and entorhinal cortex: quantitative analysis of a transgenic mouse model. *Proceedings Of The National Academy Of Sciences Of The United States Of America*, 100(8):4837–42.
- Reiman, E. M., Quiroz, Y. T., Fleisher, A. S., Chen, K., Velez-Pardo, C., Jimenez-Del-Rio, M., Fagan, A. M., Shah, A. R., Alvarez, S., Arbelaez, A., Giraldo, M., Acosta-Baena, N., Sperling, R. A., Dickerson, B., Stern, C. E., Tirado, V., Munoz, C., Reiman, R. A., Huettel, M. J., Alexander, G. E., Langbaum, J. B. S., Kosik, K. S., Tariot, P. N., and Lopera, F. (2012). Brain imaging and fluid biomarker analysis in young adults at genetic risk for autosomal dominant alzheimer's disease in the presenilin 1 e280a kindred: a case-control study. *The Lancet. Neurology*, 11(12):1048–56.

- Reisberg, B., Doody, R., Stöffler, A., Schmitt, F., Ferris, S., and Möbius, H. J. (2003). Memantine in moderate-to-severe alzheimer's disease. *The New England Journal Of Medicine*, 348(14):1333–41.
- Reisberg, B., Ferris, S. H., de Leon, M. J., and Crook, T. (1982). The global deterioration scale for assessment of primary degenerative dementia. *The American Journal Of Psychiatry*, 139(9):1136–9.
- Renner, M., Lacor, P. N., Velasco, P. T., Xu, J., Contractor, A., Klein, W. L., and Triller, A. (2010). Deleterious effects of amyloid beta oligomers acting as an extracellular scaffold for mglur5. *Neuron*, 66(5):739–54.
- Restivo, L., Vetere, G., Bontempi, B., and Ammassari-Teule, M. (2009). The formation of recent and remote memory is associated with time-dependent formation of dendritic spines in the hippocampus and anterior cingulate cortex. *The Journal Of Neuroscience : The Official Journal Of The Society For Neuroscience*, 29(25):8206–14.
- Reymann, K. G. and Frey, J. U. (2007). The late maintenance of hippocampal ltp: requirements, phases, 'synaptic tagging', 'late-associativity' and implications. *Neuropharmacology*, 52(1):24–40.
- Roberson, E. D., Halabisky, B., Yoo, J. W., Yao, J., Chin, J., Yan, F., Wu, T., Hamto, P., Devidze, N., Yu, G.-Q., Palop, J. J., Noebels, J. L., and Mucke, L. (2011). Amyloid- $\beta$ /fyn-induced synaptic, network, and cognitive impairments depend on tau levels in multiple mouse models of alzheimer's disease. *The Journal Of Neuroscience : The Official Journal Of The Society For Neuroscience*, 31(2):700–11.
- Roberson, M. R. and Harrell, L. E. (1997). Cholinergic activity and amyloid precursor protein metabolism. *Brain Research. Brain Research Reviews*, 25(1):50–69.
- Rogaev, E. I., Sherrington, R., Rogaeva, E. A., Levesque, G., Ikeda, M., Liang, Y., Chi, H., Lin, C., Holman, K., and Tsuda, T. (1995). Familial alzheimer's disease in kindreds

- with missense mutations in a gene on chromosome 1 related to the alzheimer's disease type 3 gene. *Nature*, 376(6543):775–8.
- Rogers, S. L., Doody, R. S., Mohs, R. C., and Friedhoff, L. T. (1998). Donepezil improves cognition and global function in alzheimer disease: a 15-week, double-blind, placebo-controlled study. donepezil study group. *Archives Of Internal Medicine*, 158(9):1021–31.
- Rolls, E. T. (2007). An attractor network in the hippocampus: theory and neurophysiology. *Learning & Memory (Cold Spring Harbor, N.Y.)*, 14(11):714–31.
- Rolls, E. T. (2008). Top-down control of visual perception: attention in natural vision. *Perception*, 37(3):333–54.
- Rolls, E. T. (2013a). A biased activation theory of the cognitive and attentional modulation of emotion. *Frontiers In Human Neuroscience*, 7:74.
- Rolls, E. T. (2013b). The mechanisms for pattern completion and pattern separation in the hippocampus. *Frontiers In Systems Neuroscience*, 7:74.
- Ross, B. C. (2014). Mutual information between discrete and continuous data sets. *Plos One*, 9(2):e87357.
- Rountree, S. D., Chan, W., Pavlik, V. N., Darby, E. J., Siddiqui, S., and Doody, R. S. (2009). Persistent treatment with cholinesterase inhibitors and/or memantine slows clinical progression of alzheimer disease. *Alzheimer'S Research & Therapy*, 1(2):7.
- Rousche, P. J. and Normann, R. A. (1998). Chronic recording capability of the utah intracortical electrode array in cat sensory cortex. *Journal Of Neuroscience Methods*, 82(1):1–15.
- Routtenberg, A., Cantallops, I., Zaffuto, S., Serrano, P., and Namgung, U. (2000). Enhanced learning after genetic overexpression of a brain growth protein. *Proceedings Of The National Academy Of Sciences Of The United States Of America*, 97(13):7657–62.

- Roux, L., Hu, B., Eichler, R., Stark, E., and Buzsáki, G. (2017). Sharp wave ripples during learning stabilize the hippocampal spatial map. *Nature Neuroscience*, 20(6):845–853.
- Rowe, C. C., Ellis, K. A., Rimajova, M., Bourgeat, P., Pike, K. E., Jones, G., Fripp, J., Tochon-Danguy, H., Morandieu, L., O’Keefe, G., Price, R., Raniga, P., Robins, P., Acosta, O., Lenzo, N., Szoéke, C., Salvado, O., Head, R., Martins, R., Masters, C. L., Ames, D., and Villemagne, V. L. (2010). Amyloid imaging results from the australian imaging, biomarkers and lifestyle (aibl) study of aging. *Neurobiology Of Aging*, 31(8):1275–83.
- Roy, D. S., Arons, A., Mitchell, T. I., Pignatelli, M., Ryan, T. J., and Tonegawa, S. (2016). Memory retrieval by activating engram cells in mouse models of early alzheimer’s disease. *Nature*, 531(7595):508–12.
- Ryan, L., Nadel, L., Keil, K., Putnam, K., Schnyer, D., Trouard, T., and Moscovitch, M. (2001). Hippocampal complex and retrieval of recent and very remote autobiographical memories: evidence from functional magnetic resonance imaging in neurologically intact people. *Hippocampus*, 11(6):707–14.
- Ryan, T. J., Roy, D. S., Pignatelli, M., Arons, A., and Tonegawa, S. (2015). Engram cells retain memory under retrograde amnesia. *Science*, 348(6238):1007–1013.
- Sabbagh, M., Cummings, J., Christensen, D., Doody, R., Farlow, M., Liu, L., Mackell, J., and Fain, R. (2013). Evaluating the cognitive effects of donepezil 23 mg/d in moderate and severe alzheimer’s disease: analysis of effects of baseline features on treatment response. *Bmc Geriatrics*, 13:56.
- Sanchez, P. E., Zhu, L., Verret, L., Vossel, K. A., Orr, A. G., Cirrito, J. R., Devidze, N., Ho, K., Yu, G.-Q., Palop, J. J., and Mucke, L. (2012). Levetiracetam suppresses neuronal network dysfunction and reverses synaptic and cognitive deficits in an alzheimer’s disease model. *Proceedings Of The National Academy Of Sciences Of The United States Of America*, 109(42):E2895–903.

- Santoro, A. (2013). Reassessing pattern separation in the dentate gyrus. *Frontiers In Behavioral Neuroscience*, 7:96.
- Sargolini, F., Fyhn, M., Hafting, T., McNaughton, B. L., Witter, M. P., Moser, M.-B., and Moser, E. I. (2006). Conjunctive representation of position, direction, and velocity in entorhinal cortex. *Science (New York, N.Y.)*, 312(5774):758–62.
- Sawinski, J., Wallace, D. J., Greenberg, D. S., Grossmann, S., Denk, W., and Kerr, J. N. D. (2009). Visually evoked activity in cortical cells imaged in freely moving animals. *Proceedings Of The National Academy Of Sciences Of The United States Of America*, 106(46):19557–62.
- Scheltens, P., Leys, D., Barkhof, F., Huglo, D., Weinstein, H. C., Vermersch, P., Kuiper, M., Steinling, M., Wolters, E. C., and Valk, J. (1992). Atrophy of medial temporal lobes on mri in "probable" alzheimer's disease and normal ageing: diagnostic value and neuropsychological correlates. *Journal Of Neurology, Neurosurgery, And Psychiatry*, 55(10):967–72.
- Schmitzer-Torbert, N. and Redish, A. D. (2004). Neuronal activity in the rodent dorsal striatum in sequential navigation: separation of spatial and reward responses on the multiple t task. *Journal Of Neurophysiology*, 91(5):2259–72.
- Schneider, J. A., Arvanitakis, Z., Bang, W., and Bennett, D. A. (2007). Mixed brain pathologies account for most dementia cases in community-dwelling older persons. *Neurology*, 69(24):2197–204.
- Schneider, L. S., Dagerman, K. S., Higgins, J. P. T., and McShane, R. (2011). Lack of evidence for the efficacy of memantine in mild alzheimer disease. *Archives Of Neurology*, 68(8):991–8.
- Schöll, M., Lockhart, S. N., Schonhaut, D. R., O'Neil, J. P., Janabi, M., Ossenkoppemele, R., Baker, S. L., Vogel, J. W., Faria, J., Schwimmer, H. D., Rabinovici, G. D., and

- Jagust, W. J. (2016). Pet imaging of tau deposition in the aging human brain. *Neuron*, 89(5):971–82.
- Sclan, S. G. and Reisberg, B. (1992). Functional assessment staging (fast) in alzheimer's disease: reliability, validity, and ordinality. *International Psychogeriatrics*, 4 Suppl 1:55–69.
- Scott, L., Feng, J., Kiss, T., Needle, E., Atchison, K., Kawabe, T. T., Milici, A. J., Hajós-Korcsok, E., Riddell, D., and Hajós, M. (2012). Age-dependent disruption in hippocampal  $\vartheta$  oscillation in amyloid- $\beta$  overproducing transgenic mice. *Neurobiology Of Aging*, 33(7):1481.e13–23.
- Scoville, W. B. and Milner, B. (1957). Loss of recent memory after bilateral hippocampal lesions. *Journal Of Neurology, Neurosurgery, And Psychiatry*, 20(1):11–21.
- Selkoe, D. J. (2002). Alzheimer's disease is a synaptic failure. *Science (New York, N.Y.)*, 298(5594):789–91.
- Sepulcre, J., Schultz, A. P., Sabuncu, M., Gomez-Isla, T., Chhatwal, J., Becker, A., Sperling, R., and Johnson, K. A. (2016). In vivo tau, amyloid, and gray matter profiles in the aging brain. *The Journal Of Neuroscience : The Official Journal Of The Society For Neuroscience*, 36(28):7364–74.
- Sevigny, J., Chiao, P., Bussière, T., Weinreb, P. H., Williams, L., Maier, M., Dunstan, R., Salloway, S., Chen, T., Ling, Y., O'Gorman, J., Qian, F., Arastu, M., Li, M., Chollate, S., Brennan, M. S., Quintero-Monzon, O., Scannevin, R. H., Arnold, H. M., Engber, T., Rhodes, K., Ferrero, J., Hang, Y., Mikulskis, A., Grimm, J., Hock, C., Nitsch, R. M., and Sandrock, A. (2016). The antibody aducanumab reduces  $\alpha\beta$  plaques in alzheimer's disease. *Nature*, 537(7618):50–6.
- Shah, S. and Reichman, W. E. (2006). Treatment of alzheimer's disease across the spectrum of severity. *Clinical Interventions In Aging*, 1(2):131–42.

- Shankar, G. M., Bloodgood, B. L., Townsend, M., Walsh, D. M., Selkoe, D. J., and Sabatini, B. L. (2007). Natural oligomers of the alzheimer amyloid-beta protein induce reversible synapse loss by modulating an nmda-type glutamate receptor-dependent signaling pathway. *The Journal Of Neuroscience : The Official Journal Of The Society For Neuroscience*, 27(11):2866–75.
- Shankar, G. M., Li, S., Mehta, T. H., Garcia-Munoz, A., Shepardson, N. E., Smith, I., Brett, F. M., Farrell, M. A., Rowan, M. J., Lemere, C. A., Regan, C. M., Walsh, D. M., Sabatini, B. L., and Selkoe, D. J. (2008). Amyloid-beta protein dimers isolated directly from alzheimer’s brains impair synaptic plasticity and memory. *Nature Medicine*, 14(8):837–42.
- Shi, S., Hayashi, Y., Esteban, J. A., and Malinow, R. (2001). Subunit-specific rules governing ampa receptor trafficking to synapses in hippocampal pyramidal neurons. *Cell*, 105(3):331–43.
- Shipton, O. A. and Paulsen, O. (2014). Glun2a and glun2b subunit-containing nmda receptors in hippocampal plasticity. *Philosophical Transactions Of The Royal Society Of London. Series B, Biological Sciences*, 369(1633):20130163.
- Shors, T. J. and Matzel, L. D. (1997). Long-term potentiation: what’s learning got to do with it? *The Behavioral And Brain Sciences*, 20(4):597–614; discussion 614–55.
- Siemers, E. R., Sundell, K. L., Carlson, C., Case, M., Sethuraman, G., Liu-Seifert, H., Dowsett, S. A., Pontecorvo, M. J., Dean, R. A., and Demattos, R. (2016). Phase 3 solanezumab trials: Secondary outcomes in mild alzheimer’s disease patients. *Alzheimer’S & Dementia : The Journal Of The Alzheimer’S Association*, 12(2):110–20.
- Silverman, B. W. (1986). *Density estimation for statistics and data analysis*, volume 26. CRC press.
- Singh, T. J., Grundke-Iqbali, I., McDonald, B., and Iqbali, K. (1994). Comparison of the

- phosphorylation of microtubule-associated protein tau by non-proline dependent protein kinases. *Molecular And Cellular Biochemistry*, 131(2):181–9.
- Siskova, Z., Justus, D., Kaneko, H., Friedrichs, D., Henneberg, N., Beutel, T., Pitsch, J., Schoch, S., Becker, A., von der Kammer, H., and Remy, S. (2014). Dendritic structural degeneration is functionally linked to cellular hyperexcitability in a mouse model of alzheimer's disease. *Neuron*, 84(5):1023–33.
- Skaggs, W. E. and McNaughton, B. L. (1996). Theta phase precession in hippocampal. *Hippocampus*, 6:149–172.
- Skaggs, W. E., McNaughton, B. L., and Gothard, K. M. (1993). An information-theoretic approach to deciphering the hippocampal code. In Hanson, S. J., Cowan, J. D., and Giles, C. L., editors, *Advances in Neural Information Processing Systems 5*, pages 1030–1037. Morgan-Kaufmann.
- Smith, D. A. (2009). Treatment of alzheimer's disease in the long-term-care setting. *American Journal Of Health-System Pharmacy : Ajhp : Official Journal Of The American Society Of Health-System Pharmacists*, 66(10):899–907.
- Smith, M. A., Zhu, X., Tabaton, M., Liu, G., McKeel, D. W., Cohen, M. L., Wang, X., Siedlak, S. L., Dwyer, B. E., Hayashi, T., Nakamura, M., Nunomura, A., and Perry, G. (2010). Increased iron and free radical generation in preclinical alzheimer disease and mild cognitive impairment. *Journal Of Alzheimer'S Disease : Jad*, 19(1):363–72.
- Smith, T. D., Adams, M. M., Gallagher, M., Morrison, J. H., and Rapp, P. R. (2000). Circuit-specific alterations in hippocampal synaptophysin immunoreactivity predict spatial learning impairment in aged rats. *The Journal Of Neuroscience : The Official Journal Of The Society For Neuroscience*, 20(17):6587–93.
- Solstad, T., Boccara, C. N., Kropff, E., Moser, M.-B., and Moser, E. I. (2008). Representation of geometric borders in the entorhinal cortex. *Science (New York, N.Y.)*, 322(5909):1865–8.

- Sommer, B., Köhler, M., Sprengel, R., and Seburg, P. H. (1991). Rna editing in brain controls a determinant of ion flow in glutamate-gated channels. *Cell*, 67(1):11–9.
- Sperling, R. A., Laviolette, P. S., O’Keefe, K., O’Brien, J., Rentz, D. M., Pihlajamaki, M., Marshall, G., Hyman, B. T., Selkoe, D. J., Hedden, T., Buckner, R. L., Becker, J. A., and Johnson, K. A. (2009). Amyloid deposition is associated with impaired default network function in older persons without dementia. *Neuron*, 63(2):178–88.
- Spires, T. L. and Hyman, B. T. (2004). Neuronal structure is altered by amyloid plaques. *Reviews In The Neurosciences*, 15(4):267–78.
- Squire, L. R. (1992). Memory and the hippocampus: a synthesis from findings with rats, monkeys, and humans. *Psychological Review*, 99(2):195–231.
- Squire, L. R. (2009). The legacy of patient h.m. for neuroscience. *Neuron*, 61(1):6–9.
- Squire, L. R., Stark, C. E. L., and Clark, R. E. (2004). The medial temporal lobe. *Annual Review Of Neuroscience*, 27:279–306.
- Squire, L. R. and Zola-Morgan, S. (1991). The medial temporal lobe memory system. *Science (New York, N.Y.)*, 253(5026):1380–6.
- Steinovorth, S., Corkin, S., and Halgren, E. (2006). Ecphory of autobiographical memories: an fmri study of recent and remote memory retrieval. *Neuroimage*, 30(1):285–98.
- Stevens, C. F. (1998). A million dollar question: does ltp = memory? *Neuron*, 20(1):1–2.
- Storandt, M. and Hill, R. D. (1989). Very mild senile dementia of the alzheimer type. ii. psychometric test performance. *Archives Of Neurology*, 46(4):383–6.
- Stranahan, A. M. and Mattson, M. P. (2010). Selective vulnerability of neurons in layer ii of the entorhinal cortex during aging and alzheimer’s disease. *Neural Plasticity*, 2010:108190.

- Strien, N. M. v., Cappaert, N. L. M., and Witter, M. P. (2009). The anatomy of memory: an interactive overview of the parahippocampal-hippocampal network. *Nature Reviews Neuroscience*, 10(4):272–82.
- Sumioka, A., Yan, D., and Tomita, S. (2010). Tarp phosphorylation regulates synaptic ampa receptors through lipid bilayers. *Neuron*, 66(5):755–67.
- Suthana, N. and Fried, I. (2014). Deep brain stimulation for enhancement of learning and memory. *Neuroimage*, 85 Pt 3:996–1002.
- Sutherland, R. J., Sparks, F. T., and Lehmann, H. (2010). Hippocampus and retrograde amnesia in the rat model: a modest proposal for the situation of systems consolidation. *Neuropsychologia*, 48(8):2357–69.
- Sutherland, R. J., Weisend, M. P., Mumby, D., Astur, R. S., Hanlon, F. M., Koerner, A., Thomas, M. J., Wu, Y., Moses, S. N., Cole, C., Hamilton, D. A., and Hoesing, J. M. (2001). Retrograde amnesia after hippocampal damage: recent vs. remote memories in two tasks. *Hippocampus*, 11(1):27–42.
- Suzuki, N., Cheung, T. T., Cai, X. D., Odaka, A., Otvos, L., Eckman, C., Golde, T. E., and Younkin, S. G. (1994). An increased percentage of long amyloid beta protein secreted by familial amyloid beta protein precursor (beta app717) mutants. *Science (New York, N.Y.)*, 264(5163):1336–40.
- Svoboda, E., McKinnon, M. C., and Levine, B. (2006). The functional neuroanatomy of autobiographical memory: a meta-analysis. *Neuropsychologia*, 44(12):2189–208.
- Swanson, G. T., Kamboj, S. K., and Cull-Candy, S. G. (1997). Single-channel properties of recombinant ampa receptors depend on rna editing, splice variation, and subunit composition. *The Journal Of Neuroscience : The Official Journal Of The Society For Neuroscience*, 17(1):58–69.

- Swanson, L. W., Sawchenko, P. E., and Cowan, W. M. (1981). Evidence for collateral projections by neurons in ammon's horn, the dentate gyrus, and the subiculum: a multiple retrograde labeling study in the rat. *The Journal Of Neuroscience : The Official Journal Of The Society For Neuroscience*, 1(5):548–59.
- Swerdlow, R. H., Burns, J. M., and Khan, S. M. (2014). The alzheimer's disease mitochondrial cascade hypothesis: progress and perspectives. *Biochimica Et Biophysica Acta*, 1842(8):1219–31.
- Szabo, V., Ventalon, C., De Sars, V., Bradley, J., and Emiliani, V. (2014). Spatially selective holographic photoactivation and functional fluorescence imaging in freely behaving mice with a fiberscope. *Neuron*, 84(6):1157–69.
- Takehara-Nishiuchi, K., Nakao, K., Kawahara, S., Matsuki, N., and Kirino, Y. (2006). Systems consolidation requires postlearning activation of nmda receptors in the medial prefrontal cortex in trace eyeblink conditioning. *The Journal Of Neuroscience : The Official Journal Of The Society For Neuroscience*, 26(19):5049–58.
- Takeuchi, T., Duszkiewicz, A. J., and Morris, R. G. M. (2014). The synaptic plasticity and memory hypothesis: encoding, storage and persistence. *Philosophical Transactions Of The Royal Society Of London. Series B, Biological Sciences*, 369(1633):20130288.
- Tan, C.-C., Yu, J.-T., Wang, H.-F., Tan, M.-S., Meng, X.-F., Wang, C., Jiang, T., Zhu, X.-C., and Tan, L. (2014). Efficacy and safety of donepezil, galantamine, rivastigmine, and memantine for the treatment of alzheimer's disease: a systematic review and meta-analysis. *Journal Of Alzheimer'S Disease : Jad*, 41(2):615–31.
- Tanaka, K. Z., Pevzner, A., Hamidi, A. B., Nakazawa, Y., Graham, J., and Wiltgen, B. J. (2014). Cortical representations are reinstated by the hippocampus during memory retrieval. *Neuron*, 84(2):347–54.
- Tang, S.-C., Lathia, J. D., Selvaraj, P. K., Jo, D.-G., Mughal, M. R., Cheng, A., Siler, D. A., Markesberry, W. R., Arumugam, T. V., and Mattson, M. P. (2008). Toll-like receptor-4

- mediates neuronal apoptosis induced by amyloid beta-peptide and the membrane lipid peroxidation product 4-hydroxynonenal. *Experimental Neurology*, 213(1):114–21.
- Tanzi, R. E. and Bertram, L. (2001). New frontiers in alzheimer's disease genetics. *Neuron*, 32(2):181–4.
- Tariot, P. N., Farlow, M. R., Grossberg, G. T., Graham, S. M., McDonald, S., and Gergel, I. (2004). Memantine treatment in patients with moderate to severe alzheimer disease already receiving donepezil: a randomized controlled trial. *Jama*, 291(3):317–24.
- Taube, J. S., Muller, R. U., and Ranck, J. B. (1990). Head-direction cells recorded from the postsubiculum in freely moving rats. i. description and quantitative analysis. *The Journal Of Neuroscience : The Official Journal Of The Society For Neuroscience*, 10(2):420–35.
- Terwel, D., Muyllaert, D., Dewachter, I., Borghgraef, P., Croes, S., Devijver, H., and Van Leuven, F. (2008). Amyloid activates gsk-3beta to aggravate neuronal tauopathy in bigenic mice. *The American Journal Of Pathology*, 172(3):786–98.
- Tolias, A. S., Ecker, A. S., Siapas, A. G., Hoenselaar, A., Keliris, G. A., and Logothetis, N. K. (2007). Recording chronically from the same neurons in awake, behaving primates. *Journal Of Neurophysiology*, 98(6):3780–90.
- Tomer, R., Ye, L., Hsueh, B., and Deisseroth, K. (2014). Advanced clarity for rapid and high-resolution imaging of intact tissues. *Nature Protocols*, 9(7):1682–97.
- Tomita, S., Stein, V., Stocker, T. J., Nicoll, R. A., and Bredt, D. S. (2005). Bidirectional synaptic plasticity regulated by phosphorylation of stargazin-like tarsps. *Neuron*, 45(2):269–77.
- Treiber, K. A., Carlson, M. C., Corcoran, C., Norton, M. C., Breitner, J. C. S., Piercy, K. W., Deberard, M. S., Stein, D., Foley, B., Welsh-Bohmer, K. A., Frye, A., Lyketsos, C. G., and Tschanz, J. T. (2011). Cognitive stimulation and cognitive and functional

- decline in alzheimer's disease: the cache county dementia progression study. *The Journals Of Gerontology. Series B, Psychological Sciences And Social Sciences*, 66(4):416–25.
- Tschanz, J. T., Corcoran, C. D., Schwartz, S., Treiber, K., Green, R. C., Norton, M. C., Mielke, M. M., Piercy, K., Steinberg, M., Rabins, P. V., Leoutsakos, J.-M., Welsh-Bohmer, K. A., Breitner, J. C. S., and Lyketsos, C. G. (2011). Progression of cognitive, functional, and neuropsychiatric symptom domains in a population cohort with alzheimer dementia: the cache county dementia progression study. *The American Journal Of Geriatric Psychiatry : Official Journal Of The American Association For Geriatric Psychiatry*, 19(6):532–42.
- Turrigiano, G. G. (2008). The self-tuning neuron: synaptic scaling of excitatory synapses. *Cell*, 135(3):422–35.
- Turrigiano, G. G., Leslie, K. R., Desai, N. S., Rutherford, L. C., and Nelson, S. B. (1998). Activity-dependent scaling of quantal amplitude in neocortical neurons. *Nature*, 391(6670):892–6.
- Um, J. W., Kaufman, A. C., Kostylev, M., Heiss, J. K., Stagi, M., Takahashi, H., Kerrisk, M. E., Vortmeyer, A., Wisniewski, T., Koleske, A. J., Gunther, E. C., Nygaard, H. B., and Strittmatter, S. M. (2013). Metabotropic glutamate receptor 5 is a coreceptor for alzheimer  $\alpha\beta$  oligomer bound to cellular prion protein. *Neuron*, 79(5):887–902.
- Um, J. W., Nygaard, H. B., Heiss, J. K., Kostylev, M. A., Stagi, M., Vortmeyer, A., Wisniewski, T., Gunther, E. C., and Strittmatter, S. M. (2012). Alzheimer amyloid- $\beta$  oligomer bound to postsynaptic prion protein activates fyn to impair neurons. *Nature Neuroscience*, 15(9):1227–35.
- Van Der Putt, R., Dineen, C., Janes, D., Series, H., and McShane, R. (2006). Effectiveness of acetylcholinesterase inhibitors: diagnosis and severity as predictors of response in routine practice. *International Journal Of Geriatric Psychiatry*, 21(8):755–60.

- Van Hoesen, G. W. and Solodkin, A. (1993). Some modular features of temporal cortex in humans as revealed by pathological changes in alzheimer's disease. *Cerebral Cortex (New York, N.Y. : 1991)*, 3(5):465–75.
- Vann, S. D., Brown, M. W., Erichsen, J. T., and Aggleton, J. P. (2000). Fos imaging reveals differential patterns of hippocampal and parahippocampal subfield activation in rats in response to different spatial memory tests. *The Journal Of Neuroscience : The Official Journal Of The Society For Neuroscience*, 20(7):2711–8.
- Vargha-Khadem, F., Gadian, D. G., Watkins, K. E., Connelly, A., Van Paesschen, W., and Mishkin, M. (1997). Differential effects of early hippocampal pathology on episodic and semantic memory. *Science (New York, N.Y.)*, 277(5324):376–80.
- Vazdarjanova, A. and Guzowski, J. F. (2004). Differences in hippocampal neuronal population responses to modifications of an environmental context: evidence for distinct, yet complementary, functions of ca3 and ca1 ensembles. *The Journal Of Neuroscience : The Official Journal Of The Society For Neuroscience*, 24(29):6489–96.
- Verret, L., Mann, E. O., Hang, G. B., Barth, A. M. I., Cobos, I., Ho, K., Devidze, N., Masliah, E., Kreitzer, A. C., Mody, I., Mucke, L., and Palop, J. J. (2012). Inhibitory interneuron deficit links altered network activity and cognitive dysfunction in alzheimer model. *Cell*, 149(3):708–21.
- Victor, J. D. (2002). Binless strategies for estimation of information from neural data. *Physical Review. E, Statistical, Nonlinear, And Soft Matter Physics*, 66(5 Pt 1):051903.
- Villette, V., Poindessous-Jazat, F., Simon, A., Léna, C., Roullot, E., Bellessort, B., Epelbaum, J., Dutar, P., and Stéphan, A. (2010). Decreased rhythmic gabaergic septal activity and memory-associated theta oscillations after hippocampal amyloid-beta pathology in the rat. *The Journal Of Neuroscience : The Official Journal Of The Society For Neuroscience*, 30(33):10991–1003.

- Viskontas, I. V., McAndrews, M. P., and Moscovitch, M. (2002). Memory for famous people in patients with unilateral temporal lobe epilepsy and excisions. *Neuropsychology*, 16(4):472–80.
- Vlček, K. and Laczó, J. (2014). Neural correlates of spatial navigation changes in mild cognitive impairment and alzheimer’s disease. *Frontiers In Behavioral Neuroscience*, 8:89.
- Vos, S. J., Xiong, C., Visser, P. J., Jasielec, M. S., Hassenstab, J., Grant, E. A., Cairns, N. J., Morris, J. C., Holtzman, D. M., and Fagan, A. M. (2013). Preclinical alzheimer’s disease and its outcome: a longitudinal cohort study. *The Lancet. Neurology*, 12(10):957–65.
- Vossel, K. A., Beagle, A. J., Rabinovici, G. D., Shu, H., Lee, S. E., Naasan, G., Hegde, M., Cornes, S. B., Henry, M. L., Nelson, A. B., Seeley, W. W., Geschwind, M. D., Gorno-Tempini, M. L., Shih, T., Kirsch, H. E., Garcia, P. A., Miller, B. L., and Mucke, L. (2013). Seizures and epileptiform activity in the early stages of alzheimer disease. *Jama Neurology*, 70(9):1158–66.
- Walsh, D. M., Klyubin, I., Fadeeva, J. V., Cullen, W. K., Anwyl, R., Wolfe, M. S., Rowan, M. J., and Selkoe, D. J. (2002). Naturally secreted oligomers of amyloid beta protein potently inhibit hippocampal long-term potentiation in vivo. *Nature*, 416(6880):535–9.
- Walsh, D. M. and Selkoe, D. J. (2007). A beta oligomers - a decade of discovery. *Journal Of Neurochemistry*, 101(5):1172–84.
- Wang, S.-H. and Morris, R. G. M. (2010). Hippocampal-neocortical interactions in memory formation, consolidation, and reconsolidation. *Annual Review Of Psychology*, 61:49–79, C1–4.
- Wang, X., Pinter, M. J., and Rich, M. M. (2016). Reversible recruitment of a homeostatic reserve pool of synaptic vesicles underlies rapid homeostatic plasticity of quantal content.

- The Journal Of Neuroscience : The Official Journal Of The Society For Neuroscience*, 36(3):828–36.
- Wenthold, R. J., Petralia, R. S., Blahos J, I. I., and Niedzielski, A. S. (1996). Evidence for multiple ampa receptor complexes in hippocampal ca1/ca2 neurons. *The Journal Of Neuroscience : The Official Journal Of The Society For Neuroscience*, 16(6):1982–9.
- Westerman, M. A., Cooper-Blacketer, D., Mariash, A., Kotilinek, L., Kawarabayashi, T., Younkin, L. H., Carlson, G. A., Younkin, S. G., and Ashe, K. H. (2002). The relationship between abeta and memory in the tg2576 mouse model of alzheimer’s disease. *The Journal Of Neuroscience : The Official Journal Of The Society For Neuroscience*, 22(5):1858–67.
- Wheeler, A. L., Teixeira, C. M., Wang, A. H., Xiong, X., Kovacevic, N., Lerch, J. P., McIntosh, A. R., Parkinson, J., and Frankland, P. W. (2013). Identification of a functional connectome for long-term fear memory in mice. *Plos Computational Biology*, 9(1):e1002853.
- Whitehead, G., Regan, P., Whitcomb, D. J., and Cho, K. (2017). Ca(2+)-permeable ampa receptor: A new perspective on amyloid-beta mediated pathophysiology of alzheimer’s disease. *Neuropharmacology*, 112(Pt A):221–227.
- Whitehouse, P. J., Price, D. L., Struble, R. G., Clark, A. W., Coyle, J. T., and Delon, M. R. (1982). Alzheimer’s disease and senile dementia: loss of neurons in the basal forebrain. *Science (New York, N.Y.)*, 215(4537):1237–9.
- Whitt, J. L., Petrus, E., and Lee, H.-K. (2014). Experience-dependent homeostatic synaptic plasticity in neocortex. *Neuropharmacology*, 78:45–54.
- Wilkinson, D. and Murray, J. (2001). Galantamine: a randomized, double-blind, dose comparison in patients with alzheimer’s disease. *International Journal Of Geriatric Psychiatry*, 16(9):852–7.

- Williams, D. R. and Lees, A. J. (2009). Progressive supranuclear palsy: clinicopathological concepts and diagnostic challenges. *The Lancet. Neurology*, 8(3):270–9.
- Willshaw, D., Dayan, P., and Morris, R. (2015). Memory, modelling and marr: a commentary on marr (1971)‘simple memory: a theory of archicortex’. *Phil. Trans. R. Soc. B*, 370(1666):20140383.
- Wilson, M. A. and McNaughton, B. L. (1993). Dynamics of the hippocampal ensemble code for space. *Science (New York, N.Y.)*, 261(5124):1055–8.
- Wilson, R. S., Bacon, L. D., Fox, J. H., and Kaszniak, A. W. (1983). Primary memory and secondary memory in dementia of the alzheimer type. *Journal Of Clinical Neuropsychology*, 5(4):337–44.
- Wisniewski, K. E., Wisniewski, H. M., and Wen, G. Y. (1985). Occurrence of neuropathological changes and dementia of alzheimer’s disease in down’s syndrome. *Annals Of Neurology*, 17(3):278–82.
- Wood, E. R., Dudchenko, P. A., and Eichenbaum, H. (1999). The global record of memory in hippocampal neuronal activity. *Nature*, 397(6720):613–6.
- World Health Organization (2013). Priority medicines for europe and the world update report. [Online; accessed 12-February-2017].
- Xie, K., Fox, G. E., Liu, J., and Tsien, J. Z. (2016). 512-channel and 13-region simultaneous recordings coupled with optogenetic manipulation in freely behaving mice. *Frontiers in systems neuroscience*, 10.
- Yang, W., Miller, J.-e. K., Carrillo-Reid, L., Pnevmatikakis, E., Paninski, L., Yuste, R., and Peterka, D. S. (2016). Simultaneous multi-plane imaging of neural circuits. *Neuron*, 89(2):269–284.
- Yang, W. and Yuste, R. (2017). In vivo imaging of neural activity. *Nature Methods*, 14(4):349–359.

- Yassa, M. A. and Reagh, Z. M. (2013). Competitive trace theory: A role for the hippocampus in contextual interference during retrieval. *Frontiers In Behavioral Neuroscience*, 7:107.
- Yener, G. G., Güntekin, B., Oniz, A., and Başar, E. (2007). Increased frontal phase-locking of event-related theta oscillations in alzheimer patients treated with cholinesterase inhibitors. *International Journal Of Psychophysiology : Official Journal Of The International Organization Of Psychophysiology*, 64(1):46–52.
- Yiu, A. P., Rashid, A. J., and Josselyn, S. A. (2011). Increasing creb function in the ca1 region of dorsal hippocampus rescues the spatial memory deficits in a mouse model of alzheimer’s disease. *Neuropsychopharmacology : Official Publication Of The American College Of Neuropsychopharmacology*, 36(11):2169–86.
- Yizhar, O., Fenno, L. E., Davidson, T. J., Mogri, M., and Deisseroth, K. (2011). Optogenetics in neural systems. *Neuron*, 71(1):9–34.
- Yoshida, H. and Ihara, Y. (1993). Tau in paired helical filaments is functionally distinct from fetal tau: assembly incompetence of paired helical filament-tau. *Journal Of Neurochemistry*, 61(3):1183–6.
- Young, B. J., Fox, G. D., and Eichenbaum, H. (1994). Correlates of hippocampal complex-spike cell activity in rats performing a nonspatial radial maze task. *The Journal Of Neuroscience : The Official Journal Of The Society For Neuroscience*, 14(11 Pt 1):6553–63.
- Zaleta, A. K., Carpenter, B. D., Porensky, E. K., Xiong, C., and Morris, J. C. (2012). Agreement on diagnosis among patients, companions, and professionals after a dementia evaluation. *Alzheimer Disease And Associated Disorders*, 26(3):232–7.
- Zamanillo, D., Sprengel, R., Hvalby, O., Jensen, V., Burnashev, N., Rozov, A., Kaiser, K. M., Köster, H. J., Borchardt, T., Worley, P., Lübke, J., Frotscher, M., Kelly, P. H.,

- Sommer, B., Andersen, P., Seburg, P. H., and Sakmann, B. (1999). Importance of ampa receptors for hippocampal synaptic plasticity but not for spatial learning. *Science (New York, N.Y.)*, 284(5421):1805–11.
- Zeithamova, D., Dominick, A. L., and Preston, A. R. (2012). Hippocampal and ventral medial prefrontal activation during retrieval-mediated learning supports novel inference. *Neuron*, 75(1):168–79.
- Zempel, H., Thies, E., Mandelkow, E., and Mandelkow, E.-M. (2010). Abeta oligomers cause localized ca(2+) elevation, missorting of endogenous tau into dendrites, tau phosphorylation, and destruction of microtubules and spines. *The Journal Of Neuroscience : The Official Journal Of The Society For Neuroscience*, 30(36):11938–50.
- Zhan, J., Brys, M., Glodzik, L., Tsui, W., Javier, E., Wegiel, J., Kuchna, I., Pirraglia, E., Li, Y., Mosconi, L., Saint Louis, L. A., Switalski, R., De Santi, S., Kim, B. C., Wisniewski, T., Reisberg, B., Bobinski, M., and de Leon, M. J. (2009). An entorhinal cortex sulcal pattern is associated with alzheimer’s disease. *Human Brain Mapping*, 30(3):874–82.
- Zhang, F., Aravanis, A. M., Adamantidis, A., de Lecea, L., and Deisseroth, K. (2007). Circuit-breakers: optical technologies for probing neural signals and systems. *Nature Reviews. Neuroscience*, 8(8):577–81.
- Zhang, X., Tian, Y., Zhang, C., Tian, X., Ross, A. W., Moir, R. D., Sun, H., Tanzi, R. E., Moore, A., and Ran, C. (2015). Near-infrared fluorescence molecular imaging of amyloid beta species and monitoring therapy in animal models of alzheimer’s disease. *Proceedings Of The National Academy Of Sciences Of The United States Of America*, 112(31):9734–9.
- Zhang, Y., Venkitaramani, D. V., Gladding, C. M., Zhang, Y., Kurup, P., Molnar, E., Collingridge, G. L., and Lombroso, P. J. (2008). The tyrosine phosphatase step mediates ampa receptor endocytosis after metabotropic glutamate receptor stimulation. *The Journal Of Neuroscience : The Official Journal Of The Society For Neuroscience*, 28(42):10561–6.

- Zhao, R., Fowler, S. W., Chiang, A. C. A., Ji, D., and Jankowsky, J. L. (2014). Impairments in experience-dependent scaling and stability of hippocampal place fields limit spatial learning in a mouse model of alzheimer's disease. *Hippocampus*, 24(8):963–78.
- Zhao, S., Ting, J. T., Atallah, H. E., Qiu, L., Tan, J., Gloss, B., Augustine, G. J., Deisseroth, K., Luo, M., Graybiel, A. M., and Feng, G. (2011). Cell type-specific channelrhodopsin-2 transgenic mice for optogenetic dissection of neural circuitry function. *Nature Methods*, 8(9):745–52.
- Zhao, W.-Q., Santini, F., Breese, R., Ross, D., Zhang, X. D., Stone, D. J., Ferrer, M., Townsend, M., Wolfe, A. L., Seager, M. A., Kinney, G. G., Shughrue, P. J., and Ray, W. J. (2010). Inhibition of calcineurin-mediated endocytosis and alpha-amino-3-hydroxy-5-methyl-4-isoxazolepropionic acid (ampa) receptors prevents amyloid beta oligomer-induced synaptic disruption. *The Journal Of Biological Chemistry*, 285(10):7619–32.
- Zhou, M., Zhang, F., Zhao, L., Qian, J., and Dong, C. (2016). Entorhinal cortex: a good biomarker of mild cognitive impairment and mild alzheimer's disease. *Reviews In The Neurosciences*, 27(2):185–95.
- Zhou, Q., Homma, K. J., and Poo, M.-m. (2004). Shrinkage of dendritic spines associated with long-term depression of hippocampal synapses. *Neuron*, 44(5):749–57.
- Zhu, C. W. and Sano, M. (2006). Economic considerations in the management of alzheimer's disease. *Clinical Interventions In Aging*, 1(2):143–54.
- Zhu, X., Perry, G., Moreira, P. I., Aliev, G., Cash, A. D., Hirai, K., and Smith, M. A. (2006). Mitochondrial abnormalities and oxidative imbalance in alzheimer disease. *Journal Of Alzheimer'S Disease : Jad*, 9(2):147–53.
- Ziv, Y., Burns, L. D., Cocker, E. D., Hamel, E. O., Ghosh, K. K., Kitch, L. J., El Gamal, A., and Schnitzer, M. J. (2013). Long-term dynamics of ca1 hippocampal place codes. *Nature Neuroscience*, 16(3):264–6.